01 Jul 1978

Webs for cold formed steel flexural members structural behavior of transversely reinforced beam webs

Wei-wen Yu
Missouri University of Science and Technology, wwy4@mst.edu

Nguyen Phung

CIVIL ENGINEERING STUDY 78 – 5
STRUCTURAL SERIES

Final Report

WEBS FOR COLD-FORMED STEEL FLEXURAL MEMBERS
STRUCTURAL BEHAVIOR OF TRANSVERSELY REINFORCED
BEAM WEBS

by

Nguyen Phung
Research Assistant

Wei-Wen Yu
Project Director

July, 1978

DEPARTMENT OF CIVIL ENGINEERING
UNIVERSITY OF MISSOURI-ROLLA
ROLLA, MISSOURI

PREFACE

Since 1973, a research project on webs for cold-formed steel flexural members has been conducted at the University of Missouri-Rolla under the sponsorship of American Iron and Steel Institute. This study deals with the structural behavior of beam webs subjected to bending stress, shear stress, combined bending and shear, web crippling and the effect of bending on web crippling load. In addition, it includes a study of beam webs reinforced by either transverse or longitudinal stiffeners.

This report presents the research findings on transversely rein-forced cold-formed steel beam webs. The results obtained from the study of beam webs subjected to other types of stress and the combinations thereof are presented in some other reports of the University of Missouri-Rolla referred to in the bibliography.

TABLE OF CONTENTS

LIST OF ILLUSTRATIONS

LIST OF TABLES

I. INTRODUCTION

A. General

The application of cold-formed steel structural members began several decades ago. In recent years, this type of structural member has been widely used in building construction and other areas. In general, the use of these members can provide many advantages, such as favorable strength-to-weight ratio, versatility, ease of prefabrication and mass production, fast and easy erection and installation, and simple connection in the structures (1,2).

In the United States, the unreinforced webs of cold-formed steel beams having a slenderness ratio less than or equal to 150 are designed on the basis of Sections 3.4 and 3.5 of the Specification issued by American Iron and Steel Institute (AISI) (3) for shear stress, bending stress, combined bending and shear stresses, and web crippling. The reasons behind and the justification for these design provisions are discussed by Dr. Winter in his commentary on the 1968 Edition of the AISI Specification (4).

During the past decade, numerous new types of cold-formed steel sections have been developed for use in building construction and other applications. The design of these unusual shapes may be beyond the original scope of Sections 3.4 and 3.5 of the current AISI Specification. For this reason, a research project on "Webs for Cold-Formed Steel Flexural Members," was initiated in 1973 at the University of Missouri-Rolla (UMR) under the sponsorship of the American Iron and Steel Institute. The purpose of this research project has been to study the structural behavior of unreinforced and reinforced beam webs subjected to bending stress, shear stress, web crippling load, and combinations thereof.

1

The structural behavior of cold-formed steel unreinforced beam webs in bending, shear, combined bending and shear, web crippling, and combined bending and web crippling was studied by LaBoube and Hetrakul as the first phase of this research project on beam webs. In these studies, an attempt was made to extend the limiting h/t ratio to 200 or more for the unreinforced beam webs. Their research findings on these areas are summarized in Refs. 5 through 10.

As the second phase of this project, the structural behavior of beam webs with transverse and longitudinal stiffeners has been studied. This report deals with the strength of transversely reinforced beam webs subjected to bending, shear, and web crippling. Studies of the beam webs with longitudinal stiffeners are discussed in a subsequent report.

B. Purpose of Investigation

In view of the fact that the current AISI Specification does not include any specific design provisions for reinforced beam webs, the objective of the investigation reported on herein was to study the structural behavior of transversely reinforced beam webs subjected to bending stress, shear stress, and web crippling load. The research findings will undoubtedly provide the background information needed to develop the new design criteria for transversely reinforced beam webs having h/t ratios greater than 200.

C. Scope of Investigation

The present study consisted of an analytical and experimental investigation concerning the structural behavior of cold-formed steel transversely reinforced beam webs subjected to bending, shear, and web crippling.

The first phase of the investigation dealt with an in-depth review of available publications and research reports on the related subjects. Section II of this report contains a summary of this literature survey.

In Sections III and IV, the experimental studies of the structural behavior of transversely reinforced beam webs subjected to bending and shear stresses are discussed.

Section V contains the research findings for beam webs with transverse stiffeners when they are subjected to web crippling load.

Finally, Section VI is a summary of the conclusions and design recommendations.

II. LITERATURE SURVEY

A. General

This section contains a review of some of the important research work that is related to the structural behavior of plates and beam webs with transverse stiffeners subjected to bending stress, shear stress, and web crippling load.

The current design criteria being used in various specifications for the design of transversely reinforced beam webs are also presented.

B. Bending Strength of Plates and Beam Web Elements

The buckling problem of a flat rectangular plate under bending was studied analytically by Timoshenko and Gere (11), Schuette and McCulloch (12), and Johnson and Noel (13). The critical elastic buckling stress can be expressed by the following equation:

$$f_{cr} = k\pi^2 E / [12(1 - \mu^2)(h/t)^2] \tag{1}$$

in which k = buckling coefficient, E = modulus of elasticity, μ = Poisson's ratio, h = depth of the plate, and t = thickness of the plate.

The buckling coefficient depends on the aspect ratio of the plate element, the edge support conditions, and the variation of the longitudinal bending stress. The numerical values of the buckling coefficient for a simply supported rectangular plate subjected to linearly varying bending stress were summarized by Bleich (14) and are tabulated in Table 1. Figure 1, which is reproduced from Bulson's book (15), is a graphic representation of a simply supported, rectangular plate subjected to a linearly varying bending stress.

The bending capacity of plate girders was investigated analytically and experimentally at Lehigh University (16,17) during the period

of 1957 to 1960. The objective of the study was to determine the static load-carrying capacity of transversely stiffened plate girders, and special attention was given to the postbuckling strength of the web elememts. Ten full-size plate girders were subjected to bending during this study. For these specimens, the h/t ratios range from 185 to 388, and the aspect ratios vary from 0.75 to 1.50. On the basis of the study, Eq. 2 was derived for the purpose of computing the ultimate bending stress of the plate girders.

$$\sigma_u = \sigma_y[1-0.0005 \frac{A_w}{A_f} (\frac{h}{t} - \frac{975}{\sqrt{\sigma_y}})] \tag{2}$$

in which σ_u = ultimate bending stress governed by the web, A_w = cross-sectional area of the web, A_f = cross-sectional area of the flange, and σ_y = yield point of steel. Equation 2 is currently used in the AISC Specification (18) for the design of hot-rolled and welded plate girders subjected to bending.

The structural behavior of cold-formed steel beam webs subjected to bending stress was studied by Bergfelt (19), Bergfelt et al.(20), Thomasson (21), and Hoglund (22). These Swedish investigators have introduced the concept of combining the effective web depth for the compression portion of the web element with the effective width of the compression flange for computing the bending capacity. Several formulas were proposed to calculate the effective web depth for trapezoidal steel decks and thin plate girders (19-22).

In 1973, a research project to study Webs for Cold-Formed Steel Flexural Members was initiated at the University of Missouri-Rolla. The objective was to investigate the strength of beam webs subjected to bending stress, shear stress, web crippling load, and combinations thereof. As the first phase of the research, the bending capacity of unreinforced webs having h/t ratios

less than 250 were investigated (5). In this study, four methods have been developed for predicting the moment capacity of cold-formed steel beams when the bending moment is governed by the strength of webs. These methods use either a full web depth or an effective web depth. Because the effective web depth method requires a tedious trial and error procedure in computing the ultimate bending capacity of the beam section, the postbuckling strength method as given in Eq. 3 is used in this report.

$$M_u = \Phi \, S_x \, f_{cr} \tag{3}$$

in which f_{cr} = critical web buckling stress, ksi.

$$f_{cr} = k\pi^2 E / [12(1-\mu^2)(h/t)^2] \tag{4}$$

$k \quad = \ 4 + 2(1+\beta)^3 + 2(1+\beta) =$ buckling coefficient

$\beta \quad = \ \left| f_t/f_c \right| =$ bending stress ratio in the web

$S_x \quad =$ section modulus computed based on the full

widths of tension flange and web and the

effective width of the compression flange

determined on the basis of f_{cr}

$\Phi \quad =$ postbuckling strength factor $= \alpha_1 \alpha_2 \alpha_3 \alpha_4 \tag{5}$

$$\alpha_1 \ = 0.017(h/t) - 0.790 \tag{6}$$

$$\alpha_2 \ = 0.0462 \left| f_c/f_t \right| + 0.538 \tag{7}$$

$\alpha_3 \ = 1.16 - 0.16(w/t/(w/t)_{lim})$, when

$(w/t)/(w/t)_{lim} \leq 2.25 \tag{8}$

$= 0.8$, when $(w/t)/(w/t)_{lim} > 2.25$

$$\alpha_4 \ = 0.561 \ (F_y/33) + 0.10 \tag{9}$$

In addition to Eq. 3, which utilizes a postbuckling strength factor, the effective web depth formulas were presented by LaBoube and Yu (5) for the purpose of determining the bending capacity of cold-formed steel beam webs.

C. Shear Strength of Plates and Beam Web Elements

The strength of beam web elements subjected to shear stress may be governed by either shear yielding or shear buckling. If the transverse stiffeners are provided, the postbuckling strength occasioned by the tension field action may govern the shear capacity of the reinforced beam webs.

1. Shear Yielding

When a beam web with a relatively small h/t ratio is subjected to shear stress, the maximum shearing stress developed at the neutral axis corresponds very well with the shear yield stress given by Von Mises yield theory, i.e.,

$$\tau_y = F_y/\sqrt{3} = 0.58\, F_y \tag{10}$$

in which F_y is the yield point of the material established by tensile tests.

In 1935, Lyse and Godfrey (23) found that for a beam web to attain shear yielding, the h/t ratio must be less than 70.

2. Shear Buckling

For beam webs with large h/t ratios, the web will fail in shear buckling. The critical shear stress, τ_{cre}, in the elastic range of a plate has been studied by Timoshenko and Gere (11), Skan and Southwell (24), Seydel (25), and Stein and Neff (26) and is given by Eq. 11.

$$\tau_{cre} = k\pi^2 E/[12(1-\mu^2)(h/t)^2] \tag{11}$$

in which k = the buckling coefficient, E = the modulus of elasticity, μ = Poisson's ratio, h = the depth of the web element, and t = the thickness of the web element.

The buckling coefficient, k, is a function of the support conditions along the edges of the web element and the aspect ratio, $\alpha = a/h$, in which a is the length of the web element. For a specific value of α, the numerical value of k can be determined by using Eqs. 12 and 13 for simply supported plates;

$$k = 4 + 5.34/\alpha^2, \text{ when } \alpha \leq 1.0 \tag{12}$$

and

$$k = 5.34 + 4/\alpha^2, \text{ when } \alpha > 1.0 \tag{13}$$

Figure 2, which is reproduced from Bleich's book (14), is a graphic representation of the buckling coefficient, k.

For webs having moderate h/t ratios, the theoretical shear buckling stress as determined by Eq. 11 may exceed the proportional limit in shear, therefore the web may buckle in the inelastic range.

The subject of determining the critical shear stress in the inelastic range has been studied by many investigators (27-30). It has been found that the inelastic shear buckling stress for a plate can be computed by using the following equation:

$$\tau_{cri} = \eta \tau_{cre} = \eta \frac{k\pi^2 E}{12(1-\mu^2)(h/t)^2} \tag{14}$$

in which η is a plasticity reduction factor.

In 1948, Stowell (27) found that the plasticity reduction factor is a function of the tangent modulus, E_t, and the Young's modulus, E. It can be expressed as follows:

$$\eta = \sqrt{E_t/E} \tag{15}$$

Gerard (28), in 1962, proposed another expression for the plasticity reduction factor that depends on the secant shear modulus, G_s, and the

initial shear modulus, G_o. This expression is given by Eq. 16.

$$\eta = G_s/G_o \tag{16}$$

Equations 15 and 16 are not practical for determining the plasticity reduction factor because they require the actual stress-strain curve of each given material. Therefore, in 1973, Rockey et al. (29) recommended a formula (Eq. 17) for inelastic bucking stress. This equation was derived from an assumed proportional limit in shear, τ_p, of $0.8\tau_y$ and from a reduction procedure presented by Bleich (14) for column buckling.

$$\tau_{cri} = \tau_y - \frac{(\tau_y - \tau_p)\tau_p}{\tau_{cre}} = \tau_y[1-0.16\tau_y/\tau_{cre}] \tag{17}$$

Equation 17 which is used for computing the inelastic shear buckling stress, does not take into account the strain-hardening effect of the material for beam webs having low slenderness ratios for which the actual failure stress exceeds the yield stress. In order to obtain an estimate of the shear strength for this low web slenderness ratio, Basler and Thurlimann (30) proposed an empirical formula for the inelastic shear buckling stress given by Eq. 18 when the theoretical shear buckling stress exceeds the proportional limit, which is $0.8\tau_y$.

$$\tau_{cr} = \sqrt{\tau_{pr}\tau_{cre}} = \sqrt{0.8\tau_y\tau_{cre}} \tag{18}$$

This expression was derived from the experimental data for beam webs having depth-to-thickness ratios of 50 through 70 that were obtained by Lyse and Godfrey (23).

3. Tension Field Action

The shear buckling stress was accepted as a basis for the designing

of plate girders until the early 1960's, because the formulas used for

predicting the critical buckling stresses are relatively simple and have

been known for many years. However, tests(31) have shown that subsequent to

buckling the stress in the web panel is redistributed, and a considerable

postbuckling strength may be developed as a result of tension field action.

Postbuckling strength is realized in most design specifications by

using smaller factor-of-safety for web buckling than for shear yielding.

Early tests conducted by Djubek (31) and Lepre(32) show that the

postbuckling strength of a plate girder web in shear may be

considerably larger than the buckling load even for webs without

transverse stiffeners.

In the case of stiffened plate girder webs, Wilson (33) was the

first investigator to explain the postbuckling behavior of a plate by

means of a model made of a very thin flexible web with stiffeners. He

then pointed out that the web-stiffener combination acted as a Pratt-

truss in which the stiffeners take up the duty of the posts of the

truss and the web acts as an inclined tie.

In the 1960's, extensive studies, both analytical and experimental, were

made by Basler $\underline{et}$ $\underline{al}$.(16), and Basler (34) on the postbuckling behavior of the

stiffened plate girders that are typical in civil engineering structures

such as bridges and buildings. In his analytical study, Basler (34)

considered that the flanges are rather flexible in their resistance

to the vertical stresses developed from the tension field and that these

stresses are supported by the transverse stiffeners.

It was pointed out by Basler (34) that the ultimate shear stress,

τ_u, is equal to the sum of the beam action contribution, τ_{cr}, and the

tension field action contribution as given in Eq. 19;

$$\tau_u = \tau_{cr} + \frac{1}{2} \sigma_t \sin\theta_d \qquad (19)$$

in which

τ_{cr} = shear buckling stress

σ_t = tension field stress

θ_d = angle of panel diagonal with flange

By means of Mohr's circle, Basler (34) analyzed the state of the combined buckling stress, τ_{cr}, and the tension field stress, σ_t, and developed an expression for σ_t such that the Von Mises yield condition is satisfied. This expression is given by the following equation:

$$\frac{\sigma_t}{\sigma_y} = \sqrt{1+(\tau_{cr}/\tau_y)^2[\frac{9}{4}\sin^2 2\theta-3]} - \frac{3}{2}(\tau_{cr}/\tau_y)\sin 2\theta \qquad (20)$$

in which θ is the inclination of the tension field stress σ_t, and τ_y is the shear yield point of the material.

In order to obtain a simpler expression for σ_t, Basler (34) assumed that the inclination of the tension field stress is equal to 45°. If the linear approximation of the Mises yield condition is used, the tension field stress, σ_t, can be determined by the following simple expression:

$$\sigma_t = \sigma_y[1-\tau_{cr}/\tau_y] \qquad (21)$$

By substituting Eq. 21 for σ_t in Eq. 19, one obtains:

$$\tau_u = \tau_{cr} + \frac{1}{2} \sigma_y[1-\tau_{cr}/\tau_y]\sin\theta_d \qquad (22)$$

It was pointed out first by Gaylord (35) and later by Fujii (36) and Selberg (37) that Basler's formula (Eq. 22) gives the shear strength for a complete tension field instead of a limited band as shown in Table 2. Therefore, Basler's formula overestimates the shear strength of a

girder, because the flanges are incapable of supporting the lateral load imposed by the inclined tension field. The correct formula for the limited band is

$$\tau_u = \tau_{cr} + \sigma_y[1-\tau_{cr}/\tau_y]\frac{\sin\theta_d}{2(1+\cos\theta_d)} \tag{23}$$

If one expresses the functions $\sin\theta_d$ and $\cos\theta_d$ in terms of the aspect ratio, $\alpha = a/h$, and substitutes σ_y by $\sqrt{3}\ \tau_y$, Eq. 23 becomes

$$\tau_u = \tau_{cr} + \frac{\sqrt{3}(\tau_y-\tau_{cr})}{2(\sqrt{1+\alpha^2}+\alpha)} \tag{24}$$

This modified Basler's formula is derived from the incomplete tension field theory of the stiffened plate girder webs.

Following Basler's work, many investigators developed several different models for the tension field of the transversely reinforced girder webs. These models demonstrate that the rigidity of the flanges has a profound effect on the shear capacity of the plate girders. Table 2, which is reproduced from Ref. 38, is a summary of these models. It shows the tension field, the positions of the plastic hinges, the edge conditions assumed in computing the shear buckling stress, and the names of the investigators.

Among the 10 models listed in Table 2, Rockey's model is the one most commonly used for determining the effect of the flanges upon the shear strength of plate girders. The tension field assumed by Rockey consists of a single band in which the tension field stress direction is taken in the direction of the panel diagonal. The shear failure occurs when the hinges form in the flanges to produce a combined mechanism. The vertical component of the tension field stress is added to the shear buckling stress, and the resulting ultimate shear is expressed by the following

equation:

$$\tau_u = \tau_{cr} + \sigma_t [2c/h + \cot\theta - \cot\theta_d] \sin^2\theta \qquad (25)$$

in which c is the distance measured along the flange from the transverse

stiffener to the plastic hinge and is given by Eq. 26.

$$c = \frac{2}{\sin\theta} \sqrt{\frac{m_p}{\sigma_t \cdot t}} \qquad 0 < c < a \qquad (26)$$

In Eq. 26, m_p is the plastic moment of resistance of the flange.

It is to be noted from Eq. 26 that if the flanges cannot develop the

plastic moment such as in the case of cold-formed steel beams (i.e. let

$m_p = 0$), then c = 0. By inserting this value into Eq. 25 and maximizing τ_u

by differentiating it with respect to θ, the true Basler's formula,

Eq. 24, can be obtained.

4. Transverse Stiffener Requirements

In beam webs, the intermediate stiffeners must be sufficient stiff to

preserve straight boundaries when the web buckles. They must be strong

enough to sustain the compressive stresses developed by the tension

field action.

(a) Stiffness Requirement

Various theoretical methods have been developed for the ratio of the

optimum stiffener rigidity to the panel rigidity of the beam web. Three

such methods are

    i. Moore's Method (39); $\gamma = 14/(a/h)^3$ (27)

    ii. Bleich's Method (14); $\gamma = 4[7(h/a)^2 - 5]$ (28)

    iii. McGuire's Method based $\gamma = 3.75/(a/h)^4$ (29)
           on Timoshenko's equation
           and a safety factor of 2
           (11,68);

in which
$$\gamma = \frac{EI_s}{Da} = \frac{12(1-\mu^2)EI_s}{Eat^3} \tag{30}$$

I_s = optimum stiffener moment of inertia with respect to an axis in the plane of the web.

By inserting a value of $\mu = 0.3$ into Eqs. 29 and 30, one obtains

$$I_s = \frac{0.344h^4}{(a/t)^3} \tag{31}$$

The following AISC requirement for stiffener stiffness gives reasonable agreement with 1/2 value of I_s given in Eq. 31 for shallow and deep webs: (68)

$$I_s = (h/50)^4 \tag{32}$$

The above equation is used in Section 1.10.5.4 of the 1969 Edition of the AISC Specification (18).

It should be noted that the AISC formula given by Eq. 32 depends on h alone. Because it appears to be inadequately related to web-buckling parameters, a more realistic expression for the following stiffener moment of inertia was derived by Bleich (14):

$$I_s = 2.5ht^3(h/a - 0.7a/h) \tag{33}$$

In deriving this expression, Bleich used the theoretical data obtained by Stein and Fralich (40) for an infinitely long web with simply supported edges and equally spaced stiffeners.

(b) Strength Requirement

Transverse stiffeners should also be designed to resist the vertical components of the tension field forces. In such a situation, they are considered to be compression members and therefore must be checked for local and column buckling. According to Basler's solution (34), the axial

force, F_s, developed by the tension field is

$$F_s = 0.5F_y \text{ at } (1-\tau_{cr}/\tau_y)(1-\alpha/\sqrt{1+\alpha^2}+\alpha) \tag{34}$$

in which F_y is the yield point of the web material.

The AISC equation for determining the cross-sectional area, A_s, of stiffeners that are symmetrical about the plane of the web is derived from Eq. 34 by dividing F_s by the yield point of stiffener material, F_{ys}. The value of A_s is given in Eq. 35.

$$A_s = F_s/F_{ys} \tag{35}$$

If stiffeners are one-sided, A_s should be multiplied by a factor to account for their eccentricity (41).

(c) Spacing Requirement

In his work on plate girder design, Basler (34) indicated that the minimum spacing between two transverse stiffeners was selected to facilitate fabrication, handling, and erection of the girders. The smaller dimensions, either a or h, should not exceed 260t and, therefore,

$$\frac{a}{h} < (\frac{260}{h/t})^2 < 3.0 \tag{36}$$

(d) End Panel Requirement

For an end panel, Basler (34) pointed out that when web yielding occurs there is no neighboring plate to serve as an anchor for the development of a tension stress field. The smaller dimension of the end panel, a or h, should not be greater than the value given below:

$$\frac{11,000t}{\sqrt{f_u}} \tag{37}$$

in which f_u is the maximum shear stress of the web in psi. If f_u is in

ksi, the above expression becomes

$$\frac{348t}{\sqrt{f_u}} \qquad (38)$$

D. Web Crippling Strength

1. Beam Webs Loaded Between Transverse Stiffeners

The buckling problem of a rectangular plate subjected to edge loading was studied by Sommerfeld (42), Timoshenko (43), Leggett (44), Hopkins (45), Yamaki (46), White and Cottingham (47), and Khan and Johns (48).

The web crippling strength of hot-rolled and cold-formed steel beam webs was investigated by Lyse and Godfrey (23), Winter and Pian (49), Zetlin (50), and Rockey, Bagchi, and El-gaaly (51-57). The following discussion deals with unreinforced and reinforced beam webs.

(a) Flat Plates and Unreinforced Beam Webs

In 1910, Timoshenko (43) developed an approximate solution for a plate compressed by two equal and opposite concentrated forces. By means of the energy method, he found that the critical buckling load can be expressed by the following equation:

$$P_{cr} = K\pi D/h \qquad (39)$$

in which D is the flexural rigidity of the plate, $[Et^3/12(1-\mu^2)]$, h is the depth of a plate and K is the buckling coefficient which is equal to 4 for a simply supported long plate and equal to 8 for a clamped long plate.

In 1953, Yamaki (46) found that for a simply supported rectangular plate loaded by either concentrated or distributed loads on two opposite edges, the buckling coefficient, K, is a function of the aspect ratio, $\alpha = a/h$ and the N/a ratio of the patch load as shown in Figs. 3 and 4. It should be

noted that Yamaki (46) investigated only the buckling strength of a
plate that has an aspect ratio larger than 0.8.

Girkmann (58), in 1936, was the first investigator to study the
buckling problem of a rectangular plate subjected to a simple edge load, but
his results are not in a form that is readily usuable for engineering purposes.
In 1955, the elastic stability of a simply supported plate subjected to
partial edge loading was studied theoretically by Zetlin (50). He
derived the critical buckling load as shown in the following equation:

$$P_{cr} = K\pi^2 D/a^2 \tag{40}$$

in which K is the buckling coefficient depending on the ratios of N/a and
a/h of the plate element. It is to be noted that studies made by Girkmann
and Zetlin are concerned mainly with the computation of elastic
critical loads, and for most of the cases, the methods used involve a high
degree of mathematical complexity and are difficult to apply in any
parametric study of this type of problem.

In order to overcome the above mentioned disadvantage, in March 1977,
Khan et al.(59) used the energy method to obtain the critical buckling
load for a simply supported rectangular plate under a distributed
compressive load. The critical buckling load is defined by Eq. 41.

$$P_{cr} = K\pi^2 D/h \tag{41}$$

in which K is the buckling coefficient,which depends on the aspect ratio,
$\alpha = a/h$, and the ratio $\beta = N/a$. The buckling coefficient,K,is shown
graphically in Fig. 5 and is also tabulated in Table 3.

For hot-rolled steel beams, the web crippling strength of I sections
was investigated experimentally by Lyse and Godfrey (23). Based on

the test results, the maximum bearing stress under a concentrated load can be expressed as follows:

$$f_p = \frac{R}{t(N+2k)} \qquad (42)$$

in which f_p is the bearing stress, R is the applied load, t is the thickness of the web, N is the bearing length, and k is the distance from the outer face of the flange to the toe of the web fillet of the rolled sections. Equation 42 is now being used by the AISC Specification for the design of hot-rolled shapes and welded plate girders for interior web crippling loads.

During the 1940's and 1950's, an extensive research program on the web crippling strength of cold-formed steel beams was conducted at Cornell University by Winter and Pian (49), and Zetlin (50). Based on their test results, they found that the web crippling strength of single, unreinforced webs depends primarily on the ratios of N/t, h/t,and R/t and the yield point of material. As a consequence, the following formulas were derived to predict the web crippling load for cold-formed steel sections having single unreinforced webs when they are subjected to interior one-flange or two-flange loadings:

1. $R/t \leq 1.0$

$$P_u = \frac{t^2 F_y}{10^3}[1.22{-}0.22F_y/33]\,[17000{+}125\frac{N}{t} - 0.5\frac{N}{t}\frac{h}{t} - 30\frac{h}{t}] \qquad (43)$$

2. $1.0 < R/t \leq 4.0$

$$(P_u)_1 = P_u[1.06{-}0.06R/t] \qquad (44)$$

In the above equations, P_u and $(P_u)_1$ are the predicted ultimate loads in kips per web.

Since 1973, extensive experimental work has been conducted at the University of Missouri-Rolla to study further the web crippling strength of cold-formed steel unreinforced beam webs. These research findings were reported by Hetrakul and Yu (9,10).

(b) Reinforced Beam Webs

In recent years, the web crippling strength of cold-formed steel beam webs with transverse stiffeners under partial edge loading has been studied by Rockey, Bagchi, and El-gaaly as reported in Refs. 51 to 57. Rockey and El-gaaly showed that the buckling load for a simply supported rectangular plate subjected to partial edge loading can be determined by Eq. 45.

$$P_{cr}/at = K\pi^2 D/h^2 t \tag{45}$$

in which K is the buckling coefficient depending on the ratios of a/h and N/a, and a is the spacing of the transverse stiffeners. The values of K computed by the finite element method were presented by Bagchi and Rockey(54). In addition, the postbuckling strength of reinforced beam webs under patch loads represented by the ratio of P_u/P_{cr} has also been evaluated. It was found that the relationship between P_u/P_{cr}, N/a, and h/t can be expressed as shown in Eq. 46.

$$P_u/P_{cr} = (4.5+6.4N/a)(h/t)(10^{-3}) \tag{46}$$

For hot-rolled steel beams, the web crippling of W shapes stiffened by transverse stiffeners was studied by Basler (60) in 1961. Basler indicated that a uniformly distributed load applied between two transverse stiffeners may cause the web to buckle vertically. The critical vertical buckling stress can be calculated on the basis of the following formula, which was proposed by Basler (60):

$$F_{cr} = K_c \frac{\pi^2 E}{12(1-\mu^2)(h/t)^2} \qquad (47)$$

in which K_c is the buckling coefficient depending on the aspect ratio of

the web panel and the restraint conditions at the compressed edges of the

web plate. The value of K_c is given by Eqs. 48 and 49.

when the flange is restrained against rotation,

$$K_c = 5.5 + 4/(a/h)^2 \qquad (48)$$

and when the flange is not so restrained,

$$K_c = 2 + 4/(a/h)^2 \qquad (49)$$

2. Beam Webs Loaded at the Location of Transverse Stiffeners

In aircraft structures (61), thin sheets under uniform compression

are always stiffened by angles or channels to resist the compression force

and to prevent the sheet panel from buckling prematurely. Based on

the buckling and postbuckling behavior of plate elements, studies (62,63)

have been made to determine the portion of the steel sheet or beam web

that will act as a stiffener column. The research findings of these

studies are discussed in the subsequent sections.

(a) Buckling of Compression Element

The local buckling problem of compression elements has been studied

by many investigators (62-64). Equation 50 can be used to compute the elastic

critical stress.

$$f_{cr} = k\pi^2 E/[12(1-\mu^2)(w/t)^2] \qquad (50)$$

in which f_{cr} is the critical buckling stress, E is the modulus of elasticity,

t is the thickness of the plate, μ is the Poisson's ratio, w is the width of

the plate, and k is the buckling coefficient.

Figures 6 and 7, which are reproduced from Bulson's book (15), are graphic representations of the buckling coefficient for stiffened and unstiffened plate elements under uniformly distributed compressive stresses. It was found that for long plates, the values of k are 4.0 and 0.425 for stiffened and unstiffened elements, respectively.

In 1932, Von Karman (64) was the first investigator to study the effective width of a stiffened element. This width can be expressed by Eq. 51.

$$b = 1.9t\sqrt{E/F_y} \tag{51}$$

in which b is the effective width of the plate element, t is the thickness of the plate, and F_y is the yield point of the steel.

Based on his extensive investigation of cold-formed steel members, Winter (62), in 1947, indicated that Eq. 51 can be applied to a plate element in which the stress is below the yield point; therefore, this equation can be rewritten as:

$$b = Ct\sqrt{E/f_{max}} \tag{52}$$

in which f_{max} is the maximum edge stress of the plate and may be less than the yield point of the steel. The term C was determined experimentally by Winter and is expressed by the following equation:

$$C = 1.9[1-0.415(t/w)\sqrt{E/f_{max}}] \tag{52}$$

Consequently, the effective width of the stiffened element can be determined by Eq. 53.

$$b/w = \sqrt{f_{cr}/f_{max}} [1-0.22\sqrt{f_{cr}/f_{max}}] \tag{53}$$

The limiting ratio of w/t for the plate element below which the stiffened plate element is fully effective up to failure is given as shown in Eq. 54 (63).

$$(w/t)_{lim} = \pi\sqrt{0.038\,E/(1-\mu^2)}\ \sqrt{k/F_y} \tag{54}$$

By substituting E = 29,500 ksi and k = 4.0, Eq. 54 becomes

$$(w/t)_{lim} = 220.53/\sqrt{F_y} \tag{55}$$

For the case of unstiffened plate elements, the effective width can be expressed by the following equation (63):

$$b/w = 1.19\sqrt{f_{cr}/f_{max}}\ [1-0.3\sqrt{f_{cr}/f_{max}}]\,, \tag{56}$$

and the limiting value of the ratio, w/t, is determined by Eq. 57.

$$(w/t)_{lim} = 63.87/\sqrt{F_y} \tag{57}$$

(b) Effective Width of Plate Elements with Stiffeners

In the design of aircraft structures (61), the effective width of a plate element with stiffeners under compression has been calculated on the basis of the effective width formula presented by Eq. 52 in which the coefficient C is equal to 1.70 and 1.20 for the interior and end plate panels, respectively. The load-carrying capacity of the section composed of the effective area of the plate panel and the area of the stiffener can be determined on the basis of column design (61).

In cold-formed steel structures, stiffeners may be made of rolled or formed sheet sections. Their load-carrying capacities, which are based on the column design, may exceed the local buckling stress of plate elements of stiffeners, and as a result the stiffeners may fail by local buckling at a stress level lower than that of the yield point of the

stiffener material.

For hot-rolled sections or built-up members, Bleich (14) pointed out that the stiffeners are frequently welded or riveted to one side of the plate. This arrangement results in a considerable increase in the flexural rigidity of the stiffener, because the adjacent zones of the plate take part in the bending of the deflected shape. Therefore, in computing the moment of inertia of stiffener, a recommendation was made to include the effective section of the stiffener a strip of plate having a width equal to 30 times the web thickness in the computation of the moment of inertia about the axis through the centroid of the composite section.

In 1937, Chwalla (65) analyzed the effective width of the plate for the case of a flat bar stiffener welded to a plate subjected to shear stress. It was found that the rule given by Bleich (14) provides a conservative result.

E. Current Design Criteria

1. AISI Specification

The 1968 Edition of the AISI Specification (3) includes only the design provisions for unreinforced beam webs having an h/t ratio not greater than 150. There are no specific design criteria to cover the design of beam webs with transverse stiffeners subjected to bending, shear, and web crippling.

2. AISC Specification

(a) Beam Webs Subjected to Bending

Web buckling was taken into consideration in Section 1.10.6 of the current AISC Specification (18) by reducing the allowable stress in the compression flange of the reinforced beam webs. This section specifies that when $h/t > 760/\sqrt{F_b}$ the allowable stress in the compression flange

should not exceed

$$F_b' = F_b \left[1-0.0005 \frac{A_w}{A_f} \left(\frac{h}{t} - \frac{760}{\sqrt{F_b}}\right)\right] \qquad (58)$$

in which F_b = applied bending stress given in Section 1.5.1

of the AISC Specification (18)

A_w = full area of the web element

A_f = full area of the flange element.

(b) Beam Webs Subjected to Shear

The 1969 Edition of the AISC Specification (18) includes the following design criteria for webs with transverse stiffeners for hot-rolled shapes or welded plate girders subjected to shear stress. These design criteria are based on the research findings of Basler and others (16, 17,30).

i. Transverse stiffeners are required when the h/t ratio is more than 260 and the maximum shear stress f_v is more than that permitted by Formula (1.10-1) of the AISC Specification (18).

ii. The allowable shear stress of transversely reinforced beam webs is governed by the following formula:*

$$F_v = \frac{F_y}{2.89}\left[C_v + \frac{1-C_v}{1.15\sqrt{1+(a/h)^2}}\right] \leq 0.4 F_y \qquad (59)$$

in which $C_v = \tau_{cr}/\tau_y$
$= \frac{45,000k}{F_y(h/t)^2}$, when $C_v \leq 0.8$ \qquad (60)

---

*This formula is to be applied when $C_v < 1.0$ and when the ratio a/h does not exceed $[260/(h/t)]^2$ and 3.0.

$$= \frac{190}{h/t}\sqrt{\frac{k}{F_y}}, \text{ when } C_v > 0.8 \tag{61}$$

$$k = 4 + 5.34/(a/h)^2, \text{ when } a/h \leq 1.0$$

$$= 5.34 + 4/(a/h)^2, \text{ when } a/h > 1.0$$

iii. The spacing of intermediate stiffeners shall be such that the web shear stress will not exceed the value F_v given by Formulas (1.10-1) or (1.10-2), as applicable, and the ratio a/h shall not exceed $[260/(h/t)^2]$ nor 3. The spacing between the stiffeners at the end panels and the panels containing large holes shall be such that the smaller panel dimension, a or h, shall not exceed $348t/\sqrt{f_v}$, in which f_v is the actual shear stress in psi.

iv. The moment of inertia of a pair of intermediate stiffeners or a single intermediate stiffener with reference to an axis in the plane of the web shall not be less than $(h/50)^4$.

v. The gross area in square inches of intermediate stiffeners should not be less than that computed by the following equation:

$$A_{st} = \frac{1-C_v}{2}\left[a/h - \frac{(a/h)^2}{\sqrt{1+(a/h)^2}}\right]YDht \tag{62}$$

ı which C_v, a, h, and t have been previously defined

$Y = \dfrac{\text{yield stress of web material}}{\text{yield stress of stiffener material}}$

D = 1.0 for stiffeners furnished in pairs

= 1.8 for a single angle stiffener

= 2.4 for a single plate stiffener

vi. Intermediate stiffeners should be connected for a total

shear transfer, in kips per linear inch, either for a single

stiffener or a pair of stiffeners, if not less than that

computed by Eq. 63.

$$f_{vs} = h\sqrt{(F_y/340)^3} \qquad (63)$$

in which F_y is the yield stress of steel.

(c) Web Crippling Strength

Section 1.10.10.2 of the AISC Specification includes the following

design criteria for designing beam webs with transverse stiffeners

subjected to web crippling.

(1) Beam Webs Loaded Between Transverse Stiffeners

i. Webs of plate girders shall also be so proportioned or

stiffened that the sum of the compression stresses resulting

from the concentrated and distributed loads that bear

directly on or through a flange plate upon the compression

edge of the web plate and are not suppoted directly by the

bearing stiffeners, shall not exceed

$$[5.5+4/(a/h)^2] \frac{10,000}{(h/t)^2}, \text{ ksi} \qquad (64)$$

when the flange is restrained against rotation nor

$$[2+4/(a/h)^2] \frac{10,000}{(h/t)^2}, \text{ ksi} \qquad (65)$$

when the flange is not so restrained.

ii. These stresses shall be computed as follows: Concentrated
loads and loads distributed over a partial length of the panel
shall be divided by the product of the web thickness and either
the girder depth or the length of the panel in which the
load is placed, whichever is the lesser panel dimension. Any
other distributed loading in kips per linear inch of
length shall be divided by the web thickness.

(2) Beam Webs Loaded at the Location of Transverse Stiffeners

In the 1969 Edition of the AISC Specification (18), the design of the
stiffeners was based on the following limitations:

i. The bearing stiffeners shall be designed as columns sujected
to provisions of Section 1.5.1 on the assumption that
column section comprises the stiffeners and a centrally
located strip of the web whose width is either equal to not
more than 25 times its thickness at the interior stiffeners
or equal to not more than 12 times its thickness when
stiffeners are located at the ends of the web.

ii. In calculating the strength of the web-stiffener column as
described above, the effective length shall be taken as not
less than three-fourths of the length of the stiffeners in
computing the ratio ℓ/r.

iii. Only that portion of the stiffener outside of the flange

angle fillet or the flange-to-web welds shall be considered
effective in bearing.

3. AASHO Specification

    (a) Beam Webs Subjected to Bending

In the 1973 AASHTO Specification (66), the bending strength of rolled
shapes and plate girders is governed by the strength of the flange
provided that the transverse and longitudinal stiffeners are furnished
in accordance to Sections 1.7.72 and 1.7.73 of this specification. No
design provisions are included in the current AASHTO Specification to
predict the bending strength of beam webs governed by web buckling.

    (b) Beam Webs Subjected to Shear Stress

The 1973 Edition of the AASHTO Specification (66) includes the
following design provisions for transverse stiffeners to prevent
the shear buckling of the webs.

    i. Except as otherwise provided below, the webs of plate girders

        shall be stiffened at intervals that are not greater than the

        distance given by Eq. 66 but not greater than the clear

        unsupported depth of the web plate between flanges.

$$d = \frac{11,000t}{\sqrt{f_v}} \tag{66}$$

        in which t is the thickness of the web plate, in., and f_v

        is the average calculated unit shearing stress in the cross

        section of the web plate at the point considered, psi.

        The distance between stiffeners at the end parel of

        simply supported girders shall be one-half the value

        specified in Eq. 66.

ii. Transverse intermediate stiffeners may be omitted if the
web plate thickness is more than the thickness determined
by Eq. 67 or more than D/150.

$$t = \frac{D\sqrt{f_v}}{7,500} \qquad (67)$$

in which D = depth of the web, in in.; t and f_v are defined
in Eq. 66.

iii. The moment of inertia of any type of transverse stiffener
should not be less than

$$I_o = \frac{d_o t^3}{10.92} [25(D/d)^2 - 20] \qquad (68)$$

in which d and d_o are the required and the actual distances
between stiffeners, in.

(c) Beam Webs Subjected to Web Crippling

Section 1.7.74 of the 1973 AASHTO Specification (66) specifies the
following requirements to prevent web crippling:

i. Transverse stiffeners shall be provided over the end and
intermediate bearings of continuous welded or riveted
girders.

ii. These stiffeners shall be designed as a column that comprises
the stiffeners and a centrally located strip of the web
plate whose width is equal to not more than 18 times its
thickness.

iii. Only the portions of the stiffeners outside the flange-to-web

plate welds shall be considered effective in bearing.

iv. The thickness of the bearing stiffener plate shall not be less than

$$\frac{b'}{12}\sqrt{\frac{F_y}{33,000}} \qquad (69)$$

in which b' is the width of the stiffener, in., and F_y is the yield point of the stiffener material, psi.

v. The allowable compressive stress and the bearing pressure on the stiffeners shall not exceed the values permitted in Section 1.7.1 of the AASHTO Specification (66).

III. STRUCTURAL BEHAVIOR OF BEAM WEBS SUBJECTED TO BENDING

A. General

In the first phase of this portion of the research project, the bending

strength of cold-formed steel beam webs having h/t ratios less than or equal

to 200 were studied. Modified design formulas are proposed for the purpose

of evaluating the postbuckling strength and the effective web depth of

unreinforced beam webs under bending (5). In this part of the investiga-

tion, the moment capacity of reinforced beam webs with h/t ratios larger

than 200 was studied experimentally. The objective of the study was to

verify the above modified design formulas obtained from the test results of

beam specimens having web slenderness ratios greater than 200.

B. Analytical Study

The bending capacity of beam webs governed by the strength of

web elements is a function of the web slenderness ratio, the aspect ratio

of the web element, the bending stress ratio, the yield point of the material,

and the flat-width-to-thickness ratio of the compression flange. A study

of these parameters reveals that for beam members having web elements with

h/t ratios larger than

$$(h/t)_{lim} = 163.29 \sqrt{\frac{k}{F_y}} *$$
(70)

the web strength will govern the bending capacity of the beam. In Eq. 70,

k is the buckling coefficient for web elements subjected to bending. The

postbuckling strength of beam webs under bending increases as the ratios

---

*F_y is in kips per square inches

of h/t, f_c/f_t, and the yield point of the web material increase. In addition, the intereaction of the flanges and webs plays a significant role in the postbuckling strength of the web element. This is reflected by the ratio of $(w/t)/(w/t)_{lim}$, in which $(w/t)_{lim}$ is equal to $171\sqrt{f}$ as specified in Section 2.3.1.1 of the current AISI Specification (3,5).

Because the analytical study of the plate assemblies of cold-formed steel beam members is extremely complicated, an experimental investigation was conducted in this phase of the research to study the ultimate bending capacity of reinforced beam webs having h/t ratios larger than 200.

C. Experimental Investigation

The objective of the present investigation was to determine the postbuckling strength of reinforced beam webs having h/t ratios larger than 200 when they are subjected to bending stress. The experimental results were compared with the postbuckling strength formulas (5) that were developed previously for use in predicting the bending strength of the unreinforced beam webs with h/t ratios up to 250.

The strength of the beam webs under bending was studied with due consideration given to the slenderness ratio, the edge support conditions provided by varying the flat-width-to-thickness ratio of the flange, the aspect ratio of the web element, and the mechanical properties of the steel. The h/t ratios for the beam specimens used in the study vary from 200 to 325.

A total of 22 beam specimens were evaluated. Sixteen of them which were fabricated from channels and hat sections (Figs. 8 and 9), have been described by LaBoube and Yu (5). The remaining six beam members having h/t ratios from 200 to 325 were fabricated as shown in Fig. 8 and were tested in the Engineering Research Laboratory of the University of

gage length.

(b) Testing of Beam Specimens

All the beam specimens were tested in an 8-ft. wide, 9-ft. high and 21-ft. long loading frame, which is anchored to an 18-ft. wide and 60-ft. long test bay in the Engineering Research Laboratory (5).

i. Test Setup

Figure 11 shows the test setup,which provides a pure moment region in the central portion of the beam. Rollers and bracing plates were used at each end,and the beam was loaded by two concentrated loads by means of a cross beam (Fig. 11). An electric load cell was placed between the jack and the cross beam to measure the applied load. In addition, vertical rollers were positioned at both ends to prevent the beam from moving laterally and rotating. Bracings were also provided to the central portion of the beam specimens.

ii. Test Procedure

During each test, loads were applied in 1/4 kip increments from zero to 75% of the predicted theoretical buckling load. Then, smaller increments were used up to and beyond the predicted buckling load. For each increment of loading, the applied load and strain gage readings were recorded and printed out on tape by using a 40-channel data acquisition system (Fig. 12). In addition, lateral deformations of the central portion of one web were measured at the following applied loading conditions:

Initial loading

Actual observed buckling load

Predicted web buckling load

Failure load

The lateral deformations of the web were measured to the nearest one thousandth of an inch (0.001 in.) by using five linear potentiometers attached to a movable frame (Fig. 13). The readings of the potentiometers were also recorded on both printed and punched paper tapes by the data acquisition system. These tapes were used to evaluate the data by a data reduction system (Fig. 14).

For each applied load, the vertical deflection at midspan was recoreded by using two dial gages, one under each tension flange of the channel section.

3. Results of Tests

During the test, the following applied loads were obtained and recorded as applicable

$(P_{cr})^f_{test}$ - the critical load initiating flange buckling caused by bending stress

$(P_{cr})^W_{test}$ - the critical load initiating web buckling caused by bending stress

$(P_y)_{test}$ - the load in which the bending stress in the extreme fibers of the flange reached the yield point

$(P_u)_{test}$ - the maximum failure load for the beam specimen

The experimental data are given in Table 8.

4. Evaluation of Test Data

The theoretical buckling loads of the web and the flange, $(P_{cr})^W_{theo}$ and $(P_{cr})^f_{theo}$, given in Table 9 were computed from Eqs. 71 and 72 respectively.

$$f_{cr} = k\pi^2 E / [12(1-\mu^2)(h/t)^2] \tag{71}$$

$$f_{cr} = k\pi^2 E / [12(1-\mu^2)(w/t)^2] \tag{72}$$

In the above equations, k = buckling coefficient, E = 29,500 ksi, μ = 0.3, h/t = depth-thickness ratio of beam web, w/t = flat-width-to-thickness ratio of the compression flange.

The buckling coefficient, k, was assumed to be a constant value of 4.0 for evaluating the theoretical flange buckling load, $(P_{cr})^f_{theo}$. For calculating the web buckling load, $(P_{cr})^W_{theo}$, the value of k is given by Eq. 73

$$k = 4 + 2(1+\beta)^3 + 2(1+\beta) \tag{73}$$

in which $\beta = |f_t/f_c|$ = bending stress ratio.

With the critical stress, f_{cr}, the theoretical buckling loads, $(P_{cr})^W_{theo}$ and $(P_{cr})^f_{theo}$, were calculated by using Eq. 74

$$(P_{cr})_{theo} = \frac{2S_x f_{cr}}{\ell} \tag{74}$$

in which f_{cr} is the appropriate critical buckling stress, S_x is the section

modulus of the effective area of beam section determined on the basis of

the applicable value of f_{cr}, and ℓ is the distance between the end support

and the concentrated load applied to the beam specimen.

Table 9 also lists the theoretical yield load, $(P_y)_{theo}$, for each

test specimen. This value was computed by using Eq. 75

$$(P_y)_{theo} = \frac{2S_x F_y}{\ell} \tag{75}$$

in which S_x is the section modulus of the effective area of the beam specimen

determined on the basis of the yield point of steel, F_y.

In addition, the ultimate bending strengths of 22 beam specimens were

computed on the basis of the postbuckling strength formula as indicated

by Eq. 76 . These values are listed in Table 10.

$$(M_u)_{cr} = \Phi S_x f_{cr} \tag{76}$$

in which Φ , S_x, and f_{cr} are defined in Eq. 3.

The experimental results obtained from the 22 test specimens have been

carefully studied. The following topics are discussed in the subsequent

sections: (a) failure mode, (b) comparison of the experimental and

theoretical buckling loads and yield loads, (c) postbuckling strength of

webs subjected to bending stress, (d) comparison of the experimental and

predicted ultimate bending strength.

(a) Failure Modes

Different failure modes were observed in this study. Tbble 8 gives the

types of failure mode for each beam specimen. It is to be noted that except

for the hat sections, all the remaining channel section beam specimens

failed by web buckling. This can be explained by the use of large values of the h/t ratios in this series of tests. The hat section specimens failed by flange buckling followed by web buckling and flange yielding. It seems that for the hat sections, stresses in the flange and in the web were redistributed before the flange yielded.

Figures 15 and 16 are photographs of the failure modes, and Figs. 17 to 20 are typical profiles of the deformed webs under different loading conditions.

(b) Comparison of the Experimental and Theoretical Buckling Loads and Yield Loads

A comparison of the experimental and theoretical flange buckling load for each beam specimen is presented in Table 9. A review of this table reveals that the values of $(P_{cr})^f_{test}/(P_{cr})^f_{theo}$ for the hat sections vary from 0.938 to 1.473 and have a mean value of 1.145. This indicates that the theoretical buckling stress of the flanges is in fairly good agreement with the tested values.

Comparisons were made for the experimental and theoretical web buckling loads. Table 9 lists the ratios of $(P_{cr})^w_{test}/(P_{cr})^w_{theo}$ which vary from 0.415 to 1.201 and have a mean value of 0.741. The large variation of the ratios of $(P_{cr})^w_{test}/(P_{cr})^w_{theo}$ indicates the difficulty in determining the buckling load experimentally. In addition the premature buckling may have been the result of using deep flexible webs with initial imperfections in the thin webs.

It was also noted in this series of tests that only three specimens (MB-19-1, MB-19-2, and MB-20-1) reached the yielding stress on the compression flange. However, the ratios of $(P_y)_{test}/(P_y)_{theo}$ are 0.728, 0.691, and 0.598 respectively. This premature yielding can be explained by the redistribution of stress for deep flexible webs.

(c) Postbuckling Strength of Webs Subjected to Bending Stress

Table 9 lists the ratio of $(P_u)_{test}/(P_{cr})_{theo}$ for each of the 22

beam specimens. This ratio represents the postbuckling strength of each

web under bending stress. A review of the ratio of $(P_u)_{test}/(P_{cr})_{theo}$ indi-

cates that the postbuckling strength of beam webs subjected to bending is a

function of the h/t ratio of the web, the w/t ratio of the compression

flange, the bending stress ratio, and the yield point of the material. Table

9 also reveals that the ratio of $(P_u)_{test}/(P_{cr})_{theo}$ vary from 1.599 to

4.528. Therefore, it can be concluded that the beam webs provides very

conservative results for predicting the ultimate bending capacity of

cold-formed steel beam members.

(d) Comparison of the Experimental and Predicted Ultimate

Bending Strength

The ultimate bending strengths of the beam webs, $(M_u)_{cr}$, as computed

on the basis of the postbuckling equation (Eq. 76) are listed in Table 10.

This table also contains the ratio of $(M_u)_{test}/(M_u)_{comp}$ which indicate

the accuracy of the predicted equation (Eq. 76). A study of Table 10

shows that the ratio of $(M_u)_{test}/(M_u)_{comp}$ vary from 0.842 to 1.136 and

have an average value of 1.001 and a standard deviation of 0.072. All the

computed values are within $\pm 20\%$ of the tested values. Based on the above

discussions, it seems that the postbuckling equation (Eq. 76) ,

which is derived from the experimental data for the beam webs having h/t

ratios ranging from 77 to 250 can also be used to predict the ultimate

bending capacity for reinforced beam webs with h/t ratios ranging from 250

to 325.

D. Summary and Design Recommendations

1. Summary

In order to study the bending capacity of cold-formed steel beam webs

having h/t ratios greater than 200 and to develop the additional design criteria as necessary, an experimental investigation was conducted. Twenty-two specimens were tested, and from the results that are presented in this report, the following conclusions can be drawn:

(a) For beam webs having h/t > 200, the buckling strength of the web elements should not be used in predicting the ultimate bending capacity of cold-formed steel beam members.

(b) The buckling stress of the compression flange can be adequately predicted by the theoretical equation with k = 4.0.

(c) The postbuckling strength of beam webs subjected to bending stress is a function of the h/t ratio, the bending stress ratio, the w/t ratio of the compression flange, and the yield point of the material.

(d) The postbuckling strength formula expressed by Eq. 76 can be used to predict the ultimate bending capacity of beam webs with h/t ratios ranging from 200 to 325.

2. Design Recommendations

Based on the findings of these experiments, the following design recommendations are submitted for consideration:

For beam webs having h/t > 200, the compressive stress in a flat web that results from bending in its plane* shall not be exceeded either by F or ΦF_{bw} where

$$F = \text{basic design stress} = 0.60 F_y$$

$$F_{bw} = \frac{16000 k}{(h/t)^2} \tag{77}$$

$$\Phi = \alpha_1 \alpha_2 \alpha_3 \alpha_4 \tag{78}$$

---

*The compressive stress in the web is computed from the section modulus, S_x, based on the effective flange area of the beam section determined on the basis of F_{bw} or F, whichever is smaller.

$$\alpha_1 = 0.017(h/t) - 0.790 \tag{79}$$

$$\alpha_2 = 0.462/\beta + 0.538 \tag{80}$$

$$\alpha_3 = 1.16 - 0.16(w/t/(w/t)_{lim}), \text{ when}$$

$$w/t/(w/t)_{lim} \leq 2.25$$

$$= 0.8, \text{ when } w/t/(w/t)_{lim} > 2.25 \tag{81}$$

$$\alpha_4 = 0.561(F_y/33) + 0.100 \tag{82}$$

$$k = 4 + 2(1+\beta)^3 + 2(1+\beta) \tag{83}$$

$$\beta = |f_t/f_c| \tag{84}$$

Equation 77 was derived from Eq. 1 by using a safety factor of 5/3.

IV. STUDY OF BEAM WEBS SUBJECTED TO
SHEAR STRESS

A. General

The shear strength of stiffened beam webs of hot-rolled shapes and welded plate girders has been studied by many investigators (16,30). Their research findings have been instrumental in having the design criteria included in the current AISC Specification (18), but for cold-formed steel members, little work has been done in the study of the structural behavior of beam webs with transverse stiffeners subjected to shear stress. For this reason, an analytical and experimental examination of the shear strength of cold-formed steel beam webs was undertaken under the sponsorship of American Iron and Steel Institute. The objective of the this study was to determine the buckling and postbuckling strength of beam webs with transverse stiffeners when the webs were subjected primarily to shear stress.

B. Analytical Study

The strength of a transversely reinforced beam web subjected to shear stress is a function of the depth-to-thickness ratio of the web, the support conditions along its edges, the aspect ratio of the web element, the mechanical properties of the material, and the web's initial imperfections.

A study of the different shear models presented in the literature survey (Table 2) reveals that the so-called true Basler's theory may be used to predict the shear strength of reinforced cold-formed steel beam webs, because the flexural rigidity of the flanges of such beams can be neglected. The ultimate shear stress, then, can be computed by using Eq. 24. However, because the shear strength of reinforced, cold-formed steel beam webs has not been extensively investigated, an experimental study was conducted in

the initial phase of the research to verify the application of the

true Basler's theory and to develop new design criteria for the

reinforced beam webs when they are subjected to shear stress.

C. Experimental Investigation

The objective of the experimental investigation was to determine the

strength of reinforced webs subjected primarily to shear. In the study,

consideration was given to the slenderness ratio of the web, the aspect

ratio of the web element, the flange width-to-thickness ratio, which

reflects the boundary conditions along the edges, and the mechanical

properties of the web material.

The experimental results were compared with the theoretical equation

based on the true Basler's theory for predicting the postbuckling shear

strength of beam webs with transverse stiffeners.

A total of 32 beam specimens were tested. They were

fabricated as shown in Figs. 8 and 21. All of the tests were conducted

in the Engineering Research Laboratory of the University of Missouri-

Rolla.

The following discussions deal with (1) preparation of the beam specimens,

(2) testing of the beam specimens (3) results of the tests, and (4) evaluation

of the test data.

1. Preparation of the Beam Specimens

Beam specimens , which were built up by combining two channel sections,

were used to investigate the ultimate shear strength of reinforced beam webs

subjected to shear stress. As shown in Figs. 8 and 21, the channels were

braced by 1 x 1 x 1/8 in. angles at both the compression and tension flanges.

Table 11 gives the cross-sectional dimensions for all the test specimens.

The transverse stiffeners were connected to the beam webs by using 3/4 in.

diameter bolts. In the case of intermediate stiffeners, the distance between two bolts was close enough to resist the shearing force caused by the veritical component of the tension field stress. For bearing stiffeners used at supports or the locations of applied loads, the number of bolts required should be such that they can sustain the shearing force between stiffeners and the web elements. When additional steel plates were used to stiffen the flanges, they were connected to the flanges by Epoxy 907 at the location of the concentrated loads and at supports so that the bearing plate could be in full contact with the surface of the additional cover plate and the transverse stiffeners (Figs. 22-26).

In order to prevent premature failure induced by web buckling at the locations of maximum moment of the beam specimens (Fig. 27), additional cover plates (Table 12) and small side channels (Table 12 and Fig. 28) were provided. Self-tapping screws (12-14 x 3/4 in. Tek No. 3 fasteners) were used to attach the side channels to the beam webs as well as the additional cover plates to the flanges. In addition lateral braces were provided to prevent the beam specimens from buckling laterally. The intervals between the braces were designed in accordance with the lateral buckling criteria of each individual channel. The dimensions and applicable design parameters of all the specimens are given in Table 13.

In order to ensure that the stiffeners would function properly to resist the vertical component of the load developed from the tension field stress, intermediate and bearing stiffeners were fabricated from both hot-rolled angles and small cold-formed steel U shapes. Figures 29 and 30 show the dimensions of these stiffeners. The yield point and the span length of each specimen are listed in Table 13.

In an attempt to check the critical shear buckling stress experimentally, foil strain gages were mounted on the beam webs as shown in Figs. 31 and 32 for different test setups. Strain gages were also mounted on the compression and tension flanges (Figs. 31 and 32) to determine the bending stress of of the beam specimens.

In addition to the use of strain gages, grid lines at 1/2 in. intervals were plotted on the opposite sides of each beam web. They were used for recording the buckling pattern and for measuring the profile of the deformed web . All measurements were recorded and printed on tape by a 40 channel data acquisition system (Fig. 12).

2. Testing of Specimens

(a) Tensile Coupon Tests

The mechanical properties of the steel used for the beam specimens were established by standard tensile coupon tests. All the coupons were prepared in accordance with ASTM E8 and tested in a 150,000-lb. Tinius Olson universal testing machine. Table 7 lists the test data on yield point, ultimate tensile strength, and elongation measured from a 2-in. gage length.

(b) Testing of Beam Specimens

All the beam specimens were tested in the 8-ft. wide, 9-ft. high and 21-ft. long loading frame, which is anchored to the 18-ft. wide and 60-ft. long test bay in the Engineering Research Laboratory.

i. Test Setup

Four different types of test setups were used in this part of the experimental investigation. For test Setup-A, the beam specimen was loaded by a concentrated load at the midspan (Fig. 22); for test Setup-B, C, and D, the concentrated loads were applied to the beam specimens by means of a cross

I-beam as shown in Figs. 23, 24 and 25, respectively.

Each beam specimen was tested with simply supported
conditions by using rollers and bearing plates at the supports
and at the location of the applied concentrated load.
The load was applied by means of a hydraulic jack. An
electric load cell was placed between the jack and the
bearing plate (Test Setup-A) or between the jack and the
cross I-beam (Test Setup-B, C and D) for the purpose of
measuring the applied load.

Test Setup-A as shown in Fig. 22 was used for 11 test
specimens in which two adjacent shear panels are bounded
by bearing stiffeners. In order to study the effect of
the intermediate stiffeners upon the shear strength of
reinforced beam webs, Test Setup-B was used for the next
16 beam specimens. In addition, in order to investigate
the effect of a warping or buckling restraint on the for-
mation of shear buckling for the specimens using Test
Setup-A, two additional tests were conducted by using Test
Setup-C as shown in Fig. 24. These specimens have a large
central panel to separate two end shear panels. Finally,
Test Setup-D was used for beam specimens having large
aspect ratios ($\alpha=3.0$) as indicated in Fig. 25.

In order to prevent the beam specimen from moving
laterally, braces were also provided as shown in Fig. 26.

The moment and shear diagrams for different loading
systems are given in Fig. 27.

11. Test Procedure

During each test, loads were applied in one-kip increments

from zero to approximately 75% of the predicted theoretical

buckling load. Then smaller increments were used before and

after the predicted buckling load. For each increment of

loading, the applied jack load and strain gage readings were

recorded and printed out on tape by using a 40-channel data

acquisition system (Fig. 12). In addition, lateral

displacements of one web were measured at several selected

applied loads, which included the following loading

conditions:

Initial loading

Observed shear buckling load

Predicted shear buckling load

Failure load

The lateral deformations of the web were measured to

the nearest one thousandth of an inch (0.001 in.) by using

five linear potentiometers attached to a movable frame

(Fig. 13). Results of the pilot tests indicated that the

accuracy of the lateral displacement measurement apparatus

was such that repeatability of the readings was assured.

The readings of the potentiometers were also recorded and

printed out on tape by the data acquisition system (Fig. 12).

3. Results of Tests

For each test specimen, the following applied jack loads were obtained

and recorded:

$(P_{cr})_{test}$ – the critical load initiating web buckling caused

by shear stress

$(P_u)_{test}$ – the maximum failure load for the beam specimen

The experimental loads and their corresponding shear forces for all beam specimens are given in Table 14. Also listed in this table are the values of maximum bending moment, $(M')_{test}$, which were computed from $(P_u)_{test}$.

The critical buckling load, $(P_{cr})_{test}$, was determined by using a strain-reversal method in which the load-strain curve was plotted for every pair of strain gages mounted inside and outside of the web element. The critical load, P_{cr}, was taken as the compressive load corresponding to the maxomum strain on the load-strain curve of the strain gage mounted on the convex side of the buckled web element. Fig.33 illustrates a typical load-strain diagram.

The shear stress corresponding to the critical buckling load was computed by the average stress method, i.e.,

$$(\tau_{cr})_{test} = \frac{(V_{cr})_{test}}{A_w} = \frac{(V_{cr})_{test}}{2ht} \tag{85}$$

in which $(V_{cr})_{test}$ is the tested shear force at the initiation of web buckling, A_w represents the area of the beam webs, h is the clear distance between the flanges, and t is the thickness of an individual beam web. Table 14 lists the value of $(\tau_{cr})_{test}$ for every beam specimen.

The experimentally determined ultimate shear stress corresponding to the failure load, $(P_u)_{test}$, was computed on the basis of two different methods: the average stress method and the exact method.

The average shear stress due to the failure load, τ_{ave}^{fail}, was evaluated by using Eq. 86.

$$\tau_{ave}^{fail} = \frac{(V_u)_{test}}{A_w} = \frac{(V_u)_{test}}{2ht} \tag{86}$$

in which $(V_u)_{test}$ is the tested maximum shear force of the beam specimen.

In the exact method, the experimental shear stress at failure, τ^{fail}_{exact}, was determined by the following basic equation of strength of material:

$$\tau^{fail}_{exact} = \frac{(V_u)_{test} Q}{It} \qquad (87)$$

in which

$(V_u)_{test}$ = tested external shear force of the section in question

Q = statical moment of that portion of the section lying above or below the line on which τ is desired, taken about the neutral axis

I = moment of inertia of the full area of the section about the neutral axis

t = width of the section where shear stress is desired.

The maximum shear stresses computed on the basis of Eqs. 86 and 87 are given in Table 14. Also listed in this table is the ratio of $\tau^{fail}_{exact}/\tau^{fail}_{ave}$, which indicates that this ratio varies from 1.014 to 1.221. It should be noted that the maximum shear stress determined by Eq. 87 occurs at the neutral axis of the cross section, whereas, the shear stress calculated on the basis of Eq. 86 is a constant value across the beam section (Fig. 34). The above mentioned tested results were used to verify the following theoretical values.

The theoretical critical shear buckling stresses, τ_{cr}, were calculated by Eq. 11 for sharp yielding steels and by Eq. 18 for gradual yielding steel. In the application of Eq. 18, the value of τ_{cr} was determined for the actual tested value of $\tau_{pr} = 0.69\tau_y$ (6). The theoretical ultimate

shear stresses, τ_u, were determined on the basis of the incomplete

tension field action (Eq. 24). These theoretical values are also

given in Table 14.

The ultimate moment resisting capacities of the beam specimens were

determined as follows:

The bending moments of the sections governed by the strength of

flanges, M_y, were computed by using Eq. 88 and are listed in Table 15.

$$M_y = S_x' F_y \tag{88}$$

in which S_x' is the section modulus for the beam specimen based on a conside-

ration of either the shear lag or the effective width, whichever is smaller.

The bending moments of the sections governed by the bending strength

of the webs, $(M_u)_{cr}$, were evaluated on the basis of the postbuckling

strength of the web (5) as shown in Eq. 89.

$$(M_u)_{cr} = S_x f_{cr} \phi \tag{89}$$

in which S_x = section modulus based on the effective width of

the compression flange and full widths of the

tension flange and web, in.^{3}

f_{cr} = critical buckling stress in webs subjected to

bending, ksi

$$= \frac{k\pi^2 E}{12(1-\mu^2)(h/t)^2}$$

k = buckling coefficient = $4 + 2(1+\beta)^3 + 2(1+\beta)$

$$\beta = |f_t / f_c|$$

f_c = maximum compressive bending stress in web, ksi

f_t = maximum tensile stress in web, ksi

E = modulus of elasticity = 29.5×10^3 ksi

μ = Poisson's ratio = 0.3

h/t = web slenderness ratio or depth to thickness ratio of the web

Φ = postbuckling strength factor of the web (5)

$$= \alpha_1 \alpha_2 \alpha_3 \alpha_4$$

α_1 = 0.017(h/t) − 0.790

α_2 = 0.462(f_c/f_t) + 0.538

α_3 = 1.16 − 0.16(w/t)/(w/t)$_{lim}$ $\leq$ 1.0, when

$\quad$ (w/t)/(w/t)$_{lim}$ $\leq$ 2.25

$\quad$ = 0.8, when (w/t)/(w/t)$_{lim}$ > 2.25

α_4 = 0.561 (F_y/33) + 0.10

(w/t)$_{lim}$ = 171/$\sqrt{f}$, according to Section 2.3.1.1 of the AISI Specification

f = actual stress in the compression flange computed on the basis of the effective design width, ksi.

The ultimate bending capacity of the beam specimens, $(M_u)_{comp}$, is the

smaller value of M_y or $(M_u)_{cr}$ computed by Eqs. 88 and 89. Table 15 lists the values of M_y, $(M_u)_{cr}$, and $(M_u)_{comp}$ for 32 beam specimens.

4. Evaluation of Test Data

The results of 32 shear tests have been carefully reviewed and evaluated. The following topics are discussed in detail : (a) failure modes, (b) comparison of the experimental and theoretical shear buckling stresses, (c) postbuckling strength of transversely reinforced beam webs subjected to shear stress, (d) comparison of the experimental and theoretical ultimate shear stresses based on the incomplete tension field theory.

(a) Failure Modes

The typical failure modes for reinforeced beam webs in shear are shown in Figs. 35 and 36,which indicate that the beam specimens failed by a profound tension field action that anchored with the transverse stiffeners and no plastic hinges were formed in the flanges between two transverse stiffeners. However, it was believed that premature failure by combined bending and shear was observed in three beam specimens (S-3-1, S-3-2, and S-3-5) as a result of the insufficient bending capacity caused by shear lag of small span length specimens. To study this behavior, two additional specimens (S-3-6, S-3-7), which had additional cover plates added to both tension and compression flanges were tested. Based on the test results of these specimens (Table 14), it seems that the bending moment has little effect upon the shear capacity of the reinforced beam webs (S-3-5, S-3-6, S-3-7).

To study the effect of the intermediate stiffeners, four specimens (S-2-1, S-2-2, S-2-3 and S-2-4) were tested. Test Setup-A was used for specimens S-2-1 and S-2-2 with bearing stiffeners and the specimens

S-2-3 and S-2-4 were tested by using Test Setup-B with cold-formed steel intermediate stiffeners (Fig. 23). These stiffeners were designed so that their moment of inertia and cross section could be satisfied by Eqs. 33 and 35. From the results of the tests (Table 14), it can be seen that the cold-formed steel intermediate stiffeners perform properly in developing the tension field stress.

Specimens Nos. S-3-3 and S-3-4 were tested by using Test Setup-C to investigate the warping or buckling restraint occasioned by the symmetry of Test Setup-A, which was used for specimens S-3-1 and S-3-2. The failure loads, $(P_u)_{test}$, of specimens S-3-3 and S-3-4 were compared with those of S-3-1 and S-3-2 as given in Table 14. From the test results, it can be seen that there is no restraining effect resulting from the symmetry of the test setup.

Figures 37 to 41 illustrate the typical profiles of the deformed webs at five different locations on the web panel.

(b)   Comparison of Experimental and Theoretical Shear Buckling

Stress

The experimental buckling loads, $(P_{cr})_{test}$, were determined by using a strain reversal method. This was done by applying a pair of strain gages to both sides of the web element in the direction perpendicular to the tension field of the web panel (Figs. 31 and 32). The experimental shear buckling stresses, $(\tau_{cr})_{test}$, were then computed by using Eq. 85 and are listed in Table 16.

For specimens tested with Test Setup-A, only one pair of strain gages was used at the center of the web panel (Fig. 31). Figure 42 shows a typical load-strain curve for beam S-4-1 in which the value of $(P_{cr})_{test}$ was found to be 7.51 kips.

It was found in some of the above mentioned specimens that the buckled shape was not located at the center-line of the web. As a result, more than one pair of strain gages was needed to record the deformations of buckling. Therefore, for the remaining specimens (Test Setup-B, C ,and D) ,three pairs of strain gages were used. Figures 43, 44 and 45 show three typical load-strain curves for beam S-5-1. The buckling loads were found to be identical for these three pairs, and the value was 13.04 kips.

The computed values of the ratio $(\tau_{cr})_{test}/\tau_{cr}$ are listed in Table 16. This ratio is an indication of the relationship between the experimental and theoretical buckling stresses. The values of $(\tau_{cr})_{test}/\tau_{cr}$ range from 0.660 to 1.240 and have an average of 0.872. In most of the specimens, the experimental buckling loads were found to be less than the theoretical buckling loads. The premature buckling observed from the tests may be caused by initial imperfections in the thin-walled cold-formed beam webs.

On the basis of the above discussion and as a result of the nature of the buckling pattern, it was difficult to determine the exact shear buckling loads. However, with an average value of 0.872 for the ratio of $(\tau_{cr})_{test}/\tau_{cr}$, the test results provide a reasonable indication of the buckling behavior of the beam webs subjected to shear stress.

(c) Postbuckling Strength of Transversely Reinforced Beam Webs Subjected to Shear

The postbuckling strength of webs is represented by the ratio of $\tau_{ave}^{fail}/\tau_{cr}$ which is given in Table 16 for 32 beam specimens. The ratios range from 1.357 (Specimen S-1-2) to 4.869 (Specimen S-9-2) and have an average value of 2.169.

A study of the test results indicates that the postbuckling strength depends on the web slenderness ratio, the aspect ratio of the web panel, and the yield point of of the material.

In order to evaluate the effect of the flange on the postbuckling strength, four specimens were tested (S-2-1, S-2-3, S-4-1, and S-4-2). The dimensions of these specimens are practically identical except that the widths of the flanges are different. Based on the test data given in Table 16, it can be seen that the flanges had little or no effect on the postbuckling strength of the transversely reinforced beam webs.

(d) Comparison of the Experimental and Theoretical Ultimate

Shear Stresses Based on the Incomplete Tension Field Theory

In an attempt to verify the true Basler's formula for cold-formed steel reinforced beam webs subjected to shear stress, the ratio of τ_{ave}^{fail}/τ_u was established (Table 16). This ratio is an indication of the relationship between the experimental and theoretical ultimate shear stresses. As given in Table 16, the ratio of τ_{ave}^{fail}/τ_u vary from 0.991 to 1.212 and have an average value of 1.116 and a standard deviation of 0.055.

Also tabulated in Table 16 are the ratios of $\tau_{exact}^{fail}/\tau_y$ and τ_{ave}^{fail}/τ_y. The former ranges from 0.542 to 0.897, whereas the latter varies from 0.542 to 0.792. These values indicate that for the beam webs with the h/t ratios larger than 150, the beam specimens cannot develop shear yielding. For specimens with small h/t ratios, LaBoube and Yu (6) reported that shear yielding does occur, because the critical buckling stress in shear exceeds the shear yield point of the material.

D. Summary and Design Recommendations

1. Summary

In order to study the structural behavior of transversely reinforced

beam webs subjected to shear stress, a total of 32 beam tests were conducted. Based on the test results, the following conclusions can be drawn:

(a) The elementary beam theory based on shear buckling cannot be used to predict the shear strength of transversely reinforced beam webs, because a considerable amount of postbuckling strength is developed.

(b) Although the exact buckling load for beam webs is difficult to obtain from tests, the use of the strain-reversal method provides a fairly good correlation between the experimental and theoretical shear buckling loads for beam webs with transverse stiffeners.

(c) The postbuckling strength of reinforced beam webs under shear is a function of the web slenderness ratio, the aspect ratio of the web panel, and the yield point of the web material.

(d) The compactness of the flanges of the cold-formed steel beam specimens has little or no effect on the ultimate shear capacity.

(e) The true Basler's formula based on incomplete tension field action provides a good prediction of the ultimate shear capacity of cold-formed steel beam webs.

(f) The proportional limit for cold-formed steel is generally less than that for hot-rolled steel; a proposed value of $0.7\tau_y$ may be used for inelastic shear buckling.

(g) For intermediate stiffeners, if the requirements given in Eqs. 33 and 34 are met, the ultimate shear capacity can be fully developed.

2. Design Recommendations

The postbuckling strength of reinforced beam webs with transverse stiffeners subjected to shear stress has been noted in this investigation. The following design recommendations which incorporate a factor of safety equal to 1.67 are submitted for consideration:

i. For reinforced beam webs with transverse stiffeners, the average shear stress, f_v, in kips per square inch, shall not exceed the value given by Formula 90

$$F_v = \frac{F_y}{2.89}[C_v + \frac{1-C_v}{1.15(\sqrt{1+(a/h)^2}+a/h)}] \leq 0.4F_y \qquad (90)$$

in which $\qquad C_v = \frac{46180k}{F_y(h/t)^2}$, when C_v is less than 0.7

$$= \frac{180}{(h/t)}\sqrt{\frac{k}{F_y}}, \text{ when } C_v \text{ is more than } 0.7$$

$k = 4.00 + \frac{5.34}{(a/h)^2}$, when a/h is less than 1.0

$$= 5.34 + \frac{4}{(a/h)^2}, \text{ when a/h is more than } 1.0$$

t = thickness of the web, in.

a = distance between transverse stiffeners, in.

h = clear distance between flanges, in.

ii. The moment of inertia of a pair of intermediate stiffeners

or a single intermediate stiffener with reference to the

axis in the plane of the web, shall not be less than the

value given by Eq. 91 below

$$I_s = 5 ht^3 (h/a - 0.7a/h) \qquad (91)$$

iii. The required cross sectional area of intermediate stiffeners

is evaluated by using Eq. 34. For the sake of uniformity

between AISC and AISI Specifications, the same correction

factors for eccentricity used in the AISC Specification are

recommended.

The gross area in square inches of intermediate

stiffeners shall not be less than that computed by Eq. 92.

$$A_{st} = \frac{1-C_v}{2} [\frac{a}{h} - \frac{(a/h)^2}{\sqrt{1+(a/h)^2}+a/h}] YDht \qquad (92)$$

in which C_v, a, h, and t are defined in Item i.

$$Y = \frac{\text{yield stress of web steel}}{\text{yield stress of stiffener steel}}$$

D = 1.0 for stiffeners furnished in pairs

= 1.8 for single angle or channel stiffeners

= 2.4 for single plate stiffeners

iv. The transverse stiffeners are not required when the h/t ratio

is less than 200 and the average shear stress is less than

59

that permitted by Eqs. 93 or 94.

$$F_v = 15,965 \frac{k}{(h/t)^2}, \text{ for } C_v < 0.7 \tag{93}$$

$$F_v = 62.2 \frac{\sqrt{kF_y}}{(h/t)} \leq 0.4F_y, \text{ for } C_v > 0.7 \tag{94}$$

The notations used in these formulas were defined in Item i.

It should be noted that in Eq. 90, the value of $C_v = 46,180 \ k/[F_y(h/t)^2]$ is based the theoretical shear buckling stress in the elastic range and $E = 29,500$ ksi. The value of $C_v = 180\sqrt{k/F_y}/(h/t)$ is based on an assumption that $\tau_p = 0.7 \ \tau_y$. For the sake of uniformity between the AISC and AISI Specifications, the following AISC values may be used:

$$C_v = 45,000 \ k/[F_y(h/t)^2], \text{ when } C_v \text{ is less than } 0.8$$

$$C_v = 180\sqrt{k/F_y}/(h/t), \text{ when } C_v \text{ is more than } 0.8$$

For the same reason, the following allowable shear stresses proposed in Ref. 6 may be used in lieu of Eqs. 93 and 94:

$$F_v = 15,550 \frac{k}{(h/t)^2}, \text{ for } C_v < 0.8$$

$$F_v = 65.7 \frac{\sqrt{kF_y}}{(h/t)} \leq 0.40 \ F_y, \text{ for } C_v > 0.8$$

In Eq. 91, the required moment of inertia for intermediate stiffeners, I_s, is based on Eq. 33 and a factor of safety of 2.0.

V. STUDY OF WEB CRIPPLING STRENGTH
OF TRANSVERSELY REINFORCED BEAM WEBS

V.1. Beam Webs Loaded Between Transverse Stiffeners

A. General

The web crippling strengths of cold-formed steel unreinforced beam webs having h/t ratios less than 150 have been studied previously at Cornell University by Winter and Zetlin (49,50). In the first phase of the present research project, this problem was also studied at the University of Missouri-Rolla (9,10) for possible extension of the h/t ratio of the beam webs up to 200.

In the case of beam webs having h/t ratios larger than 200, the web may buckle in the flexural mode before it fails through localized crippling. For this reason, transverse stiffeners may be used to prevent premature failure occasioned by web buckling.

Since the web crippling strength of reinforced cold-formed steel beam webs has not been fully investigated, the purpose of this study has been to determine the web crippling loads of cold-formed steel beam webs when they are loaded between transverse stiffeners.

B. Analytical Study

This section deals with the analytical study of plates and beam web elements when they are subjected to one-flange and two-flange web crippling loads.

1. Buckling Behavior of Plates

    (a) One-Flange Loading

An analytical study of the buckling strength of thin flat plates with one-flange partial edge loading has been conducted by Khan et al. (59), who defined the critical load by using Eq. 41. In this equation, K is the buckling

coefficient,which is a function of two parameters α and β, in which $\alpha = a/h$, and β is the larger value of N/a and N/h (Fig.46(a)).

Based on the data tabulated in Table 3 for the value of K and by using a Statstical Analysis System, SAS-76 (67), the following two formulas have been derived in the present study to compute the buckling coefficient for simply supported plates subjected to partial edge loading on one edge with any combinations of α and β.

$$K = (2.04+1.52/\alpha^3)(1.0+0.48\beta^2); \quad \text{for } \alpha > 1.0 \tag{95}$$

$$K = (5.59-2.62\alpha+0.54/\alpha^2)(1.0+0.48\beta^2); \quad \text{for } \alpha \leq 1.0 \tag{96}$$

Table 17 gives the values of K_{comp}, which is based on Eqs. 95 and 96, and the ratio of K_{theo}/K_{comp} in which K_{theo} is the buckling coefficient obtained by Khan et al. (Table 3). The ratios of K_{theo}/K_{comp} have a mean value of 0.998 and a standard deviation of 0.038, which indicates that Eqs. 95 and 96 provide a good prediction of the buckling coefficient.

(b) Two-Flange Loading

The buckling problem of plates under locally distributed loads applied on two opposite edges has been studied by Yamaki (46). In his study, the energy method was used to obtain the critical buckling load of the form as given by Eq. 39.

It should be noted that Yamaki studied only the buckling strength of a plate for which the aspect ratio, a/h, is greater than 0.8. The buckling behavior of a plate with an aspect ratio smaller than 0.8 has not been investigated. Therefore, the following discussion deals with a solution for the buckling load of a rectangular plate under a uniformly distributed

load applied to two opposite edges for an aspect ratio ranging from 0.2 to 3.0.

The energy method used by Yamaki (46) has been further developed in this analysis,and the buckling coefficient,K,has been determined by means of an eigenvalue problem.

Consider a plate element having a length,a, depth,h, and subjected to uniformly distributed loads, p = P/N, acting on two opposite edges as shown in Fig. 46(b). The origin of the coordinates is chosen at the center of the rectangular plate,and the x- and y- axes are shown in Fig. 46(b).

The strain energy in bending of a plate, U, and the work of external forces, W, are

$$U = \frac{D}{2} \int_{-a/2}^{+a/2} \int_{-h/2}^{+h/2} [\frac{\partial^2 \omega}{\partial x^2} + \frac{\partial^2 \omega}{\partial y^2}]^2 dxdy \qquad (97)$$

and

$$W = \frac{P}{2} \int_{-a/2}^{+a/2} \int_{-h/2}^{+h/2} (\partial \omega/\partial y)^2 dxdy \qquad (98)$$

in which ω = the deflection surface of the plate

   D = the flexural rigidity of the plate

   The   deflection of the plate can be taken as

$$\omega = \sin(n\pi/h)(y + h/2) \sum_{m = 1,3,5}^{\infty} a_m \cos(m\pi x/a) \qquad (99)$$

in which n is an integer representing the number of half-waves in the direction of y.

In order to simplify the calculation, the following notations are introduced:

$$\alpha = a/h, \qquad \beta = N/a, \qquad \lambda = ph^2/\pi^2 D,$$

(100)

and

$$S_n = \sin(n\pi x)/n\pi x$$

Then, by substituting the expression for ω in Eqs. 97 and 98, one obtains

$$U = \frac{\pi^4 aD}{8h^3} \sum_{m=1,3,5}^{\infty} a_m^2 \left[\frac{m^2}{\alpha^2} + n^2\right]^2$$

(101)

and

$$W = \frac{pNn^2\pi^2}{8h} \sum_{\substack{i=1,3,5 \\ j=1,3,5}}^{\infty} \sum^{\infty} a_i a_j \frac{S_{i+j}}{2} + \frac{S_{i-j}}{2}$$

(102)

The condition required to get the minimum value of p is as follows:

$$\frac{\partial}{\partial a_m}(U - W) = 0$$

(103)

The inserting of Eqs. 101 and 102 into Eq. 103 gives the following system of homogeneous linear equation:

$$\sum_{r=1,3,5}^{\infty} a_r \left[\frac{S_{m+r}}{2} + \frac{S_{m-r}}{2}\right] - a_m \frac{n^2}{\lambda\beta}\left[1 + \frac{m^2}{n^2\alpha^2}\right]^2 = 0 \qquad m=1,3,5\ldots$$

(104)

This system of equations can be written in the matrix form as follows:

$$\begin{bmatrix} 1+S_1 - \dfrac{n^2}{\lambda\beta}[1+\dfrac{1}{n^2\alpha^2}]^2 & S_1+S_2 & - \\[2em] S_1+S_2 & 1+S_2 - \dfrac{n^2}{\lambda\beta}[1+\dfrac{3^2}{n^2\alpha^2}] & - \\[2em] - & - & - \end{bmatrix} \begin{bmatrix} a_1 \\[2em] a_3 \\[2em] - \end{bmatrix} = \begin{bmatrix} 0 \\[2em] 0 \\[2em] - \end{bmatrix} \qquad (105)$$

For the non-trivial solution of this system, the determinant of the coefficients of this equation is zero .

$$\begin{vmatrix} 1+S_1 - \dfrac{n^2}{\lambda\beta}[1+\dfrac{1}{n^2\alpha^2}]^2 & S_1+S_2 & - \\[2em] S_1+S_2 & 1+S_2 - \dfrac{n^2}{\lambda\beta}[1+\dfrac{3^2}{n^2\alpha^2}] & - \\[2em] - & - & - \end{vmatrix} = 0 \qquad (106)$$

or

$$\begin{vmatrix} a_{11} - \lambda_1^* & a_{12} & - \\[2em] a_{21} & a_{22} - \lambda_2^* & - \\[2em] - & - & - \end{vmatrix} = 0 \qquad (107)$$

in which $\qquad \lambda* = 1/\lambda$ $\hspace{4cm}$ (108)

$$a_{11} = (1+S_1) \; / \; \frac{n^2}{\beta}(1+ \frac{1}{n^2\alpha^2})^2 \hspace{3cm} (109)$$

$$a_{12} = (S_1+S_2) \; / \; \frac{n^2}{\beta}(1+ \frac{1}{n^2\alpha^2})^2 \hspace{2.5cm} (110)$$

$$a_{22} = (1+S_1) \; / \; \frac{n^2}{\beta}(1+ \frac{3^2}{n^2\alpha^2})^2 \hspace{2.7cm} (111)$$

$$a_{21} = (S_1+S_2) \; / \; \frac{n^2}{\beta}(1+ \frac{3^2}{n^2\alpha^2})^2 \hspace{2.3cm} (112)$$

The value of $\lambda*$ is an eigenvalue of the corresponding system given in Eq. 107. When α and β are given, the value of $\lambda*$ can be solved for different values of n or different buckling modes. The greatest value of $\lambda*$ or smallest value of λ, thus obtained, corresponds to the critical value of a uniformly distributed load p (p = $\lambda\pi^2 D/h$),and its corresponding value of n gives the number of half-waves in the direction of y.

Several values of λ are tabulated in Table 18 for different combinations of α and β. Table 19 gives the values of λ for five different buckling modes for three different values of β (β = 0.25, 0.5, and 1.0). Figure 47 shows the variation of λ versus the aspect ratio, α, of the plate element.

A comparison of λ based on Yamaki's solution and this analysis is represented in Table 20 for the case of a square plate. These two values have been found to be almost identical.

The buckling loads, then, can be computed by the following formula

$$P_{cr} = \lambda\alpha\beta\pi^2 D/h \qquad (113)$$

$$= K\pi^2 D/h \qquad (114)$$

in which $\qquad K = \lambda\alpha\beta \qquad (115)$

The buckling coefficient K obtained from Eq. 115 is listed in Table 21 and is shown in Fig. 48.

By using the data given in Table 21 and a Statistical Analysis System, SAS-76(67), the following two formulas were developed to compute the buckling coefficient, K, for use in Eq. 114 and for a simply supported plate subjected to locally distributed loads applied on two opposite edges for any combinations of α and β:

$$K = (0.58+0.31\alpha+0.73/\alpha^2+0.25/\alpha^3)(1.0+1.2\beta^2), \quad \text{for } \alpha > 1.0 \quad (116)$$

$$K = (4.7-3.1\alpha+0.22/\alpha^2)(1.0+1.2\beta^2), \quad \text{for } \alpha \leq 1.0 \quad (117)$$

in which $\alpha = a/h$ and $\beta = N/a$.

Table 22 gives the computed values of the buckling coefficient, K_{comp}, which is based on Eqs. 116 and 117. The theoretical buckling coefficient,

---

* Equation 116 and 117 can be simplyfied as follows:

$$K = \alpha(0.52+1.38/\alpha^3)(1+1.2\beta^2) \qquad (116a)$$

$$K = \alpha(0.16+1.86/\alpha)(1+1.2\beta^2) \qquad (117a)$$

K_{theo}, which were calculated on the basis of Eq. 115, are also listed

in this table. The accuracy of Eqs. 116 and 117 is demonstrated by

the ratio of K_{theo}/K_{comp} given in Table 22. These ratios vary from

0.908 to 1.052 and have a mean value of 0.981 and a standard deviation

of 0.040.

2. Ultimate Failure Load

It is known that the web crippling problem is extremely

complicated for theoretical analysis (49), because it involves a combination

of non uniform stress distribution under applied loads, local yielding

in the immediate region of the applied loads, elastic and inelastic

stability of the web element, and the bending moment in the plane of the web

as aresult of eccentric loading. Therefore, the design criteria for the

unreinforced beam webs included in Section 3.5 of the AISI Specification

were developed from information obtained in an experimental study

conducted at Cornell University by Winter and Pian (49) and Zetlin (50).

On the basis of this study, the ultimate web crippling loads of

unreinforced beam webs were found to be a function of N/t, h/t, R/t, and F_y.

For the case of transversely reinforced beam webs, the aspect ratio, a/h,

which indicates the effect of the transverse stiffeners, should be

considered as an additional parameter in predicting the web crippling

strength of beam webs with stiffeners. In addition, the presence of

stiffeners tends to prevent premature buckling failure, and as a result

the h/t ratio does not have much effect on the web crippling loads.

C. Experimental Investigation

The objective of this portion of the investigation was to determine

the ultimate web crippling loads and the postbuckling strength of

reinforced beam webs when they are loaded between transverse stiffeners. In this study, consideration was given to the effect of various parameters, such as (1) the web slenderness ratio,h/t,(2) the bearing length to thickness ratio,(3) the aspect ratio,a/h,(4) the N/a ratio of the patch load,(5) the corner radius to thickness ratio,R/t,(6) the yield point of the steel,and (7) the thickness of the web steel. The intention was to obtain the necessary background information to develop a new design criteria for transversely reinforced beam webs to withstand web crippling loads.

A total of 120 tests were conducted for the following two different loading conditions as shown in Fig. 49:

<div align="center">

One-Flange Loading (60 specimens)

Two-Flange Loading (60 specimens)

</div>

All the tests were performed in the Engineering Research Laboratory of the University of Missouri-Rolla. The following discussion deals with (1) preparation of beam specimens, (2) testing of beam specimens, (3) results of tests, (4) evaluation of the test data, and (5) development of the design methods.

1. Preparation of Beam Specimens

Box beam specimens built up by combining two channel sections as shown in Fig. 8 were used to investigate the web crippling strength of beam webs when they are loaded between transverse stiffeners. The channels were braced by 3/4 x 3/4 x 1/8 in. angles at the top flange and by 1/8 x 3/4 in. rectangular bars at the bottom flange.

Small cold-formed steel channel sections were used as transverse stiffeners. These stiffeners were connected to the web with self-tapping screws (#12-14 x 3/4 in. Tek No. 3 Fasteners).

The cross-sectional dimensions of all 120 beam specimens are listed in

Tables 23 and 24 and their pertinent parameters are given in Tables 25

and 26.

Grid lines were plotted at 1/2 in. intervals on one side of the

beam web so that the profile of the deformed web could be measured.

All measurements were recorded and printed out on tape by a data

acquisition system (Fig. 12).

2. Testing of Specimens

(a) Tensile Coupon Tests

The mechanical properties of the steel used for the 120 beam specimens

were established by standard tensile coupon tests as discussed in Section

III.C.2.(a). Table 7 lists the test data on yield point, ultimate tensile

strength, and elongation measured from a 2-in. gage length of the steel

sheets.

(b) Testing of Beam Specimens

i. Test Setup

One-Flange Loading -- Two different test setups as shown in

Figs. 50 and 51 were used for the one-flange loading condition.

The specimen was tested in a simply supported condition by

using bearing plates at both ends and under a concentrated

load at midspan. The load was applied by a hydraulic jack

and transmitted to the beam specimen by an electric load

cell placed between the jack and the bearing plate. An

electric load cell was used to measure the applied load. In

addition, lateral braces were attached to prevent the

beam specimen from moving laterally (Fig. 52).

Figure 52 shows the test setup and details of the lateral

supports.

Two-Flange Loading -- Sixty specimens were tested under two-flange loading conditions. Each beam specimen was tested by using the bearing plate above and below the beam specimen at mid-length as shown in Figs. 53 and 54. The testing machine was the same as that described above for one-flange loading.

ii. Test Prodecure

During the test, loads were applied in 10% increments of the predicted ultimate load. For each increment of loading, the applied jack load was recorded and printed out on tape by using a 40-channel data acquisition system (Fig. 12). In addition, lateral displacements of one web were measured at several selected applied loads, which included the following loading conditions:

Initial loading

Predicted buckling load

Failure load

These readings were also recorded and printed out on tape by the data acquisition system.

3. Results of Tests

For each test specimen, the failure load per web, $(P_u)_{test}$, was obtained and recorded. Tables 27 and 28 list the values of $(P_u)_{test}$ of 120 beam specimens for the one-flange and two-flange loading conditions.

The theoretical buckling loads, $(P_{cr})_{comp}$, were evaluated from Eqs. 41, 95, and 96 for the one-flange test specimens and from Eqs. 114, 116, and 117 for the two-flange test specimens. These values are given in Table 27 and 28. Also listed in these tables are the postbuckling

strength factor represented by the ratio of $(P_u)_{test}/(P_{cr})_{comp}$.

In an attempt to study the effect of the bending moment on the web crippling load of transversely reinforced beam webs subjected to one-flange loading, the ultimate bending capacity of these sections was calculated on the basis of the bending strength governed by the flanges and the webs.

The bending strength of the beam specimen governed by the flange was computed by using Eq. 118,

$$M_y = S'_x F_y \tag{118}$$

in which S'_x = section modulus for a beam specimen based on either the shear lag or the effective width of the compression flange, whichever is smaller, $in.^3$

F_y = yield point of steel, ksi

The bending strength of the beam specimen governed by the web was computed by using Eq. 119,

$$(M_u)_{cr} = S_x f_{cr} \Phi \tag{119}$$

in which f_{cr} = critical web buckling stress, ksi

$$= k\pi^2 E / [12(1-\mu^2)(h/t)^2] \tag{120}$$

k = buckling coefficient = $4 + 2(1+\beta)^3 + 2(1+\beta)$

$$\beta = |f_t/f_c| \tag{121}$$

S_x = section modulus based on the full widths of the tension flange and the web and on the effective width of the compression flange determined on the basis of Section 2.3.1.1 of the AISI Specification with $f = 0.6f_{cr}$ or $0.6F_y$, whichever is smaller.

Φ = postbuckling strength factor (5)

$$= \alpha_1 \alpha_2 \alpha_3 \alpha_4 \tag{122}$$

$$\alpha_1 = 0.017(h/t) - 0.790 \tag{123}$$

$$\alpha_2 = 0.0462(f_c/f_t) + 0.538 \tag{124}$$

$$\alpha_3 = 1.16 - 0.16(w/t/(w/t)_{lim}), \quad \text{when} \tag{125}$$

$$(w/t)/(w/t)_{lim} \leq 2.25$$

$$= 0.8, \quad \text{when} \quad (w/t)/(w/t)_{lim} > 2.25 \tag{126}$$

$$\alpha_4 = 0.561(F_y/33) + 0.10 \tag{127}$$

The ultimate bending capacity of the beam specimen, $(M_u)_{comp}$, is determined by M_y or $(M_u)_{cr}$ based on Eqs. 118 and 119, whichever is smaller. These values are also listed in Table 29.

4. Evaluation of Test Data

The results of 120 tests have been carefully evaluated in this study, and are discussed in the subsequent sectios on (a) failure modes, (b) a comparison of the experimental failure load and theoretical buckling load, and (c) the effect of the bending moment on the

one-flange web crippling load.

(a) Failure Modes

It was observed that all the test specimens failed by forming a

local cripple curve as shown in Figs. 55 and 56. This cripple curve

corresponds closely to a segment of a circle in which the depth is

proportional to the width of the bearing plate and is independent of the

h/t ratios.

Figures 57 and 58 illustrate typical profiles of the deformed webs for

one-flange and two-flange loading test specimens. These profiles were

measured at the central section of the tested panel at various loading

conditions.

(b) Comparison of the Experimental Failure Load and Theoretical

Buckling Load

One-Flange Loading — The theoretical buckling loads,$(P_{cr})_{comp}$, and

the experimental failure loads,$(P_u)_{test}$, are tabulated in Table 27. It is to

be noted from this table that except for six beam specimens (WC-OF-1-1,

WC-OF-1-2, WC-OF-4-3, WC-OF-4-4, MWC-OF-4-3,and MWC-OF-4-4), the tested

failure loads of the remaining 54 specimens exceed their respective

theoretical buckling loads. The maximum ratio of $(P_u)_{test}/(P_{cr})_{comp}$

increases as the ratios of h/t, a/h, N/a,and the yield point increase.

Two-Flange Loading -- In the case of two-flange loading, Table 28

indicates that the experimental failure load always exceeds the theoretical

buckling load. The postbuckling strength indicated by the ratio of

$(P_u)_{test}/(P_{cr})_{comp}$ varies from 1.041 to 6.885. The postbuckling strength

also increases with an increase in the ratios of h/t, a/h, and N/a, and

F_y.

(c)   Effect of Bending Moment on the One-Flange Web Crippling

   Load

In order to study the effect of the bending moment on the web crippling load, two ratios were established. They are $(P_u)_{test}/(P_u)_{comp}$ and $(M_u)_{test}/(M_u)_{comp}$ in which

   $(P_u)_{test}$ = tested ultimate failure load, kips

   $(P_u)_{comp}$ = computed failure load, based on Eq. 129, kips

   $(M_u)_{test}$ = tested ultimate bending moment, in-kips

   $(M_u)_{comp}$ = computed ultimate bending moment

The values of $(P_u)_{test}/(P_u)_{comp}$ and $(M_u)_{test}/(M_u)_{comp}$ are listed in Table 27. The ratios of $(M_u)_{test}/(M_u)_{comp}$ vary from 0.037 to 0.274. The ratios of $(P_u)_{test}/(P_u)_{comp}$ range from 0.886 to 1.228 and have a mean value of 1.000 and a standard deviation of 0.091.

Figure 59 shows the variation of $(M_u)_{test}/(M_u)_{comp}$ versus $(P_u)_{test}/(P_u)_{comp}$.

Also plotted in Fig. 59 is the intereaction curve between the bending and web crippling load of transversely reinforced beam webs that was developed by Rockey (57).

$$(M_u/M_{uo})^3 + (P_u/P_{uo})^3 = 1.0 \qquad\qquad (128)$$

The notations used in Eq. 128 are defined as follows:

   M_u = ultimate bending moment in the presence of patch load, in-kips

   M_{uo} = ultimate bending moment in the absence of patch load, in-kips

P_u = ultimate patch load in the presence of bending moment, kips

P_{uo} = ultimate patch load in the absence of bending moment, kips

Table 29 also reveals that the ratios of $(M_u)_{test}/(M_u)_{comp}$ for the 60 beam specimens under one-flange web crippling loads are always less than 0.30. As a result, the effect of the bending moment on the web crippling load can be neglected.

5. Development of Design Methods

In order to provide background information for the design of transversely reinforced beam webs subjected to web crippling load, two design methods were developed. They are the ultimate load method and the postbuckling strength method.

This section includes detailed discussions of the aforementioned method and a comparison of the tested and computed web crippling loads based on two different methods.

(a) Ultimate Load Method

In view of the fact that the ultimate load of beam webs with transverse stiffeners subjected to web crippling load depends primarily on the ratios of N/t, a/h, and R/t, the thickness and the yield point of the webs, the following two-formulas were developed by using a Statistical Analysis System, SAS-76(67), and the data from the 120 beam specimens tested in this investigation.

i. One-Flange Loading

$$(P_u)_{comp} = \frac{t^2 F_y}{10^3} C_1 C_2 [12000 + 198 \frac{N}{t}][1.20 - 0.20\frac{a}{h}] \qquad (129)$$

ii. Two-Flange Loading

$$(P_u)_{comp} = \frac{t^2 F_y}{10^3} C_1 C_2 [13056 + 142 \frac{N}{t}][1.08 - 0.08\frac{a}{h}] \qquad (130)$$

in which $(P_u)_{comp}$ = the predicted ultimate web crippling load, in kips per web

$$C_1 \qquad = 1.22 - 0.22k \leq 1.0 \qquad (131)$$

$$C_2 \qquad = 1.06 - 0.06n \leq 1.0 \qquad (132)$$

$$k \qquad = F_y/33 \qquad (133)$$

$$n \qquad = R/t \qquad (134)$$

The comparison of the tested and computed ultimate loads based on Eqs. 129 and 130 is discussed in item (c) below.

(b) Postbuckling Strength Method

The second design method is based on the available postbuckling strength, which is a function of the ratios of h/t, a/h, and N/a and the yield point of steel.

On the basis of the experimental results obtained from 120 web crippling tests, Eq. 135 was derived to evaluate the ultimate web crippling load, $(P'_u)_{comp}$, by using a postbuckling strength factor for transversely reinforced beam webs.

$$(P'_u)_{comp} = \phi_c P_{cr} \qquad (135)$$

in which $(P'_u)_{comp}$ is the computed failure load for web crippling in kips per web, P_{cr} is the theoretical buckling load calculated on the basis of Eqs. 41 and 114 for one- and two-flange loading conditions, in kips per web, and ϕ_c is the postbuckling strength factor for transversely reinforced beam webs under web crippling.

The value of ϕ_c was computed by the following two experimental equations for one- and two-flange loading conditions:

   i.   One-Flange Loading --

$$\phi_c = \psi_1\psi_2\psi_3\psi_4 \qquad (136)$$

in which

$$\psi_1 = 0.0146(h/t) - 0.914 \qquad (137)$$

$$\psi_2 = 0.88(a/h) \qquad (138)$$

$$\psi_3 = 0.58 + 1.42(N/a) \qquad (139)$$

$$\psi_4 = 0.33 + 0.57(F_y/33) \qquad (140)$$

Figures 60, 61, 62, and 63 are the plots of the tested postbuckling strength factors versus the parameters of h/t, a/h, N/a, and $F_y/33$ from which the respective ψ terms were derived.

   ii.   Two-Flange Loading --

$$\phi_c' = \psi_1'\psi_2'\psi_3'\psi_4' \qquad (141)$$

in which

$$\psi_1' = 0.00476(h/t) - 0.194 \qquad (142)$$

$$\psi_2' = 3.25(a/h) \qquad (143)$$

$$\psi_3' = 0.82 + 0.60(N/a) \qquad (144)$$

$$\psi_4' = 0.33 + 0.57(F_y/33) \qquad (145)$$

Figures 64, 65, 66, and 67 are plots of the tested postbuckling strength

factors versus the parameters of h/t, a/h, N/a, and $F_y/33$ from which the

respective ψ' terms were derived,

The accuracy of Eqs. 136 and 141 is discussed in the following

section.

       (c) Comparison of the Tested and Computed Ultimate Web

           Crippling Loads Based on Two Methods

Comparisons were made for the experimental and computed web crippling

loads based on the ultimate load method and the postbuckling strength

method. The following discussions presentsthe mean value and the standard

deviation of the ratios between the tested and computed web crippling

loads for one-flange and two-flange loadings.

       i. One-Flange Loading

           The tested and computed web crippling loads based on the

           Ultimate Load Method are compared in Fig. 68 which indicates

           that Eq. 129 adequately predicts the web crippling loads to

           within $\pm 20\%$ of the tested values. The ratio of

           $(P_u)_{test}/(P_u)_{comp}$ is calculated and is given in Table 27.

           These ratios vary from 0.886 to 1.228 and have a mean value of

           1.000 and a standard deviation of 0.091.

           A   comparison of the tested and computed loads based

           on the Postbuckling Strength Method is represented by the

           ratios of $(P_u)_{test}/(P'_u)_{comp}$ given in Table 27. This

           table reveals that these ratios vary from 0.873 to 1.240 and

           have a mean value of 1.007 and a standard deviation of

           0.107.   A comparison of the tested and computed postbuckling

           strength factors (Eq. 136) is shown in Fig. 69, which indicates

that Eq. 136 adequately predicts the postbuckling strength

factor within $\pm 20\%$ of the tested value.

ii. Two-Flange Loading

A comparison of the tested and computed web crippling

loads based on the Ultimate Load Method is represented

graphically by Fig. 70. All the data points are within

$\pm 20\%$ of the tested values. In Table 28, the ratios of

$(P_u)_{test}/(P_u)_{comp}$ vary from 0.922 to 1.099 and have an

average value of 1.009 and a standard deviation of 0.054.

Therefore, it can be concluded that Eq. 130 correlates

well with the tested ultimate web crippling loads.

With regard to the second method, the comparison was

also made between the computed and tested loads that are

listed in Table 28. A study of this table shows that the

ratios of $(P_u)_{test}/(P_u')_{comp}$ vary from 0.800 to 1.270. Their

mean value and standard of deviation are 1.005 and 0.193

respectively. Fig. 71 shows a graphic comparison of

the tested and computed postbuckling strength factors. All

the computed data are practically within $\pm 20\%$ of the tested

values.

D. Summary and Design Recommendations

1. Summary

In order to study the crippling strength of cold-formed steel beam

webs loaded between transverse stiffeners and to develop new design

criteria as necessary, a total of 120 beam tests were conducted.

Based upon the results of these tests, the following conclusions can be

drawn:

(a) The current AISI Specification includes design provisions
for only the web crippling strength of unreinforced
beam webs having an h/t ratio of no more than 150. Modified
design formulas have been proposed by Hetrakul and Yu (9) to
extent this ratio to 200.

(b) For beam webs with h/t ratios larger than 200, transverse
stiffeners should be provided to prevent premature failure
by web buckling.

(c) The postbuckling strength of reinforced beam webs loaded
between transverse stiffeners subjected to web crippling is a
function of h/t, a/h, N/a, and the yield point of the material.

(d) For beam webs subjected to one-flange loading, design
formulas were developed for h/t ratios larger than 200. Eqs.
129 and 136 correlate well with the tested web crippling
loads.

(e) For beam webs subjected to two-flange loading, Eqs. 130 and
141 were developed on the basis of the experimental data
of beam specimens having h/t ratios larger than 300. These
equations agree well with the tested values.

(f) According to the scatter likely to be found in the web
crippling tests and for the sake of uniformity with the
unreinforced webs (5), a safety factor of 1.85 is desirable
for the development of the design criteria.

2. Design Recommendations

Based on the findings of this research, the following design formulas
are recommended for the design of transversely reinforced beam webs
subjected to web crippling loads.

To avoid crippling of transversely reinforced beam webs having h/t ratios larger than 200, concentrated loads and reactions should not exceed the value P_{max} given below.

    2.1 For reactions or for concentrated loads located on the span of the beams between two transverse stiffeners

    (a) Ultimate Load Method

$$P_{max} = t^2 F_y C_1 C_2 [6490 + 107\frac{N}{t}][1.20 - 0.20\frac{a}{h}]10^{-3} \tag{146}$$

in which
$$C_1 = 1.22 - 0.22(F_y/33) \leq 1.00$$

$$C_2 = (1.06 - 0.06\frac{R}{t}) \leq 1.0$$

    (b) Postbuckling Strength Method

$$P_{max} = \phi_c P_a \tag{147}$$

in which
$$\phi_c = \psi_1 \psi_2 \psi_3 \psi_4 \tag{148}$$

$$\psi_1 = 0.0146(h/t) - 0.914$$

$$\psi_2 = 0.88(a/h)$$

$$\psi_3 = 0.58 + 1.42(N/a)$$

$$\psi_4 = 0.33 + 0.59(F_y/33)$$

$$P_a = k\frac{14412t^3}{h}$$

$$k \quad = (2.04+1.52/\alpha^3)(1.0+0.48\beta^2), \text{ for } \alpha > 1.0$$

$$= (5.59-2.62\alpha+0.54/\alpha^2)(1.0+0.48\beta^2), \text{ for } \alpha \leq 1.0$$

$$\alpha \quad = a/h$$

$$\beta \quad = \text{larger value of } N/a \text{ and } N/h$$

2.2 For two opposite concentrated loads applied simultaneously to both top and bottom flanges between two transverse stiffeners

(a) Ultimate Load Method

$$P_{max} = t^2 F_y C_1 C_2 [7057 + 77 \frac{N}{t}][1.08-0.08\frac{a}{h}]10^{-3} \tag{149}$$

(b) Postbuckling Strength Method

$$P_{max} = \phi'_c P_a \tag{150}$$

in which
$$\phi'_c = \psi'_1\psi'_2\psi'_3\psi'_4 \tag{151}$$

$$\psi'_1 = 0.00476(h/t) - 0.194$$

$$\psi'_2 = 3.25(a/h)$$

$$\psi'_3 = 0.82 + 0.60(N/a)$$

$$\psi'_4 = 0.33 + 0.57(F_y/33)$$

$$P_a = k\frac{14412t^3}{h}$$

$$k = (0.58+0.31\alpha+0.73/\alpha^2+0.25/\alpha^3)x$$

$$(1.0+1.2\beta^2), \text{ for } \alpha > 1.0$$

$$= (4.7-3.1\alpha+0.22/\alpha^2)(1.0+1.2\beta^2), \text{ for } \alpha \leq 1.0$$

$$\alpha = a/h$$

$$\beta = N/a$$

In the above formulas, P_{max} is the allowable load in kips per web.

V.2. Beam Webs Loaded at the Location of Transverse Stiffeners

A. General

In cold-formed steel beams, heavy concentrated loads usually exceed the web crippling strength of the reinforced beam webs when they are loaded between transverse stiffeners as discussed in the previous sections. In this case, transverse stiffeners must be provided at the locations of applied concentrated loads or reactions to carry the compressive stress in the vicinity of the concentrated loads. The idea of using transverse stiffeners to prevent premature failure caused by web crippling is considered in the current AISI Specification (3). Section 2.4.4.(b) of this specification specifies that the h/t ratio of the beam web can be extended tp 200 if the members are provided with an adequate means of transmitting concentrated loads or reactions, i.e., transverse stiffeners.

This investigation has been directed toward the study of the load carrying capacity of transverse stiffeners when they are located within the spans or at the ends of the beam members and subjected directly to concentrated loads or reactions.

B. Analytical Study

The load carrying capacity of transverse stiffeners,when they are provided at the locations of the applied loads or reactions,can be determined on the basis of column formulas provided that the adjacent portion of the web is considered as a part of the stiffener column. The determination of this effective portion is very complicated for analytical analysis, because it involves the web crippling strength of a combination of beam webs and stiffeners, the elastic and inelastic instability of stiffeners, and the local buckling of the plate elements of the stiffeners. For these reasons, an experimental study was made

to provide enough bacground information for the design of the cold-formed steel transverse stiffeners.

C. Experimental Investigation

The objective of the investigation was to determine the web crippling strength of beam webs when they are loaded at the location of the transverse stiffeners. The experimental results will provided a basis for the development of design criteria for the stiffeners. Consideration was given to the slenderness ratio of the web, the dimensions of the stiffeners, the thicknesses of the webs and stiffeners, and the mechanical properties of the material.

A total of 61 beam specimens were tested for the following two types of stiffeners:

Interior Transverse Stiffeners (33 tests)

End Transverse Stiffeners (28 tests)

These test specimens were fabricated from the channel sections shown in Fig. 8. All the tests were performed in the Engineering Research Laboratory of the University of Missouri-Rolla.

Topics to be discussed in this section are (1) the preparation of the beam specimens, (2) testing of the beam specimens, (3) results of the tests, (4) evaluation of the test data, and (5) development of the design method.

1. Preparation of Beam Specimens

The built-up beam specimens were fabricated in the same maner as described in Section V.C.1 of this report. Table 30 and 31 list the dimensions of the beam sections shown in Fig. 8. The h/t ratios of the web vary from 150 to 300, the web thicknesses are 0.0382, 0.0478, and 0.0592 in. respectively.

The transverse stiffeners were made of channel sections as shown in Fig. 72. All the plate elements of the stiffeners were designed such that the flat-width-to-thickness ratios, w/t, were less than the limiting ratios defined by Eqs. 55 and 57 for stiffened and unstiffened elements. The transverse stiffener dimensions are given in Tables 32 and 33 and are shown in Fig. 73.

The transverse stiffeners were attached to the webs by 3/4-in. diameter bolts for beam specimens with h/t ratios less than 250 and by self-tapping screws (#12 x 14 x 3/4 Tek Screws) for beam specimens with h/t ratios greater than 250. The channels were braced by 3/4 x 3/4 x 1/8 in. angles at both the top and bottom flanges.

In an attempt to determine the actual stresses in the stiffeners and the beam webs, eight foil strain gages (Nos. S1, S2, S3, S4, W1, W2, W3 and W4) were mounted on the stiffeners as well as on the beam webs as shown in Fig. 74.

In order to prevent the beam specimens from moving laterally, lateral braces were provided on both the top and bottom flanges; Figs. 75 and 76 show details of these braces.

2. Testing of Specimens

(a) Tensile Coupon Tests

The tensile coupon tests were carried out by using the standard procedure described in Section III.C.2.(a) of this report. Table 7 contains the test data on yield point, ultimate tensile strength, and elongation measured from a 2-in. gage length.

(b) Testing of Beam Specimens

i. Test Setup

The test setup for beam specimens having intermediate and

end transverse stiffeners are shown in Figs. 75 and 77

respectively. The loading machine used in this series of

test is described in Section III.C.2.(b). Fig. 76 is a

photograph of test setup for intermediate transverse

stiffener tests.

ii. Test Procedure

After the specimen was setup in the testing frame and

instrumented, the test was conducted as follows: The test

specimen was first loaded to approximately 10% of the

expected failure load. Strain gage readings were then

compared for different locations on the stiffeners. If an

individual strain gage varied more than 5%, the load

was considered eccentric,and the specimen was unloaded.

The specimen then was realigned,and the load cell was

relocated. Once a concentrated load condition was achieved,

the loads were applied in 250 lb increments from zero

to the failure load. At the end of each increment, the load

was permitted to stabilize,and the strain gage readings were

taken and recorded by an acquisition system.

3. Results of Tests

For each specimen, the tested failure load per stiffener, $(P_u)_{test}$,

was obtained and recorded. Tables 34 and 35 list the value of $(P_u)_{test}$ for

all the beam specimens. The critical loads,P_{cr}, of one stiffener alone

were calculated by using Eq. 152. These values are tabulated in Tables 34 and

and 35 for intermediate and end transverse stiffener test specimens.

$$P_{cr} = A\sigma_{cr} \qquad (152)$$

in which P_{cr} is the critical buckling load of the stiffener column, kips, A is the cross sectional area of the stiffener, in.^{2}, and σ_{cr} is the critical buckling stress of the stiffener column, ksi.

The critical stress of the stiffener column, σ_{cr}, was determined by using either Eq. 153 or 154, whichever was applicable.

$$\sigma_{cr} = \pi^2 E/(KL/r)^2, \text{ for } (KL/r) > \sqrt{2\pi^2 E/F_y} \qquad (153)$$

$$\sigma_{cr} = F_y - (F_y^2/4\pi^2 E)(KL/r)^2, \text{ for } (KL/r) \leq \sqrt{2\pi^2 E/F_y} \qquad (154)$$

in which F_y is the yield point of the stiffener, ksi, L is the total length of the stiffener, in., K is the effective length factor = 1.0, r is the radius of gyration of the stiffener's cross section, in., and E is the modulus of elasticity = 29,500 ksi.

The yield load, P_y, of the stiffener was calculated by using Eq. 155 and is listed in Tables 34 and 35.

$$P_y = AF_y \qquad (155)$$

in which A and F_y have been previously defined.

The computed ultimate loads of the stiffener, $(P_{us})_{comp}$, were determined by either P_{cr} or P_y of Eqs. 152 and 155, whichever was smaller. These values are also tabulated in Tables 34 and 35.

4. Evaluation of Test Data

The results of 61 beam tests were carefully studied. The topics which are discussed in this section are (a) failure modes, (b) comparison of the tested failure load and computed ultimate load of the stiffener column

(c) crushing stress, and (d) effect of connectors between the beam webs and transverse stiffeners.

(a) Failure Modes

Two types of failure modes were observed during the testing of the 61 beam specimens. The first failure mode is evidenced by crushing at the end of transverse stiffeners. This is a typical failure mode for beams having h/t ratios less than 250. These specimens were designated by ITS-C or ETS-C for interior and end transverse stiffeners respectively. Figures 78 and 79 are photographs of this type of failure mode. For beam specimens with h/t ratios larger than 250, the second mode of failure was observed. This is due to the buckling failure of the web-stiffener column. These specimens were designated as ITS-S or ETS-S. Figures 80 and 81 show the typical beam specimens that failed as a result of column buckling.

A combination of end crushing and column instability caused eight specimens to fail. The specimens used in the intermediate stiffener tests are ITS-C-3-1, ITS-C-3-2, ITS-C-4-1, and ITS-C-4-2, and the specimens used in the end transverse stiffenr tests are ETS-C-3-1, ETS-C-3-2, ETS-C-4-1 and ETS-C-4-2 . The h/t ratios of these specimens are approximately equal to 250.

(b) Comparison of the Tested Failure Load and Computed Ultimate
Load of the Stiffener Column

Intermediate Stiffener Tests -- Table 34 lists the tested failure load, $(P_u)_{test}$, and the computed ultimate load of the stiffeners, $(P_{us})_{comp}$, of 33 beam specimens having intermediate stiffeners. The ratios of $(P_u)_{test}/(P_{us})_{comp}$ were calculated and are tabulated in Table 34. A study of this table indicates that the atios of $(P_u)_{test}/(P_{us})_{comp}$ vary from 1.210 to 1.870 and have an aveaage value of 1.501. In addition, Table 34 reveals that 13 beam specimens designated as ITS-C-1-1 to

ITS-C-6-2 failed as a result of being crushed at the end of the stiffeners, whereas their computed ultimate loads were governed by the buckling load of the stiffener column, P_{cr}.

End Transverse Stiffener Tests - For this case, the tested failure loads, $(P_u)_{test}$, the computed ultimate loads of the stiffener column, $(P_{us})_{comp}$, and the ratios of $(P_u)_{test}/(P_{us})_{comp}$ are listed in Table 35. Examination of this table shows that the ratios of $(P_u)_{test}/(P_{us})_{comp}$ vary from 1.154 to 1.708 and have a mean value of 1.394.

Based on the aforementioned discussions concerning a comparison of the tested failure load and the computed ultimate load of the stiffener column, it seems that the strength of stiffener alone does not adequately predict the load-carrying capacity of the transverse stiffeners attached to the beam webs, and a portion of the web should be considered as a part of the web-stiffener column.

(c) Discussion of the Crushing Stress

Because cold-formed steel transverse stiffeners are made of thin plate elements, end crushing always causes short stiffeners to fail at a stress that is less than the yield stress of steel.

On the basis of the experimental results of 17 tests on intermediate stiffeners and 14 tests on end transverse stiffeners that failed as a result of being crushed at the end, an attempt was made to evaluate the crushing stress of cold-formed steel transverse stiffeners. Table 36 lists the experimental value of crushing stress, f_c, the yield points of web and stiffener materials, and the average yield point, F_{ya}, of the web-stiffener section, which is determined by Eq. 156.

$$F_{ya} = CF_{ys} + (1-C)F_{yw} \qquad (156)$$

in which F_{ys} and F_{yw} are the yield points of the stiffener and the web steel, ksi, C is the ratio of A_s/A_c, A_s is the cross section of the stiffener, in.^{2}, and A_c^* is the area of the web-stiffener's cross section.

Table 36 reveals that the ratio of f_c/F_{ya} has a mean value of 0.859. Therefore, the crushing stress of cold-formed transverse stiffeners used in this investigation can be simply determined by the following equation:

$$F_c = 0.86F_{ya} \qquad (157)$$

in which F_{ya} is defined in Eq. 156.

    (d)   Effect of Connections Between Beam Webs and Transverse

           Stiffeners

The effect of connections between beam webs and stiffeners on the structural behavior of cold-formed transverse stiffeners is very complicated. It depends mainly upon the types of connections used, the size of the connections, the distances between beam flanges and the end connectors, and the distances between intermediate connectors.

In this investigation, bolted connections and self-tapping screws were used, because they were more convinient to use to fabricate the beam specimens than other types of connections, such as welding or riveting.

For the type of connections used, the strain gage readings indicated that the measured stress in the web was about 10% less than the stress in the stiffeners. However, in calculating the effective width of the beam webs, it was conservatively assumed that the

---

*In calculating A_c, a portion of the beam webs, as defined by Eq. 158 or 159 was used for the intermediate or end transverse stiffeners.

stresses in the webs are equal to the ones in the stiffeners.

5. Development of Design Methods

Design methods were developed to provide criteria for cold-formed steel transverse stiffeners when they are placed at the locations of applied loads or reactions. These methods are discussed in the following sections:

(a) Crushing Criterion

As noted previously, short stiffeners may fail by end crushing at a stress level that is lower than that for the yield point of stiffener steel. In this case, the crushing criterion as discussed below may control the load-carrying capacities of the stiffeners.

Intermediate Stiffeners -- Based on the experimental crushing stress, f_c, of the 17 intermediate stiffener test specimens tabulated in Table 37, the effective widths of the beam webs of these specimens under end crushing failure were computed and tabulated in Table 37. This table reveals that the average effective width in this case is 18.58 times the web thickness. For practical purposes, the effective width can be computed by using Eq. 158.

$$b_{ec} = 18(t_w)$$ (158)

in which b_{ec} is the effective width of the beam webs for intermediate stiffeners under end crushing failure, in., t_w is the thickness of beam webs, in.

End Transverse Stiffeners -- The experimental crushing stress of 14 beam specimens that failed by end crushing are tabulated in Table 38. Based on these values, the effective widths were computed and tabulated.

Table 38 also indicates that except for four beam specimens (ETS-C-1-1, ETS-C-2-2, ETS-C-3-2, and ETS-C-4-1) the average value of the ratio b_e/t_w is 10.65. Therefore, it is recommended that the effective width of the end transverse stiffeners under end crushing failure be determined by Eq. 159.

$$b_{ec} = 10(t_w) \qquad (159)$$

Figure 82 shows the effective widths of beam webs for end crushing failure conditions.

(b) Stability Criterion

Transverse stiffeners may fail by column buckling if the beam web is relatively deep. In this series of tests, 20 specimens having intermediate stiffeners and 20 specimens having end transverse stiffeners failed as a result of instability. The h/t ratios of these specimens were higher than 250. This section deals with the development of the stability criteria of intermediate and end transverse stiffeners.

Intermediate Stiffeners -- Table 39 lists the tested failure loads, $(P_u)_{test}$, and the tested effective widths, $(b_e)_{test}$ of 20 beam specimens that failed by column buckling. An interative method was used to compute the effective widths, $(b_e)_{test}$, on the basis of Eqs. 153 and 154. The ratios of $(b_e)_{test}/t_w$ and D/t_w are also listed in this table. The data in the table indicate that the tested effective width, $(b_e)_{test}$, increases as the web thickness, t_w, and the ratio D/t_w increase.

From the experimental results of 20 tests that failed by column buckling (Table 39), the following formula was derived to compute the

effective width of beam webs:

$$b_e = 25t_w[0.00241(D/t_w)+0.720] \leq 42t_w \qquad (160)$$

in which b_e is the effective width of the beam webs, in., D is the total length

of the transverse stiffeners, in. and t_w is the thickness of the beam webs, in.

The upper limit of Eq. 160 was determined by setting a value of

D/t_w equals to 400. This limiting value is very close to the value of

$(w/t)_{lim}$ as shown by Eq. 55 for F_y equal to 33 ksi.

Figure 83 is a plot of the ratio of the $(b_e)_{test}/25t_w$ versus the ratio of

D/t_w from which Eq. 161 was derived.

Figure 84, which is a graphic comparison of the tested and computed

effective widths, reveals that Eq. 160 adequately predicts the effective

width of beam webs having intermediate stiffeners subjected to web

stiffener column buckling.

In addition, Table 39 lists the ratio of the tested and computed

effective widths, $(b_e)_{test}/(b_e)_{comp}$. This ratio varies from 0.770 to

1.235. It has an average value of 1.006 and a standard deviation of

0.114.

End Transverse Stiffeners -- The procedure used to develop the effec-

tive width for end transverse stiffener beam specimens was the same as that

used for intermediate stiffeners as discussed in the previous section.

Twenty specimens of this series of tests failed by column buckling.

These specimens and their respective widths, which were calculated by itera-

tive method, are listed in Table 40. Based on the experimental results

given in this table, the following formula was derived by using a Statistical

Analysis System, SAS-76(67).

$$b_e = 12t_w[0.00437(D/t_w)+0.833] \leq 30t_w \qquad (161)$$

in which b_e is the effective width of beam webs with end transverse stiffeners under stability failure, in. The terms D and t_w are defined for Eq. 160. The upper limit of Eq. 161 was determined by setting a value of D/t_w equal to 400.

Figure 85 is a plot of the ratio $(b_e)_{test}/12t_w$ versus the ratio D/t_w from which Eq. 161 was derived. Table 40 contains a tabulation of the ratios of $(b_e)_{test}/(b_e)_{comp}$ which vary from 0.842 to 1.124. Their mean value is 1.000 and their standard deviation 0.097. Figure 86 shows a comparison of the tested and computed effective widths of beam webs having end transverse stiffeners under stability failure.

(c) Local Buckling Criterion

To prevent premature failure as the result of the buckling of the plate elements of cold-formed transverse stiffeners, the widths of stiffened and unstiffened plate elements should not be greater than the limiting values provided by Eq. 55 and 57, respectively, in which F_y is the yield point of stiffener steel.

(d) Comparison of the Tested and Computed Ultimate Loads for
Beam Webs Loaded at the Location of Transverse Stiffeners

A comparison was made of the experimental and computed load carrying capacities of intermediate and end transverse stiffeners attached to the beam webs when they are provided at the locations of the applied loads or reactions. The following discussions concern this comparison.

Intermediate Stiffeners -- The computed loads based on crushing

criterion, $(P_c)_{comp}$, were calculated by using Eq. 162

$$(P_c)_{comp} = A_c F_{ya} \qquad (162)$$

in which $A_c = 18(t_w) + A_s$, in.

F_{ya} = average yield stress, ksi, computed by Eq. 156

The computed loads based on stability criterion, $(P_{cr})_{comp}$, were evaluated by using Eq. 163

$$(P_{cr})_{comp} = A_b \sigma_{cr} \qquad (163)$$

in which

σ_{cr} = critical buckling stress of the web-stiffener column having a cross section, A_b, in.^{2}, ksi.

A_b = web-stiffener cross-sectional area, in.^{2}, composed of the area of the stiffener and the area of the beam web having a width as computed by Eq. 160.

The computed ultimate load, $(P_u)_{comp}$, was determined from $(P_c)_{comp}$ or $(P_{cr})_{comp}$ whichever was smaller. These values are listed in Table 34. This table indicates that the ratio of $(P_u)_{test}/(P_u)_{comp}$ varied from 0.914 to 1.136 and has a mean value of 1.002 and a standard deviation of 0.056.

End Transverse Stiffener -- For end transverse stiffeners, the computed loads based on crushing criterion, $(P_c)_{comp}$, were calculated by using Eq. 162 in which the value of A_c is given by Eq. 164

$$A_c = 10(t_w) + A_w \qquad (164)$$

The computed loads based on the stability criterion, $(P_{cr})_{comp}$, were evaluated by using Eq. 163 in which the area of the beam web has a width as computed by Eq. 161. The computed ultimate load, $(P_u)_{comp}$, was determined from $(P_c)_{comp}$ or $(P_{cr})_{comp}$ whichever was smaller. Table 35, which lists the values of $(P_u)_{comp}$ and the ratios of $(P_u)_{test}/(P_u)_{comp}$ reveals that these ratios range from 0.976 to 1.089 and have an average value of 0.996. The standard deviation is 0.051.

D. Summary and Design Recommendations

In this investigation, a total of 61 tests were conducted to study the load carrying capacity of the intermediate and end transverse stiffeners when they are provided at the locations of the applied concentrated loads or reactions. The test results were carefully evaluated, and the following conclusions drawn:

1. Summary

   (a) The strength of transverse stiffeners alone provide a very conservative result in predicting the load carrying capacity of beam webs loaded at the locations of the transverse stiffeners.

   (b) A portion of the beam webs contributes to the load-carrying capacity of the web-stiffener column.

   (c) Short transverse stiffeners usually failed by end crushing stress at a stress level less than that of the yield point of stiffener steel.

   (d) Stability failure occurred for long transverse stiffeners, and the effective width of beam webs depends on the web thickness and the D/t_w ratio of the steel beam.

   (e) Connections between beam webs and transverse stiffeners have

a significant effect on the behavior of transverse stiffeners.

(f) On the basis of the experimental data obtained from this investigation, design formulas were derived to compute the effective widths of beam webs for intermediate and end transverse stiffeners under end crushing and stability failure.

(g) The column design criteria included in Section 3.6.1.1 of the current AISI Specification can be used to predict the ultimate load of a web-stiffener assembly column.

2. Design Recommendations

Based on the findings of this research, the following design formulas are recommended for the design of transverse stiffeners when they are provided at the locations of applied loads or reactions.

(a) The concentrated loads or reactions should not exceed the value, P_{max}, given below

i. Crushing Criterion

$$P_{max} = 0.52F_{ya}A_c \qquad (166)$$

ii. Stability Criterion

$$P_{max} = F_{al}A_b \qquad (167)$$

in which $\quad F_{ya}$ = average yield point of web-stiffener section, ksi.

$$= CF_{ys} + (1-C)F_{yw}$$

F_{ys} = yield point of stiffener material, ksi.

F_{yw} = yield point of web material, ksi.

C = A_s/A_c

A_s = cross-sectional area of stiffener, in.^{2}

A_c = $18t_w + A_s$, for intermediate stiffener, in.^{2}

= $10t_w + A_s$, for end transverse stiffener, in.^{2}

t_w = thickness of beam web, in.

A_b = $b_1 t_w + A_s$ for intermediate stiffener, in.^{2}

= $b_2 t_w + A_s$ for end transverse stiffener, in.^{2}

b_1 = $25t_w[0.00241(D/t_w) + 0.720] \leq 42t_w$

b_2 = $12t_w[0.00437(D/t_w) + 0.833] \leq 30t_w$

D = total length of transverse stiffener, in.

F_{al} = allowable column stress, determined according to Section 3.6.1.1 of the current AISI Specification for the cross section, A_b

(b) The ratio w/t of the stiffened and unstiffened elements of cold-formed steel transverse stiffeners shall not exceed $220.53/\sqrt{F_{ys}}$ and $63.87/\sqrt{F_{ys}}$ respectively.

VI. CONCLUSIONS

In this investigation, analytical and experimental investigations were undertaken to determine the structural behavior of cold-formed steel beams having transversely reinforced webs subjected to bending, shear, and web crippling. The research findings of these three cases are summarized below:

A. Bending Strength of Beam Webs

The results of 22 test specimens of beam webs having h/t ratios larger than 200 subjected to bending stress indicate that the postbuckling strength equation previously developed for unreinforced beam webs under bending can be used to predict the ultimate moment capacity of the transversely reinforced beam webs having h/t ratios larger than 200. Consequently, design recommendations were proposed for use in the design of the reinforced beam webs subjected to bending stress.

B. Shear Strength of Transversely Reinforced Beam Webs

In this study, 32 beam specimens were tested at the University of Missouri-Rolla. An evaluation of the experimental data reveals that a considerable postbuckling strength has been developed which corresponds very well with the incomplete tension field theory. In addition, the requirements of transverse stiffeners were discussed. On the basis of the results of these tests, formulas and design recommendations were developed to evaluate the shear strength of transversely reinforced beam webs and to design the cold-formed steel transverse stiffeners.

C. Web Crippling Strength of Transversely Reinforced Beam Webs

The web crippling problem of cold-formed steel transversely reinforced beam webs was studied in this phase of the investigation.

For beam webs loaded between two transverse stiffeners, the results of 120 specimens of beam webs subjected to one-flange and two-flange loadings were evaluated. The postbuckling strength of web elements under patch loads was formed to be a function of the depth-to-thickness ratio of the beam web, the aspect ratio of the web element, the N/a ratio of the patch load, and the yield point of the web material. Formulas and design recommendations were developed to predict the web crippling strength of transversely reinforced beam webs.

In the case of beam webs loaded at the location of transverse stiffeners, 61 beam specimens were tested to study the load-carrying capacities of the intermediate and end transverse stiffeners. Test results indicate that a portion of the beam webs contributes to the strength of the stiffener column in resisting the applied concentrated loads or reactions. Equations for calculating the effective widths of the beam webs were proposed and presented.

ACKNOWLEDGMENTS

BIBLIOGRAPHY

1. Winter, G., "Cold-Formed, Light Gage Steel Construction," _Journal of Structural Division_, ASCE Proceedings, Vol. 85, No. ST9, November 1959.

2. Yu, W.W., _Cold-Formed Steel Structures_, McGraw-Hill Book Company, 1973.

3. American Iron and Steel Institute, "Specification for the Design of Cold-Formed Steel Structural Members," 1968 Edition.

4. Winter, G., "Commentary on the 1968 Edition of the Specification for the Design of Cold-Formed Steel Structural Members," _Cold-Formed Steel Design Manual_, Part II, American Iron and Steel Institute, 1977.

5. LaBoube, R.A., and Yu, W.W., "Webs for Cold-Formed Steel Flexural Members--Structural Behavior of Beam Webs Subjected to Bending Stress," _Final Report_, University of Missouri-Rolla, July 1978.

6. LaBoube, R.A., and Yu, W.W., "Webs for Cold-Formed Steel Flexural Members--Structural Behavior of Beam Webs Subjected Primarily to Shear Stress," _Final Report_, University of Missouri-Rolla, July 1978.

7. LaBoube, R.A., and Yu, W.W., "Webs for Cold-Formed Steel Flexural Members--Structural Behavior of Beam Webs Subjected to a Combination of Bending and Shear," _Final Report_, University of Missouri-Rolla, July 1978.

8. LaBoube, R.A., "Strength of Cold-Formed Steel Beam Webs in Bending, Shear, and a Combination of Bending and Shear," thesis presented to the University of Missouri-Rolla, Missouri, in 1977, in partial fulfillment of the requirements for the degree of Doctor of Philosophy.

9. Hetrakul, N., and Yu, W.W., "Webs for Cold-Formed Steel Flexural Members--Structural Behavior of Beam Webs Subjected to Web Crippling and a Combination of Web Crippling and Bending," _Final Report_, University of Missouri-Rolla, Rolla, Missouri, July 1978.

10. Hetrakul, N., "Web Crippling Strength and a Combination of Bending and Web Crippling of Cold-Formed Steel Beams," thesis presented to the University of Missouri-Rolla, Missouri, in 1978, in partial fulfillment of the requirements for the degree of Doctor of Philosophy.

11. Timoshenko, S.P., and Gere, J.M., _Theory of Elastic Stability_, McGraw-Hill Book Company, 1961.

12. Schuette, E.H., and McCulloch, J.C., "Charts for the Minimum-Weight Design of Multiweb Wings in Bending," NACA TN 1323, 1947.

13. Johnson, J.H., and Noel, R.G., "Critical Bending Stress for Flat Rectangular Plates Supported Along All Edges and Elastically Restrained Against Rotation Along the Unloaded Compression Edge," _Journal of Aerospace Science_, Vol. 10, No. 8, August 1953.

14. Bleich, F., Buckling Strength of Metal Structures, McGraw-Hill Book Company, 1952.

15. Bulson, P.S., The Stability of Flat Plates, American Elsevier Publishing Company, Inc., New York, 1969.

16. Basler, K., Yen, B.T., Mueller, J.A., and Thurlimann, B., "Web Buckling Tests on Welded Plate Girders," Welding Research Council Bulletin No. 64, September 1960.

17. Basler, K., and Thurlimann, B., "Strength of Plate Girders in Bending," Journal of the Structural Division, ASCE Proceedings, Vol. 87, No. ST6, August 1961.

18. American Institute of Steel Construction, "Specification for the Design, Fabrication, and Erection of Structural Steel for Buildings," February 12, 1969.

19. Bergfelt, A., "Profile's Minces Formés A Froid," Bulletin Technique de la Suisse Romande, 18 Aout 1973, pp. 363-372.

20. Bergfelt, A., Edlund, B., and Larson, H., "Experiments on Trapezoidal Steel Sheets in Bending," Proceedings of the Third International Specialty Conference on Cold-Formed Steel Structures, University of Missouri-Rolla, November 1975, pp. 285-314.

21. Thomasson, P., "Livbuckling ens Inverkan pa Barformagan Has Trapets Profilerad Stalplat," Presented at Nordiske for Skningsdager for Stalkonstruksjoner, Oslo, Norway, August 1973.

22. Hoglund, T., "Design of Thin Plate I Girders in Shear and Bending with Special Reference to Web Buckling," Division of Building Statics and Structural Engineering, Royal Institute of Technology, Sweden, Bulletin No. 94, September 1973.

23. Lyse, I., and Godfrey, H.J., "Investigation of Web Buckling in Steel Beams," ASCE Transactions, Vol. 100, 1935, pp. 675-695.

24. Skan, S.W., and Southwell, R.V., "On the Stability under Shearing Forces of a Flat Elastic Strip," Proc. Roy. Soc. (London), Series A, Vol. 105, p. 582, 1924.

25. Seydel, E., "Über das Ausbeulen von Rechteckigen Isotropen oder Orthogonalanisotropen Platten bei Schubbeanspruching," Ingenieur-Archiv, Vol. 4, P. 169, 1933.

26. Stein, M., and Neff, J., "Buckling Stress of Simply Supported Rectangular Flat Plates in Shear," NACA Tech. Note No. 1222, 1947.

27. Stowell, E., Z., "Critical Shear Stresses of an Infinitely Long Plate in Plastic Region," NACA Tech. Note No. 1611, 1948.

28. Gerard, G., Introduction to Structural Stability Theory, McGraw-Hill Book Company, 1962.

29. Rockey, K.C., Evans, H.R., and Porter, D.M., "Ultimate Load Capacity of Stiffened Webs Subjected to Shear and Bending," Conference on Steel Box Girder Bridges, 1973.

30. Basler, K., and Thurlimann, B., "Plate Girder Resesearch," Proceedings of the National Engineering Conference, American Institute of Steel Construction, 1961.

31. Djubek, J., "The Design Theory of Slender Webplate Bars," Starebnicky Casopis, Sam XU, 8, Bratislava, 1967.

32. Lepre, U., "L'equilibre des plaques minces elastiques et plastiques á grande fléche," Rec. Ing., Vol. 34, 1956.

33. Wilson, J.M., "On Specifications for Strength of Iron Bridges," Trans. ASCE, Vol. 15, Part I, pp. 104-401, 489-490, 1886.

34. Basler, K., "Strength of Plate Girders in Shear," Journal of Structural Division, ASCE Proceedings, Vol. 87, No. ST7, October 1961, pp. 151-180.

35. Gaylord, E.H., Discussion of K. Basler, "Strength of Plate Girders in Shear," Trans. ASCE, Vol. 128, Part II, 1963, p. 712.

36. Fujii, T., "On an Improved Theory for Dr. Basler's Theory," IABSE 8th Cong., Final Report, New York, 1968.

37. Selberg, A., "On the Shear Capacity of Girder Webs," University of Trondheim Report, 1973.

38. Johnston, B.G. (Ed.), Guide to Stability Design Criteria for Metal Structures, 3rd. ed., John Wiley & Sons, Inc., New York, 1976.

39. Moore, R.L., "An Investigation of the Effectiveness of Stiffeners on Shear-Resistant Plate Girder Webs," NACA Tech. Note No. 862, 1942.

40. Stein, M., and Fralich, R.W., "Critical Shear Stress of Infinitely Long Simply Supported Plate With Transverse Stiffeners," J. Aeron. Sci., Vol. 17, 1950.

41. Salmon, C.G., and Johnson, J.E., Steel Structures, Intext Educational Publishers Corporation, November, 1972.

42. Sommerfeld, A., Z. fur Math Phys., Vol. 54, 1906.

43. Timoshenko, S.P., Z. fur Math Phys., Vol. 58, 1910.

44. Leggett, D.M.A., Proc. Cambridge Phil. Soc., Vol. 33, 1937.

45. Hopkins, H.G., Proc. Cambridge Phil. Soc., Vol. 45, 1947.

46. Yamaki, N., "Buckling of a Rectangular Plate Under Locally Distributed Force Applied on the Two Opposite Edges," 1st and 2nd Report, The Institute of High Speed Mechanics, Tohoku University, Japan, Vol. 3, 1953.

47. White, R.N., and Cottingham, W.S., "Stability of Plates under Partial Edge Loading, "Journal of Engineering Mechanics Division, ASCE Proceedings, Vol. 88, No. EM5, October 1962.

48. Khan, M.Z., and Johns, K.C., "Buckling of Web Plates under Combined Loadings," Universite de Sherbrooke, Sherbrooke, Quebec.

49. Winter, G., and Pian, R.H.J., "Crushing Strength of Thin Steel Webs," Cornell Bulletin No. 35, Part I, 1946.

50. Zetlin, Lev., "Elastic Instability of Flat Plates Subjected to Partial Edge Loads," Journal of the Structural Division, ASCE Proceedings, Vol. 81, September 1955.

51. Rockey, K.C., and Bagchi, D.K., "Buckling of Plate Girders Webs under Partial Edge Loadings," International Journal of Mechanical Science, Pergamon Press, Vol. 12, 1970.

52. Bagchi, D.K., and Rockey, K.C., "A Note on the Buckling of a Plate Girder Web Due to Partial Edge Loadings," International Association for Bridge and Structural Engineering, Final Report, September 1968.

53. Rockey, K.C., and El-gaaly, M.A., "Ultimate Strength of Plates When Subjected to In-Plane Patch Loading," International Association for Bridge and Structural Engineering, Proceedings of the Seminar on Design of Plate and Box Girders for Ultimate Strength, 1971.

54. Rockey, K.C., El-gaaly, M.A., and Bagchi, D.K., "Failure of Thin Walled Members under Patch Loading," Journal of Structural Division, ASCE Proceedings, Vol. 98, No. ST12, December 1972.

55. Rockey, K.C., and El-gaaly, M.A., "Stability of Load Bearing Trapezoidal Diaphragms," International Association for Bridge and Structural Engineering, Publications, Vol. 32-II, 1972.

56. Rockey, K.C., and El-gaaly, M.A., "Ultimate Strength of Plates When Subjected to In-Plane Patch Loading," International Association for Bridge and Structural Engineering, Colloquium on Design of Plate and Box Girders for Ultimate Strength, held in London, England, in March, 1971, published July 1972.

57. El-gaaly, M.A., and Rockey, K.C., "Ultimate Strength of Thin-Walled Members under Patch Loading and Bending," Current Research and Design Trends, Proceedings of the Second Specialty Conference on Cold-Formed Steel Structure, University of Missouri-Rolla, October 1973.

58. Girkmann, K., "Stability of the Webs of Plate Girders Taking Account of Concentrated Loads," Final Report, International Association for Bridge and Structural Engineering, 1936.

59. Khan, M.Z., Johns, K.C., and Hayman, B., "Buckling of Plates with Partially Loaded Edges," Journal of the Structural Division, ASCE Proceedings, Vol. 103, No. ST3, March 1977.

60. Basler, K., "New Provisions for Plate Girder Design," Proc., 1961, National Engineering Conference, AISC, New York.

61. Perry, D.J., Aircraft Structures, McGraw-Hill Book Company, 1950.

62. Winter, G., "Strength of Thin Steel Compression Flanges," Bulletin No. 35/3, Cornell University Engineering Experimental Station, Ithaca, New York, 1947.

63. Kalyanaraman, V., Pekoz, T., and Winter, G., "Unstiffened Compression Elements, Journal of the Structural Division, ASCE Proceedings, Vol. 103, No. ST9, September 1977.

64. Von Karman, T., Sechler, E.E., and Donnell, L.H., "Strength of Thin Plates in Compression," Transaction ASME, Vol. 54, APM 54-5, 1932.

65. Chwalla, E., "Theorie der Einseitig Angeordneten Stegblechsteife der Bauingenieur," Vol. 10, 1937.

66. American Association of State Highway and Transportation Officials, "Standard Specifications for Highway Bridges," 11th ed., 1973.

67. Barr, A.J., Goodnight, J.H., Sall, J.P., and Helwig, J.T., A User's Guide to SAS 76, Sparks Press of Raleigh, February 1977.

68. McGuire, W., Steel Structures, Prentice-Hall, Inc., 1968.

NOTATION

The following symbols are used in this report:

A_f = full area of the flange element, in inches^2;

A_s, A_{st} = cross-sectional area of tranverse stiffener in inches^2;

A_w = cross-sectional area of beam web, in inches^2;

a = distance between two transverse stiffeners, in inches;

b = effective width of plate element, in inches;

b_e = effective width of beam web, in inches;

$(b_e)_{comp}$ = computed effective width of beam web, in inches;

$(b_e)_{test}$ = tested effective width of beam web, in inches;

C_1, C_2 = correction factors for yield point of steel and corner radius;

D = flexural rigidity of plate

E = modulus of elasticity, in kips per square inch;

F_{cr} = critical vertical buckling stress, in kips per square inch;

F_b = applied bending stress, in kips per square inch;

F_b' = allowable bending stress in the compression flange, in kips per square inch;

F_s = axial force developed by the tension field, in kips;

F_w, F_v = allowable shear stress of transversely reinforced beam web, in kips per square inch;

F_y = yield point of material, in kips per square inch;

F_{ys} = yield point of stiffener steel, in kips per square inch;

F_{yw} = yield point of web steel, in kips per square inch;

f = actual stress in the compression flange, in kips per square inch;

f_c = maximum compressive bending stress in web, in kips per square inch;

f_{cr} = critical buckling stress in bending, in kips per square inch;

f_p = maximum bearing stress, in kips per square inch;

f_t = maximum tensile bending stress in web, in kips per square inch;

H = total length of transverse stiffener, in inches;

h = clear distance between flanges measured along the plane of the web, in inches;

I = moment of inertia of full section, in inches^4;

I_s = moment of inertia of transverse stiffener, in inches^4;

K = buckling coefficient in compressive patch load;

K_c = vertical buckling coefficient of a plate;

K_e = effective length factor for transverse stiffener column;

k = buckling coefficient in bending;

M_{cr} = bending moment computed on the basis of critical buckling stress of web element, in inch-kips;

$(M_u)_c$, $(M_u)_{comp}$ = computed ultimate bending moment, in inch-kips;

$(M_u)_{cr}$ = computed bending moment based on web buckling; in inch-kips;

$(M_u)_t$, $(M_u)_{test}$ = tested ultimate bending moment, in inch-kips;

M_y = computed bending moment governed by the flange yielding, in inch-kips;

$(M')_{test}$ = tested maximum bending moment of beam specimen, in inch-kips;

N = length of bearing plate, in inches;

n = number of half-waves;

P = concentrated patch load, in kips;

P_{cr} = theoretical buckling load, in kips;

$(P_{cr})_c$ = computed critical buckling load, in kips;

$(P_{cr})_{test}^f$ = tested critical flange buckling load, in kips;

$(P_{cr})_{test}^w$ = tested critical web buckling load, in kips;

P_u = ultimate web crippling load, in kips;

$(P_u)_c$, $(P_u')_c$ = computed web crippling load, in kips;

$(P_u)_t$ = tested web crippling load, in kips;

$(P_u)_{test}$ = failure load, in kips;

P_y = yield load of transverse stiffener, in kips;

$(P_y)_{test}$ = tested yield load of beam specimens in bending, in kips;

p = uniformly distributed patch load, in kips per linear inch;

Q = statical moment of area taken about the neutral axis, in inches^3;

R = inside bend corner radius, in inches;

r = radius of gyration of transverse stiffener cross section, in inches;

S_x = section modulus based on F_y, in inches^3;

S_x' = section modulus based on f_{cr}, in inches^3;

t = thickness of web steel, in inches;

$(V_{cr})_{test}$ = tested shear buckling force, in kips;

$(V_u)_{test}$ = tested shear force at failure, in kips;

w = flat-width of compression flange, in inches;

Y = ratio of web steel yield point to stiffener steel yield point;

α = aspect ratio of plate element;

α_1 = postbuckling strength factor in bending for h/t;

α_2 = postbuckling strength factor in bending for $|f_c/f_t|$;

α_3 = postbuckling strength factor in bending for $(w/t)/(w/t)_{lim}$;

α_4 = postbuckling strength factor in bending for F_y;

β = $|f_t/f_c|$ for plate in bending;

β = N/a or N/h for plate under patch loading;

θ = inclination of the tension field stress;

θ_d = angle of panel diagonal with flange;

μ = Poisson's ratio;

σ_t = tension field stress, in kips per square inch;

σ_y = yield point of steel; in kips per square inch;

τ_{avg}^{fail} = average shear stress at failure, in kips per square inch;

τ_{cr} = critical shear buckling stress, in kips per square inch;

τ_{cre} = critical elastic shear buckling stress, in kips per square inch;

τ_{cri} = critical inelastic shear buckling stress, in kips per square inch;

$(\tau_{cr})_{test}$ = tested critical shear buckling stress, in kips per square inch;

τ_{exact}^{fail} = failure shear stress based on beam theory in kips per square inch;

τ_{pr} = proportional limit in shear, in kips per square inch;

τ_u = theoretical ultimate shear stress, in kips per square inch;

τ_y = shear yield stress, in kips per square inch;

Φ = postbuckling strength factor in bending;
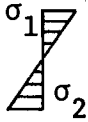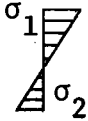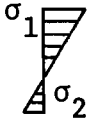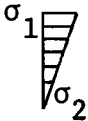
ϕ_c, ϕ_c' = postbuckling strength factor in web crippling;

ψ_1, ψ_2, ψ_3, ψ_4 = postbuckling strength factor under one-flange web crippling load for h/t, a/h, N/a and F_y;

ψ_1', ψ_2', ψ_3', ψ_4' = postbuckling strength factor under two-flange web crippling load for h/t, a/h, N/a and F_y;

TABLE 1
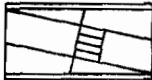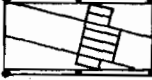
BUCKLING COEFFICIENT k FOR SIMPLY SUPPORTED PLATES SUBJECTED
TO NONUNIFORM LONGITUDINAL COMPRESSIVE STRESSES (14)

Type of Stress Distribution	$\alpha = a/h$							
	0.4	0.5	0.6	0.667	0.75	0.8	1.0	1.5
$\dfrac{\sigma_1}{\sigma_2} = -1$	29.1	25.6	24.1	23.9	24.1	24.4	25.6	24.1
$\dfrac{\sigma_1}{\sigma_2} = -\dfrac{3}{2}$	23.6	--	17.7	--	15.7	16.4	16.9	15.7
$\dfrac{\sigma_1}{\sigma_2} = -3$	18.7	--	12.9	—	11.5	11.2	11.0	11.5
$\dfrac{\sigma_1}{\sigma_2} = \infty$	15.1	--	9.7	--	8.4	8.1	7.8	8.4

σ_1 - Compressive bending stress

σ_2 - Tensile bending stress

TABLE 2

SUMMARY OF NUMEROUS MODELS ON
SHEAR STRENGTH OF PLATE GIRDERS (38)

Investigator	Mechanism	Web Buckling Edge Support
Basler		S / S S / S
Takeuchi		S / S S / S
Fujii		S / F S / F
Komatsu		S / F S / F
Chern and Ostapenko		S / F S / F
Rockey		S / S S / S
Höglund		S / S S / S
Horzoy		*
Sharp and Clark		S / F/2 S / F/2
Steinhardt and Schröter		S / S S / S

*Web buckling component neglected

TABLE 3

BUCKLING COEFFICIENT FOR SIMPLY SUPPORTED
PLATES PARTIALLY LOADED ON ONE EDGE

α \ β	0.25	0.50	0.75	1.00
0.33	10.0	11.00	12.40	13.70
0.50	6.60	7.33	8.45	9.55
0.75	4.38	4.94	5.82	6.78
1.00	3.42	3.90	4.65	5.57
2.00	2.41	2.59	2.84	3.15
3.00	2.72	2.43	2.66	2.95
4.00	2.21	2.34	2.54	2.80

TABLE 4

DIMENSIONS OF BENDING TEST SPECIMENS
(CHANNEL SECTIONS)

Beam Specimen No.	Cross-Section Dimensions (inches)												Span Length (in.)	ℓ (in.)
	Thick.	B1	B2	B3	B4	d1	d2	D1	D2	BB	BP	t_p		
B-1-1	0.0406	1.509	1.566	1.545	1.559	0.712	0.680	8.680	8.644	7	--	—	86	26.00
B-1-2	0.0405	1.562	1.606	1.616	1.566	0.696	0.698	8.575	8.605	7	--	--	86	26.00
B-2-1	0.0415	1.525	1.560	1.536	1.582	0.686	0.624	11.750	11.625	7	--	--	105	35.00
B-2-2	0.0411	1.572	1.550	1.575	1.600	0.661	0.641	11.656	11.656	7	--	--	105	35.00
B-3-1	0.0420	1.550	1.561	1.549	1.546	0.662	0.663	13.375	13.438	7	--	--	112	36.00
B-3-2	0.0415	1.560	1.575	1.560	1.575	0.661	0.660	13.406	13.406	7	--	--	112	36.00
B-19-1*	0.0490	1.494	1.464	1.463	1.480	0.635	0.672	9.828	9.833	9	--	--	136	48.00
B-19-2*	0.0465	1.492	1.457	1.455	1.478	0.647	0.652	9.769	9.789	9	--	--	136	48.00
B-20-1*	0.0466	1.504	1.481	1.472	1.471	0.656	0.658	12.390	12.450	9	--	--	136	43.13
B-20-2*	0.0460	1.487	1.456	1.489	1.488	0.639	0.628	12.390	12.400	9	--	--	136	43.13
MB-19-1*	0.0479	1.477	1.474	1.488	1.503	0.645	0.632	9.753	9.768	9	6.089	0.0488	136	48.00
MB-19-2*	0.0489	1.480	1.521	1.469	1.501	0.646	0.624	9.831	9.789	9	6.089	0.0488	136	48.00
MB-20-1*	0.0465	1.457	1.447	1.459	1.455	0.662	0.643	12.380	12.380	9	8.023	0.0490	136	43.13
MB-20-2*	0.0491	1.477	1.466	1.490	1.472	0.652	0.627	12.410	12.380	9	8.023	0.0490	136	43.13

Notes: 1. See Fig. 8 for the symbols used for dimensions
2. Inside bend radius was assumed to be equal to thickness
3. See Fig. 11 for the definition of ℓ
4. Beam specimens are designated as follows:

B	-	3	-	2
Beam Section		Channel No.		Test No.

5. *These test specimens have been reported in Ref. 5

TABLE 5

DIMENSIONS OF BENDING TEST SPECIMENS
(HAT SECTIONS)

Beam Specimen No.	Cross-Section Dimensions (inches)								Span Length (in.)	ℓ (in.)
	Thick. (in.)	B1	B2	B3	D1	D2	BPL	t_p		
H-5-1*	0.0498	9.775	1.373	1.474	9.725	9.810	--	--	136.00	48.00
H-5-2*	0.0480	9.808	1.424	1.396	9.836	9.685	--	--	136.00	48.00
H-6-1*	0.0505	12.450	1.784	1.812	12.390	12.460	--	--	136.00	43.13
H-6-2*	0.0490	12.420	1.800	1.781	12.410	12.500	--	--	136.00	43.13
H-7-1*	0.0484	9.796	3.393	3.339	9.833	9.653	6.089	0.0488	136.00	48.00
H-7-2*	0.0492	9.780	3.284	3.422	9.723	9.781	6.089	0.0488	136.00	48.00
H-8-1*	0.0490	12.500	4.588	4.744	12.500	12.390	6.089	0.0488	136.00	43.13
H-8-2*	0.0470	12.400	4.657	4.735	12.430	12.410	6.089	0.0488	136.00	43.13

Notes: 1. See Fig. 9 for the symbols used for dimensions
        2. Inside bend radius was assumed to be equal to thickness
        3. See Fig. 11 for definition of ℓ
        4. Beam specimens are designated as follows:

| H   -   5   -   2 |
| Hat Section   Channel No.   Test No. |

        5. *These test specimens have been reported in Ref.5

TABLE 6

PERTINENT PARAMETERS OF BENDING TEST SPECIMENS

Beam Specimen No.	h/t	w/t	$(w/t)_{lim}$	F_y (ksi)	f_c/f_t	$a*$ (in.)
B-1-1	211.35	33.87	30.84	51.24	0.99	26.00
B-1-2	210.10	35.11	30.84	51.24	0.98	26.00
B-2-1	279.63	33.17	30.84	51.24	1.00	35.00
B-2-2	281.60	33.98	30.84	51.24	0.99	35.00
B-3-1	317.20	33.04	30.84	51.24	1.00	36.00
B-3-2	321.04	33.77	30.84	51.24	0.99	36.00
B-19-1	209.46	26.49	33.35	43.82	1.00	16.00
B-19-2	208.52	28.09	33.35	43.82	1.00	16.00
B-20-1	265.17	28.27	33.35	43.82	1.00	14.38
B-20-2	267.57	28.33	33.35	43.82	1.00	14.38
MB-19-1	201.92	26.84	33.35	43.82	1.46	16.00
MB-19-2	198.61	27.10	33.35	43.82	1.44	16.00
MB-20-1	264.24	27.33	33.35	43.82	1.52	14.38
MB-20-2	250.75	26.08	33.35	43.82	1.49	14.38
H-5-1	194.99	192.29	33.35	43.82	0.92	16.00
H-5-2	202.92	200.33	33.35	43.82	0.92	16.00
H-6-1	244.73	242.53	33.35	43.82	0.92	14.38
H-6-2	253.10	249.47	33.35	43.82	0.93	14.38
H-7-1	201.16	198.40	33.35	43.82	1.59	16.00
H-7-2	198.80	194.78	33.35	43.82	1.58	16.00
H-8-1	253.10	251.10	33.35	43.82	1.53	14.38
H-8-2	262.47	259.83	33.35	43.82	1.56	14.38

*a equals to the unsupported length in the middle third of the test specimens

TABLE 7

MECHANICAL PROPERTIES OF
STEEL SHEETS

F_y (ksi)	F_u (ksi)	Elongation Percent*	Comments
53.79	73.08	29	Sharp Yielding
51.24	59.82	15	Sharp Yielding
47.63	59.96	18	Sharp Yielding
44.80	60.66	38	Sharp Yielding
44.07	51.09	36	Sharp Yielding
43.82	55.73	29	Sharp Yielding
43.06	50.74	35	Sharp Yielding
41.18	49.50	38	Sharp Yielding
39.64	48.44	42	Sharp Yielding
38.80	49.90	42	Sharp Yielding
36.88	48.31	32	Sharp Yielding
33.46	49.94	28	Gradual Yielding

*2-in. gage length

TABLE 8

EXPERIMENTAL DATA FOR BENDING TEST SPECIMENS

Beam Specimen No.	$(P_{cr})^w_{test}$ (kips)	$(P_{cr})^f_{test}$ (kips)	$(P_y)_{test}$ (kips)	$(P_u)_{test}$ (kips)	$(M_u)_{test}$ (in-kips)	Failure Mode
B-1-1	2.68	--	--	5.96	77.48	WB
B-1-2	2.50	--	--	6.25	81.25	WB
B-2-1	2.15	--	--	6.43	112.53	WB
B-2-2	2.00	--	--	6.40	112.00	WB
B-3-1	1.50	--	--	7.20	129.60	WB
B-3-2	1.75	--	--	7.38	132.84	WB
B-19-1	0.80	--	--	4.70	112.80	WB
B-19-2	2.10	--	--	4.75	114.00	WB
B-20-1	1.10	--	--	5.90	127.22	WB
B-20-2	1.40	--	--	6.35	136.92	WB
MB-19-1	1.10	--	5.00	5.10	122.40	WB-FY
MB-19-2	1.10	--	4.90	5.27	126.48	WB-FY
MB-20-1	1.10	--	6.53	6.60	142.31	WB-FY
MB-20-2	1.60	--	--	6.65	143.39	WB
H-5-1	1.40	0.81	--	4.03	96.72	FB-WB-FY
H-5-2	1.00	0.50	--	3.85	92.40	FB-WB-FY
H-6-1	1.10	0.60	--	5.73	123.55	FB-WB-FY
H-6-2	1.20	0.80	--	5.70	122.91	FB-WB-FY
H-7-1	0.80	0.60	--	4.30	103.20	FB-WB-FY
H-7-2	0.90	0.60	--	4.20	100.80	FB-WB-FY
H-8-1	1.40	0.80	--	6.27	135.20	FB-WB-FY
H-8-2	1.30	0.81	--	6.00	129.38	FB-WB-FY

Note: Failure modes are designated as follows:
WB : web buckling
WB-FY : web buckling followed by flange yielding
FB-WB-FY : flange buckling followed by web buckling and flange yielding

TABLE 9

COMPARISON OF EXPERIMENTAL AND THEORETICAL DATA FOR BENDING TEST SPECIMENS

Beam Specimen No.	$(P_{cr})^w_{theo}$ (kips)	$(P_{cr})^f_{theo}$ (kips)	$(P_y)_{theo}$ (kips)	$\dfrac{(P_{cr})^w_{test}}{(P_{cr})^w_{theo}}$	$\dfrac{(P_{cr})^f_{test}}{(P_{cr})^f_{theo}}$	$\dfrac{(P_y)_{test}}{(P_y)_{theo}}$	$\dfrac{(P_u)_{test}}{(P_{cr})^w_{theo}}$
B-1-1	2.66	--	9.38	1.008	--	--	2.241
B-1-2	2.68	--	9.26	0.933	--	--	2.332
B-2-1	1.79	--	11.10	1.201	--	--	3.592
B-2-2	1.74	--	10.92	1.149	--	--	3.575
B-3-1	1.69	--	13.47	0.888	--	--	4.260
B-3-2	1.63	--	13.32	1.074	--	--	4.528
B-19-1	1.93	--	5.81	0.415	--	--	2.435
B-19-2	2.06	--	6.16	1.019	--	--	2.306
B-20-1	1.94	--	9.37	0.567	--	--	3.041
B-20-2	1.86	--	9.16	0.753	--	--	3.414
MB-19-1	1.61	--	6.87	0.683	--	0.728	3.168
MB-19-2	1.72	--	7.09	0.640	--	0.691	3.064
MB-20-1	1.49	--	10.92	0.738	--	0.598	4.430
MB-20-2	1.76	--	11.58	0.909	--	--	3.778
H-5-1	2.52	0.55	5.04	0.614	1.473	--	1.599
H-5-2	2.24	0.49	4.80	0.493	1.020	--	1.719
H-6-1	2.92	0.64	8.67	0.415	0.938	--	1.962
H-6-2	2.60	0.59	8.41	0.504	1.356	--	2.192
H-7-1	1.79	0.61	6.05	0.447	0.984	--	2.402
H-7-2	1.90	0.64	6.18	0.474	0.938	--	2.211
H-8-1	2.06	0.70	10.42	0.680	1.143	--	3.044
H-8-2	1.84	0.62	9.90	0.707	1.306	--	3.261

TABLE 10

COMPARISON OF EXPERIMENTAL AND COMPUTED ULTIMATE BENDING CAPACITIES
OF BENDING TEST SPECIMENS

Beam Specimen No.	f_{cr} (ksi)	S_x (in.^{3})	$M_{cr}=S_x f_{cr}$ (in-kips)	$(M_u)_{cr}=\phi M_{cr}$ (in-kips)	F_y (ksi)	S'_x (in.^{3})	$M_y=S'_x F_y$ (in-kips)	$(M_u)_{test}$ (in-kips)	$\dfrac{(M_u)_{test}}{(M_u)_{comp}}$*
B-1-1	14.33	2.41	34.54	92.04	51.24	2.38	121.95	77.48	0.842
B-1-2	14.50	2.40	34.80	91.11	51.24	2.35	120.41	81.25	0.892
B-2-1	8.18	3.83	31.33	118.65	51.24	3.79	194.20	112.53	0.948
B-2-2	8.07	3.78	30.50	115.90	51.24	3.73	191.13	112.00	0.966
B-3-1	6.36	4.77	30.34	134.07	51.24	4.73	242.37	129.60	0.967
B-3-2	6.21	4.73	29.37	130.46	51.24	4.68	239.80	132.84	1.018
B-19-1	16.15	3.18	51.36	115.50	43.82	3.18	139.54	112.80	0.977
B-19-2	14.69	3.37	49.51	118.96	43.82	3.37	147.85	114.00	0.958
B-20-1	9.11	4.61	42.00	134.77	43.82	4.61	201.99	127.22	0.944
B-20-2	8.91	4.51	40.18	130.88	43.82	4.51	197.53	136.92	1.046
MB-19-1	10.28	3.76	38.65	107.73	43.82	3.76	164.93	122.40	1.136
MB-19-2	10.61	3.88	41.17	111.69	43.82	3.88	170.09	126.48	1.132
MB-20-1	6.00	5.38	32.28	128.89	43.82	5.38	235.56	142.31	1.104
MB-20-2	6.67	5.70	38.02	141.54	43.82	5.70	249.68	143.39	1.013
H-5-1	18.51	3.20	59.25	96.76	43.82	2.76	120.94	96.72	1.000
H-5-2	17.10	3.08	52.75	90.26	43.82	2.63	115.25	92.40	1.024
H-6-1	11.75	5.26	61.79	135.13	43.82	4.27	186.95	123.55	0.914
H-6-2	10.82	5.14	55.64	127.54	43.82	4.14	181.29	122.91	0.964
H-7-1	10.34	4.16	43.01	96.08	43.82	3.32	145.30	103.20	1.074
H-7-2	10.81	4.22	45.60	99.59	43.82	3.38	148.32	100.80	1.012
H-8-1	6.53	6.80	44.43	130.84	43.82	5.13	224.76	135.20	1.033
H-8-2	6.08	6.51	39.57	123.62	43.82	4.87	213.55	129.38	1.047

Mean									1.001
Standard Deviation									0.072

*The value of $(M_u)_{comp}$ is determined by $(M_u)_{cr}$ or M_y whichever is smaller.
The values of S_x and S'_x were computed on the basis of f_{cr} and F_y, respectively.

TABLE 11

CROSS SECTION DIMENSIONS OF SHEAR TEST SPECIMENS

Beam Specimen No.	Cross-Section Dimensions (in.)												
	Thick.	B1	B2	B3	B4	d1	d2	D1	D2	BB	TFPL	BFPL	TPL
S-1-1	0.0502	1.756	1.746	1.892	1.885	0.514	0.527	7.399	7.391	7	3.484	3.488	0.1004
S-1-2	0.0500	1.875	1.875	1.724	1.745	0.520	0.502	7.342	7.376	7	3.492	3.488	0.1004
S-1-3	0.0498	1.750	1.741	1.884	1.875	0.506	0.508	7.377	7.383	7	3.484	3.488	0.1004
S-1-4	0.0505	1.873	1.885	1.742	1.746	0.513	0.510	7.391	7.385	7	3.844	3.840	0.1004
S-1-5	0.0503	1.875	1.882	1.745	1.740	0.524	0.515	7.415	7.425	7	3.840	3.844	0.1004
S-2-1	0.0384	1.319	1.328	1.289	1.294	0.575	0.561	5.917	5.915	7	2.454	2.450	0.0764
S-2-2	0.0384	1.295	1.299	1.282	1.281	0.555	0.540	5.960	5.958	7	2.450	2.454	0.0764
S-2-3	0.0382	1.375	1.308	1.280	1.205	0.514	0.550	5.951	6.075	7	2.460	2.460	0.0382
S-2-4	0.0382	1.184	1.267	1.280	1.175	0.563	0.555	6.112	6.122	7	2.464	2.464	0.0382
S-3-1	0.0460	2.961	2.966	2.925	2.908	0.641	0.721	7.045	7.091	7	--	--	--
S-3-2	0.0458	2.910	2.963	2.970	2.938	0.688	0.652	7.079	7.092	7	--	--	--
S-3-3	0.0457	3.001	2.981	3.005	2.985	0.625	0.592	7.155	7.198	7	--	--	--
S-3-4	0.0460	2.962	2.975	2.998	2.994	0.587	0.604	7.226	7.190	7	--	--	--
S-3-5	0.0457	2.992	2.960	2.944	2.950	0.643	0.696	7.051	7.068	7	--	--	--
S-3-6	0.0458	2.932	2.983	2.968	2.971	0.642	0.629	7.074	7.248	7	5.948	5.952	0.0495
S-3-7	0.0465	2.973	2.922	2.918	2.975	0.633	0.693	7.105	7.045	7	5.948	5.952	0.0495
S-4-1	0.0382	2.362	2.353	2.373	2.370	0.550	0.576	6.112	6.093	7	4.712	4.716	0.0382
S-4-2	0.0382	2.371	2.371	2.340	2.340	0.526	0.601	6.078	6.075	7	4.714	4.714	0.0382
S-4-3	0.0381	2.373	2.390	2.365	2.304	0.582	0.641	6.008	6.000	7	--	--	--
S-4-4	0.0388	2.392	2.397	2.360	2.321	0.556	0.620	6.012	5.760	7	--	--	--
S-5-1	0.0380	2.383	2.370	2.353	2.360	0.541	0.533	8.101	8.045	7	--	--	--
S-5-2	0.0381	2.362	2.368	2.340	2.355	0.532	0.553	8.105	8.073	7	--	--	--
S-6-1	0.0381	2.325	2.327	2,263	2.265	0.578	0.658	9.966	9.981	7	--	--	--
S-6-2	0.0378	2.354	2.355	2.318	2.318	0.482	0.608	10.023	10.016	7	--	--	--
S-7-1	0.0381	0.259	1.253	1.216	1.185	0.580	0.635	9.881	9.958	7	3.028	3.032	0.0382
S-7-2	0.0379	1.295	1.269	1.247	1.207	0.473	0.562	9.933	9.954	7	3.032	3.028	0.0382

TABLE 11 (continued)

Beam Specimen No.	Cross-Section Dimensions (in.)												
	Thick.	B1	B2	B3	B4	d1	d2	D1	D2	BB	TFPL	BFPL	TPL
S-7-3	0.0385	1.255	1.253	1.227	1.224	0.549	0.568	9.949	9.940	7	3.030	3.030	0.0382
S-7-4	0.0391	1.261	1.264	1.247	1.241	0.557	0.578	9.937	9.889	7	3.026	3.034	0.0382
S-8-1	0.0409	1.555	1.550	1.575	1.575	0.680	0.701	8.652	8.630	7	--	--	--
S-8-2	0.0402	1.535	1.552	1.583	1.575	0.683	0.701	8.627	8.716	7	--	--	--
S-9-1	0.0383	1.265	1.273	1.255	1.255	0.591	0.568	11.700	11.688	7	3.030	3.036	0.0382
S-9-2	0.0379	1.314	1.289	1.240	1.277	0.562	0.593	11.656	11.688	7	3.028	3.032	0.0382

Notes: 1. See Figures 8 and 21 for the symbols used for dimensions.
2. Inside bend radius was assumed to be equal to thickness.
3. Shear specimens are designated as follows:

$$S \quad - \quad 9 \quad - \quad 1$$

S	9	1
Shear Test Section	Channel No.	Test No.

123

TABLE 12

DETAILS OF ADDITIONAL COVER PLATES AND SIDE CHANNELS
(TEST SETUP-C)

Beam Specimen No.	Plate Dimensions (in.)				Channel Dimensions (in.)			
	ATFP	ABFP	TAPL	Length	D	B	d	t
S-2-3	--	--	--	--	3.95	1.50	0.5	0.0480
S-2-4	--	--	--	--	3.95	1.50	0.5	0.0480
S-4-3	4.708	4.712	0.0382	10	3.95	1.50	0.5	0.0480
S-4-4	4.712	4.708	0.0382	10	3.95	1.50	0.5	0.0480
S-5-1	4.714	4.714	0.0382	12	5.95	1.20	0.5	0.0395
S-5-2	4.708	4.712	0.0382	12	5.95	1.20	0.5	0.0395
S-6-1	4.712	4.708	0.0382		7.88	1.20	0.5	0.0395
S-6-2	4.714	4.714	0.0382	20	7.88	1.20	0.5	0.0395
S-7-1	--	--	--	--	7.88	1.20	0.5	0.0395
S-7-2	--	--	--	--	7.88	1.20	0.5	0.0395
S-7-3	3.028	3.032	0.0382	9	--	--	--	--
S-7-4	3.030	3.030	0.0382	9	--	--	--	--
S-9-1	3.032	3.028	0.0382	19	9.83	1.20	0.5	0.0395
S-9-2	3.030	3.030	0.0382	19	9.83	1.20	0.5	0.0395

Notes: 1. Refer to Fig. 28 for the symbols used for dimensions.
2. See Fig. 23 for the location of side channels

TABLE 13

PERTINENT PARAMETERS OF SHEAR TEST SPECIMENS

Beam Specimen No.	h/t	w/t	$(w/t)_{lim}$	a/h	Span Length (in.)	F_y (ksi)
S-1-1	145.31	30.88	25.55	0.994	17.000	44.80
S-1-2	145.18	33.50	25.55	0.809	14.250	44.80
S-1-3	146.19	31.05	25.55	1.013	17.250	44.80
S-1-4	144.30	33.21	25.55	1.492	24.250	44.80
S-1-5	145.51	33.35	25.55	1.973	31.375	44.80
S-2-1	152.06	30.47	25.76	1.009	14.278	44.07
S-2-2	153.18	29.78	25.76	1.001	14.278	44.07
S-2-3	155.41	31.12	25.76	0.979	14.125	44.07
S-2-4	158.13	28.08	25.76	0.962	14.125	44.07
S-3-1	151.65	60.42	29.56	1.003	16.500	33.46
S-3-2	152.72	60.12	29.56	1.001	16.500	33.46
S-3-3	155.05	61.45	29.56	0.988	21.000	33.46
S-3-4	154.70	60.53	29.56	0.984	21.000	33.46
S-3-5	152.49	61.12	29.56	3.014	31.500	33.46
S-3-6	154.35	60.57	29.56	2.971	31.500	33.46
S-3-7	150.15	59.39	29.56	3.008	31.500	33.46
S-4-1	157.76	57.74	25.76	0.977	14.278	44.07
S-4-2	157.08	58.07	25.76	0.981	14.278	44.07
S-4-3	155.59	58.51	25.76	0.981	17.440	44.07
S-4-4	149.70	57.71	25.76	1.001	17.440	44.07
S-5-1	210.45	58.54	25.76	0.985	23.625	44.07
S-5-2	210.31	58.07	25.76	0.983	23.625	44.07
S-6-1	259.78	57.05	25.76	1.402	26.016	44.07
S-6-2	263.08	58.29	25.76	1.395	26.016	44.07
S-7-1	258.37	28.97	25.76	0.991	29.250	44.07
S-7-2	260.37	29.83	25.76	0.988	29.250	44.07
S-7-3	256.31	28.57	25.76	0.494	14.625	44.07
S-7-4	251.53	28.29	25.76	0.496	14.625	44.07
S-8-1	209.27	33.96	23.89	0.993	19.500	51.24
S-8-2	213.72	34.40	23.89	0.989	19.500	51.24
S-9-1	303.33	29.13	25.76	1.001	34.875	44.07
S-9-2	305.97	30.34	25.76	1.003	34.875	44.07

TABLE 14

EXPERIMENTAL DATA FOR SHEAR TEST SPECIMENS

Beam Specimen No.	$(P_u)_{test}$ (kips)	$(P_{cr})_{test}$ (kips)	$(V_u)_{test}$ (kips)	$(V_{cr})_{test}$ (kips)	$(M')_{test}$ (in-kips)	$(\tau_{cr})_{test}$ (ksi)	τ^{fail}_{exact} (ksi)	τ^{fail}_{ave} (ksi)	$\dfrac{\tau^{fail}_{exact}}{\tau^{fail}_{ave}}$
S-1-1(A)*	28.02	14.25	14.01	7.13	105.08	9.74	20.77	19.13	1.086
S-1-2(A)	30.28	15.09	15.14	7.55	88.95	10.40	21.16	20.86	1.014
S-1-3(A)	26.04	11.02	13.02	5.51	96.02	7.60	19.47	17.96	1.084
S-1-4(A)	23.16	10.98	11.58	5.49	125.93	7.46	16.69	15.73	1.061
S-1-5(A)	20.22	7.80	10.11	3.90	145.97	5.30	14.54	13.73	1.059
S-2-1(A)	16.30	9.46	8.15	4.73	48.00	10.55	19.68	18.17	1.083
S-2-2(A)	15.60	7.50	7.80	3.75	45.93	8.30	18.69	17.27	1.082
S-2-3(B)	23.10	12.97	7.70	4.32	44.76	9.52	18.97	16.98	1.117
S-2-4(B)	24.51	13.03	8.17	4.34	47.49	9.40	20.05	17.70	1.168
S-3-1(A)	19.03	9.55	9.52	4.78	66.64	7.45	16.84	14.83	1.136
S-3-2(A)	19.61	11.15	9.81	5.58	68.67	8.71	17.33	15.30	1.133
S-3-3(C)	19.11	12.98	9.56	6.49	66.92	10.02	16.65	14.75	1.129
S-3-4(C)	19.57	10.75	9.79	5.38	68.53	8.22	16.97	14.95	1.135
S-3-5(D)	18.38	13.75	6.13	4.58	64.31	7.14	10.86	9.55	1.137
S-3-6(D)	20.27	13.25	6.76	4.42	70.93	6.68	10.92	10.21	1.070
S-3-7(D)	20.48	15.25	6.83	5.08	73.61	7.79	11.24	10.47	1.074
S-4-1(B)	16.30	7.51	8.15	3.76	48.00	8.17	19.14	17.70	1.081
S-4-2(B)	15.98	6.99	7.99	3.50	47.05	7.63	18.78	17.43	1.077
S-4-3(B)	23.30	15.01	7.77	5.00	45.17	11.07	19.58	17.20	1.138
S-4-4(B)	25.00	14.55	8.33	4.85	48.42	10.76	20.98	18.48	1.135
S-5-1(B)	26.08	--	8.69	--	68.43	--	16.64	14.30	1.164
S-5-2(B)	28.11	13.04	9.37	4.35	73.79	7.12	17.88	15.35	1.165
S-6-1(B)	24.03	5.49	8.01	1.83	69.46	2.43	12.67	10.62	1.193
S-6-2(B)	24.21	4.50	8.07	1.50	69.98	2.00	12.87	10.73	1.199
S-7-1(B)	30.56	--	10.68	--	99.30	--	15.88	13.58	1.169
S-7-2(B)	29.15	6.53	10.53	2.18	94.74	2.91	15.22	12.99	1.172

TABLE 14 (continued)

Beam Specimen No.	$(P_u)_{test}$ (kips)	$(P_{cr})_{test}$ (kips)	$(V_u)_{test}$ (kips)	$(V_{cr})_{test}$ (kips)	$(M')_{test}$ (in-kips)	$(\tau_{cr})_{test}$ (ksi)	τ_{exact}^{fail} (ksi)	τ_{ave}^{fail} (ksi)	$\dfrac{\tau_{exact}^{fail}}{\tau_{ave}^{fail}}$
S-7-3(B)	44.06	--	14.69	--	71.60	--	21.48	18.37	1.169
S-7-4(B)	46.59	19.51	15.53	6.50	75.71	8.52	22.60	19.33	1.169
S-8-1(A)	20.21	6.75	10.11	3.38	85.94	4.83	17.58	14.43	1.218
S-8-2(A)	20.92	7.75	10.46	3.88	88.91	5.62	18.49	15.14	1.221
S-9-1(B)	34.01	7.01	11.34	2.34	131.77	2.63	15.10	12.74	1.185
S-9-2(B)	34.04	6.50	11.35	2.17	131.91	2.47	15.28	12.90	1.184

*Denotes test setup which was used

TABLE 15

ULTIMATE BENDING MOMENT CAPACITY OF SHEAR TEST SPECIMENS

Beam Specimen No.	f_{cr} (ksi)	S_x (in.^{3})	$(M_u)_{cr}$ (in-kips)	S'_x (in.^{3})	M_y (in-kips)	$(M_u)_{comp}$ (in-kips)
S-1-1	29.04	5.061	214.98	4.454	199.54	199.54
S-1-2	29.09	5.075	212.94	4.399	197.08	197.08
S-1-3	28.69	5.022	212.43	4.422	198.11	198.11
S-1-4	29.45	5.386	227.03	4.955	221.98	221.98
S-1-5	28.96	5.411	226.92	5.075	227.36	226.92
S-2-1	26.52	2.333	95.60	2.073	91.36	91.36
S-2-2	26.13	2.338	95.70	2.079	91.62	91.62
S-2-3*	25.39	1.813	73.13	1.546	68.13	68.13
S-2-4*	24.52	1.819	73.68	1.567	69.06	69.06
S-3-1	26.66	2.631	76.06	1.881	62.94	62.94
S-3-2	26.29	2.646	76.32	1.888	63.17	63.17
S-3-3	25.51	2.681	76.19	2.117	70.83	70.83
S-3-4	25.63	2.670	77.15	2.123	71.04	71.04
S-3-5	26.73	2.633	76.08	2.259	75.59	75.59
S-3-6	26.89	4.790	139.60	4.482	149.97	139.60
S-3-7	27.44	4.699	137.76	4.405	147.39	137.76
S-4-1	24.64	2.669	93.19	2.270	100.04	93.19
S-4-2	24.85	2.645	92.43	2.252	99.25	92.43
S-4-3*	25.33	1.560	54.70	2.288	100.83	100.83
S-4-4*	27.36	1.530	55.10	2.249	99.11	99.11
S-5-1*	13.85	2.488	71.64	3.413	150.41	150.41
S-5-2*	13.86	2.497	72.10	3.419	150.68	150.68
S-6-1*	9.09	3.453	85.56	4.544	200.25	200.25
S-6-2*	8.86	3.420	83.35	4.515	198.98	198.98
S-7-1*	9.19	3.414	97.91	3.486	153.63	153.63
S-7-2*	9.05	3.401	96.55	3.456	152.31	152.31

TABLE 15 (continued)

Beam Specimen No.	f_{cr} (ksi)	S_x (in.^{3})	$(M_u)_{cr}$ (in-kips)	S'_x (in.^{3})	M_y (in-kips)	$(M_u)_{comp}$ (in-kips)
S-7-3	9.33	3.421	98.93	4.438	195.58	195.58
S-7-4	9.69	3.465	101.79	4.461	196.60	196.60
S-8-1	14.00	2.519	93.25	2.097	107.45	93.25
S-8-2	13.43	2.485	90.41	2.063	105.71	90.41
S-9-1*	6.67	3.966	99.96	5.802	255.69	255.69
S-9-2*	6.55	4.014	99.87	5.753	253.53	253.53

Notes: 1. *Web buckling is prevented by providing a side channel as shown in Fig. 23.
   2. If web buckling is prevented, $(M_u)_{comp}$ equals to M_y, otherwise $(M_u)_{comp}$ is determined by $(M_u)_{cr}$ or M_y, whichever is smaller.

TABLE 16

COMPARISON OF EXPERIMENTAL AND THEORETICAL DATA
FOR SHEAR TEST SPECIMENS

Beam Specimen No.	Theoretical Data				$\dfrac{(\tau_{cr})_{test}}{\tau_{cr}}$	$\dfrac{\tau_{ave}^{fail}}{\tau_{cr}}$	$\dfrac{\tau_{exact}^{fail}}{\tau_y}$	$\dfrac{\tau_{ave}^{fail}}{\tau_y}$	$\dfrac{\tau_{ave}^{fail}}{\tau_u}$
	τ_y (ksi)	τ_{cr} (ksi)	τ_u (ksi)	$(M_u)_{comp}$ (in-kips)					
S-1-1	25.87	11.88	16.92	199.54	0.820	1.610	0.803	0.739	1.131
S-1-2	25.87	15.37	19.71	197.08	0.677	1.357	0.818	0.806	1.058
S-1-3	25.87	11.52	16.62	198.11	0.660	1.559	0.753	0.694	1.081
S-1-4	25.87	9.14	13.54	221.98	0.816	1.721	0.645	0.608	1.162
S-1-5	25.87	8.02	11.71	226.92	0.661	1.712	0.562	0.531	1.173
S-2-1	25.94	10.69	15.95	91.36	0.987	1.700	0.774	0.714	1.139
S-2-2	25.44	10.60	15.92	91.62	0.783	1.629	0.735	0.679	1.085
S-2-3	25.44	10.56	15.98	68.13	0.902	1.608	0.746	0.667	1.063
S-2-4	25.44	10.41	15.95	69.06	0.903	1.700	0.788	0.696	1.110
S-3-1	19.32	10.80	13.85	62.94	0.690	1.373	0.872	0.768	1.071
S-3-2	19.32	10.67	13.77	63.17	0.816	1.434	0.897	0.792	1.111
S-3-3	19.32	10.51	13.69	70.83	0.953	1.403	0.862	0.763	1.077
S-3-4	19.32	10.61	13.77	71.04	0.775	1.409	0.878	0.774	1.086
S-3-5	19.32	6.72	8.48	75.59	1.063	1.421	0.562	0.494	1.126
S-3-6	19.32	6.77	8.55	139.60	0.987	1.508	0.565	0.528	1.194
S-3-7	19.32	6.90	8.64	137.76	1.129	1.517	0.542	0.542	1.212
S-4-1	25.44	10.28	15.81	93.19	0.795	1.722	0.696	0.696	1.120
S-4-2	25.44	10.31	15.81	92.43	0.740	1.691	0.685	0.685	1.102
S-4-3	25.44	10.52	15.95	100.83	1.052	1.635	0.770	0.676	1.078
S-4-4	25.44	11.10	16.25	99.11	0.969	1.665	0.825	0.726	1.137
S-5-1	25.44	5.72	12.87	150.41	--	2.500	0.654	0.562	1.111
S-5-2	25.44	5.74	12.90	150.68	1.240	2.674	0.703	0.603	1.190
S-6-1	25.44	2.91	9.16	200.25	0.835	3.649	0.498	0.417	1.159
S-6-2	25.44	2.85	9.14	198.98	0.702	3.765	0.506	0.422	1.174
S-7-1	25.44	3.77	11.60	153.63	--	3.602	0.624	0.534	1.171
S-7-2	25.44	3.72	11.58	152.31	0.782	3.492	0.598	0.511	1.122

TABLE 16 (continued)

Beam Specimen No.	Theoretical Data				$\dfrac{(\tau_{cr})_{test}}{\tau_{cr}}$	$\dfrac{\tau^{fail}_{ave}}{\tau_{cr}}$	$\dfrac{\tau^{fail}_{exact}}{\tau_{y}}$	$\dfrac{\tau^{fail}_{ave}}{\tau_{y}}$	$\dfrac{\tau^{fail}_{ave}}{\tau_{u}}$
	τ_y (ksi)	τ_{cr} (ksi)	τ_u (ksi)	$(M_u)_{comp}$ (in-kips)					
S-7-3	25.44	10.50	18.54	195.58	--	1.750	0.844	0.722	0.991
S-7-4	25.44	10.84	18.69	196.60	0.786	1.783	0.888	0.760	1.034
S-8-1	29.58	5.73	14.33	93.25	0.843	2.518	0.594	0.488	1.007
S-8-2	29.58	5.52	14.22	90.41	1.018	2.743	0.625	0.512	1.065
S-9-1	25.44	2.71	10.86	255.69	0.970	4.701	0.594	0.501	1.173
S-9-2	25.44	2.65	10.82	253.53	0.932	4.868	0.601	0.507	1.192
Mean									1.116
Standard Deviation									0.055

TABLE 17

COMPARISON OF THEORETICAL AND PREDICTED VALUES OF
BUCKLING COEFFICIENT FOR SIMPLY SUPPORTED PLATES
PARTIALLY LOADED ON ONE EDGE

α	β	K_{comp}	K_{theo}	$\dfrac{K_{theo}}{K_{comp}}$
0.33	0.25	9.97	10.00	1.003
0.33	0.50	10.85	11.00	1.014
0.33	0.75	12.30	12.40	1.008
0.33	1.00	14.33	13.70	0.956
0.50	0.25	6.63	6.60	0.995
0.50	0.50	7.21	7.33	1.017
0.50	0.75	8.18	8.45	1.033
0.50	1.00	9.53	9.55	1.002
0.75	0.25	4.72	4.38	0.928
0.75	0.50	5.13	4.94	0.963
0.75	0.75	5.82	5.82	1.000
0.75	1.00	6.78	6.78	1.000
1.00	0.25	3.61	3.42	0.934
1.00	0.50	3.93	3.90	0.980
1.00	0.75	4.46	4.65	1.029
1.00	1.00	5.19	5.57	1.057
2.00	0.25	2.29	2.41	1.052
2.00	0.50	2.50	2.59	1.036
2.00	0.75	2.83	2.84	1.004
2.00	1.00	3.30	3.15	0.955
3.00	0.25	2.16	2.28	1.056
3.00	0.50	2.34	2.43	1.038
3.00	0.75	2.66	2.66	1.000
3.00	1.00	3.10	2.95	0.952
4.00	0.25	2.13	2.21	1.038
4.00	0.50	2.31	2.34	1.013
4.00	0.75	2.62	2.54	0.969
4.00	1.00	3.05	2.80	0.918

Mean				0.998
Standard Deviation				0.038

TABLE 18

NUMERICAL VALUE OF λ IN EQUATION 113 FOR SIMPLY
SUPPORTED PLATES PARTIALLY LOADED ON BOTH EDGES

β / α	0.2	0.4	0.6	0.8	1.00
0.2	250.00	140.49	110.51	101.30	100.00
0.4	63.83	36.13	28.53	26.18	25.84
0.6	28.37	16.06	12.68	11.63	11.48
0.8	16.57	9.26	7.26	6.65	6.57
1.0	10.00	5.62	4.42	4.05	4.00
2.0	3.58	2.12	1.71	1.58	1.56
3.0	2.49	1.59	1.34	1.25	1.23

Note: $\alpha = a/h$ and $\beta = N/a$

TABLE 19

NUMERICAL VALUE OF λ IN EQUATION 113 FOR 5 DIFFERENT BUCKLING MODES

Buckling Mode	α β	0.2	0.4	0.6	0.8	1.0	2.0
1	0.25	1410.44	109.43	29.61	13.55	8.19	2.98
2	0.25	437.83	54.20	23.29	15.27	11.91	7.01
3	0.25	266.52	52.40	29.91	22.67	19.06	12.80
4	0.25	216.83	61.07	40.31	32.38	28.06	20.39
5	0.25	204.83	74.42	52.94	43.84	38.76	29.86
1	0.50	824.40	64.07	17.38	7.99	4.86	1.86
2	0.50	256.28	31.95	13.92	9.31	7.46	5.10
3	0.50	156.45	31.31	18.48	14.64	12.90	10.29
4	0.50	127.81	37.25	26.03	22.25	20.39	17.42
5	0.50	121.45	46.62	35.83	31.85	29.81	26.51
1	1.00	676.13	52.56	14.27	6.57	4.00	1.56
2	1.00	210.26	26.27	11.48	7.74	6.25	4.52
3	1.00	128.45	25.84	15.41	12.40	11.11	9.51
4	1.00	105.06	30.94	22.04	19.28	18.06	16.50
5	1.00	100.00	39.06	30.86	28.22	27.04	25.50

Note: $\alpha = a/h$ and $\beta = N/a$

TABLE 20

COMPARISON OF THE VALUES OF λ BASED
ON YAMAKI'S SOLUTION AND UMR ANALYSIS
FOR SQUARE PLATE

β	Yamaki	UMR
0.1	19.35	19.32
0.2	10.00	10.00
0.3	7.02	7.02
0.4	5.62	5.62
0.5	4.86	4.86
0.6	4.42	4.42
0.7	4.18	4.18
0.8	4.05	4.05
0.9	4.01	4.01
1.0	4.00	4.00

Note: $\beta = N/a$

TABLE 21

BUCKLING COEFFICIENT FOR SIMPLY SUPPORTED
PLATES LOADED ON BOTH EDGES

β α	0.2	0.4	0.6	0.8	1.0
0.2	10.00	11.24	13.26	16.21	20.00
0.4	5.11	5.78	6.85	8.38	10.34
0.6	3.44	3.85	4.56	5.58	6.89
0.8	2.65	2.96	3.48	4.26	5.26
1.0	2.00	2.25	2.65	3.24	4.00
2.0	1.43	1.70	2.05	2.53	3.12
3.0	1.49	1.91	2.41	3.00	3.69

Note: $\alpha = a/h$ and $\beta = N/a$

TABLE 22

COMPARISON OF THEORETICAL AND PREDICTED VALUES
OF BUCKLING COEFFICIENT FOR SIMPLY SUPPORTED PLATES
PARTIALLY LOADED ON BOTH EDGES

α	β	K_{comp}	K_{theo}	$\dfrac{K_{theo}}{K_{comp}}$
0.2	0.2	10.03	10.00	0.997
0.4	0.2	5.07	5.11	1.008
0.6	0.2	3.61	3.40	0.942
0.8	0.2	2.68	2.65	0.989
1.0	0.2	1.91	2.00	1.047
2.0	0.2	1.48	1.43	0.966
3.0	0.2	1.67	1.49	0.892
0.2	0.4	11.42	11.24	0.984
0.4	0.4	5.76	5.78	1.003
0.6	0.4	4.11	3.85	0.937
0.8	0.4	3.05	2.96	0.970
1.0	0.4	2.17	2.25	1.037
2.0	0.4	1.69	1.70	1.006
3.0	0.4	1.91	1.91	1.000
0.2	0.6	13.71	13.26	0.967
0.4	0.6	6.92	6.85	0.990
0.6	0.6	4.94	4.56	0.923
0.8	0.6	3.67	3.48	0.948
1.0	0.6	2.61	2.65	1.015
2.0	0.6	2.02	2.05	1.015
3.0	0.6	2.29	2.41	1.052
0.2	0.8	16.93	16.21	0.957
0.4	0.8	8.54	8.38	0.981
0.6	0.8	6.10	5.58	0.915
0.8	0.8	4.53	4.26	0.940
1.0	0.8	3.22	3.24	1.006
2.0	0.8	2.50	2.49	0.996
3.0	0.8	2.83	2.89	1.021
0.2	1.0	21.07	20.00	0.949
0.4	1.0	10.63	10.34	0.973
0.6	1.0	7.59	6.89	0.908
0.8	1.0	5.64	5.26	0.933
1.0	1.0	4.00	4.00	1.000
2.0	1.0	3.11	3.12	1.003
3.0	1.0	3.52	3.69	1.048

Mean				0.981
Standard Deviation				0.040

TABLE 23

DIMENSIONS OF ONE-FLANGE WEB CRIPPLING TEST SPECIMENS

Specimen No.	Dimensions (in.)											Span Length (in.)
	Thick.	B1	B2	B3	B4	d1	d2	D1	D2	R	BB	
WC-OF-1-1	0.0500	1.636	1.635	1.620	1.615	0.631	0.618	4.992	4.989	0.1094	7	4.750
WC-OF-1-2	0.0499	1.637	1.632	1.619	1.623	0.653	0.608	4.994	4.982	0.1094	7	4.750
WC-OF-2-1	0.0510	2.562	2.549	2.554	2.550	0.600	0.603	6.065	6.059	0.0781	7	6.000
WC-OF-2-2	0.0510	2.545	2.545	2.550	2.554	0.598	0.604	6.075	6.081	0.0781	7	6.000
WC-OF-3-1	0.0495	1.625	1.623	1.637	1.639	0.604	0.631	7.441	7.450	0.1094	7	7.250
WC-OF-3-2	0.0497	1.647	1.637	1.618	1.628	0.619	0.642	7.456	7.452	0.1094	7	7.250
WC-OF-4-1	0.0488	1.627	1.646	1.629	1.628	0.607	0.632	9.881	9.881	0.1094	7	9.625
WC-OF-4-2	0.0500	1.630	1.615	1.613	1.636	0.631	0.623	9.900	9.920	0.1094	7	9.625
WC-OF-5-1	0.0502	2.886	2.905	2.917	2.886	0.715	0.710	11.969	11.981	0.0938	7	12.000
WC-OF-5-2	0.0498	2.936	2.882	2.907	2.935	0.677	0.657	11.969	12.00	0.0938	7	12.000
WC-OF-7-1	0.0501	2.882	2.940	2.925	2.875	0.686	0.696	14.969	14.969	0.0938	7	15.000
WC-OF-7-2	0.0502	2.922	2.889	2.881	2.910	0.695	0.698	15.083	15.00	0.0938	7	15.000
WC-OF-6-1	0.0382	1.270	1.268	1.308	1.280	0.547	0.526	9.916	9.916	0.1250	7	7.875
WC-OF-6-2	0.0385	1.238	1.282	1.289	1.232	0.543	0.534	9.925	9.932	0.1250	7	7.875
WC-OF-6-3	0.0383	1.272	1.247	1.222	1.208	0.530	0.592	9.950	9.968	0.1250	7	7.875
WC-OF-6-4	0.0387	1.234	1.225	1.217	1.233	0.567	0.577	9.963	9.944	0.1250	7	7.875
WC-OF-6-5	0.0382	1.282	1.275	1.214	1.214	0.581	0.531	9.927	9.936	0.1250	7	7.875
WC-OF-6-6	0.0382	1.291	1.273	1.214	1.222	0.577	0.538	9.908	9.936	0.1250	7	7.875
WC-OF-6-7	0.0375	1.237	1.241	1.250	1.243	0.550	0.568	9.908	9.900	0.1250	7	7.875
WC-OF-6-8	0.0376	1.245	1.247	1.250	1.250	0.533	0.555	9.925	9.928	0.1250	7	7.875
WC-OF-6-9	0.0386	1.239	1.275	1.209	1.247	0.516	0.565	9.984	9.934	0.1250	7	7.875
WC-OF-6-10	0.0386	1.300	1.210	1.246	1.246	0.582	0.529	9.925	9.970	0.1250	7	7.875
WC-OF-3-3	0.0492	1.622	1.620	1.643	1.640	0.629	0.636	7.461	7.460	0.1094	7	11.000
WC-OF-3-4	0.0491	1.635	1.622	1.620	1.650	0.630	0.613	7.439	7.446	0.1094	7	11.000
WC-OF-3-5	0.0496	1.621	1.622	1.633	1.642	0.672	0.595	7.467	7.463	0.1094	7	11.000
WC-OF-3-6	0.0494	1.616	1.625	1.645	1.636	0.652	0.622	7.456	7.444	0.1094	7	11.000
WC-OF-3-7	0.0497	1.613	1.642	1.635	1.630	0.632	0.637	7.465	7.471	0.1094	7	11.000
WC-OF-3-8	0.0494	1.628	1.625	1.621	1.627	0.639	0.619	7.465	7.475	0.1094	7	11.000
WC-OF-3-9	0.0498	1.625	1.637	1.622	1.619	0.640	0.616	7.464	7.475	0.1094	7	11.000

TABLE 23 (continued)

Specimen No.	Dimensions (in.)											Span Length (in.)
	Thick.	B1	B2	B3	B4	d1	d2	D1	D2	R	BB	
WC-OF-3-10	0.0495	1.635	1.633	1.631	1.627	0.631	0.622	7.481	7.496	0.1094	7	11.000
WC-OF-3-11	0.0494	1.630	1.634	1.637	1.631	0.585	0.630	7.478	7.450	0.1094	7	11.000
WC-OF-3-12	0.0497	1.632	1.630	1.645	1.639	0.632	0.573	7.447	7.448	0.1094	7	11.000
WC-OF-4-3	0.0498	1.624	1.617	1.640	1.651	0.623	0.626	9.888	9.911	0.1094	7	4.875
WC-OF-4-4	0.0497	1.620	1.645	1.648	1.616	0.611	0.637	9.925	9.888	0.1094	7	4.875
WC-OF-4-5	0.0497	1.620	1.625	1.640	1.621	0.607	0.645	9.889	9.886	0.1094	7	9.625
WC-OF-4-6	0.0498	1.625	1.627	1.624	1.631	0.621	0.628	9.889	9.879	0.1094	7	9.625
WC-OF-4-7	0.0501	1.622	1.624	1.645	1.645	0.623	0.628	9.888	9.901	0.1094	7	14.500
WC-OF-4-8	0.0505	1.631	1.631	1.632	1.624	0.637	0.642	9.889	9.890	0.1094	7	14.500
WC-OF-4-9	0.0498	1.624	1.635	1.654	1.640	0.632	0.620	9.893	9.878	0.1094	7	19.250
WC-OF-4-10	0.0501	1.625	1.626	1.635	1.630	0.628	0.632	9.895	9.895	0.1094	7	19.250
WC-OF-5-3	0.0498	2.950	2.925	2.870	2.875	0.687	0.678	11.969	11.969	0.0938	7	8.000
WC-OF-5-4	0.0493	2.908	2.907	2.881	2.883	0.706	0.722	11.975	11.963	0.0938	7	8.000
WC-OF-5-5	0.0501	2.875	2.925	2.919	2.872	0.700	0.717	11.969	11.975	0.0938	7	12.000
WC-OF-5-6	0.0498	2.900	2.875	2.876	2.914	0.720	0.722	11.969	11.950	0.0938	7	12.000
WC-OF-5-7	0.0497	2.927	2.933	2.881	2.885	0.708	0.713	11.938	11.950	0.0938	7	16.000
WC-OF-5-8	0.0498	2.891	2.934	2.883	2.875	0.717	0.725	11.938	11.938	0.0938	7	16.000
WC-OF-5-9	0.0498	2.936	2.885	2.875	2.936	0.706	0.674	11.956	12.000	0.0938	7	20.000
WC-OF-5-10	0.0500	2.889	2.903	2.898	2.899	0.721	0.701	11.975	11.969	0.0938	7	20.000
WC-OF-5-11	0.0501	2.949	2.889	2.875	2.892	0.690	0.679	11.988	12.000	0.0938	7	24.000
WC-OF-5-12	0.0502	2.920	2.902	2.879	2.898	0.696	0.708	11.969	11.969	0.0938	7	24.000
WC-OF-8-1	0.0455	2.975	2.975	2.920	2.922	0.539	0.754	7.100	7.094	0.0625	7	7.000
WC-OF-8-2	0.0462	2.975	2.917	3.009	2.977	0.667	0.561	7.235	7.083	0.0625	7	7.000
MWC-OF-4-3	0.0496	1.623	1.619	1.620	1.614	0.638	0.626	9.912	9.878	0.1094	7	4.875
MWC-OF-4-4	0.0497	1.626	1.614	1.641	1.628	0.662	0.603	9.890	9.900	0.1094	7	4.875
MWC-OF-4-5	0.0493	1.622	1.628	1.623	1.612	0.646	0.615	9.897	9.918	0.1094	7	9.625
MWC-OF-4-6	0.0496	1.624	1.609	1.625	1.630	0.627	0.638	9.925	9.918	0.1094	7	9.625
MWC-OF-4-7	0.0499	1.624	1.632	1.632	1.635	0.600	0.629	9.885	9.900	0.1094	7	14.500
MWC-OF-4-8	0.0498	1.614	1.630	1.632	1.637	0.630	0.628	9.890	9.911	0.1094	7	14.500

TABLE 23 (continued)

Specimen No.	Dimensions (in.)											Span Length (in.)
	Thick.	B1	B2	B3	B4	d1	d2	D1	D2	R	BB	
MWC-OF-4-9	0.0495	1.634	1.631	1.618	1.634	0.638	0.600	9.879	9.921	0.1094	7	19.250
MWC-OF-4-10	0.0493	1.618	1.625	1.624	1.626	0.594	0.639	9.883	9.891	0.1094	7	19.250

Notes: 1. See Fig. 8 for definition of symbols.
        2. Beam specimens are designated as follows:

MWC	–	WC	–	OF	–	4	–	3
Modified Web Crippling		Web Crippling		One-Flange		Channel No.		Test No.

TABLE 24

DIMENSIONS OF TWO-FLANGE WEB CRIPPLING TEST SPECIMENS

Specimen No.	Dimensions (in.)											Span Length (in.)
	Thick.	B1	B2	B3	B4	d1	d2	D1	D2	R	BB	
WC-TF-1-1	0.0495	1.619	1.641	1.630	1.617	0.626	0.602	5.022	5.030	0.1094	7	4.750
WC-TF-1-2	0.0495	1.640	1.638	1.622	1.618	0.640	0.624	5.037	5.036	0.1094	7	4.750
WC-TF-2-1	0.0494	1.641	1.642	1.626	1.619	0.644	0.611	7.455	7.437	0.1094	7	7.250
WC-TF-2-2	0.0493	1.621	1.620	1.635	1.646	0.610	0.632	7.429	7.475	0.1094	7	7.250
WC-TF-2-3	0.0496	1.625	1.634	1.616	1.630	0.604	0.647	7.458	7.475	0.1094	7	7.250
WC-TF-2-4	0.0493	1.616	1.643	1.621	1.622	0.648	0.605	7.458	7.472	0.1094	7	7.250
WC-TF-3-1	0.0498	1.641	1.623	1.619	1.639	0.647	0.618	9.898	9.909	0.1094	7	9.625
WC-TF-3-2	0.0494	1.625	1.625	1.622	1.616	0.611	0.662	9.894	9.888	0.1094	7	9.625
WC-TF-5-1	0.0495	2.873	2.888	2.916	2.898	0.715	0.694	11.975	11.969	0.0938	7	11.875
WC-TF-5-2	0.0497	2.922	2.898	2.878	2.890	0.711	0.713	11.964	11.950	0.0938	7	11.875
WC-TF-7-1	0.0496	2.900	2.912	2.878	2.881	0.692	0.707	14.969	14.938	0.0938	7	14.875
WC-TF-7-2	0.0493	2.882	2.906	2.892	2.877	0.716	0.706	14.969	14.938	0.0938	7	14.875
WC-TF-6-1	0.0383	2.281	2.299	2.295	2.294	0.696	0.687	9.844	9.813	0.1250	7	8.000
WC-TF-6-2	0.0383	2.294	2.309	2.280	2.296	0.694	0.703	9.844	9.813	0.1250	7	8.000
WC-TF-6-3	0.0383	2.311	2.295	2.289	2.298	0.686	0.676	10.022	10.014	0.1250	7	8.000
WC-TF-6-4	0.0383	2.306	2.307	2.300	2.278	0.685	0.670	9.942	10.002	0.1250	7	8.000
WC-TF-6-5	0.0382	2.294	2.285	2.292	2.296	0.701	0.690	9.954	10.018	0.1250	7	8.000
WC-TF-6-6	0.0382	2.290	2.295	2.291	2.284	0.702	0.688	9.962	9.964	0.1250	7	8.000
WC-TF-6-7	0.0378	2.295	2.305	2.282	2.290	0.677	0.672	10.010	10.026	0.1250	7	8.000
WC-TF-6-8	0.0382	2.314	2.310	2.278	2.287	0.696	0.658	9.954	9.955	0.1250	7	8.000
WC-TF-6-9	0.0382	2.286	2.271	2.291	2.292	0.712	0.687	9.996	9.970	0.1250	7	8.000
WC-TF-6-10	0.0382	2.300	2.310	2.284	2.304	0.699	0.699	9.955	9.966	0.1250	7	8.000
WC-TF-6-11	0.0381	2.304	2.286	2.287	2.291	0.692	0.687	9.954	9.960	0.1250	7	15.000
WC-TF-6-12	0.0381	2.283	2.290	2.294	2.290	0.697	0.679	9.992	9.986	0.1250	7	15.000
WC-TF-6-13	0.0381	2.295	2.302	2.317	2.286	0.702	0.677	9.942	9.943	0.1250	7	15.000
WC-TF-6-14	0.0380	2.314	2.394	2.285	2.280	0.706	0.676	9.961	9.954	0.1250	7	15.000
WC-TF-6-15	0.0380	2.287	2.283	2.320	2.313	0.692	0.675	9.968	9.971	0.1250	7	15.000

TABLE 24 (continued)

| Specimen No. | Dimensions (in.) | | | | | | | | | | | Span Length (in.) |
	Thick.	B1	B2	B3	B4	d1	d2	D1	D2	R	BB	
WC-TF-6-16	0.0380	2.298	2.304	2.280	2.275	0.693	0.702	9.962	9.968	0.1250	7	15.000
WC-TF-6-17	0.0382	2.315	2.275	2.305	2.302	0.688	0.659	9.936	9.963	0.1250	7	15.000
WC-TF-6-18	0.0382	2.267	2.282	2.290	2.312	0.697	0.666	9.964	9.964	0.1250	7	15.000
WC-TF-6-19	0.0381	2.279	2.304	2.285	2.292	0.693	0.693	9.972	9.963	0.1250	7	15.000
WC-TF-6-20	0.0380	2.287	2.285	2.320	2.335	0.690	0.671	9.993	9.960	0.1250	7	15.000
WC-TF-8-1	0.0381	2.315	2.300	2.289	2.314	0.662	0.682	11.781	11.813	0.1250	7	15.250
WC-TF-8-2	0.0381	2.291	2.308	2.280	2.282	0.695	0.682	11.844	11.783	0.1250	7	15.250
WC-TF-7-3	0.0496	2.875	2.882	2.924	2.929	0.714	0.665	14.944	14.950	0.0938	7	23.000
WC-TF-7-4	0.0497	2.913	2.892	2.875	2.905	0.699	0.694	14.975	14.969	0.0938	7	23.000
WC-TF-8-3	0.0379	2.290	2.292	2.287	2.304	0.673	0.694	11.781	11.781	0.1250	7	23.000
WC-TF-8-4	0.0380	2.288	2.300	2.276	2.291	0.674	0.684	11.813	11.844	0.1250	7	23.000
WC-TF-8-5	0.0382	2.295	2.282	2.283	2.315	0.705	0.660	11.813	11.781	0.1250	7	8.000
WC-TF-8-6	0.0380	2.320	2.298	2.275	2.290	0.683	0.666	11.813	11.781	0.1250	7	8.000
WC-TF-8-7	0.0379	2.284	2.289	2.289	2.321	0.699	0.658	11.813	11.781	0.1250	7	11.750
WC-TF-8-8	0.0380	2.296	2.290	2.283	2.306	0.682	0.678	11.844	11.813	0.1250	7	11.750
WC-TF-7-5	0.0500	2.890	2.875	2.892	2.925	0.709	0.688	14.969	14.981	0.0938	7	20.000
WC-TF-7-6	0.0501	2.950	2.893	2.885	2.890	0.681	0.672	14.981	14.963	0.0938	7	20.000
WC-TF-8-9	0.0380	2.288	2.296	2.292	2.282	0.703	0.670	11.813	11.813	0.1250	7	5.875
WC-TF-8-10	0.0381	2.317	2.306	2.275	2.288	0.668	0.689	11.781	11.781	0.1250	7	5.875
WC-TF-7-7	0.0498	2.873	2.927	2.934	2.879	0.698	0.673	14.969	14.963	0.0938	7	12.000
WC-TF-7-8	0.0497	2.891	2.925	2.909	2.886	0.685	0.691	14.969	14.975	0.0938	7	12.000
WC-TF-8-11	0.0382	2.288	2.295	2.289	2.282	0.680	0.686	11.844	11.844	0.1250	7	12.000
WC-TF-8-12	0.0382	2.295	2.293	2.304	2.998	0.697	0.659	11.813	11.844	0.1250	7	12.000

TABLE 24 (continued)

Specimen No.	Dimensions (in.)											Span Length (in.)
	Thick.	B1	B2	B3	B4	d1	d2	D1	D2	R	BB	
WC-TF-4-1	0.0381	2.269	2.285	2.297	2.312	0.696	0.667	8.072	8.056	0.1250	7	6.000
WC-TF-4-2	0.0381	2.291	2.309	2.314	2.298	0.688	0.688	8.059	8.056	0.1250	7	6.000
WC-TF-4-3	0.0385	2.267	2.284	2.305	2.291	0.695	0.684	8.067	8.073	0.1250	7	16.000
WC-TF-4-4	0.0385	2.275	2.278	2.322	2.325	0.661	0.675	8.053	8.015	0.1250	7	16.000
WC-TF-4-5	0.0385	2.297	2.291	2.275	2.334	0.678	0.679	8.065	8.027	0.1250	7	8.000
WC-TF-4-6	0.0385	2.270	2.276	2.298	2.318	0.691	0.667	8.063	8.048	0.1250	7	8.000
WC-TF-9-1	0.0464	2.990	2.980	2.975	2.987	0.587	0.584	7.175	7.232	0.0625	7	7.000
WC-TF-9-2	0.0460	2.989	2.992	3.005	2.985	0.588	0.582	7.230	7.215	0.0625	7	7.000
WC-TF-10-1	0.0415	1:595	1.598	1.641	1.573	0.667	0.671	8.609	8.588	0.0938	7	8.500
WC-TF-10-2	0.0414	1.605	1.538	1.595	1.525	0.668	0.709	8.624	8.652	0.0938	7	8.500

Notes 1. See Fig. 8 for definition of symbols

2. Beam specimens are designated as follows:

WC	–	TF	–	8	–	5
Web Crippling		Two-Flange		Channel No.		Test No.

TABLE 25

PERTINENT PARAMETERS OF ONE-FLANGE
WEB CRIPPLING TEST SPECIMENS

Specimen No.	N (in.)	F_y (ksi)	R/t	N/t	N/a	a/h	h/t
WC-OF-1-1	2	36.88	2.19	40.00	0.421	0.971	97.82
WC-OF-1-2	2	36.88	2.19	40.08	0.421	0.972	97.96
WC-OF-2-1	2	53.79	1.53	39.22	0.333	1.007	116.86
WC-OF-2-2	2	53.79	1.53	39.22	0.333	1.004	117.18
WC-OF-3-1	3	36.88	2.21	60.61	0.414	0.987	148.42
WC-OF-3-2	3	36.88	2.20	60.36	0.414	0.985	148.07
WC-OF-4-1	4	36.88	2.24	81.97	0.416	0.984	200.47
WC-OF-4-2	4	36.88	2.19	80.00	0.416	0.981	196.20
WC-OF-5-1	5.2	38.80	1.87	103.59	0.433	1.011	236.55
WC-OF-5-2	5.2	38.80	1.88	104.42	0.433	1.010	238.66
WC-OF-7-1	6	38.80	1.87	119.76	0.400	1.009	296.79
WC-OF-7-2	6	38.80	1.87	119.52	0.400	1.004	297.63
WC-OF-6-1	1	43.06	3.27	26.18	0.127	0.800	257.54
WC-OF-6-2	1	43.06	3.25	25.97	0.127	0.799	255.90
WC-OF-6-3	2	43.06	3.26	52.22	0.254	0.796	258.02
WC-OF-6-4	2	43.06	3.23	51.68	0.254	0.797	255.19
WC-OF-6-5	3	43.06	3.27	78.53	0.381	0.799	257.98
WC-OF-6-6	3	43.06	3.27	78.53	0.381	0.800	257.95
WC-OF-6-7	4	43.06	3.33	106.67	0.508	0.801	262.11
WC-OF-6-8	4	43.06	3.32	106.38	0.508	0.799	262.00
WC-OF-6-9	5.2	43.06	3.24	134.72	0.660	0.797	256.01
WC-OF-6-10	5.2	43.06	3.24	134.72	0.660	0.799	255.70
WC-OF-3-3	1	36.88	2.22	20.33	0.091	1.494	149.63
WC-OF-3-4	1	36.88	2.23	20.37	0.091	1.498	149.57
WC-OF-3-5	2	36.88	2.21	40.32	0.182	1.494	148.51
WC-OF-3-6	2	36.88	2.21	40.49	0.182	1.496	148.81
WC-OF-3-7	3	36.88	2.20	60.36	0.273	1.493	148.27
WC-OF-3-8	3	36.88	2.21	60.73	0.273	1.492	149.21
WC-OF-3-9	4	36.88	2.20	80.32	0.364	1.493	147.99
WC-OF-3-10	4	36.88	2.21	80.81	0.364	1.489	149.29
WC-OF-3-11	5.2	36.88	2.21	105.26	0.473	1.494	149.08
WC-OF-3-12	5.2	36.88	2.20	104.63	0.473	1.497	147.85
WC-OF-4-3	1	36.88	2.20	20.08	0.205	0.497	196.79
WC-OF-4-4	1	36.88	2.20	20.12	0.205	0.497	197.32
WC-OF-4-5	2	36.88	2.20	40.24	0.208	0.983	196.94
WC-OF-4-6	2	36.88	2.20	40.16	0.208	0.984	196.45
WC-OF-4-7	3	36.88	2.18	59.88	0.207	1.481	195.49
WC-OF-4-8	3	36.88	2.17	59.41	0.207	1.480	194.02
WC-OF-4-9	4	36.88	2.20	80.32	0.208	1.967	196.51
WC-OF-4-10	4	36.88	2.18	79.84	0.208	1.965	195.51

TABLE 25 (continued)

Specimen No.	N (in.)	F_y (ksi)	R/t	N/t	N/a	a/h	h/t
WC-OF-5-3	2	38.80	1.88	40.16	0.250	0.674	238.88
WC-OF-5-4	2	38.80	1.90	40.57	0.250	0.674	240.77
WC-OF-5-5	3	38.80	1.87	59.88	0.250	1.011	236.97
WC-OF-5-6	3	38.80	1.88	60.24	0.250	1.012	238.15
WC-OF-5-7	4	38.80	1.89	80.48	0.250	1.351	238.33
WC-OF-5-8	4	38.80	1.88	80.32	0.250	1.352	237.71
WC-OF-5-9	5.2	38.80	1.88	104.42	0.260	1.684	238.51
WC-OF-5-10	5.2	38.80	1.88	104.00	0.260	1.685	237.44
WC-OF-5-11	6	38.80	1.87	119.96	0.250	2.018	237.41
WC-OF-5-12	6	38.80	1.87	119.52	0.250	2.022	236.43
WC-OF-8-1	2	33.46	1.37	43.96	0.286	0.999	153.98
WC-OF-8-2	2	33.46	1.35	43.29	0.286	0.991	152.97
MWC-OF-4-3	1	36.88	2.21	20.16	0.205	0.498	197.50
MWC-OF-4-4	1	36.88	2.20	20.12	0.205	0.498	197.10
MWC-OF-4-5	2	36.88	2.22	40.57	0.208	0.981	198.97
MWC-OF-4-6	2	36.88	2.21	40.32	0.208	0.980	198.02
MWC-OF-4-7	3	36.88	2.19	60.12	0.207	1.481	196.25
MWC-OF-4-8	3	36.88	2.20	60.24	0.207	1.479	196.81
MWC-OF-4-9	4	36.88	2.21	80.81	0.208	1.964	198.00
MWC-OF-4-10	4	36.88	2.22	81.14	0.208	1.967	198.54

Note: Refer to Figs. 50 and 51 for definition of symbols

TABLE 26

PERTINENT PARAMETERS OF TWO-FLANGE
WEB CRIPPLING TEST SPECIMENS

Specimen No.	N (in.)	F_y (ksi)	R/t	N/t	N/a	a/h	h/t
WC-TF-1-1	2	36.88	2.21	40.40	0.421	0.964	99.54
WC-TF-1-2	2	36.88	2.21	40.49	0.421	0.962	99.96
WC-TF-2-1	3	36.88	2.21	60.73	0.414	0.986	148.73
WC-TF-2-2	3	36.88	2.22	60.85	0.414	0.986	149.15
WC-TF-2-3	1	36.88	2.21	20.16	0.138	0.984	148.53
WC-TF-2-4	1	36.88	2.22	20.28	0.138	0.984	149.41
WC-TF-3-1	4	36.88	2.20	80.32	0.416	0.982	196.87
WC-TF-3-2	4	36.88	2.21	80.97	0.416	0.982	198.22
WC-TF-5-1	5	38.80	1.89	105.05	0.438	1.000	239.86
WC-TF-5-2	5	38.80	1.89	104.63	0.438	1.001	238.63
WC-TF-7-1	6	38.80	1.89	120.97	0.403	1.001	299.48
WC-TF-7-2	6	38.80	1.90	121.70	0.404	1.000	301.30
WC-TF-6-1	1	43.06	3.26	26.11	0.125	0.821	254.62
WC-TF-6-2	1	43.06	3.26	26.11	0.125	0.821	254.62
WC-TF-6-3	2	43.06	3.26	52.22	0.250	0.947	259.56
WC-TF-6-4	2	43.06	3.26	52.22	0.250	0.808	258.36
WC-TF-6-5	3	43.06	3.27	78.53	0.375	0.806	259.42
WC-TF-6-6	3	43.06	3.27	78.53	0.375	0.808	258.82
WC-TF-6-7	4	43.06	3.31	105.82	0.500	0.805	263.07
WC-TF-6-8	4	43.06	3.27	104.71	0.500	0.810	258.59
WC-TF-6-9	5	43.06	3.27	130.89	0.625	0.808	259.35
WC-TF-6-10	5	43.06	3.27	130.89	0.625	0.808	258.74
WC-TF-6-11	1	43.06	3.28	26.25	0.067	1.518	259.34
WC-TF-6-12	1	43.06	3.28	26.25	0.067	1.513	260.18
WC-TF-6-13	2	43.06	3.28	52.49	0.133	1.520	258.95
WC-TF-6-14	2	43.06	3.29	52.63	0.133	1.530	258.18
WC-TF-6-15	3	43.06	3.29	78.95	0.200	1.525	260.37
WC-TF-6-16	3	43.06	3.29	78.95	0.200	1.518	260.24
WC-TF-6-17	4	43.06	3.27	104.71	0.267	1.518	258.46
WC-TF-6-18	4	43.06	3.27	104.71	0.267	1.518	258.85
WC-TF-6-19	5.2	43.06	3.28	136.48	0.347	1.517	259.61
WC-TF-6-20	5.2	43.06	3.29	136.84	0.347	1.517	260.55
WC-TF-8-1	2	43.06	3.28	52.49	0.131	1.301	307.64
WC-TF-8-2	2	43.06	3.28	52.49	0.131	1.299	308.02
WC-TF-7-3	3	38.80	1.89	60.48	0.130	1.549	299.32
WC-TF-7-4	3	38.80	1.89	60.36	0.130	1.546	299.26
WC-TF-8-3	3	43.06	3.30	79.16	0.128	2.008	308.84
WC-TF-8-4	3	43.06	3.30	79.16	0.128	1.999	310.11
WC-TF-8-5	2	43.06	3.27	52.36	0.250	0.683	306.70
WC-TF-8-6	2	43.06	3.29	52.63	0.250	0.683	308.45
WC-TF-8-7	3	43.06	3.30	79.16	0.255	1.002	309.26

TABLE 26 (continued)

Specimen No.	N (in.)	F_y (ksi)	R/t	N/t	N/a	a/h	h/t
WC-TF-8-8	3	43.06	3.29	78.95	0.255	1.000	309.26
WC-TF-7-5	5.2	38.80	1.88	104.00	0.260	1.345	297.50
WC-TF-7-6	5.2	38.80	1.87	103.79	0.260	1.345	296.85
WC-TF-8-9	3	43.06	3.29	78.95	0.511	0.501	308.87
WC-TF-8-10	3	43.06	3.28	78.74	0.511	0.502	307.22
WC-TF-7-7	6	38.80	1.88	120.48	0.500	0.807	298.51
WC-TF-7-8	6	38.80	1.89	120.72	0.500	0.807	299.26
WC-TF-8-11	6	43.06	3.27	157.07	0.500	1.020	308.06
WC-TF-8-12	6	43.06	3.27	157.07	0.500	1.021	307.64
WC-TF-4-1	3	43.06	3.28	78.74	0.500	0.751	209.66
WC-TF-4-2	3	43.06	3.28	78.74	0.500	0.752	209.48
WC-TF-4-3	3	43.06	3.25	77.92	0.188	2.002	207.61
WC-TF-4-4	3	43.06	3.25	77.92	0.188	2.011	206.68
WC-TF-4-5	3	43.06	3.25	77.92	0.375	1.004	206.99
WC-TF-4-6	3	43.06	3.25	77.92	0.375	1.003	207.25
WC-TF-9-1	2	33.46	1.35	43.10	0.286	0.984	153.25
WC-TF-9-2	2	33.46	1.36	43.48	0.286	0.982	155.02
WC-TF-10-1	3	51.24	2.26	72.29	0.353	0.998	205.20
WC-TF-10-2	3	51.24	2.27	72.46	0.353	0.994	206.64

Note: Refer to Fig. 53 for definition of symbols

TABLE 27

COMPARISON OF TESTED AND COMPUTED ONE-FLANGE WEB CRIPPLING LOADS

Beam Specimen No.	Tested Data		Computed Data				$\dfrac{(P_u)_{test}}{(P_{cr})_{comp}}$	$\dfrac{(P_u)_{test}}{(P_u)_{comp}}$	$\dfrac{(P_u)_{test}}{(P'_u)_{comp}}$	$\dfrac{(M_u)_{test}}{(M_u)_{comp}}$
	$(P_u)_{test}$ (kips/web)	$(M_u)_{test}$ (in-kips)	$(P_{cr})_{comp}$ (kips/web)	$(P_u)_{comp}$ (kips/web)	$(P'_u)_{comp}$ (kips/web)	$(M_u)_{comp}$ (in-kips)				
WC-OF-1-1	1.660	3.94	2.675	1.673	1.339	29.80	0.621	0.992	1.240	0.132
WC-OF-1-2	1.595	3.79	2.659	1.667	1.337	29.87	0.600	0.957	1.193	0.127
WC-OF-2-1	2.225	6.68	2.095	2.305	1.950	63.69	1.062	0.966	1.141	0.105
WC-OF-2-2	2.275	6.83	2.096	2.306	1.957	69.87	1.085	0.987	1.162	0.098
WC-OF-3-1	1.890	6.46	1.695	1.967	2.083	59.23	1.115	0.961	0.907	0.109
WC-OF-3-2	1.860	6.74	1.716	1.980	2.096	59.93	1.084	0.939	0.887	0.112
WC-OF-4-1	2.120	10.20	1.224	2.245	2.415	96.70	1.732	0.944	0.878	0.105
WC-OF-4-2	2.245	10.80	1.317	2.334	2.510	99.61	1.705	0.962	0.894	0.108
WC-OF-5-1	2.920	17.52	0.998	2.788	2.605	157.18	2.926	1.047	1.121	0.111
WC-OF-5-2	2.775	16.65	0.974	2.755	2.572	155.01	2.849	1.007	1.079	0.107
WC-OF-7-1	3.160	23.70	0.794	3.051	2.675	233.75	3.980	1.036	1.181	0.101
WC-OF-7-2	2.985	22.39	0.800	3.063	2.691	236.18	3.731	0.975	1.109	0.095
WC-OF-6-1	1.105	4.55	0.660	0.905	1.080	77.25	1.654	1.221	0.997	0.059
WC-OF-6-2	1.070	4.21	0.676	0.919	1.095	77.71	1.583	1.164	0.977	0.054
WC-OF-6-3	1.405	5.53	0.680	1.185	1.375	76.75	2.066	1.186	1.022	0.072
WC-OF-6-4	1.475	5.81	0.702	1.207	1.399	77.26	2.101	1.222	1.054	0.075
WC-OF-6-5	1.775	7.38	0.700	1.453	1.691	77.78	2.679	1.222	1.109	0.095
WC-OF-6-6	1.785	7.03	0.700	1.453	1.691	77.91	2.550	1.228	1.056	0.090
WC-OF-6-7	1.995	7.86	0.696	1.732	1.998	73.24	2.866	1.152	0.998	0.107
WC-OF-6-8	1.990	7.84	0.702	1.740	2.008	73.66	2.835	1.144	0.991	0.106
WC-OF-6-9	2.360	9.29	0.817	2.160	2.635	77.46	2.889	1.093	0.896	0.120
WC-OF-6-10	2.210	8.70	0.817	2.159	2.635	78.36	2.705	1.024	0.839	0.111
WC-OF-3-3	1.125	6.19	1.076	1.208	1.233	64.50	1.046	0.931	0.912	0.096
WC-OF-3-4	1.095	6.02	1.071	1.203	1.229	64.13	1.022	1.910	0.891	0.094
WC-OF-3-5	1.510	8.31	1.103	1.534	1.473	65.50	1.369	0.984	1.025	0.127
WC-OF-3-6	1.485	8.17	1.090	1.522	1.465	64.87	1.362	0.976	1.014	0.126
WC-OF-3-7	1.755	9.65	1.109	1.847	1.704	65.31	1.583	0.950	1.030	0.148

TABLE 27 (continued)

Beam Specimen No.	Tested Data		Computed Data				$\frac{(P_u)_{test}}{(P_{cr})_{comp}}$	$\frac{(P_u)_{test}}{(P_u)_{comp}}$	$\frac{(P_u)_{test}}{(P'_u)_{comp}}$	$\frac{(M_u)_{test}}{(M_u)_{comp}}$
	$(P_u)_{test}$ (kips/web)	$(M_u)_{test}$ (in-kips)	$(P_{cr})_{comp}$ (kips/web)	$(P_u)_{comp}$ (kips/web)	$(P'_u)_{comp}$ (kips/web)	$(M_u)_{comp}$ (in-kips)				
WC-OF-3-8	1.805	9.93	1.089	1.829	1.691	64.95	1.657	0.987	1.067	0.153
WC-OF-3-9	2.040	11.22	1.116	2.162	1.937	65.46	1.828	0.944	1.053	0.171
WC-OF-3-10	1.960	10.78	1.094	2.143	1.924	65.31	1.792	0.915	1.019	0.165
WC-OF-3-11	2.215	12.18	1.089	2.500	2.188	64.21	2.034	0.886	1.012	0.190
WC-OF-3-12	2.305	12.68	1.111	2.521	2.203	64.84	2.075	0.914	1.046	0.196
WC-OF-4-3	1.420	3.46	2.218	1.503	1.602	91.50	0.640	0.945	0.886	0.038
WC-OF-4-4	1.395	3.40	2.204	1.497	1.598	91.31	0.633	0.932	0.873	0.037
WC-OF-4-5	1.605	7.72	1.219	1.709	1.751	98.36	1.317	0.939	0.917	0.078
WC-OF-4-6	1.585	7.63	1.227	1.715	1.756	98.69	1.292	0.924	0.903	0.077
WC-OF-4-7	1.955	14.17	0.859	1.877	1.834	105.81	2.276	1.042	1.066	0.134
WC-OF-4-8	1.915	13.88	0.879	1.902	1.857	107.10	2.179	1.007	1.031	0.130
WC-OF-4-9	2.120	20.41	0.754	1.940	2.158	112.74	2.812	1.093	0.982	0.181
WC-OF-4-10	2.050	19.73	0.767	1.959	2.178	113.37	2.673	1.046	0.941	0.174
WC-OF-5-3	1.825	7.30	1.433	1.926	2.039	154.39	1.274	0.948	0.896	0.047
WC-OF-5-4	1.740	6.96	1.390	1.893	2.005	153.53	1.252	0.919	0.868	0.045
WC-OF-5-5	2.115	12.69	0.992	2.189	2.100	164.57	2.132	0.966	1.007	0.077
WC-OF-5-6	1.995	11.97	0.974	2.167	2.078	163.85	2.048	0.921	0.960	0.073
WC-OF-5-7	2.545	20.36	0.734	2.352	2.094	171.50	3.467	1.082	1.215	0.119
WC-OF-5-8	2.430	19.44	0.739	2.359	2.101	171.73	3.288	1.030	1.157	0.113
WC-OF-5-9	2.750	27.50	0.654	2.571	2.362	179.53	4.205	1.070	1.164	0.153
WC-OF-5-10	2.670	26.70	0.662	2.586	2.378	180.42	4.033	1.032	1.123	0.148
WC-OF-5-11	2.725	32.70	0.627	2.632	2.658	187.44	4.346	1.035	1.025	0.174
WC-OF-5-12	2.705	32.46	0.632	2.637	2.669	187.44	4.280	1.026	1.013	0.173
WC-OF-8-1	1.570	5.50	1.309	1.448	1.374	53.44	1.199	1.084	1.143	0.103
WC-OF-8-2	1.555	5.44	1.371	1.488	1.411	55.95	1.134	1.045	1.102	0.097
MWC-OF-4-3	1.255	18.83	2.191	1.491	1.592	126.75	0.573	0.842	0.788	0.149
MWC-OF-4-4	1.345	20.18	2.204	1.497	1.597	120.73	0.610	0.898	0.842	0.167
MWC-OF-4-5	1.510	23.41	1.190	1.686	1.731	119.97	1.269	0.896	0.872	0.195

TABLE 27 (continued)

Beam Specimen No.	Tested Data		Computed Data				$\dfrac{(P_u)_{test}}{(P_{cr})_{comp}}$	$\dfrac{(P_u)_{test}}{(P_u)_{comp}}$	$\dfrac{(P_u)_{test}}{(P'_u)_{comp}}$	$\dfrac{(M_u)_{test}}{(M_u)_{comp}}$
	$(P_u)_{test}$ (kips/web)	$(M_u)_{test}$ (in-kips)	$(P_{cr})_{comp}$ (kips/web)	$(P_u)_{comp}$ (kips/web)	$(P'_u)_{comp}$ (kips/web)	$(M_u)_{comp}$ (in-kips)				
MWC-OF-4-6	1.595	24.57	1.212	1.704	1.749	120.52	1.316	0.936	0.912	0.204
MWC-OF-4-7	1.805	28.88	0.849	1.864	1.823	121.41	2.126	0.968	0.990	0.238
MWC-OF-4-8	1.845	29.52	0.843	1.859	1.817	121.85	2.189	0.992	1.015	0.242
MWC-OF-4-9	2.015	33.25	0.739	1.923	2.137	121.34	2.727	1.048	0.943	0.274
MWC-OF-4-10	1.955	32.26	0.731	1.910	2.125	119.64	2.674	1.024	0.920	0.270
Mean								1.000	1.007	
Standard Deviation								0.091	0.107	

TABLE 28

COMPARISON OF TESTED AND COMPUTED TWO-FLANGE WEB CRIPPLING LOADS

Beam Specimen No.	Tested Data (per web) $(P_u)_{test}$ (kips)	Computed Data per web			$\dfrac{(P_u)_{test}}{(P_{cr})_{comp}}$	$\dfrac{(P_u)_{test}}{(P_u)_{comp}}$	$\dfrac{(P_u)_{test}}{(P'_u)_{comp}}$
		$(P_{cr})_{comp}$ (kips)	$(P_u)_{comp}$ (kips)	$(P'_u)_{comp}$ (kips)			
WC-TF-1-1	1.615	1.551	1.538	1.410	1.041	1.050	1.145
WC-TF-1-2	1.615	1.544	1.533	1.411	1.046	1.053	1.053
WC-TF-2-1	1.835	0.985	1.764	1.676	1.863	1.040	1.095
WC-TF-2-2	1.860	0.979	1.758	1.673	1.900	1.058	1.112
WC-TF-2-3	1.255	0.848	1.307	1.214	1.480	0.960	1.034
WC-TF-2-4	1.190	0.832	1.291	1.202	1.430	0.922	0.990
WC-TF-3-1	2.035	0.764	2.026	1.874	2.664	1.004	1.086
WC-TF-3-2	2.050	0.745	1.998	1.845	2.752	1.026	1.111
WC-TF-5-1	2.510	0.626	2.419	2.090	4.153	1.038	1.201
WC-TF-5-2	2.520	0.634	2.434	2.104	4.156	1.036	1.198
WC-TF-7-1	2.505	0.489	2.625	2.081	5.327	0.954	1.204
WC-TF-7-2	2.525	0.481	2.601	2.060	5.561	0.971	1.225
WC-TF-6-1	0.805	0.389	0.866	1.014	1.812	0.930	0.794
WC-TF-6-2	0.830	0.389	0.866	1.014	2.005	0.958	0.819
WC-TF-6-3	1.070	0.412	1.059	1.170	2.597	1.010	0.915
WC-TF-6-4	1.060	0.412	1.058	1.167	2.573	1.002	0.908
WC-TF-6-5	1.255	0.444	1.244	1.362	2.827	1.009	0.921
WC-TF-6-6	1.230	0.444	1.244	1.360	2.770	0.989	0.904
WC-TF-6-7	1.505	0.479	1.410	1.595	3.142	1.067	0.944
WC-TF-6-8	1.490	0.494	1.435	1.621	3.016	1.038	0.919
WC-TF-6-9	1.675	0.558	1.626	1.957	3.002	1.030	0.856
WC-TF-6-10	1.630	0.558	1.626	1.954	2.921	1.002	0.834
WC-TF-6-11	0.840	0.216	0.810	1.023	3.426	1.037	0.821
WC-TF-6-12	0.805	0.215	0.810	1.022	3.744	0.994	0.788
WC-TF-6-13	0.960	0.220	0.989	1.089	4.364	0.971	0.882

TABLE 28 (continued)

Beam Specimen No.	Tested Data (per web) $(P_u)_{test}$ (kips)	Computed Data per web			$\dfrac{(P_u)_{test}}{(P_{cr})_{comp}}$	$\dfrac{(P_u)_{test}}{(P_u)_{comp}}$	$\dfrac{(P_u)_{test}}{(P'_u)_{comp}}$
		$(P_{cr})_{comp}$ (kips)	$(P_u)_{comp}$ (kips)	$(P'_u)_{comp}$ (kips)			
WC-TF-6-14	0.990	0.219	0.984	1.087	4.521	1.006	0.911
WC-TF-6-15	1.225	0.223	1.164	1.159	5.493	1.052	1.057
WC-TF-6-16	1.190	0.223	1.164	1.160	5.336	1.002	1.026
WC-TF-6-17	1.375	0.235	1.355	1.265	5.851	1.015	1.015
WC-TF-6-18	1.325	0.235	1.355	1.265	5.638	0.978	1.047
WC-TF-6-19	1.565	0.246	1.565	1.391	6.362	1.000	1.125
WC-TF-6-20	1.600	0.243	1.558	1.384	6.584	1.027	1.156
WC-TF-8-1	1.055	0.196	1.007	1.017	5.383	1.048	1.037
WC-TF-8-2	1.050	0.196	1.007	1.017	5.357	1.043	1.032
WC-TF-7-3	1.975	0.320	1.797	1.782	6.172	1.099	1.108
WC-TF-7-4	1.930	0.322	1.804	1.787	5.994	1.070	1.080
WC-TF-8-3	1.145	0.179	1.111	1.433	6.397	1.031	0.800
WC-TF-8-4	1.155	0.178	1.112	1.428	6.208	1.039	0.809
WC-TF-8-5	1.105	0.417	1.064	1.219	2.650	1.039	0.906
WC-TF-8-6	1.090	0.410	1.053	1.208	2.659	1.035	0.902
WC-TF-8-7	1.180	0.249	1.208	1.084	4.739	1.093	1.089
WC-TF-8-8	1.165	0.244	1.214	1.061	4.775	0.960	1.098
WC-TF-7-5	2.325	0.364	2.390	1.899	6.799	0.973	1.224
WC-TF-7-6	2.420	0.366	2.398	1.906	6.885	1.009	1.270
WC-TF-8-9	1.310	0.659	1.263	1.655	1.836	1.037	0.792
WC-TF-8-10	1.335	0.664	1.268	1.663	1.860	1.053	0.803
WC-TF-7-7	3.040	0.730	2.683	2.633	4.164	1.133	1.155
WC-TF-7-8	2.990	0.726	2.674	2.623	4.118	1.118	1.140
WC-TF-8-11	1.625	0.301	1.787	1.527	5.399	0.909	1.064
WC-TF-8-12	1.675	0.301	1.787	1.527	5.565	0.937	1.097
WC-TF-4-1	1.260	0.663	1.244	1.564	1.900	1.013	0.806
WC-TF-4-2	1.260	0.663	1.244	1.564	1.900	1.013	0.806

TABLE 28 (continued)

Beam Specimen No.	Tested Data (per web) $(P_u)_{test}$ (kips)	Computed Data/per web			$\dfrac{(P_u)_{test}}{(P_{cr})_{comp}}$	$\dfrac{(P_u)_{test}}{(P_u)_{comp}}$	$\dfrac{(P_u)_{test}}{(P'_u)_{comp}}$
		$(P_{cr})_{comp}$ (kips)	$(P_u)_{comp}$ (kips)	$(P'_u)_{comp}$ (kips)			
WC-TF-4-3	1.160	0.281	1.143	1.451	4.128	1.015	0.800
WC-TF-4-4	1.150	0.282	1.141	1.457	4.078	1.007	0.789
WC-TF-4-5	1.200	0.416	1.242	1.204	2.885	0.966	0.997
WC-TF-4-6	1.210	0.416	1.242	1.205	2.909	0.974	0.974
WC-TF-9-1	1.420	0.771	1.350	1.190	1.842	1.052	1.193
WC-TF-9-2	1.410	0.753	1.330	1.177	1.873	1.060	1.198
WC-TF-10-1	1.565	0.470	1.671	1.496	3.330	0.937	1.046
WC-TF-10-2	1.505	0.468	1.665	1.497	3.216	0.904	1.005
Mean						1.009	1.005
Standard Deviation						0.054	0.143

TABLE 29

ULTIMATE MOMENT CAPACITY OF BEAM SPECIMENS FOR ONE-FLANGE WEB CRIPPLING TESTS

Specimen No.	f_{cr} (ksi)	S_x (in.^{4})	$(M_u)_{cr}$ (in.-kips)	S_x' (in.^{4})	M_y (in.-kips)	$(M_u)_{test}$ (in.-kips)	$\dfrac{(M_u)_{test}}{(M_u)_{comp}}$*
WC-OF-1-1	64.09	1.325	76.59	0.808	29.80	3.94	0.132
WC-OF-1-2	63.91	1.326	76.68	0.810	29.87	3.79	0.127
WC-OF-2-1	44.90	2.109	103.67	1.184	63.69	6.68	0.105
WC-OF-2-2	44.66	2.116	104.07	1.299	69.87	6.83	0.098
WC-OF-3-1	27.84	2.426	120.94	1.606	59.23	6.46	0.109
WC-OF-3-2	27.97	2.457	122.50	1.625	59.93	6.74	0.112
WC-OF-4-1	15.26	3.548	145.90	2.622	96.70	10.20	0.105
WC-OF-4-2	15.93	3.632	152.40	2.701	99.61	10.80	0.108
WC-OF-5-1	10.96	6.590	215.57	4.262	157.18	17.52	0.111
WC-OF-5-2	10.77	6.524	211.23	4.203	155.01	16.65	0.107
WC-OF-7-1	6.96	9.128	249.30	6.338	233.75	23.70	0.101
WC-OF-7-2	6.92	9.209	251.19	6.404	236.18	22.39	0.095
WC-OF-6-1	9.25	2.281	77.25	1.935	83.32	4.55	0.059
WC-OF-6-2	9.36	2.278	77.71	1.948	83.88	4.21	0.054
WC-OF-6-3	9.21	2.266	76.75	1.947	83.84	5.53	0.072
WC-OF-6-4	9.42	2.249	77.26	1.972	84.91	5.81	0.075
WC-OF-6-5	9.21	2.302	77.78	1.951	84.01	7.38	0.095
WC-OF-6-6	9.23	2.305	77.91	1.948	83.88	7.03	0.090
WC-OF-6-7	8.93	2.190	73.24	1.894	81.56	7.86	0.107
WC-OF-6-8	8.93	2.203	73.66	1.899	81.77	7.84	0.106
WC-OF-6-9	9.36	2.269	77.46	1.951	84.01	9.29	0.120
WC-OF-6-10	9.38	2.293	78.36	1.973	84.96	8.70	0.111
WC-OF-3-3	27.39	2.429	120.47	1.749	64.50	6.19	0.096
WC-OF-3-4	27.41	2.418	119.84	1.739	64.13	6.02	0.094
WC-OF-3-5	27.81	2.464	122.83	1.776	65.50	8.31	0.127
WC-OF-3-6	27.69	2.441	121.52	1.759	64.87	8.17	0.126
WC-OF-3-7	27.89	2.459	122.70	1.771	65.31	9.65	0.148
WC-OF-3-8	27.54	2.446	121.51	1.761	64.95	9.93	0.153
WC-OF-3-9	28.00	2.466	123.17	1.775	65.46	11.22	0.171

TABLE 29 (continued)

Specimen No.	f_{cr} (ksi)	S_x (in^4)	$(M_u)_{cr}$ (in.-kips)	S_x' (in^4)	M_y (in.-kips)	$(M_u)_{test}$ (in.-kips)	$\dfrac{(M_u)_{test}}{(M_u)_{comp}}$*
WC-OF-3-10	27.52	2.462	122.22	1.771	65.31	10.78	0.165
WC-OF-3-11	25.59	2.426	120.51	1.741	64.21	12.18	0.190
WC-OF-3-12	28.05	2.448	122.27	1.758	64.84	12.68	0.196
WC-OF-4-3	15.84	3.612	151.19	2.481	91.50	3.46	0.038
WC-OF-4-4	15.75	3.616	150.87	2.476	91.31	3.40	0.037
WC-OF-4-5	15.81	3.592	150.22	2.667	98.36	7.72	0.078
WC-OF-4-6	15.89	3.607	151.07	2.676	98.69	7.63	0.077
WC-OF-4-7	16.05	3.633	152.85	2.869	105.81	14.17	0.134
WC-OF-4-8	16.29	3.679	155.64	2.904	107.10	13.88	0.130
WC-OF-4-9	15.88	3.622	151.65	3.057	112.74	20.41	0.181
WC-OF-4-10	16.04	3.637	152.99	3.074	113.37	19.73	0.174
WC-OF-5-3	10.80	6.528	209.57	3.979	154.39	7.30	0.047
WC-OF-5-4	10.58	6.469	206.10	3.957	153.53	6.96	0.045
WC-OF-5-5	10.92	6.566	212.87	4.244	164.57	12.69	0.077
WC-OF-5-6	10.81	6.525	210.65	4.223	163.85	11.97	0.073
WC-OF-5-7	10.80	6.514	209.18	4.420	171.50	20.36	0.119
WC-OF-5-8	10.85	6.517	210.18	4.426	171.73	19.44	0.113
WC-OF-5-9	10.78	6.540	210.40	4.627	179.53	27.50	0.153
WC-OF-5-10	10.88	6.564	212.47	4.650	180.42	26.70	0.148
WC-OF-5-11	10.88	6.580	212.63	4.831	187.44	32.70	0.174
WC-OF-5-12	10.97	6.577	213.50	4.831	187.44	32.46	0.173
WC-OF-8-1	26.88	2.567	68.77	1.597	53.44	5.50	0.103
WC-OF-8-2	26.88	2.697	72.77	1.672	55.95	5.44	0.097
MWC-OF-4-3	15.72	3.600	150.21	3.260	126.75	18.83	0.149
MWC-OF-4-4	15.79	3.620	151.31	3.279	120.93	20.18	0.167
MWC-OF-4-5	15.49	3.594	149.02	3.253	119.97	23.41	0.195
MWC-OF-4-6	15.64	3.604	150.15	3.268	120.52	24.57	0.204
MWC-OF-4-7	15.92	3.609	151.31	3.292	121.41	28.88	0.238
MWC-OF-4-8	15.83	3.616	151.34	3.304	121.85	29.52	0.242
MWC-OF-4-9	15.64	3.609	150.12	3.290	121.34	33.25	0.274
MWC-OF-4-10	15.56	3.555	147.66	3.244	119.64	32.26	0.270

*The value of $(M_u)_{comp}$ is determined by $(M_u)_{cr}$ or M_y whichever is smaller.

TABLE 30

DIMENSIONS OF INTERMEDIATE STIFFENER TEST SPECIMENS

Specimen No.	Dimensions (in.)												F_{yw} (ksi)	Total Length (in.)
	Thick.	B1	B2	B3	B4	d1	d2	D1	D2	R	BB	N		
ITS-C-1-1	0.0379	2.280	2.317	2.303	2.322	0.684	0.701	6.024	6.026	0.1250	7	2	43.06	20
ITS-C-1-2	0.0382	2.259	2.309	2.308	2.270	0.703	0.697	6.056	6.045	0.1250	7	2	43.06	20
ITS-C-1-3	0.0383	2.310	2.265	2.256	2.299	0.712	0.700	6.048	6.051	0.1250	7	2	43.06	20
ITS-C-2-1	0.0382	2.355	2.340	2.372	2.370	0.547	0.576	8.053	8.055	0.1250	7	2	43.06	25
ITS-C-2-2	0.0381	2.344	2.370	2.370	2.339	0.568	0.552	8.054	8.048	0.1250	7	2	43.06	25
ITS-C-2-3	0.0382	2.348	2.374	2.380	2.348	0.578	0.560	8.056	8.060	0.1250	7	2	43.06	25
ITS-C-3-1	0.0380	2.277	2.275	2.296	2.296	0.694	0.697	9.951	9.959	0.1250	7	2	43.06	30
ITS-C-3-2	0.0381	2.285	2.279	2.310	2.314	0.679	0.684	9.948	9.972	0.1250	7	2	43.06	30
ITS-C-4-1	0.0385	2.290	2.305	2.286	2.285	0.684	0.675	11.844	11.844	0.1250	7	2	43.06	36
ITS-C-4-2	0.0387	2.292	2.297	2.296	2.291	0.673	0.695	11.844	11.844	0.1250	7	2	43.06	36
ITS-C-4-3	0.0384	2.296	2.298	2.310	2.290	0.662	0.687	11.844	11.844	0.1250	7	2	43.06	36
ITS-C-4-4	0.0382	2.299	2.284	2.296	2.291	0.679	0.701	11.844	11.844	0.1250	7	3	43.06	36
ITS-C-4-5	0.0383	2.271	2.310	2.291	2.299	0.698	0.672	11.844	11.844	0.1250	7	3	43.06	36
ITS-C-6-1	0.0504	1.644	1.618	1.631	1.639	0.658	0.644	9.902	9.885	0.1094	7	2	36.88	30
ITS-C-6-2	0.0506	1.637	1.623	1.622	1.640	0.625	0.641	9.891	9.896	0.1094	7	2	36.88	30
ITS-C-5-1	0.0502	3.480	3.569	3.590	3.477	0.697	0.687	7.508	7.508	0.1094	7	2	36.88	24
ITS-C-5-2	0.0504	3.572	3.475	3.523	3.584	0.683	0.663	7.485	7.493	0.1094	7	2	36.88	24
ITS-S-7-1	0.0386	2.510	2.498	2.506	2.566	0.692	0.659	15.063	15.063	0.0938	7	2	47.63	45
ITS-S-7-2	0.0385	2.534	2.526	2.491	2.501	0.674	0.692	14.938	15.000	0.0938	7	2	47.63	45
ITS-S-7-3	0.0385	2.555	2.504	2.510	2.558	0.691	0.695	14.875	14.844	0.0938	7	2	47.63	45
ITS-S-8-1	0.0499	2.912	2.912	2.882	2.881	0.691	0.714	17.969	17.969	0.0625	7	3	38.80	54
ITS-S-8-2	0.0498	2.898	2.896	2.894	2.896	0.697	0.709	17.969	18.000	0.0625	7	3	38.80	54
ITS-S-9-1	0.0504	2.875	2.847	2.829	2.839	0.608	0.608	14.750	14.750	0.0781	7	3	41.18	45
ITS-S-9-2	0.0505	2.814	2.816	2.850	2.849	0.621	0.591	14.594	14.688	0.0781	7	3	41.18	45
ITS-S-10-1	0.0501	2.816	2.830	2.842	2.811	0.638	0.635	12.094	12.094	0.0781	7	3	41.18	36
ITS-S-10-2	0.0502	2.850	2.824	2.839	2.819	0.626	0.629	12.063	12.063	0.0781	7	3	41.18	36

TABLE 30 (continued)

Specimen No.	Dimensions (in.)												F_{yw} (ksi)	Total Length (in.)
	Thick.	B1	B2	B3	B4	d1	d2	D1	D2	R	BB	N		
ITS-S-11-1	0.0620	3.676	3.706	3.691	3.687	0.695	0.735	21.094	21.094	0.0781	9	3	39.64	64
ITS-S-11-2	0.0620	3.693	3.676	3.697	3.708	0.669	0.678	21.063	21.063	0.0781	9	3	39.64	64
ITS-S-11-3	0.0615	3.689	3.698	3.705	3.702	0.697	0.700	21.031	21.031	0.0781	9	3	39.64	64
ITS-S-12-1	0.0631	3.701	3.675	3.676	3.681	0.696	0.700	18.063	18.063	0.0781	9	3	39.64	54
ITS-S-12-2	0.0623	3.696	3.689	3.684	3.675	0.699	0.718	18.031	18.063	0.0781	9	3	39.64	54
ITS-S-13-1	0.0611	3.675	3.687	3.688	3.683	0.709	0.719	14.963	14.963	0.0781	9	3	39.64	45
ITS-S-13-2	0.0610	3.686	3.686	3.675	3.675	0.705	0.720	14.969	14.969	0.0781	9	3	39.64	45

Notes: 1. See Fig. 8 for the definition of symbols.

2. Beam specimens are designated as follows:

ITS	-	C	-	S	-	13	-	2
Intermediate Transverse Stiffener		Crushing Failure		Stability Failure		Channel No.		Test No.

TABLE 31

DIMENSIONS OF END TRANSVERSE STIFFENER TEST SPECIMENS

Specimen No.	Dimensions (in.)												F_{yw} (ksi)	Total Length (in.)
	Thick.	B1	B2	B3	B4	d1	d2	D1	D2	R	BB	N		
ETS-C-1-1	0.0383	2.284	2.285	2.293	2.322	0.695	0.675	6.058	6.060	0.1250	7	2	43.06	14
ETS-C-1-2	0.0382	2.306	2.292	2.288	2.301	0.700	0.698	6.063	6.054	0.1250	7	2	43.06	14
ETS-C-2-1	0.0383	2.277	2.298	2.307	2.323	0.674	0.683	8.033	8.037	0.1250	7	2	43.06	18
ETS-C-2-2	0.0382	2.273	2.278	2.292	2.310	0.698	0.689	8.010	8.034	0.1250	7	2	43.06	18
ETS-C-3-1	0.0382	2.286	2.289	2.288	2.283	0.699	0.694	9.998	9.996	0.1250	7	2	43.06	20
ETS-C-3-2	0.0384	2.287	2.283	2.288	2.320	0.678	0.686	9.981	9.986	0.1250	7	2	43.06	20
ETS-C-3-3	0.0382	2.330	2.292	2.286	2.295	0.699	0.704	9.964	9.975	0.1250	7	2	43.06	20
ETS-C-4-1	0.0384	2.320	2.296	2.287	2.319	0.661	0.688	11.844	11.844	0.1250	7	2	43.06	24
ETS-C-4-2	0.0382	2.282	2.292	2.299	2.318	0.689	0.697	11.844	11.844	0.1250	7	2	43.06	24
ETS-C-4-3	0.0382	2.304	2.294	2.279	2.326	0.698	0.678	11.844	11.844	0.1250	7	2	43.06	24
ETS-C-6-1	0.0500	1.620	1.637	1.642	1.632	0.635	0.626	9.898	9.905	0.1094	7	2	36.88	20
ETS-C-6-2	0.0502	1.621	1.644	1.645	1.636	0.630	0.623	9.903	9.801	0.1094	7	2	36.88	20
ETS-C-5-1	0.0501	3.572	3.477	3.529	3.568	0.678	0.678	7.503	7.514	0.1094	7	2	36.88	16
ETS-C-5-2	0.0502	3.498	3.572	3.608	3.483	0.688	0.692	7.493	7.518	0.1094	7	2	36.88	16
ETS-S-7-1	0.0386	2.574	2.487	2.487	2.582	0.660	0.662	14.844	14.844	0.0938	7	2	47.63	30
ETS-S-7-2	0.0386	2.536	2.447	2.457	2.562	0.667	0.667	14.938	14.968	0.0938	7	2	47.63	30
ETS-S-8-1	0.0497	2.890	2.919	2.922	2.886	0.701	0.702	17.969	17.969	0.0625	7	3	38.80	36
ETS-S-8-2	0.0497	2.919	2.896	2.881	2.893	0.698	0.713	17.975	17.975	0.0625	7	3	38.80	36
ETS-S-9-1	0.0505	2.889	2.871	2.866	2.884	0.623	0.609	14.531	14.531	0.0781	7	3	41.18	30
ETS-S-9-2	0.0504	2.873	2.871	2.874	2.875	0.621	0.618	14.500	14.531	0.0781	7	3	41.18	30
ETS-S-10-1	0.0500	2.875	2.855	2.865	2.885	0.622	0.612	11.969	12.000	0.0781	7	3	41.18	25
ETS-S-10-2	0.0502	2.836	2.850	2.862	2.864	0.629	0.613	12.063	12.031	0.0781	7	3	41.18	25

TABLE 31 (continued)

Specimen No.	Dimensions (in.)												F_{yw} (ksi)	Total Length (in.)
	Thick.	B1	B2	B3	B4	d1	d2	D1	D2	R	BB	N		
ETS-S-11-1	0.0631	3.686	3.676	3.692	3.694	0.720	0.697	21.031	21.063	0.0781	9	3	39.64	44
ETS-S-11-2	0.0617	3.695	3.683	3.699	3.698	0.688	0.692	21.063	21.094	0.0781	9	3	39.64	44
ETS-S-12-1	0.0614	3.677	3.678	3.702	3.689	0.712	0.730	18.063	18.031	0.0781	9	3	39.64	36
ETS-S-12-2	0.0622	3.684	3.687	3.690	3.680	0.708	0.725	18.019	18.031	0.0781	9	3	39.64	36
ETS-S-13-1	0.0612	3.722	3.695	3.682	3.706	0.669	0.679	14.969	14.969	0.0781	9	3	39.64	30
ETS-S-13-2	0.0618	3.706	3.702	3.675	3.694	0.657	0.691	15.063	15.000	0.0781	9	3	39.64	30

Notes: 1. See Fig. 8 for the definition of symbols

2. Beam specimens are designated as follows:

ETS	–	C	–	S	–	13	–	2
End		Crushing		Stability		Channel		Test
Transverse		Failure		Failure		No.		No.
Stiffeners								

TABLE 32

STIFFENER DIMENSIONS FOR INTERMEDIATE STIFFENER TESTS

Specimen No.	Dimensions (in.)								F_{ys} (ksi)	Total Length (in.)
	t	r	a1	a2	b1	b2	b3	b4		
ITS-C-1-1	0.0382	0.0938	1.272	1.285	0.521	0.455	0.518	0.469	43.06	6.025
ITS-C-1-2	0.0382	0.0938	1.275	1.290	0.521	0.481	0.470	0.506	43.06	6.051
ITS-C-1-3	0.0382	0.0938	1.238	1.255	0.498	0.517	0.495	0.510	43.06	6.050
ITS-C-2-1	0.0380	0.0938	1.245	1.245	0.498	0.524	0.492	0.515	43.06	8.054
ITS-C-2-2	0.0380	0.0938	1.255	1.247	0.479	0.515	0.520	0.490	43.06	8.051
ITS-C-2-3	0.0380	0.0938	1.260	1.268	0.490	0.496	0.485	0.485	43.06	8.056
ITS-C-3-1	0.0378	0.0938	1.273	1.275	0.508	0.483	0.463	0.527	43.06	9.955
ITS-C-3-2	0.0381	0.0938	1.273	1.280	0.512	0.467	0.474	0.514	43.06	9.960
ITS-C-4-1	0.0375	0.0938	1.253	1.274	0.499	0.474	0.475	0.475	43.06	11.844
ITS-C-4-2	0.0375	0.0938	1.274	1.285	0.489	0.496	0.495	0.501	43.06	11.844
ITS-C-4-3	0.0378	0.0938	1.271	1.269	0.496	0.475	0.491	0.484	43.06	11.844
ITS-C-4-4	0.0375	0.0938	1.325	1.278	0.495	0.498	0.509	0.496	43.06	11.844
ITS-C-4-5	0.0380	0.0938	1.294	1.296	0.473	0.490	0.469	0.481	43.06	11.844
ITS-C-5-1	0.0381	0.0938	1.298	1.315	0.450	0.499	0.490	0.445	43.06	7.508
ITS-C-5-2	0.0380	0.0938	1.312	1.308	0.446	0.495	0.445	0.499	43.06	7.489
ITS-C-6-1	0.0380	0.0938	1.281	1.296	0.463	0.510	0.499	0.471	43.06	9.894
ITS-C-6-2	0.0380	0.0938	1.271	1.266	0.490	0.495	0.518	0.470	43.06	9.894
ITS-S-7-1	0.0381	0.0938	1.315	1.313	0.505	0.482	0.501	0.486	43.06	15.063
ITS-S-7-2	0.0382	0.0938	1.287	1.285	0.513	0.470	0.515	0.472	43.06	14.969
ITS-S-7-3	0.0382	0.0938	1.299	1.290	0.508	0.487	0 487	0.499	43.06	14.860
ITS-S-8-1	0.0410	0.0781	1.476	1.521	0.500	0.575	0.475	0.536	47.63	17.969
ITS-S-8-2	0.0410	0.0781	1.466	1.475	0.533	0.571	0.560	0.525	47.63	17.985
ITS-S-9-1	0.0410	0.0781	1.485	1.525	0.486	0.592	0.470	0.533	47.63	14.750
ITS-S-9-2	0.0411	0.0781	1.467	1.496	0.581	0.495	0.450	0.575	47.63	14.641
ITS-S-10-1	0.0409	0.0781	1.487	1.494	0.473	0.562	0.550	0.512	47.63	12.094
ITS-S-10-2	0.0413	0.0781	1.461	1.480	0.544	0.540	0.575	0.500	47.63	12.063

TABLE 32 (continued)

Specimen No.	Dimensions (in.)								F_{ys} (ksi)	Total Length (in.)
	t	r	a1	a2	b1	b2	b3	b4		
ITS-S-11-1	0.0411	0.0781	1.461	1.502	0.584	0.515	0.475	0.550	47.63	21.094
ITS-S-11-2	0.0410	0.0781	1.465	1.501	0.585	0.512	0.473	0.548	47.63	21.063
ITS-S-11-3	0.0415	0.0781	1.455	1.491	0.580	0.513	0.547	0.497	47.63	21.031
ITS-S-12-1	0.0416	0.0781	1.464	1.501	0.593	0.495	0.578	0.479	47.63	18.063
ITS-S-12-2	0.0414	0.0781	1.512	1.464	0.556	0.471	0.568	0.519	47.63	18.047
ITS-S-13-1	0.0415	0.0781	1.454	1.455	0.509	0.591	0.502	0.590	47.63	14.963
ITS-S-13-2	0.0414	0.0781	1.460	1.462	0.583	0.503	0.500	0.575	47.63	14.969

Note: Refer to Fig.73 for definition of symbols used

TABLE 33

STIFFENER DIMENSIONS FOR END TRANSVERSE STIFFENER TESTS

Specimen No.	Dimensions (in.)								F_{ys} (ksi)	Total Length (in.)
	t	r	a1	a2	b1	b2	b3	b4		
EBS-C-1-1	0.0380	0.0938	1.323	1.313	0.431	0.503	0.512	0.434	43.06	6.059
EBS-C-1-2	0.0382	0.0938	1.325	1.320	0.436	0.521	0.439	0.508	43.06	6.059
EBS-C-2-1	0.0382	0.0938	1.267	1.277	0.489	0.509	0.433	0.516	43.06	8.035
EBS-C-2-2	0.0382	0.0938	1.291	1.280	0.455	0.511	0.501	0.474	43.06	8.022
EBS-C-3-1	0.0382	0.0938	1.250	1.254	0.514	0.491	0.516	0.471	43.06	9.997
EBS-C-3-2	0.0382	0.0938	1.268	1.287	0.510	0.483	0.478	0.502	43.06	9.984
EBS-C-3-3	0.0383	0.0938	1.310	1.308	0.504	0.441	0.509	0.440	43.06	9.970
EBS-C-4-1	0.0382	0.0938	1.276	1.287	0.450	0.515	0.499	0.508	43.06	11.844
EBS-C-4-2	0.0382	0.0938	1.289	1.275	0.464	0.507	0.464	0.525	43.06	11.844
EBS-C-4-3	0.0382	0.0938	1.329	1.316	0.501	0.455	0.493	0.468	43.06	11.844
EBS-C-5-1	0.0382	0.0938	1.274	1.271	0.494	0.509	0.511	0.476	43.06	7.509
EBS-C-5-2	0.0382	0.0938	1.311	1.267	0.497	0.445	0.490	0.504	43.06	7.506
EBS-C-6-1	0.0382	0.0938	1.276	1.269	0.507	0.480	0.508	0.482	43.06	9.902
EBS-C-6-2	0.0382	0.0938	1.287	1.255	0.502	0.483	0.515	0.464	43.06	9.852
EBS-S-7-1	0.0381	0.0938	1.269	1.276	0.555	0.442	0.542	0.453	43.06	14.844
EBS-S-7-2	0.0382	0.0938	1.250	1.259	0.450	0.550	0.472	0.521	43.06	14.953
EBS-S-8-1	0.0412	0.0781	1.475	1.473	0.565	0.520	0.510	0.569	47.63	17.969
EBS-S-8-2	0.0410	0.0781	1.509	1.469	0.503	0.525	0.566	0.540	47.63	17.975
EBS-S-9-1	0.0410	0.0781	1.499	1.492	0.433	0.596	0.595	0.462	47.63	14.531
EBS-S-9-2	0.0409	0.0781	1.520	1.497	0.483	0.550	0.595	0.475	47.63	14.516
EBS-S-10-1	0.0414	0.0781	1.463	1.461	0.565	0.525	0.566	0.522	47.63	11.915
EBS-S-10-2	0.0415	0.0781	1.473	1.515	0.543	0.525	0.505	0.545	47.63	12.047

TABLE 33 (continued)

Specimen No.	Dimensions (in.)								F_{ys} (ksi)	Total Length (in.)
	t	r	a1	a2	b1	b2	b3	b4		
EBS-S-11-1	0.0412	0.0781	1.500	1.502	0.546	0.490	0.499	0.545	47.63	21.047
EBS-S-11-2	0.0410	0.0781	1.496	1.502	0.537	0.491	0.496	0.526	47.63	21.079
EBS-S-12-1	0.0411	0.0781	1.465	1.510	0.518	0.568	0.525	0.523	47.63	18.047
EBS-S-12-2	0.0412	0.0781	1.500	1.522	0.512	0.542	0.466	0.552	47.63	18.025
EBS-S-13-1	0.0411	0.0781	1.491	1.498	0.506	0.554	0.536	0.489	47.63	14.969
EBS-S-13-2	0.0418	0.0781	1.484	1.489	0.530	0.545	0.511	0.525	47.63	15.032

Note: Refer to Fig. 73 for definition of symbols used

162

TABLE 34

COMPARISON OF TESTED AND COMPUTED DATA FOR INTERMEDIATE STIFFENER
TEST SPECIMENS

Beam Specimen No.	Tested Data $(P_u)_{test}$ (kips)	Computed Data				$\dfrac{(P_u)_{test}}{(P_{us})_{comp}}$	$\dfrac{(P_u)_{test}}{(P_u)_{comp}}$
		P_{cr} (kips)	P_y (kips)	$(P_c)_{comp}$ (kips)	$(P_{cr})_{comp}$ (kips)		
ITS-C-1-1	4.17	3.23	3.44	3.92	4.18	1.291	1.064
ITS-C-1-2	3.98	3.25	3.46	3.95	4.20	1.225	1.008
ITS-C-1-3	4.07	3.22	3.42	3.94	4.20	1.264	1.003
ITS-C-2-1	4.09	3.05	3.40	3.92	4.15	1.341	1.043
ITS-C-2-2	3.98	3.05	3.40	3.90	4.12	1.210	1.021
ITS-C-2-3	4.42	3.02	3.39	3.89	4.08	1.464	1.136
ITS-C-4-3	3.72	2.57	3.38	3.89	3.89	1.467	0.961
ITS-C-4-4	4.42	2.66	3.43	3.95	3.89	1.662	1.136
ITS-C-4-5	4.28	2.55	3.41	3.91	3.95	1.678	1.095
ITS-C-5-1	4.06	3.05	3.41	4.38	4.57	1.331	0.927
ITS-C-5-2	4.02	3.05	3.41	4.38	4.58	1.318	0.916
ITS-C-6-1	4.13	2.84	3.43	4.40	4.45	1.454	0.939
ITS-C-6-2	4.02	2.86	3.41	4.40	4.50	1.406	0.914
ITS-C-3-1	3.76	2.85	3.41	3.90	3.96	1.333	0.949
ITS-C-3-2	3.62	2.86	3.43	3.92	3.97	1.273	0.923
ITS-C-4-1	3.52	2.50	3.32	3.85	3.63	1.424	0.970
ITS-C-4-2	3.72	2.61	3.39	3.92	3.77	1.322	1.005
ITS-S-7-1	3.25	2.19	3.51	4.12	3.26	1.484	0.997
ITS-S-7-2	3.43	2.17	3.46	4.07	3.24	1.581	1.059
ITS-S-7-3	3.34	2.21	3.48	4.09	3.29	1.511	1.015
ITS-S-8-1	3.12	2.12	4.55	5.50	3.27	1.472	0.954
ITS-S-8-2	3.81	2.39	4.51	5.39	3.69	1.594	1.033
ITS-S-9-1	4.58	2.89	4.57	5.63	4.46	1.585	1.027
ITS-S-9-2	4.66	2.95	4.54	5.62	4.57	1.580	1.020

TABLE 34 (continued)

Beam Specimen No.	Tested Data $(P_u)_{test}$ (kips)	Computed Data				$\dfrac{(P_u)_{test}}{(P_{us})_{comp}}$	$\dfrac{(P_u)_{test}}{(P_u)_{comp}}$
		P_{cr} (kips)	P_y (kips)	$(P_c)_{comp}$ (kips)	$(P_{cr})_{comp}$ (kips)		
ITS-S-10-1	4.95	3.44	4.53	5.59	5.18	1.439	0.956
ITS-S-10-2	5.29	3.55	4.55	5.64	5.37	1.490	0.985
ITS-S-11-1	3.01	1.61	4.54	6.36	2.88	1.870	1.045
ITS-S-11-2	2.90	1.61	4.53	6.36	2.87	1.801	1.010
ITS-S-11-3	2.96	1.66	4.58	6.37	2.94	1.783	1.007
ITS-S-12-1	3.98	2.29	4.62	6.52	4.02	1.738	0.990
ITS-S-12-2	3.85	2.20	4.60	6.43	3.85	1.750	1.000
ITS-S-13-1	5.22	3.08	4.55	6.34	5.36	1.695	0.974
ITS-S-13-2	5.12	3.01	4.55	6.32	5.24	1.711	0.977
Mean						1.501	1.002
Standard Deviation						0.184	0.056

TABLE 35

COMPARISON OF TESTED AND COMPUTED DATA FOR END TRANSVERSE
STIFFENER TEST SPECIMENS

Beam Specimen No.	Tested Data $(P_u)_{test}$ (kips)	Computed Data P_{cr} (kips)	P_y (kips)	$(P_c)_{comp}$ (kips)	$(P_{cr})_{comp}$ (kips)	$\dfrac{(P_u)_{test}}{(P_{us})_{comp}}$	$\dfrac{(P_u)_{test}}{(P_u)_{comp}}$
ETS-C-1-1	3.68	3.19	3.44	3.50	3.70	1.154	1.051
ETS-C-1-2	3.76	3.23	3.46	3.52	3.72	1.164	1.068
ETS-C-2-1	3.79	3.03	3.42	3.48	3.66	1.251	1.089
ETS-C-2-2	3.57	3.05	3.43	3.49	3.66	1.170	1.023
ETS-C-3-3	3.77	2.81	3.44	3.50	3.51	1.342	1.077
ETS-C-4-3	3.52	2.59	3.47	3.53	3.54	1.359	0.997
ETS-C-5-1	3.88	3.13	3.45	3.77	4.02	1.240	1.029
ETS-C-5-2	3.93	3.09	3.43	3.76	3.99	1.272	1.045
ETS-C-6-1	3.70	3.88	3.44	3.76	3.89	1.285	0.984
ETS-C-6-2	3.91	2.87	3.43	3.75	3.88	1.362	1.043
ETS-C-3-1	3.43	2.86	3.42	3.48	3.58	1.199	0.986
ETS-C-3-2	3.40	2.87	3.44	3.50	3.58	1.185	0.971
ETS-C-4-1	3.37	2.57	3.41	3.48	3.33	1.311	0.968
ETS-C-4-2	3.24	2.62	3.44	3.50	3.38	1.434	0.926
ETS-S-7-1	2.99	2.21	3.45	3.57	3.21	1.353	0.958
ETS-S-7-2	3.06	2.18	3.42	3.56	3.18	1.404	0.962
ETS-S-8-1	3.30	2.34	4.54	4.84	3.38	1.410	0.976
ETS-S-8-2	3.29	2.26	4.54	4.84	3.25	1.456	1.012
ETS-S-9-1	4.20	2.95	4.55	4.85	4.34	1.424	0.968
ETS-S-9-2	4.00	2.99	4.56	4.87	4.39	1.338	0.911
ETS-S-10-1	4.70	3.59	4.55	5.26	5.21	1.309	0.902
ETS-S-10-2	4.69	3.54	4.62	5.22	5.13	1.325	0.913
ETS-S-11-1	2.63	1.54	4.59	5.38	2.56	1.708	1.027

TABLE 35 (continued

Beam Specimen No.	Tested Data	Computed Data				$\dfrac{(P_u)_{test}}{(P_{us})_{comp}}$	$\dfrac{(P_u)_{test}}{(P_u)_{comp}}$
	$(P_u)_{test}$ (kips)	P_{cr} (kips)	P_y (kips)	$(P_c)_{comp}$ (kips)	$(P_{cr})_{comp}$ (kips)		
ETS-S-11-2	2.50	1.47	4.55	5.27	2.42	1.701	1.033
ETS-S-12-1	3.67	2.24	4.55	5.32	3.57	1.638	1.028
ETS-S-12-2	3.35	2.08	4.61	5.35	3.34	1.611	1.003
ETS-S-13-1	4.56	2.85	4.56	5.28	4.62	1.600	0.987
ETS-S-13-2	4.51	2.95	4.56	5.38	4.79	1.529	0.942
Mean						1.394	0.996
Standard Deviation						0.203	0.051

TABLE 36

CRUSHING STRESS OF COLD-FORMED STEEL TRANSVERSE STIFFENERS

Specimen No.	f_c (ksi)	F_{ys} (ksi)	F_{yw} (ksi)	F_{ya} (ksi)	$\dfrac{f_c}{F_{ya}}$
ITS-C-1-1	40.53	43.06	43.06	43.06	0.941
ITS-C-1-2	37.89	43.06	43.06	43.06	0.880
ITS-C-1-3	39.18	43.06	43.06	43.06	0.910
ITS-C-2-1	35.44	43.06	43.06	43.06	0.823
ITS-C-2-2	32.33	43.06	43.06	43.06	0.751
ITS-C-2-3	40.21	43.06	43.06	43.06	0.934
ITS-C-3-1	31.15	43.06	43.06	43.06	0.723
ITS-C-3-2	32.30	43.06	43.06	43.06	0.750
ITS-C-4-1	–	43.06	43.06	43.06	–
ITS-C-4-2	–	43.06	43.06	43.06	–
ITS-C-4-3	34.34	4.306	43.06	43.06	0.798
ITS-C-4-4	43.06	43.06	43.06	43.06	1.000
ITS-C-4-5	43.06	43.06	43.06	43.06	1.000
ITS-C-5-1	30.61	43.06	36.88	41.45	0.739
ITS-C-5-2	–	43.06	36.88	–	–
ITS-C-6-1	34.41	43.06	36.88	41.69	0.825
ITS-C-6-2	32.16	43.06	36.88	41.57	0.774
ETS-C-1-1	35.02	43.06	43.06	43.06	0.813
ETS-C-1-2	38.10	43.06	43.06	43.06	0.885
ETS-C-2-1	39.43	43.06	43.06	43.06	0.916
ETS-C-2-2	40.31	43.06	43.06	43.06	0.936
ETS-C-3-1	36.57	43.06	43.06	43.06	0.849
ETS-C-3-2	32.51	43.06	43.06	43.06	0.755
ETS-C-3-3	39.57	43.06	43.06	43.06	0.919
ETS-C-4-1	40.60	43.06	43.06	43.06	0.943
ETS-C-4-2	34.27	43.06	43.06	43.06	0.796
ETS-C-4-3	35.78	43.06	43.06	43.06	0.831
ETS-C-5-1	35.96	43.06	36.88	41.47	0.867
ETS-C-5-2	37.57	43.06	36.88	41.58	0.904
ETS-C-6-1	35.38	43.06	36.88	41.59	0.851
ETS-C-6-2	38.89	43.06	36.88	41.76	0.931
Mean					0.859

TABLE 37

EFFECTIVE WIDTH OF BEAM WEBS FOR INTERMEDIATE STIFFENERS
UNDER END CRUSHING FAILURE

Specimen No.	f_c (ksi)	$P_s = A_s f_c$ (kips)	$(P_u)_{test}$ (kips)	P_w (kips)	b_e (in.)	$\dfrac{b_e}{t_w}$
ITS-C-1-1	40.53	3.23	4.17	0.94	0.612	16.15
ITS-C-1-2	37.89	3.04	3.98	0.94	0.649	17.00
ITS-C-1-3	39.18	3.12	4.07	0.95	0.633	16.53
ITS-C-2-1	35.44	2.81	3.78	0.97	0.716	18.76
ITS-C-2-2	32.33	2.55	3.58	1.03	0.834	21.83
ITS-C-2-3	40.21	3.16	4.02	0.86	0.560	14.66
ITS-C-4-3	34.34	2.69	3.72	1.03	0.781	20.34
ITS-C-4-4	43.06	3.44	4.42	0.98	0.596	15.60
ITS-C-4-5	43.06	3.40	4.28	0.88	0.534	13.93
ITS-C-5-1	30.61	2.50	4.06	1.56	1.015	20.22
ITS-C-5-2	–	–	4.02	–	–	–
ITS-C-6-1	34.41	2.73	4.13	1.40	0.807	16.02
ITS-C-6-2	32.16	2.55	4.02	1.47	0.903	17.85
ITS-C-3-1	31.15	2.46	3.76	1.30	1.098	28.90
ITS-C-3-2	32.30	2.57	3.62	1.05	0.853	22.39
ITS-C-4-1	–	–	3.56	–	–	–
ITS-C-4-2	–	–	3.45	–	–	–
Mean						18.58

Notes: (a) f_c is the experimental crushing stress of stiffeners

(b) A_s is the stiffener cross section area

(c) P_s is the experimental load carried by stiffener alone

(d) $P_w = (P_u)_{test} - P_s$ = Load carried by beam webs

(e) $b_e = P_w / t_w f_c$ = Effective width of beam web

TABLE 38

EFFECTIVE WIDTH OF BEAM WEBS FOR END TRANSVERSE STIFFENERS
UNDER END CRUSHING FAILURE

Specimen No.	f_c (ksi)	$P_s = A_s f_c$ (kips)	$(P_u)_{test}$ (kips)	P_w (kips)	b_e (in.)	$\dfrac{b_e}{t_w}$
ETS-C-1-1	35.02	2.79	3.68	0.89	0.664	17.33 *
ETS-C-1-2	38.10	3.06	3.76	0.70	0.481	12.59
ETS-C-2-1	39.43	3.12	3.79	0.67	0.444	11.58
ETS-C-2-2	40.31	3.21	3.57	0.36	0.234	6.12 *
ETS-C-3-3	39.57	3.16	3.77	0.61	0.404	10.56
ETS-C-4-3	35.78	2.88	3.52	0.64	0.468	12.26
ETS-C-5-1	35.96	2.88	3.88	1.00	0.556	11.12
ETS-C-5-2	37.57	2.99	3.93	0.94	0.498	9.93
ETS-C-6-1	35.38	2.82	3.70	0.88	0.497	9.95
ETS-C-6-2	38.89	3.09	3.91	0.82	0.420	8.37
ETS-C-3-1	36.57	2.90	3.43	0.53	0.379	9.93
ETS-C-3-2	32.51	2.60	3.40	0.80	0.641	16.69 *
ETS-C-4-1	40.60	3.21	3.37	0.16	0.103	2.67 *
ETS-C-4-2	34.27	2.73	3.24	0.51	0.390	10.20
Mean						10.65

*These tests results were not used for computing the mean value

Note :   Refer to Table 37 for the footnotes

TABLE 39

COMPARISON OF TESTED AND COMPUTED EFFECTIVE WIDTHS
OF BEAM WEBS UNDER STABILITY FAILURE FOR INTERMEDIATE STIFFENERS

Specimen No.	$(P_u)_{test}$ (kips)	$(b_e)_{test}$ (in.)	$\dfrac{(b_e)_{test}}{t_w}$	D/t_w	$\dfrac{(b_e)_{test}}{(b_e)_{comp}}$
ITS-C-3-1	3.76	1.09	28.68	261.97	0.849
ITS-C-3-2	3.62	0.99	25.98	261.42	0.770
ITS-C-4-1	3.52	1.28	33.25	307.64	0.910
ITS-C-4-2	3.72	1.43	37.24	311.68	1.017
ITS-S-7-1	3.25	1.59	41.19	390.23	0.992
ITS-S-7-2	3.43	1.97	51.17	388.81	1.235
ITS-S-7-3	3.34	1.67	43.38	385.97	1.051
ITS-S-8-1	3.12	2.10	42.08	360.10	1.060
ITS-S-8-2	3.81	2.30	46.18	361.14	1.162
ITS-S-9-1	4.58	1.96	38.89	292.66	1.091
ITS-S-9-2	4.66	1.91	37.82	289.92	1.066
ITS-S-10-1	4.95	1.42	28.34	241.40	0.871
ITS-S-10-2	5.29	1.56	31.08	240.30	0.957
ITS-S-11-1	3.01	2.82	45.48	340.23	1.181
ITS-S-11-2	2.90	2.49	40.16	339.73	1.044
ITS-S-11-3	2.96	2.43	39.51	341.97	1.024
ITS-S-12-1	3.98	2.15	34.07	286.26	0.967
ITS-S-12-2	3.85	2.21	35.47	289.68	1.000
ITS-S-13-1	5.22	1.85	30.28	244.89	0.924
ITS-S-13-2	5.15	1.91	31.31	245.39	0.955

Mean   1.006
Standard Deviation   0.114

TABLE 40

COMPARISON OF TESTED AND COMPUTED EFFECTIVE WIDTHS
OF BEAM WEBS UNDER STABILITY FAILURE FOR END TRANSVERSE STIFFENER TESTS

Specimen No.	$(P_u)_{test}$ (kips)	$(b_e)_{test}$ (in.)	$\dfrac{(b_e)_{test}}{t_w}$	D/t_w	$\dfrac{(b_e)_{test}}{(b_e)_{comp}}$
ETS-C-3-1	3.43	0.77	20.16	261.70	0.850
ETS-C-3-2	3.40	0.81	21.20	260.99	0.895
ETS-C-4-1	3.37	1.05	27.34	308.44	1.045
ETS-C-4-2	3.24	0.85	22.25	310.05	0.848
ETS-S-7-1	2.99	1.07	27.72	384.56	0.919
ETS-S-7-2	3.06	1.21	31.35	387.38	1.034
ETS-S-8-1	3.30	1.31	26.36	361.55	0.910
ETS-S-8-2	3.29	1.52	30.58	361.67	1.056
ETS-S-9-1	4.20	1.41	27.92	287.74	1.113
ETS-S-9-2	4.00	1.12	22.22	288.02	0.885
ETS-S-10-1	4.70	1.09	21.80	239.70	0.966
ETS-S-10-2	4.69	1.16	23.11	239.98	1.023
ETS-S-11-1	2.63	1.92	30.43	333.55	1.107
ETS-S-11-2	2.50	1.93	31.28	341.64	1.121
ETS-S-12-1	3.67	1.74	28.34	293.93	1.115
ETS-S-12-2	3.35	1.58	25.40	289.79	1.008
ETS-S-13-1	4.56	1.57	25.65	244.59	1.124
ETS-S-13-2	4.51	1.37	22.17	243.24	0.974

Mean 1.000
Standard Deviation 0.097
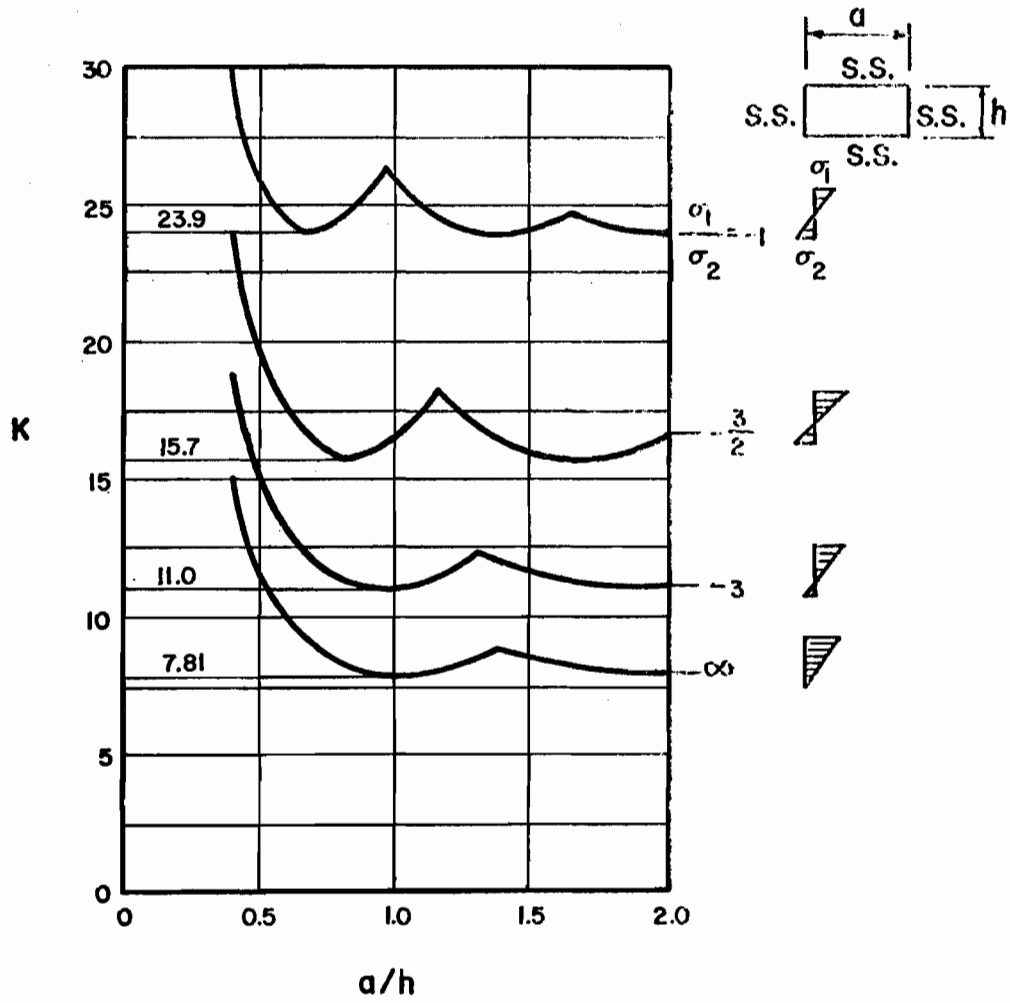
Figure 1. Buckling Coefficient k for Simply Supported Plates
Subjected to Nonuniform Longitudinal Bending Stress
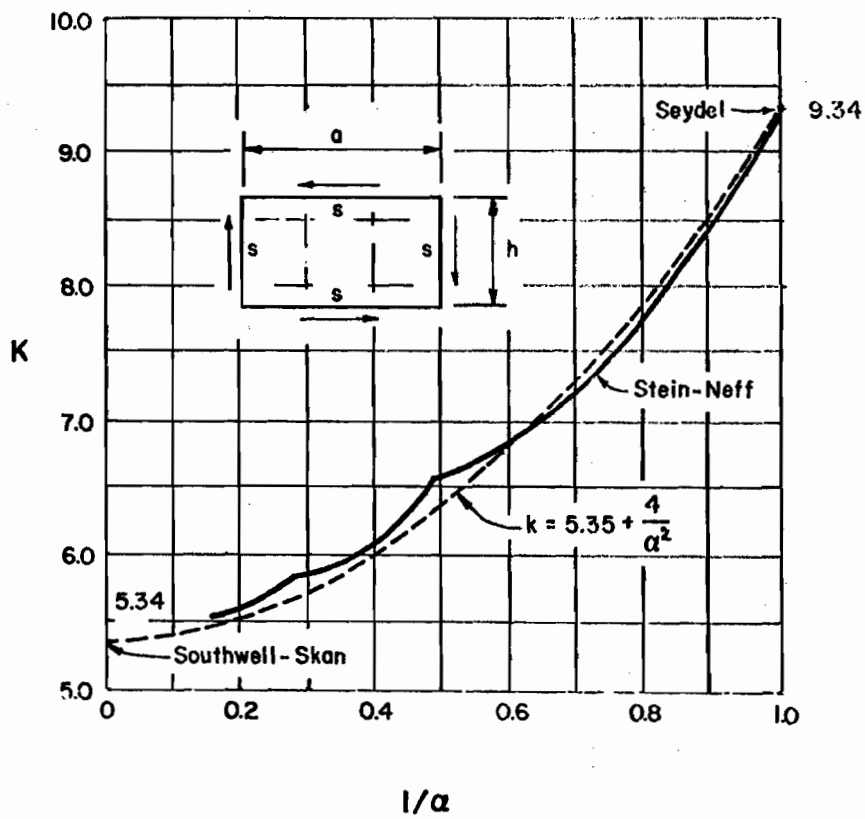
Figure 2. Buckling Coefficient k for Simply Supported Plates Subjected to Shear Stress
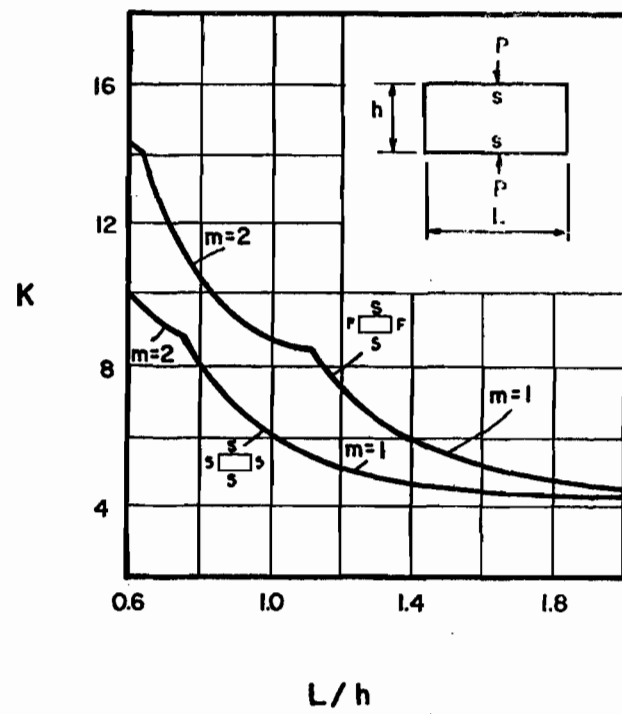
Figure 3. Buckling Coefficient K for Simply Supported Plates
Subjected to Two-Opposite Concentrated Loads
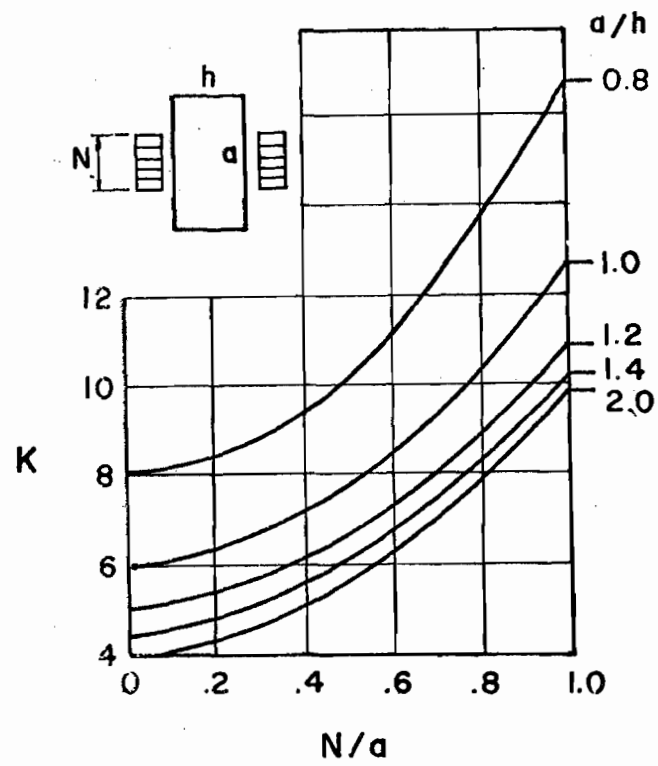
Figure 4. Buckling Coefficient K for Simply Supported Plates
Under Partial Loads on Both Edges
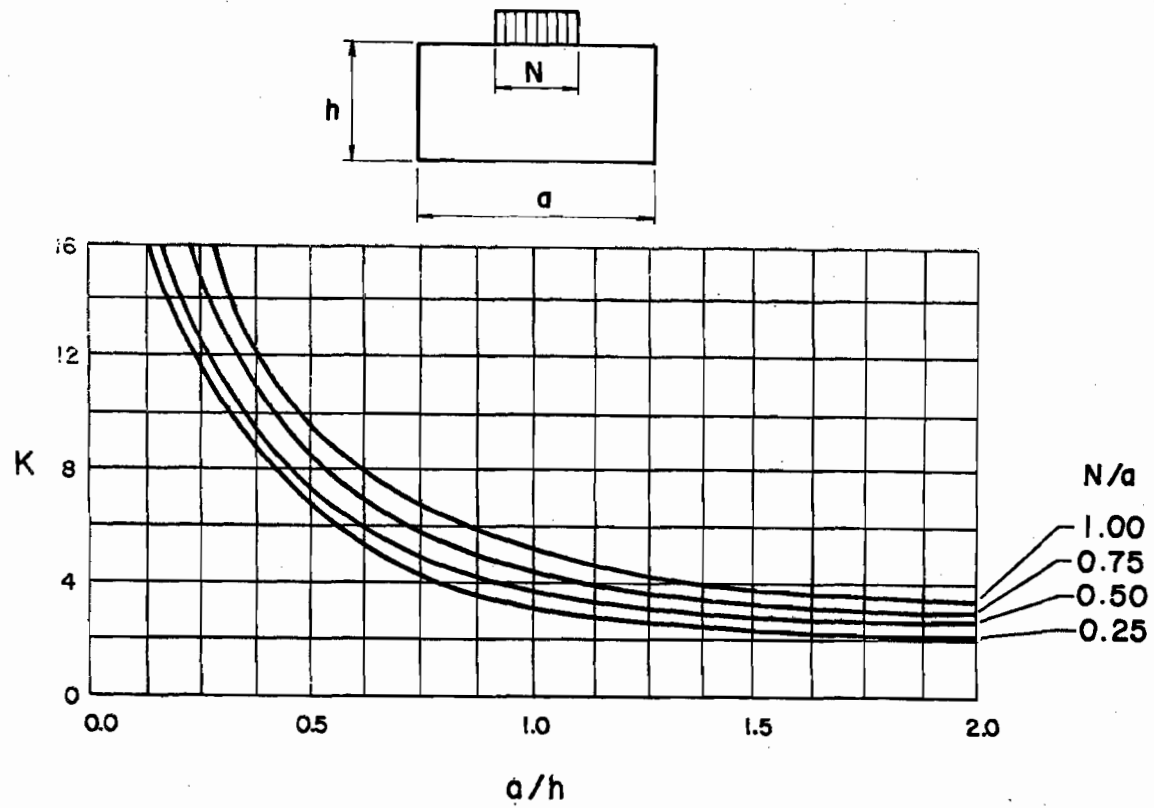
Figure 5. Buckling Coefficient K for Simply Supported Plates
Under Partial Load on One Edge
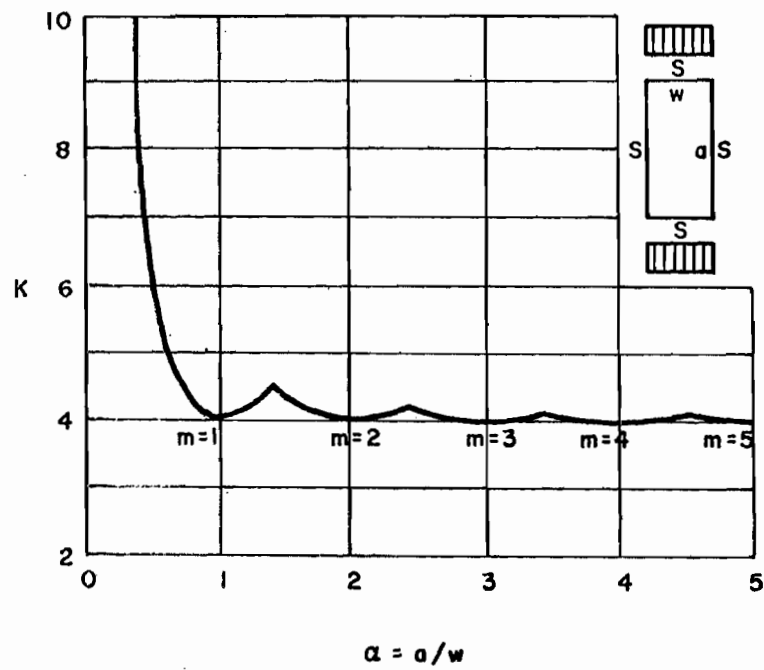
Figure 6. Buckling Coefficient for Simply Supported Plates Under Uniform Compression
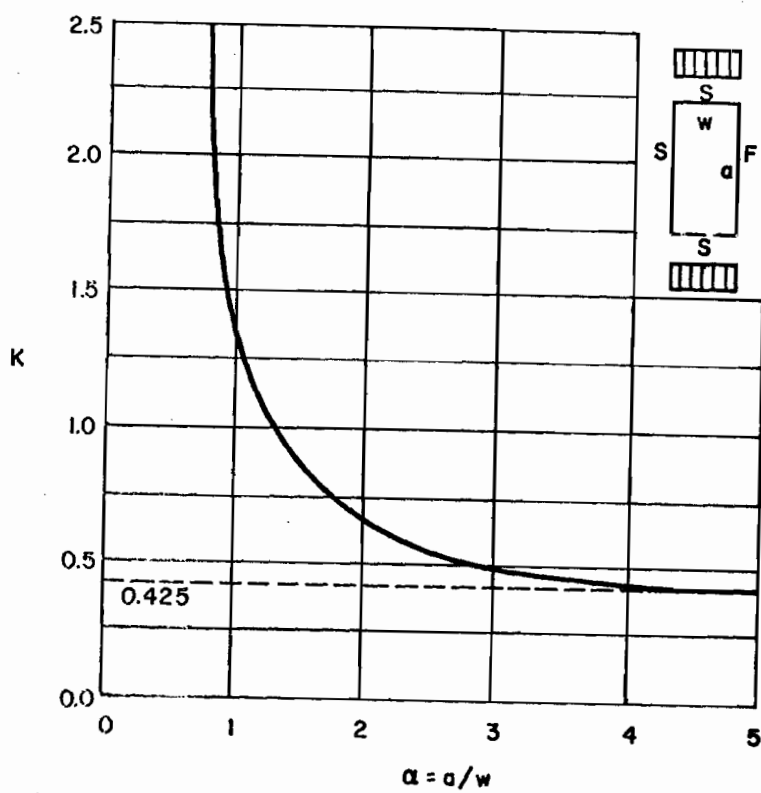
Figure 7. Buckling Coefficient for Plates With One Longitudinal
Edge Simply Supported, One Free Under Uniform
Compression
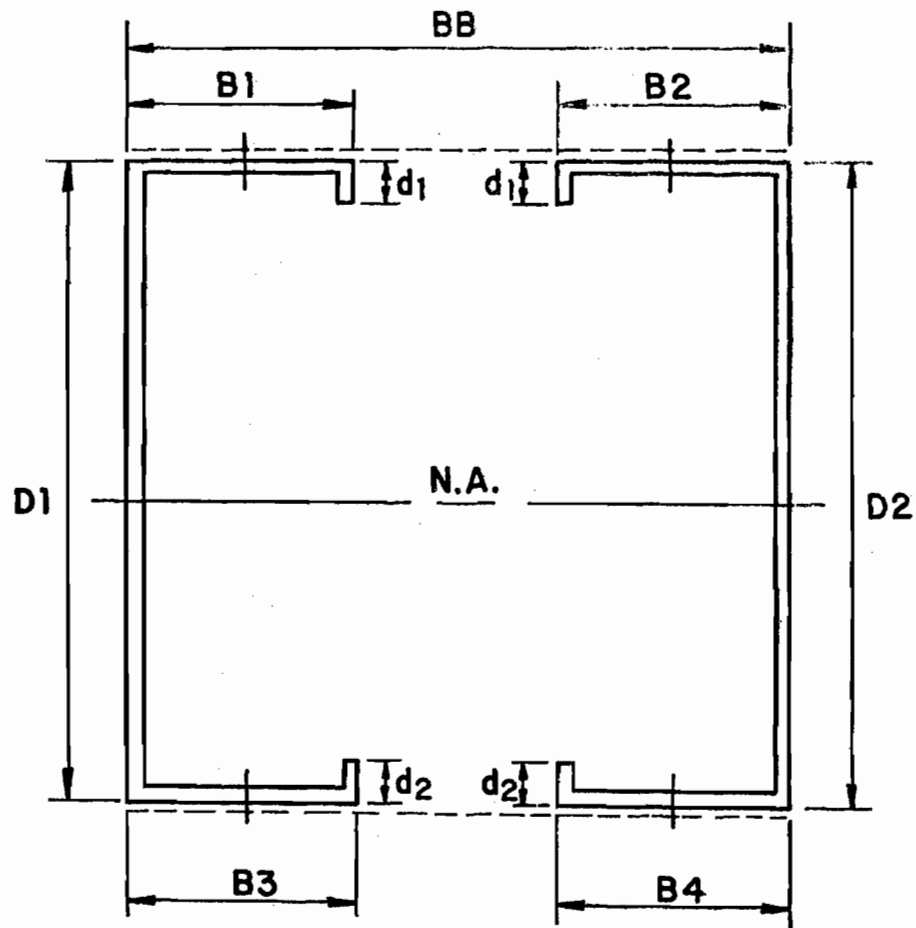
Figure 8. Dimensions of Channel Specimens
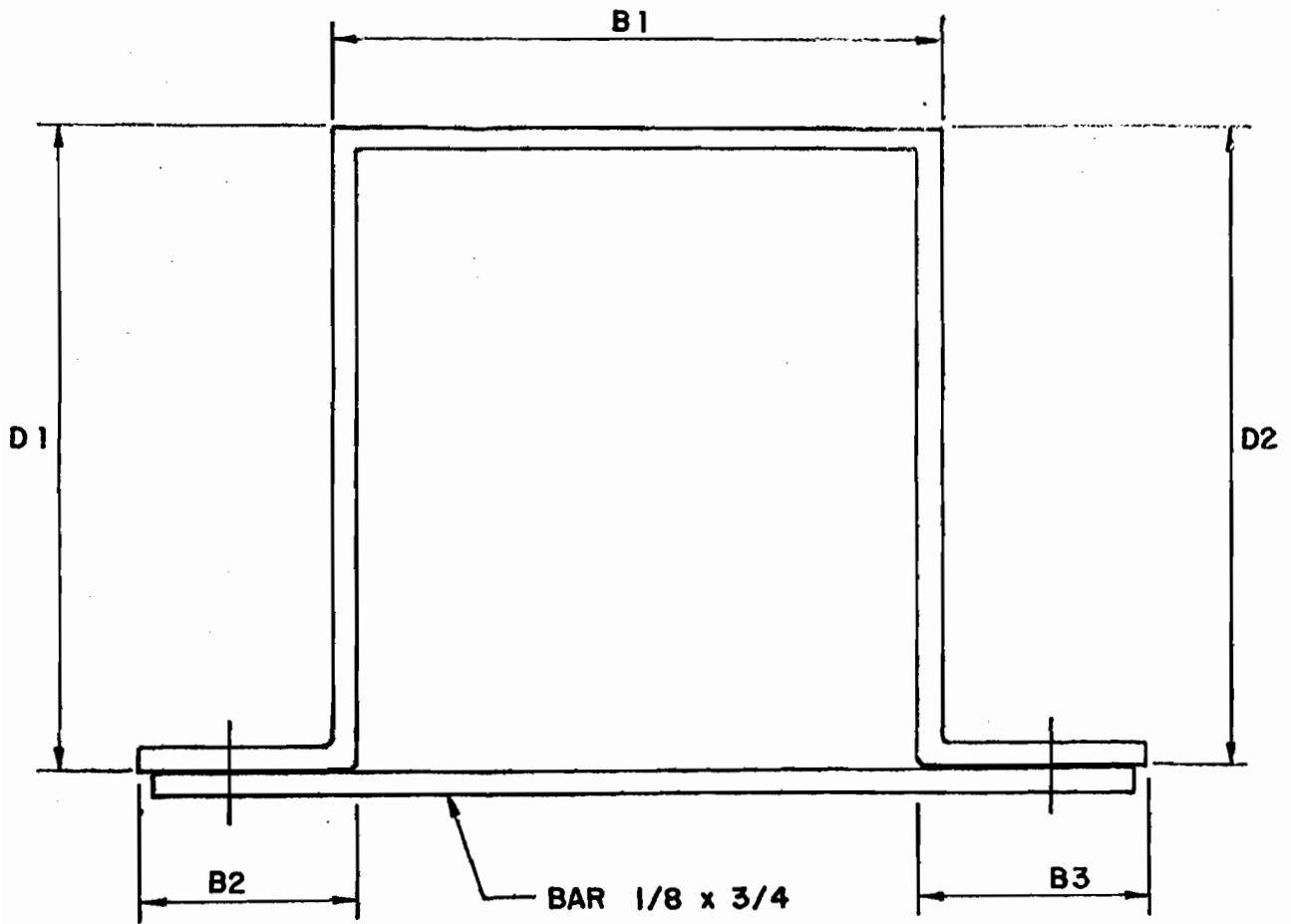
Figure 9.   Dimensions of Hat Specimens
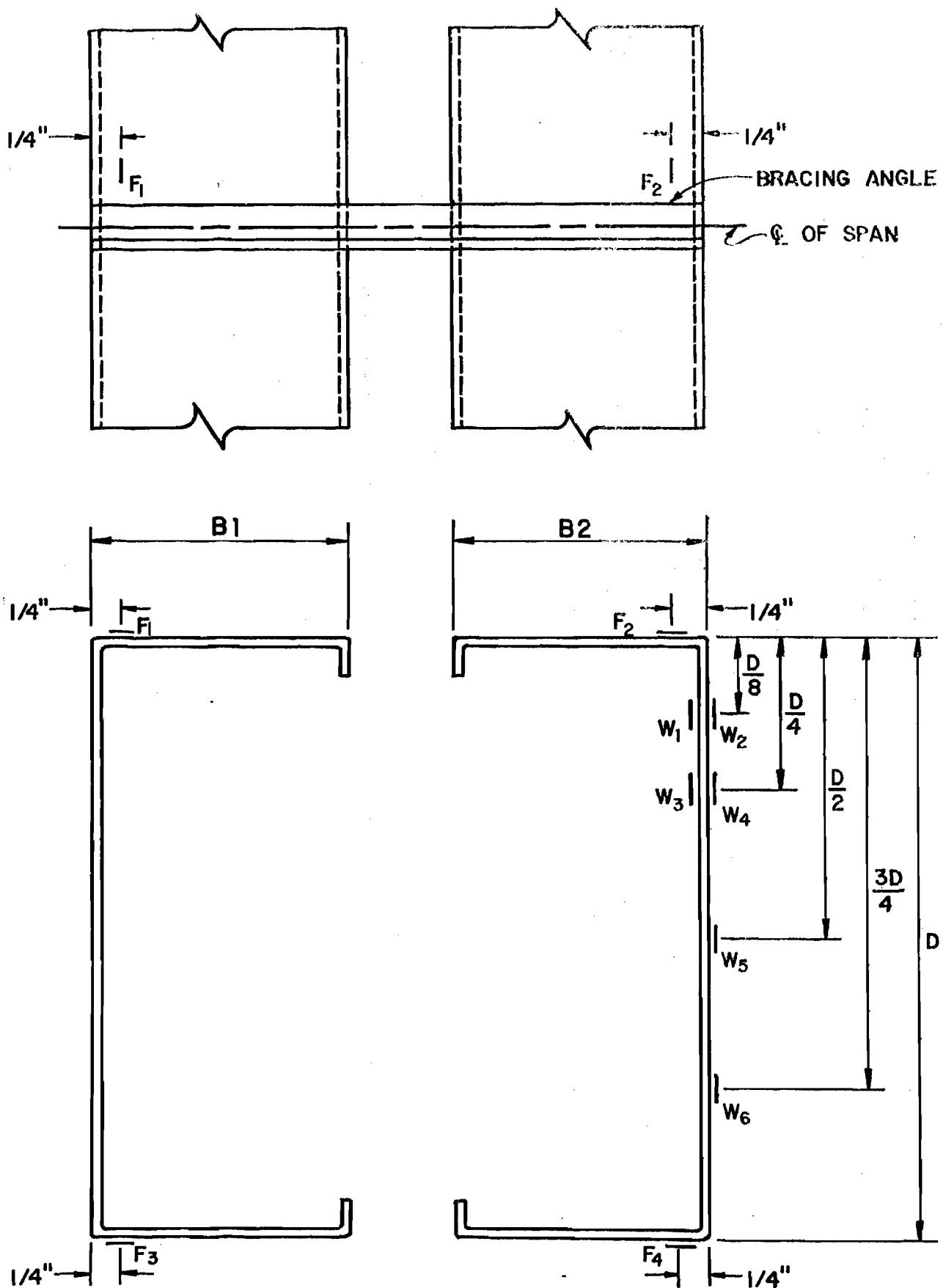
Figure 10. Locations of Strain Gages for Bending Test Specimens
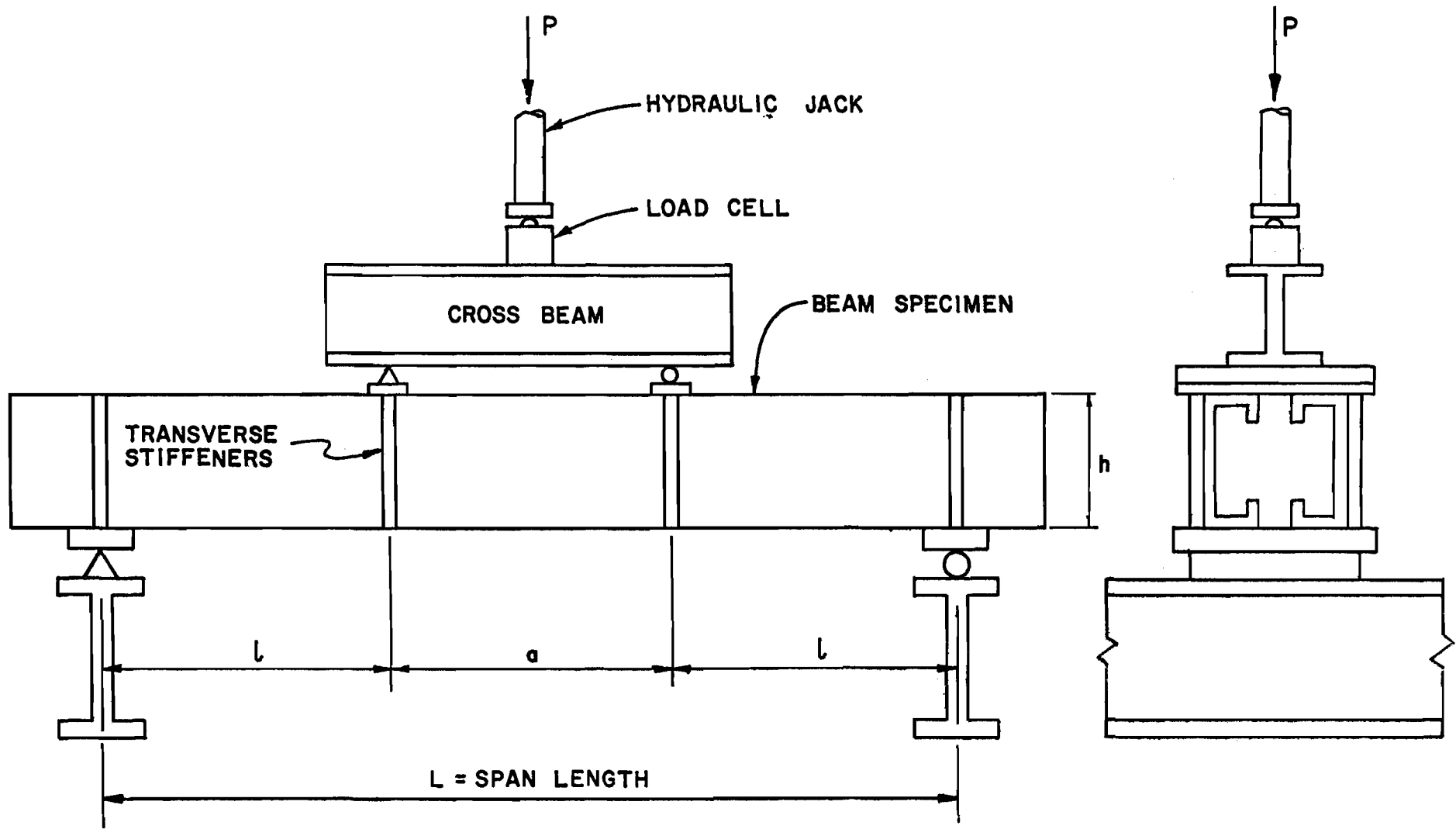
Figure 11. Bending Test Setup
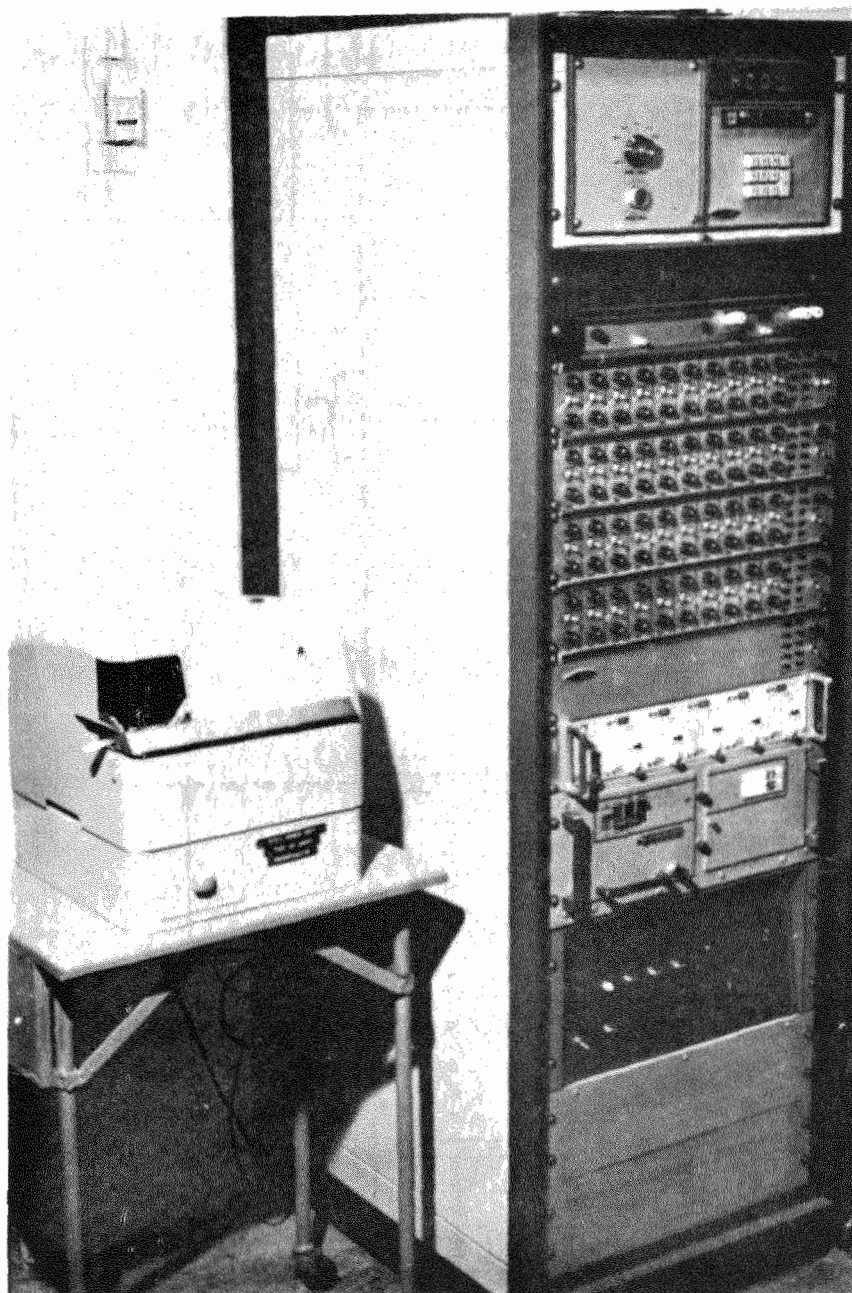
Figure 12. Data Acquisition System and Paper
Tape Punch
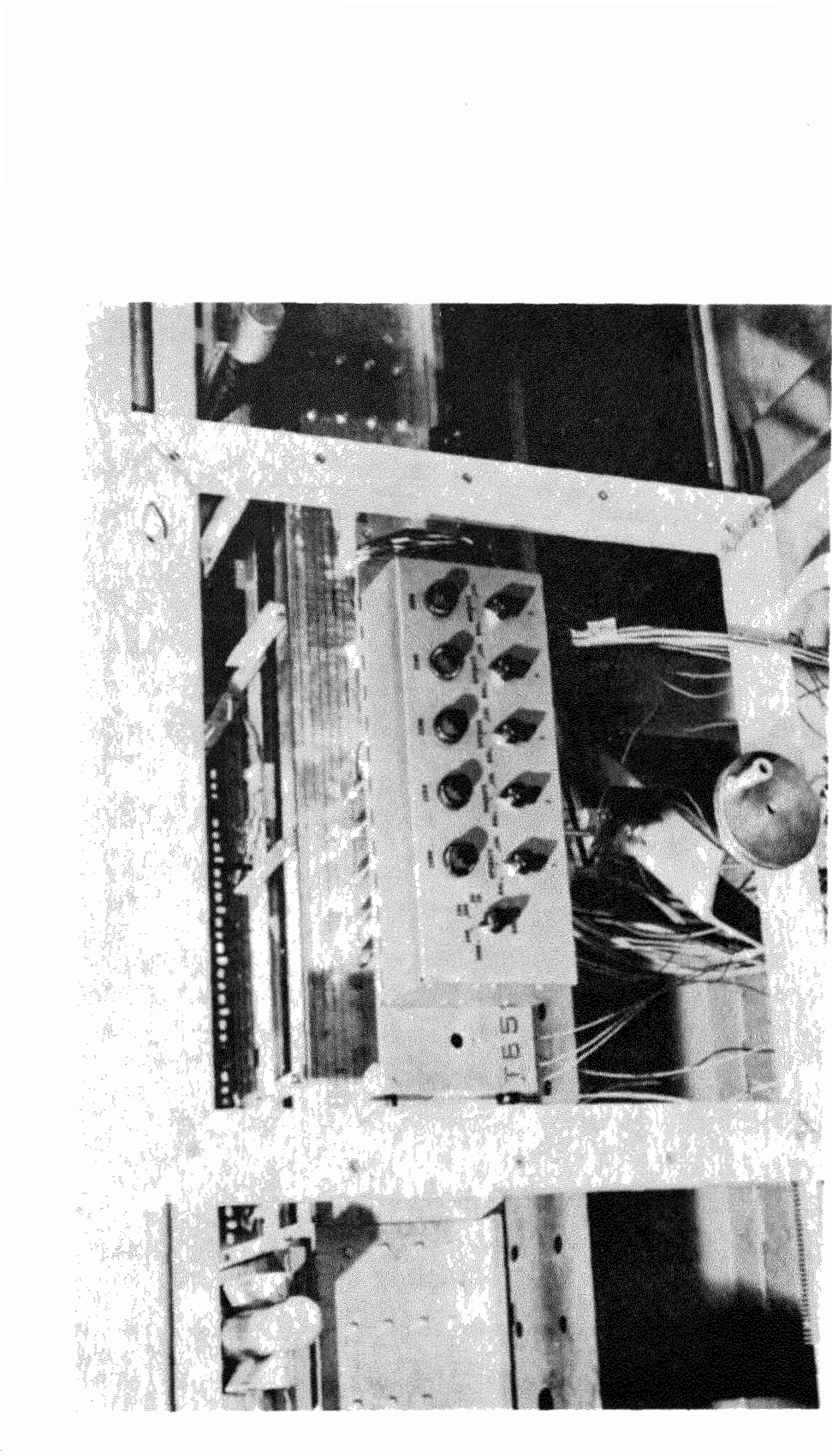
Figure 13. Lateral Deformation Measurement Unit

Figure 14. Data Reduction System
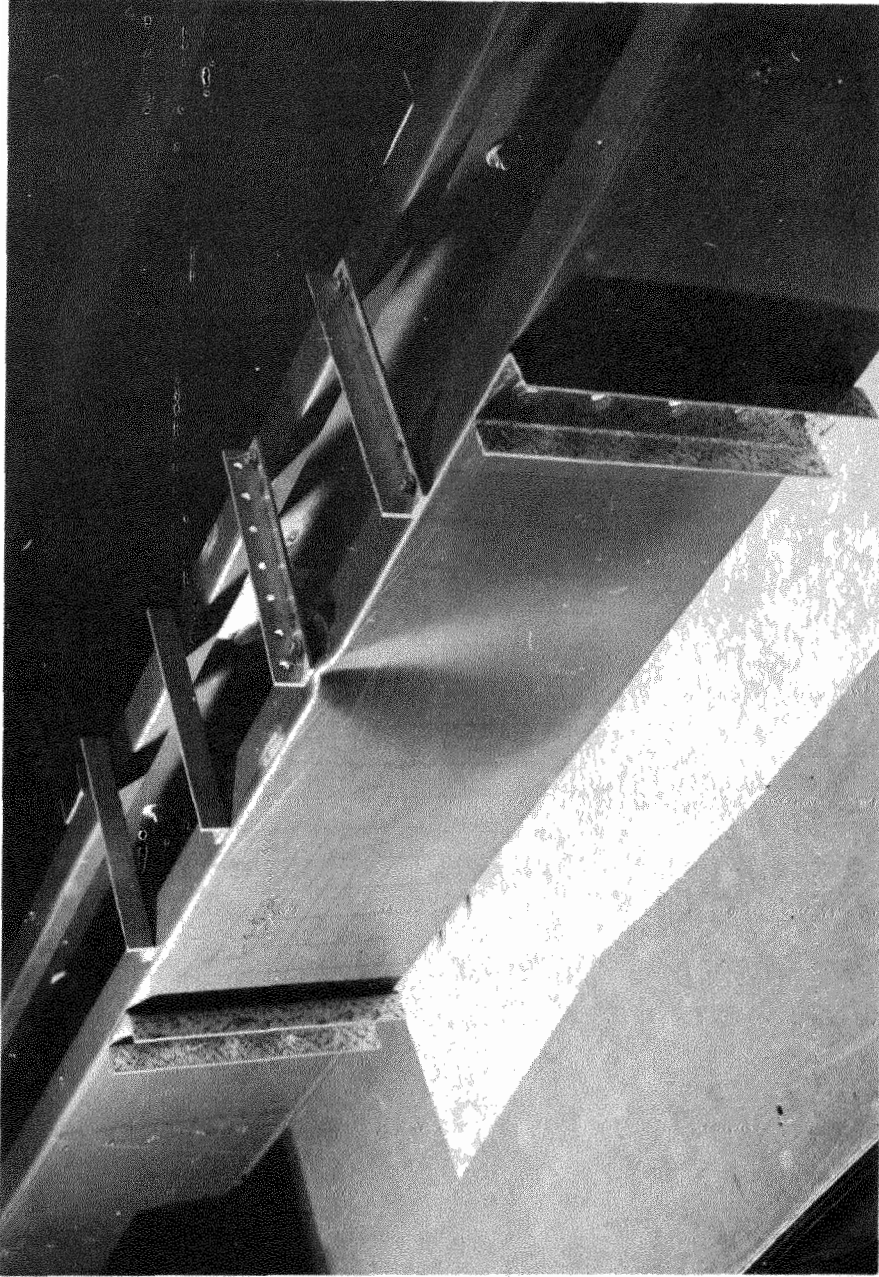
Figure 15. Typical Failure Pattern for Bending Test Specimens
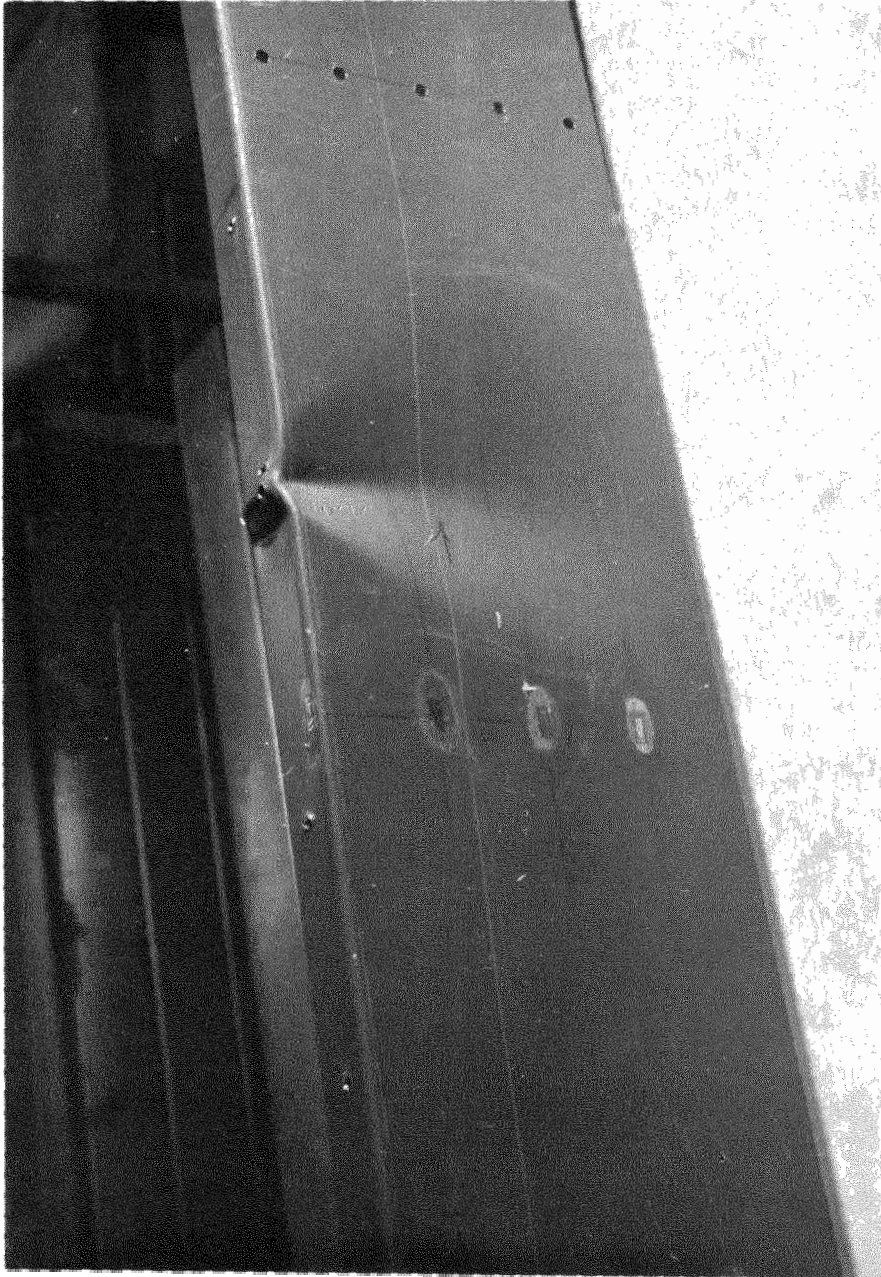
Figure 16. Photograph of Web Buckling Failure Mode for Bending Tests
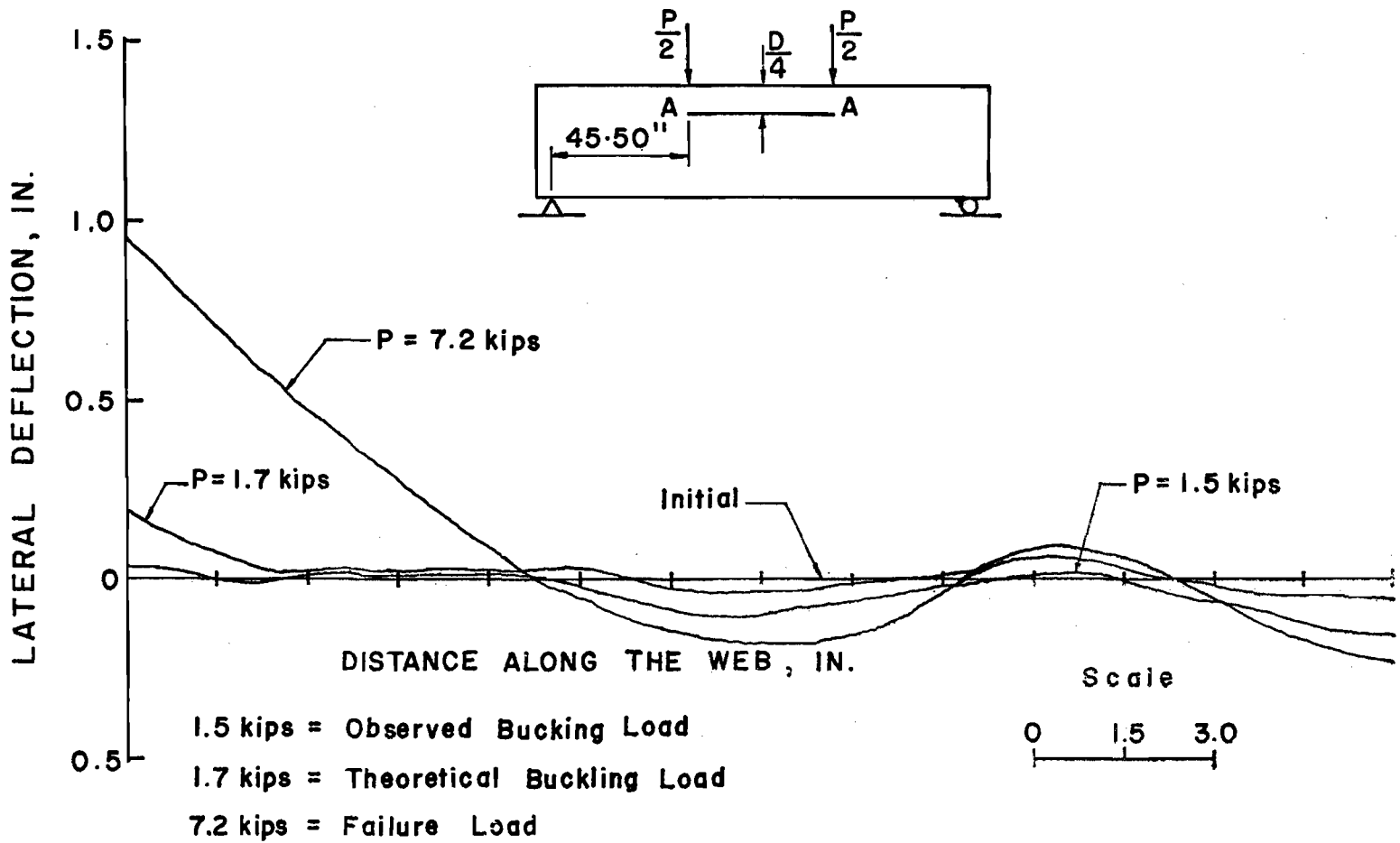
Figure 17. Web Profile of Bending Test Specimen No. B-3-1 at D/4
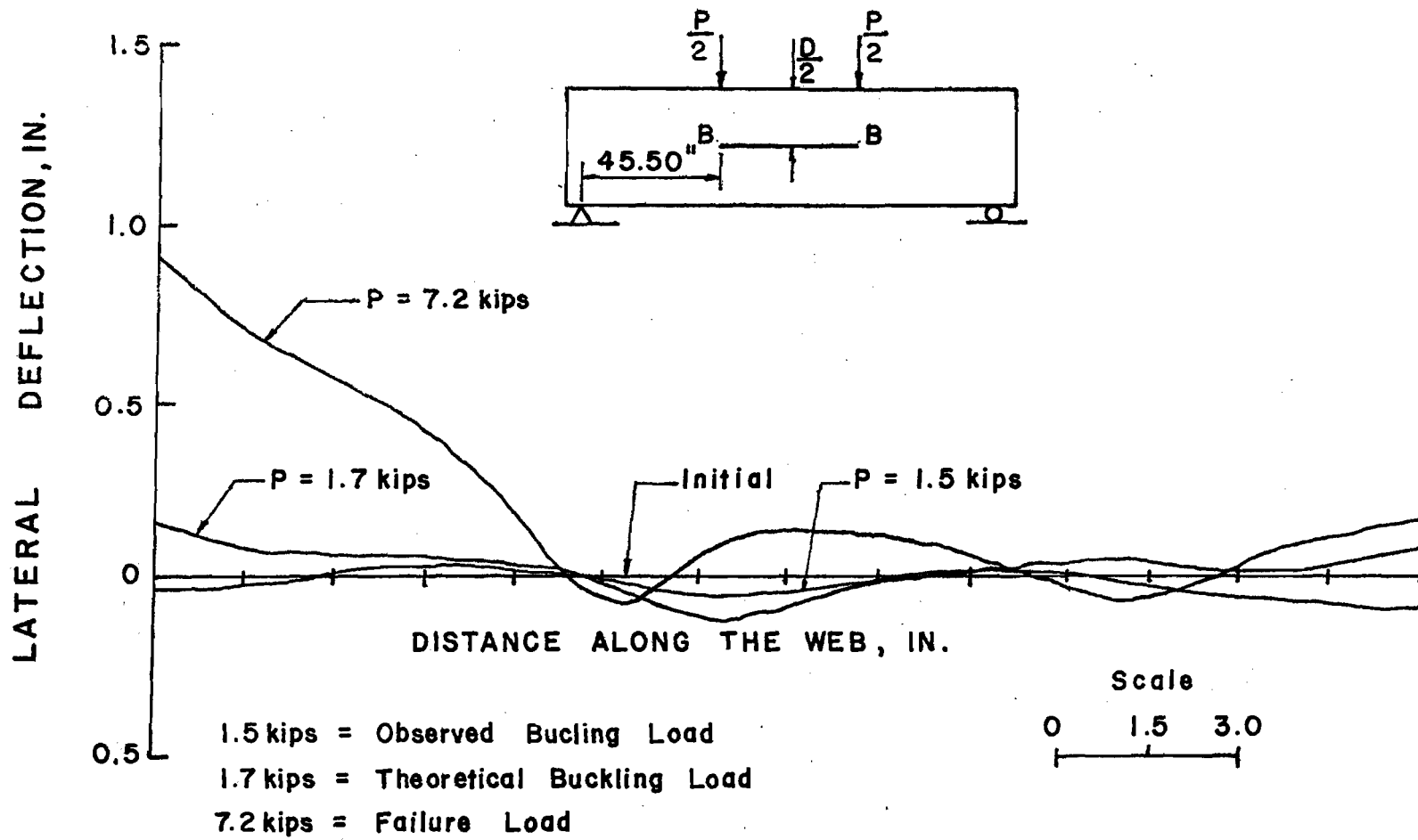
Figure 18. Web Profile of Bending Test Specimen No. B-3-1 at D/2
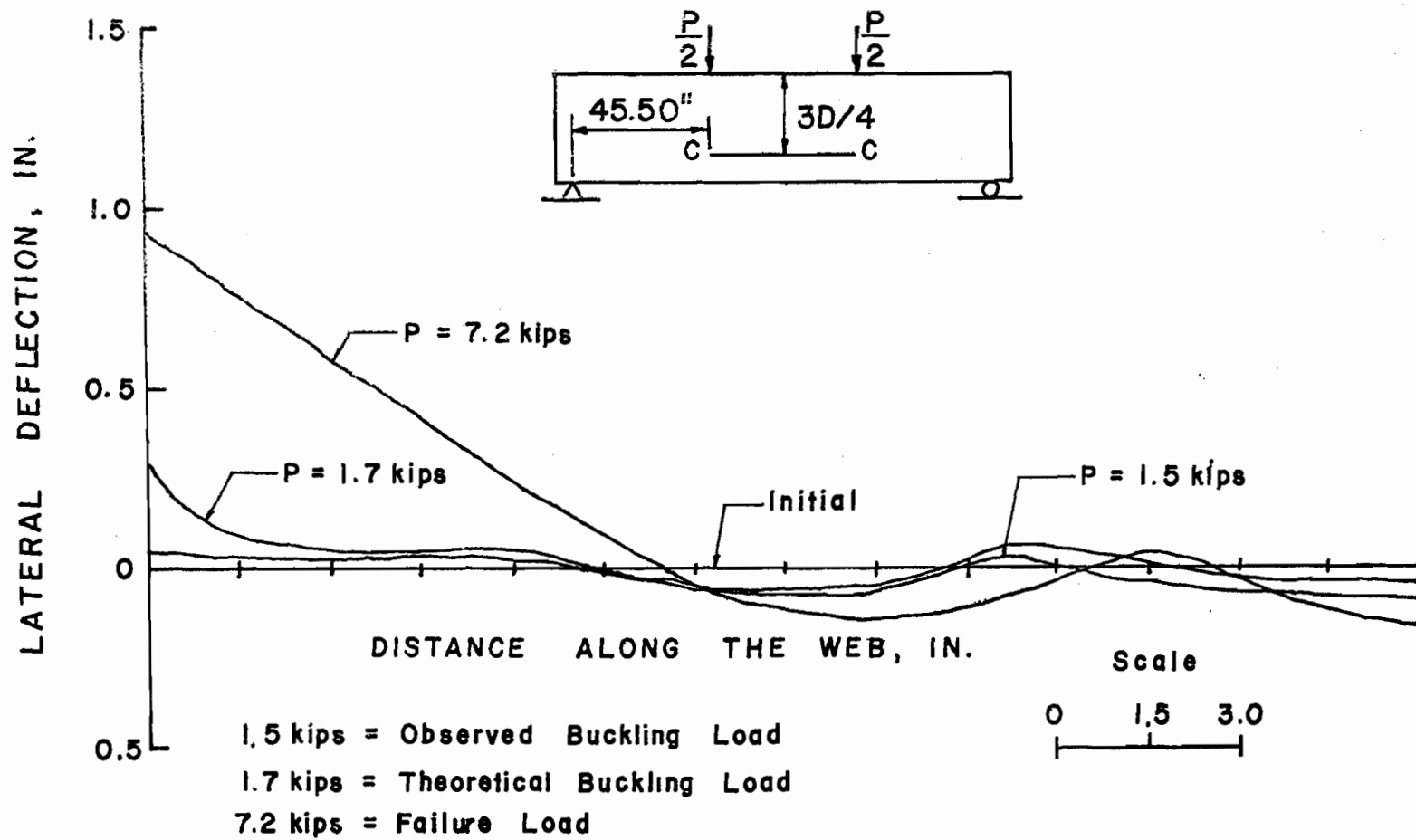
Figure 19. Web Profile of Bending Test Specimen No. B-3-1 at 3D/4

LATERAL DEFLECTION, IN.
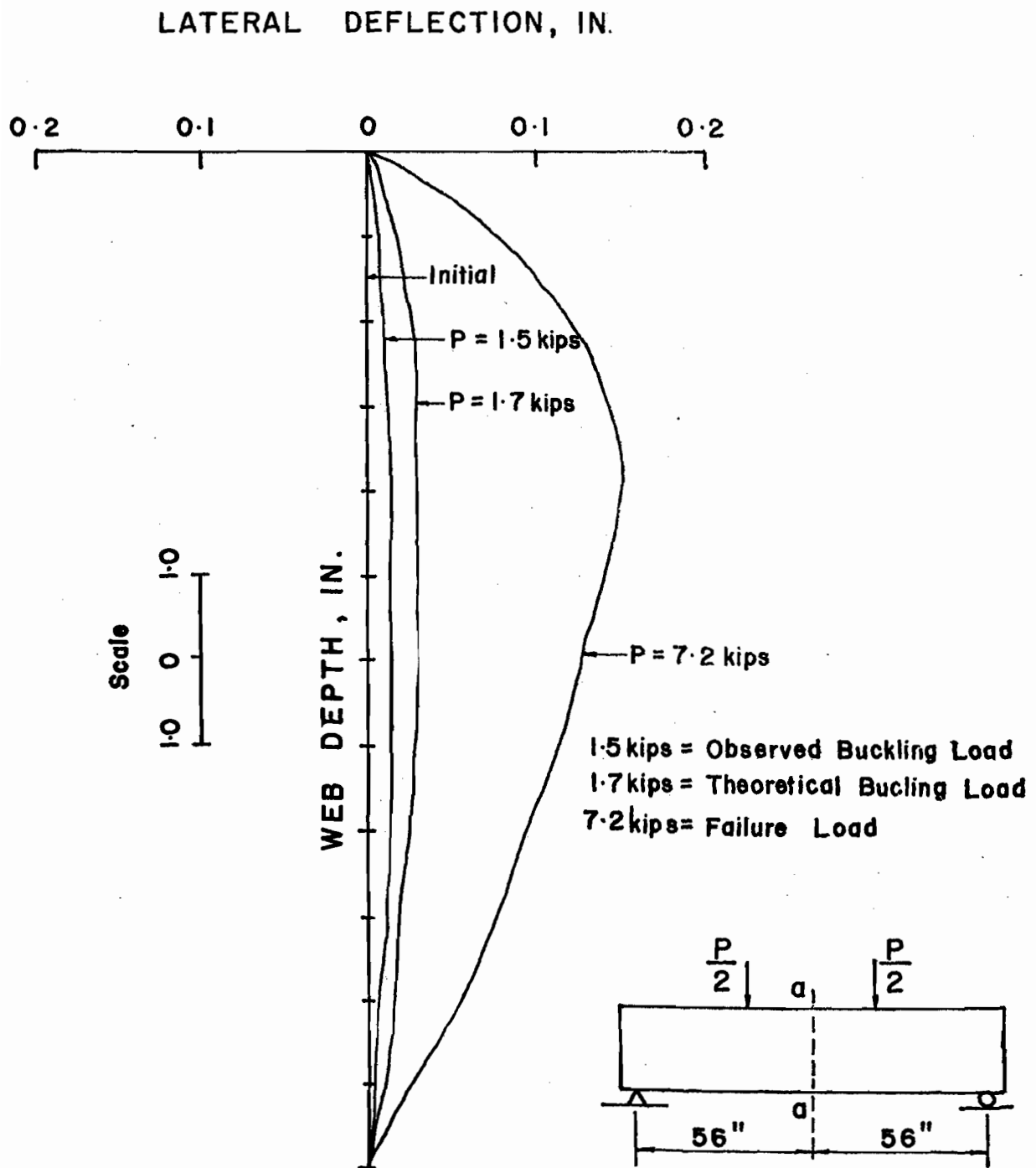
Figure 20. Web Profile of Bending Test Specimen No. B-3-1
at Cross-Section a-a
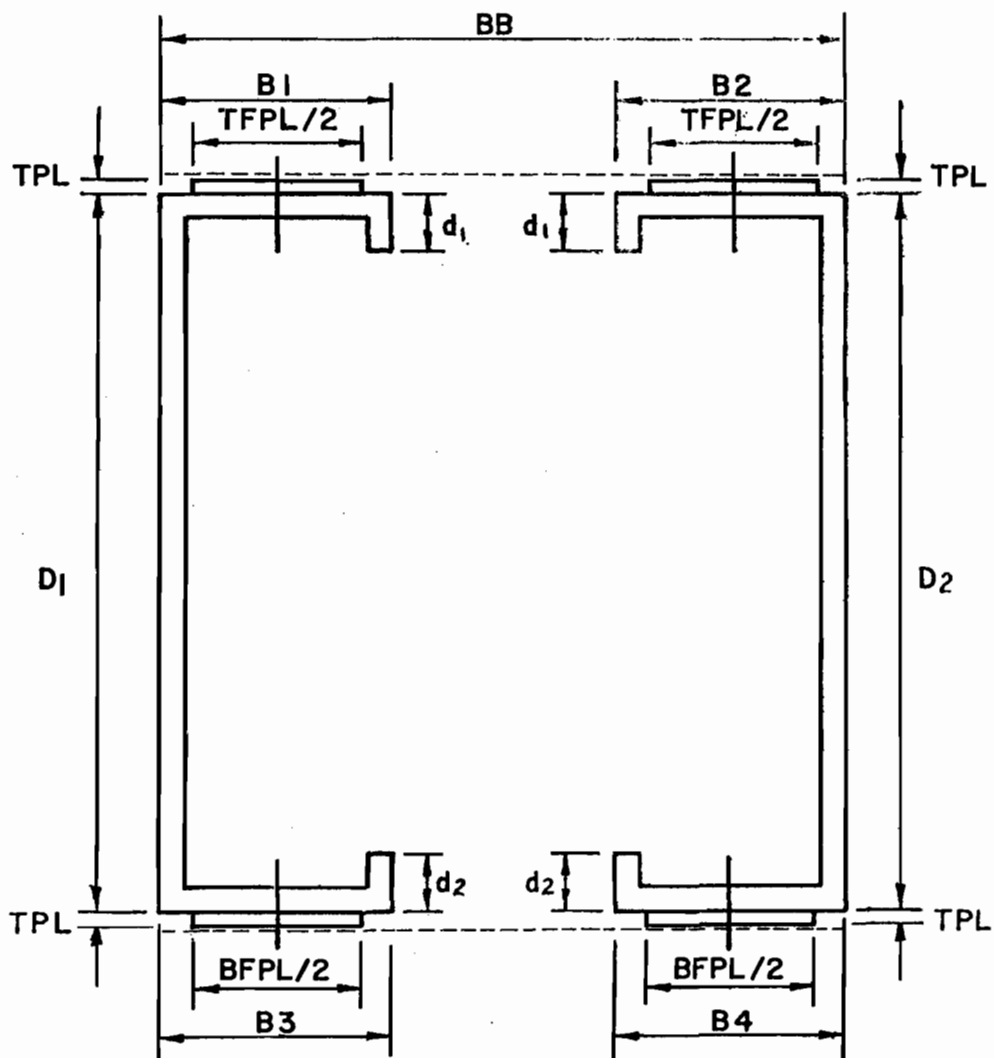
Figure 21. Dimensions of Shear Test Specimens
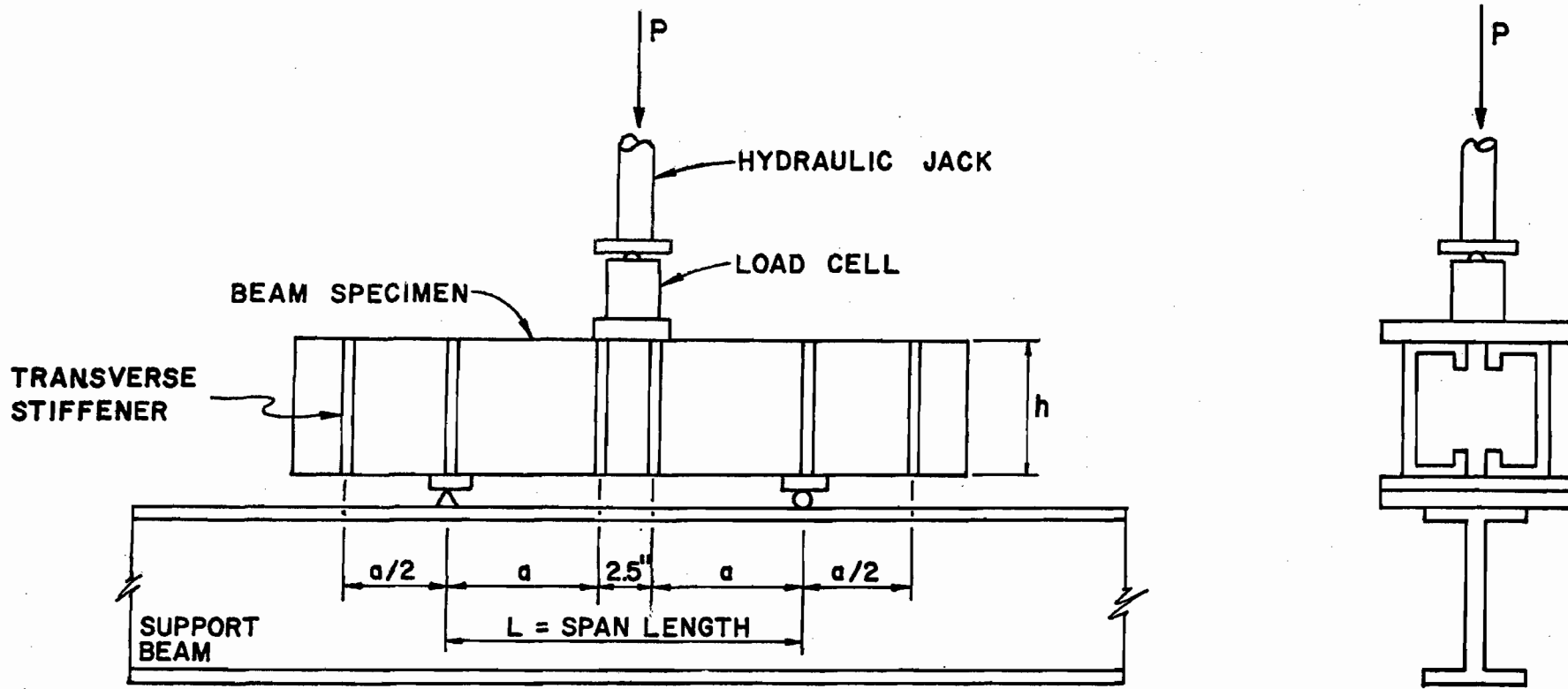
Figure 22.   Shear Test Setup-A
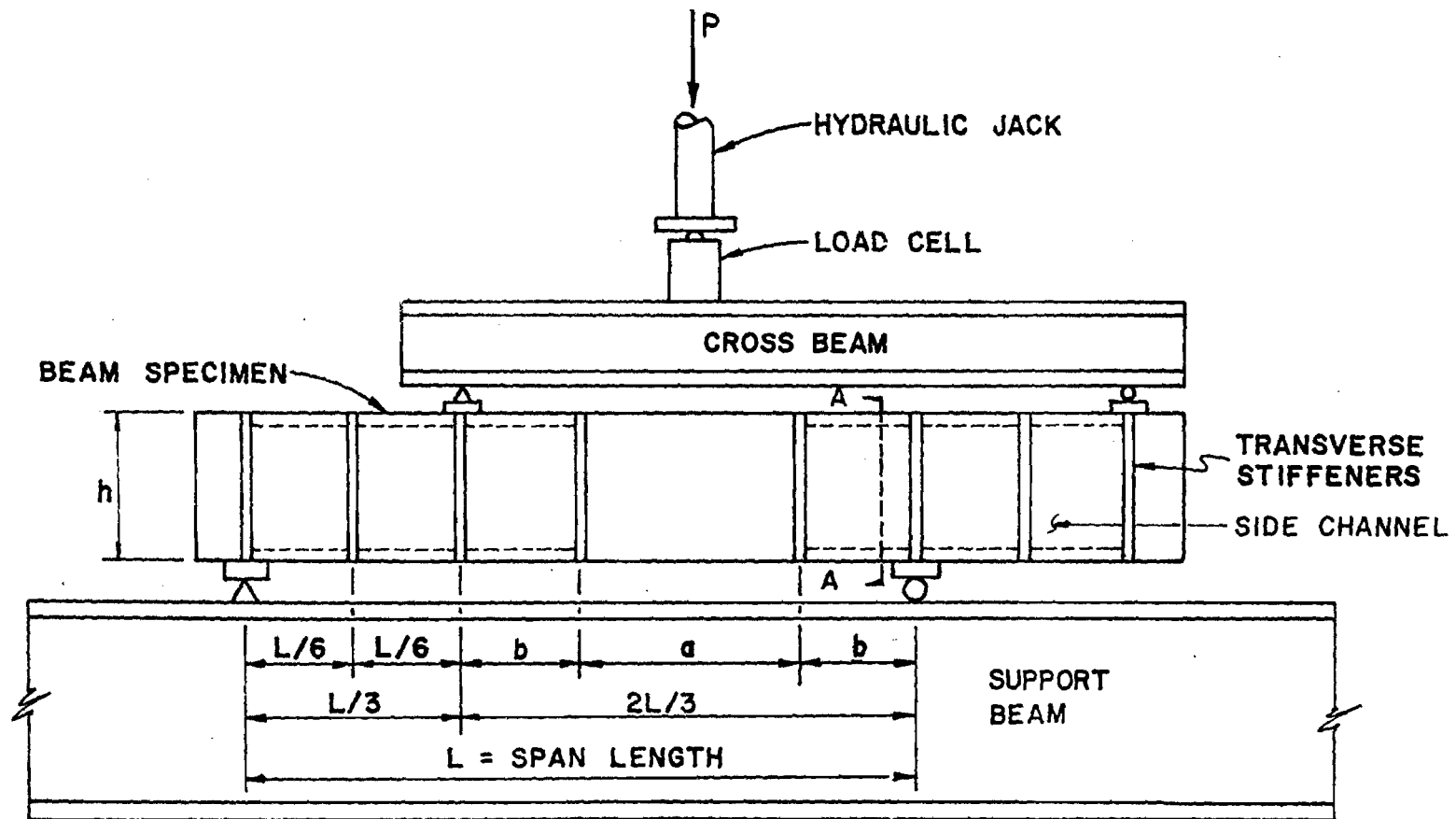
Note: $b = (2L/3 - a)/2$

Figure 23. Shear Test Setup-B
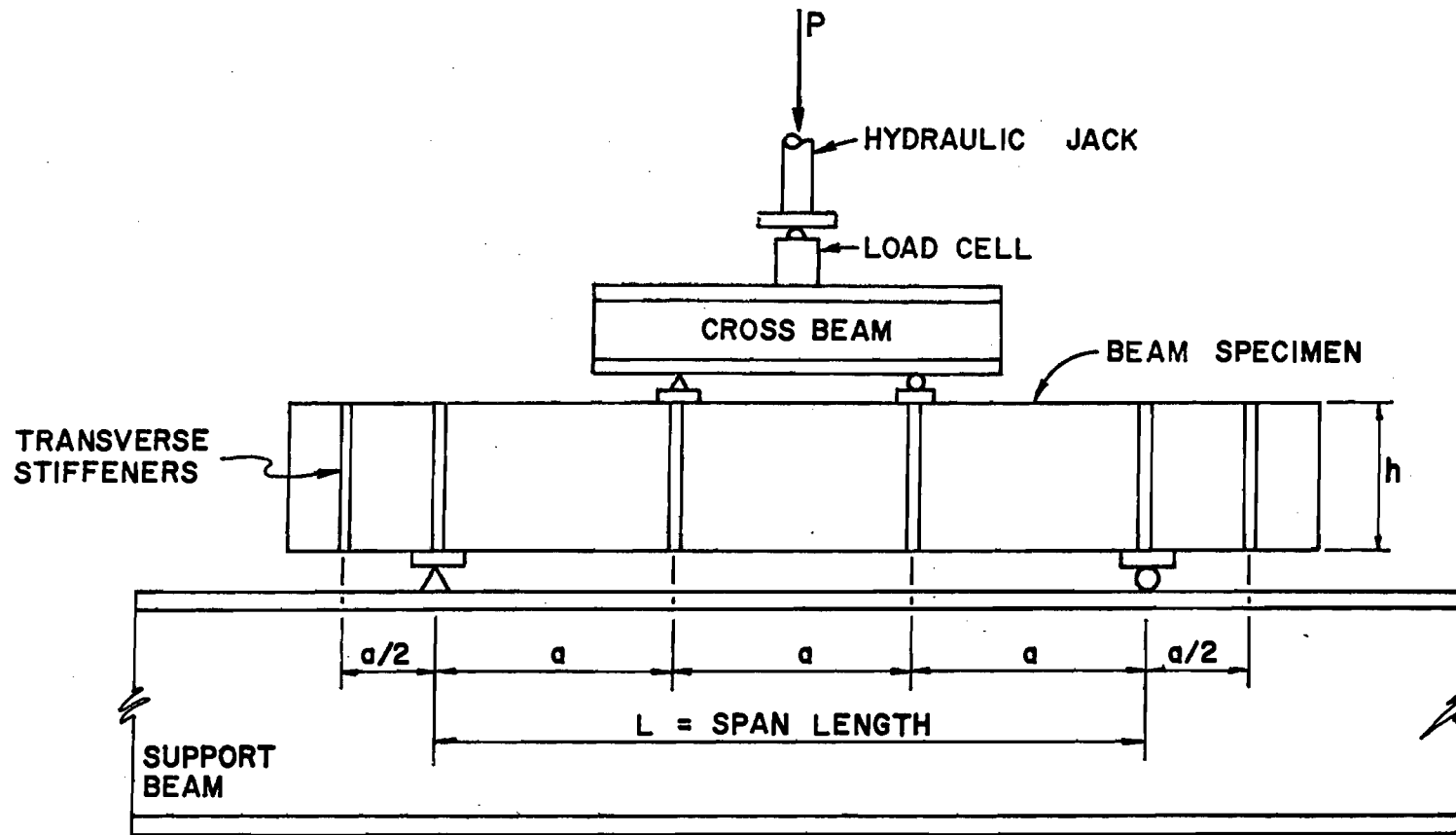
Figure 24.   Shear Test Setup-C
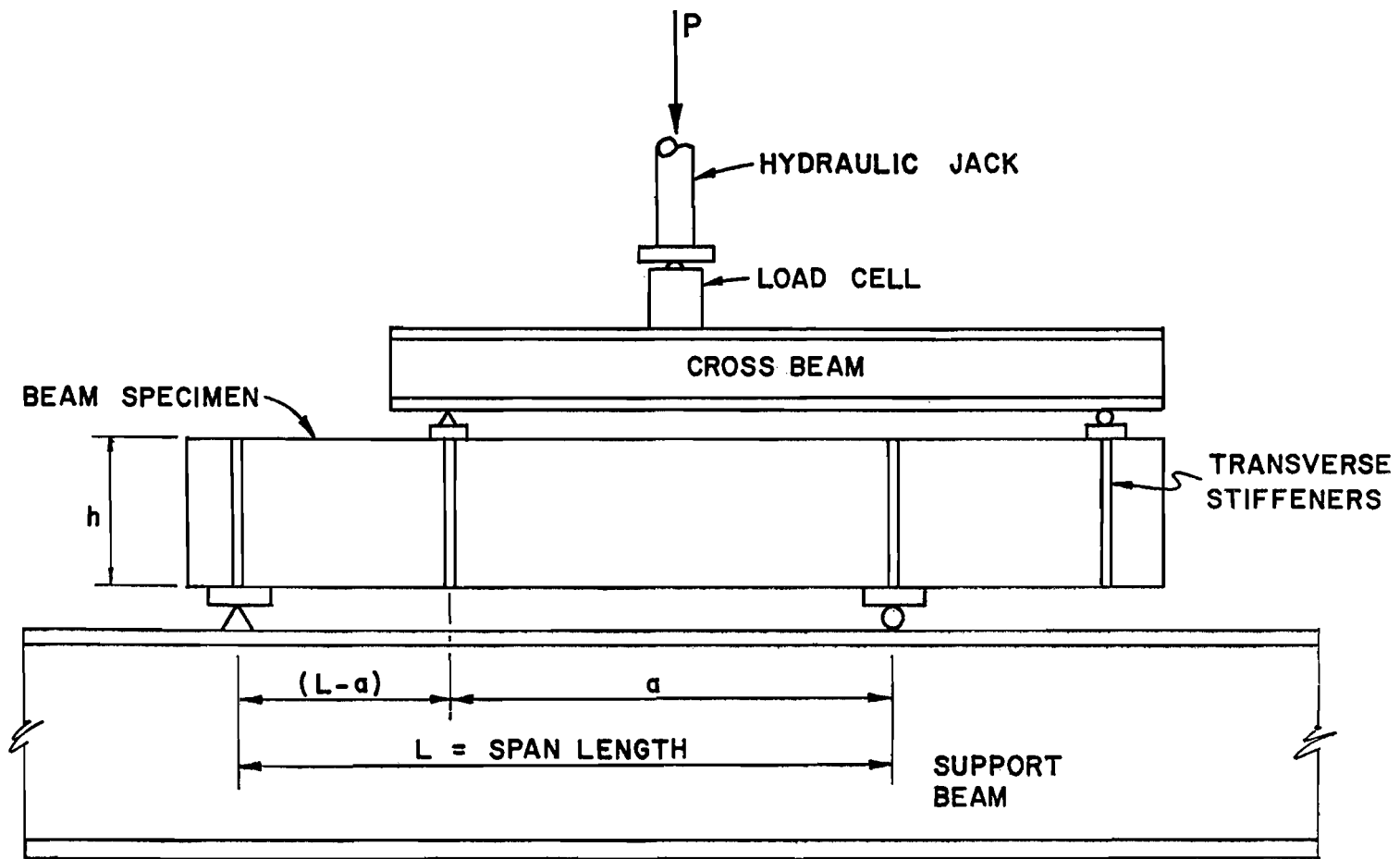
Figure 25. Shear Test Setup-D
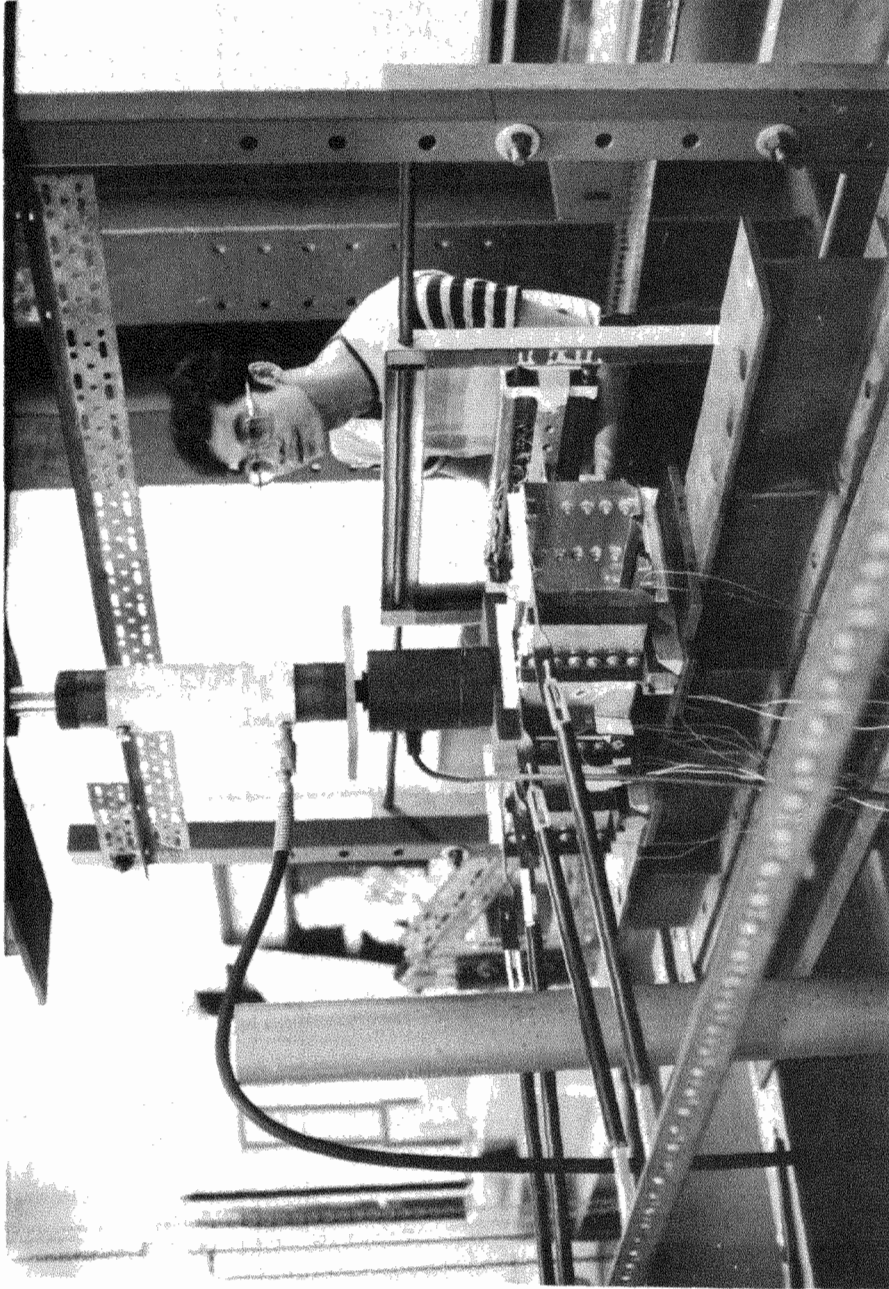
Figure 26. Photograph of Shear Test Setup
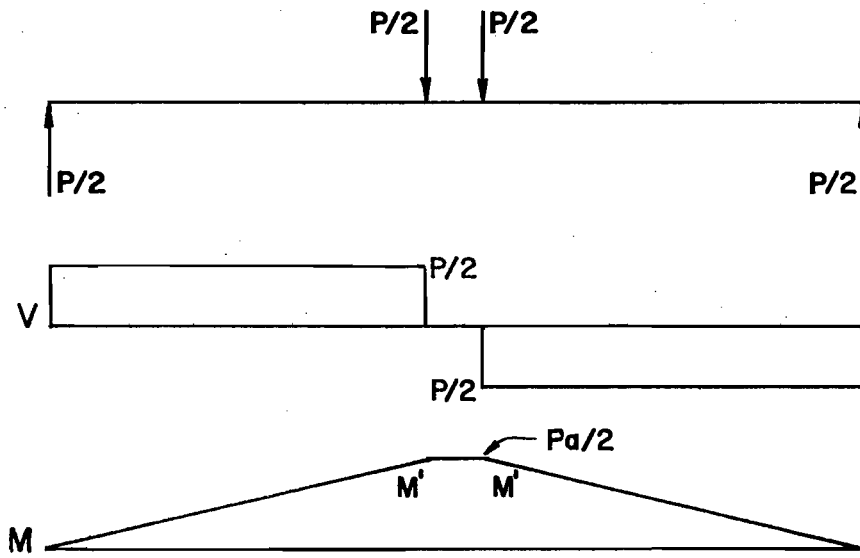
(a) Test Setup-A
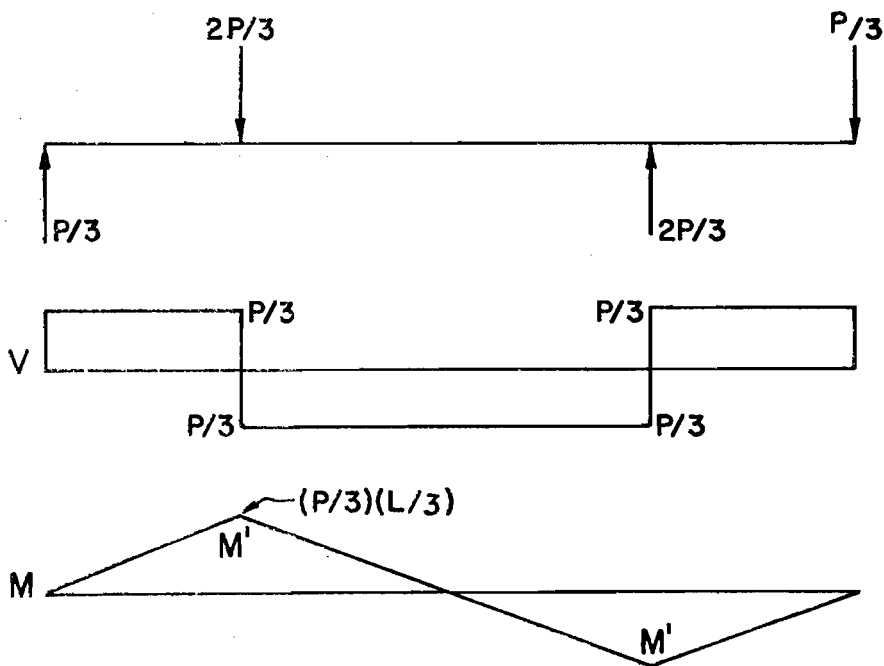
(b) Test Setup-B

Figure 27. Shear and Moment Diagrams for Various Shear Test Setups
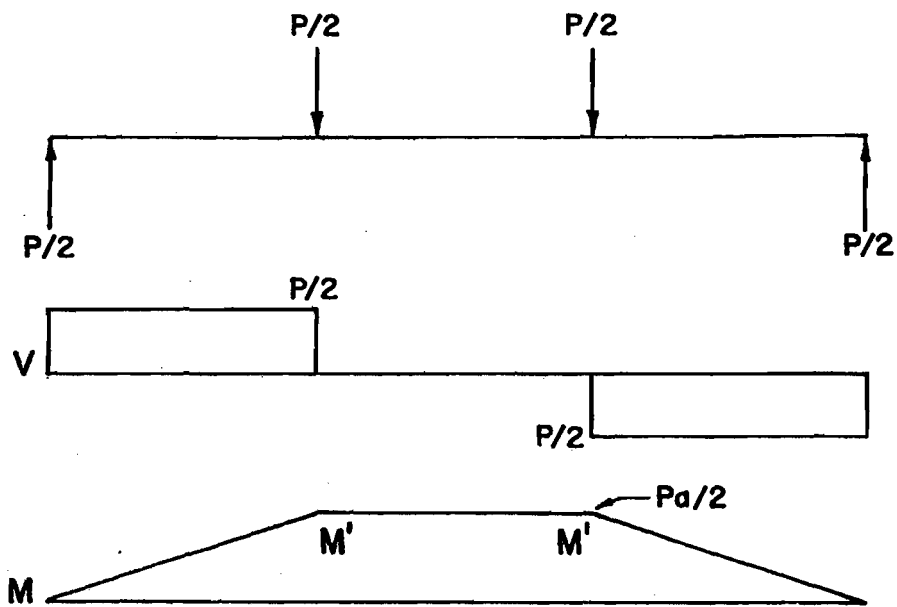
(c) Test Setup-C
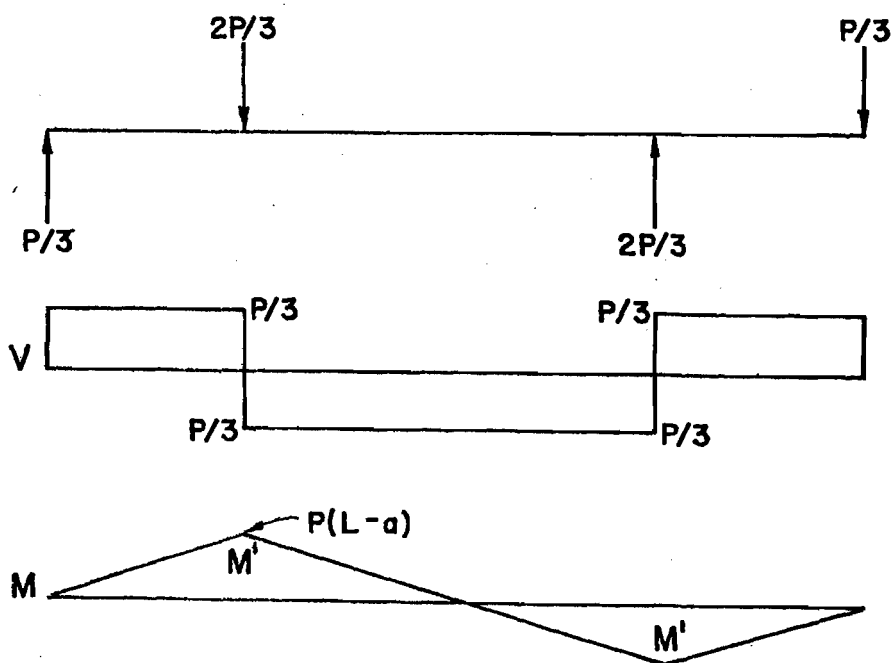
(d) Test Setup-D

Figure 27. (continued)
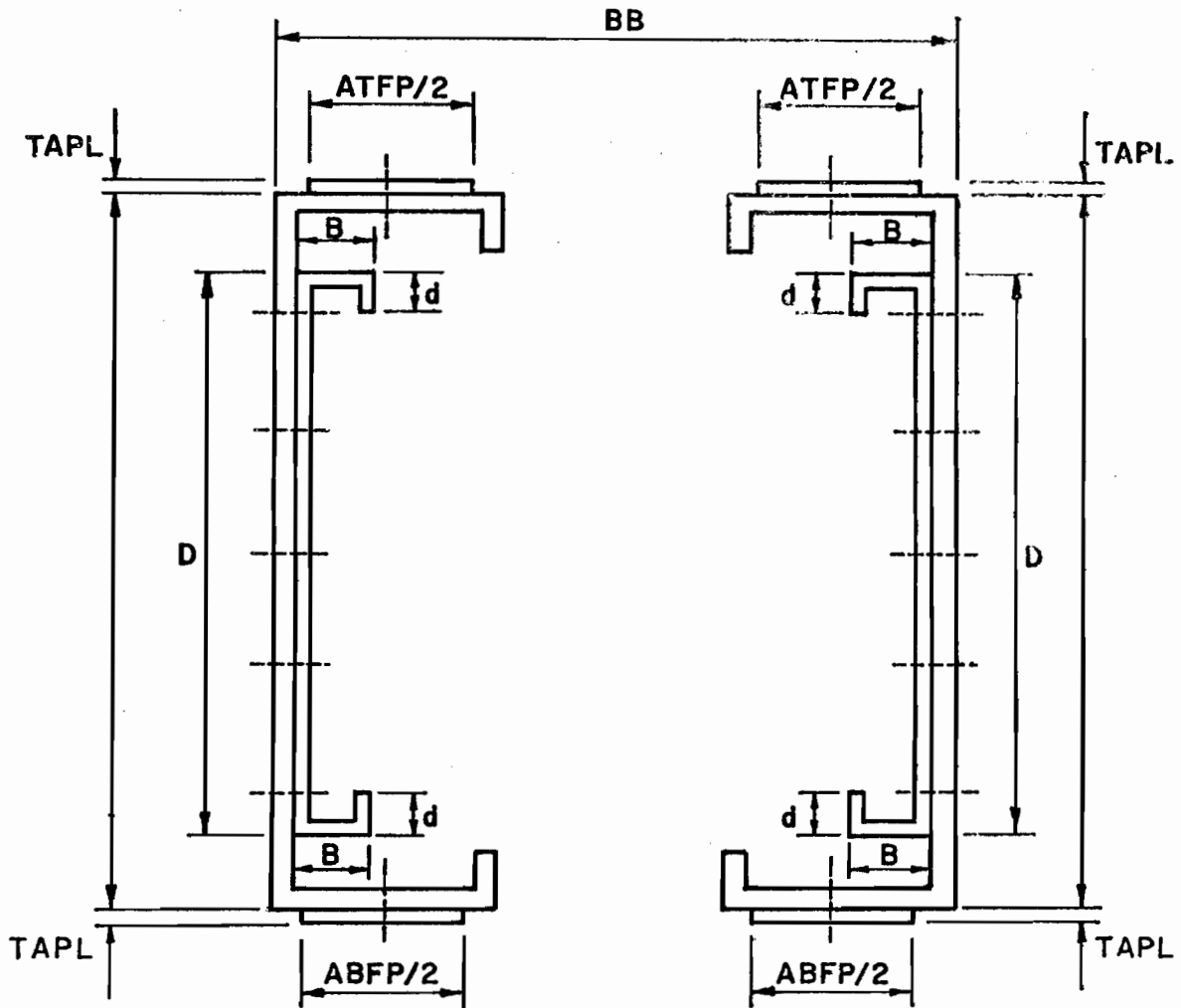
Note: See Fig. 23 for the location of Section A-A

Figure 28. Dimensions of Cross-Section A-A
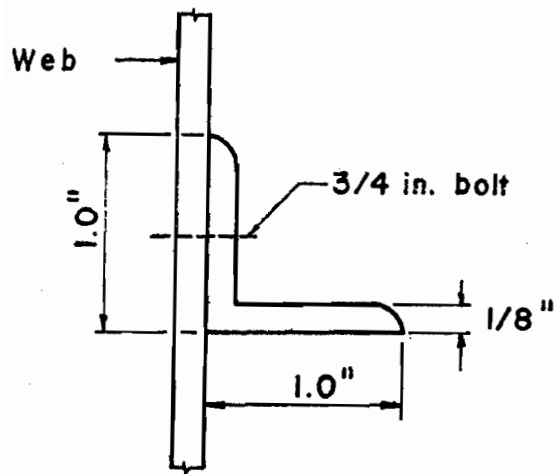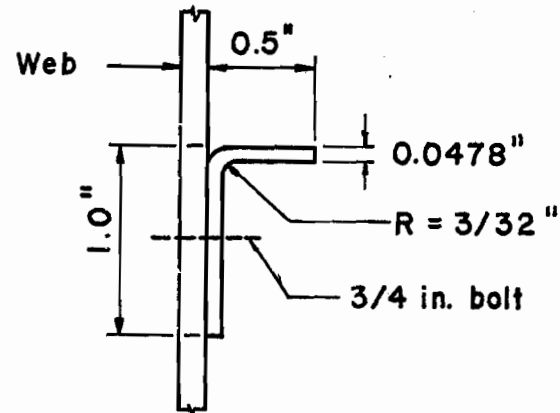
Figure 29.   Details of Intermediate Stiffeners for Shear Tests
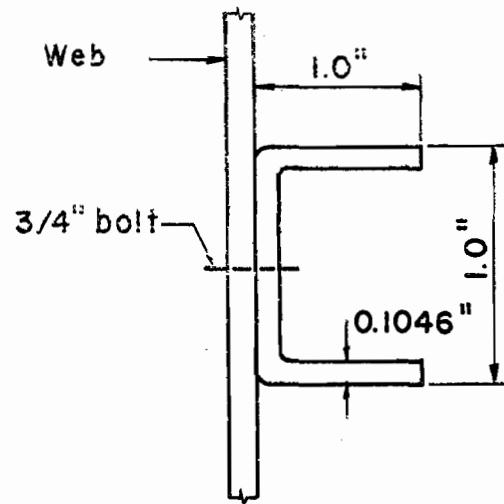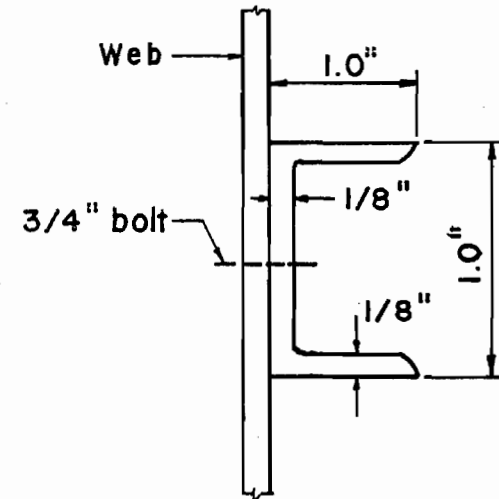
Figure 30. Details of Bearing Stiffeners for Shear Tests
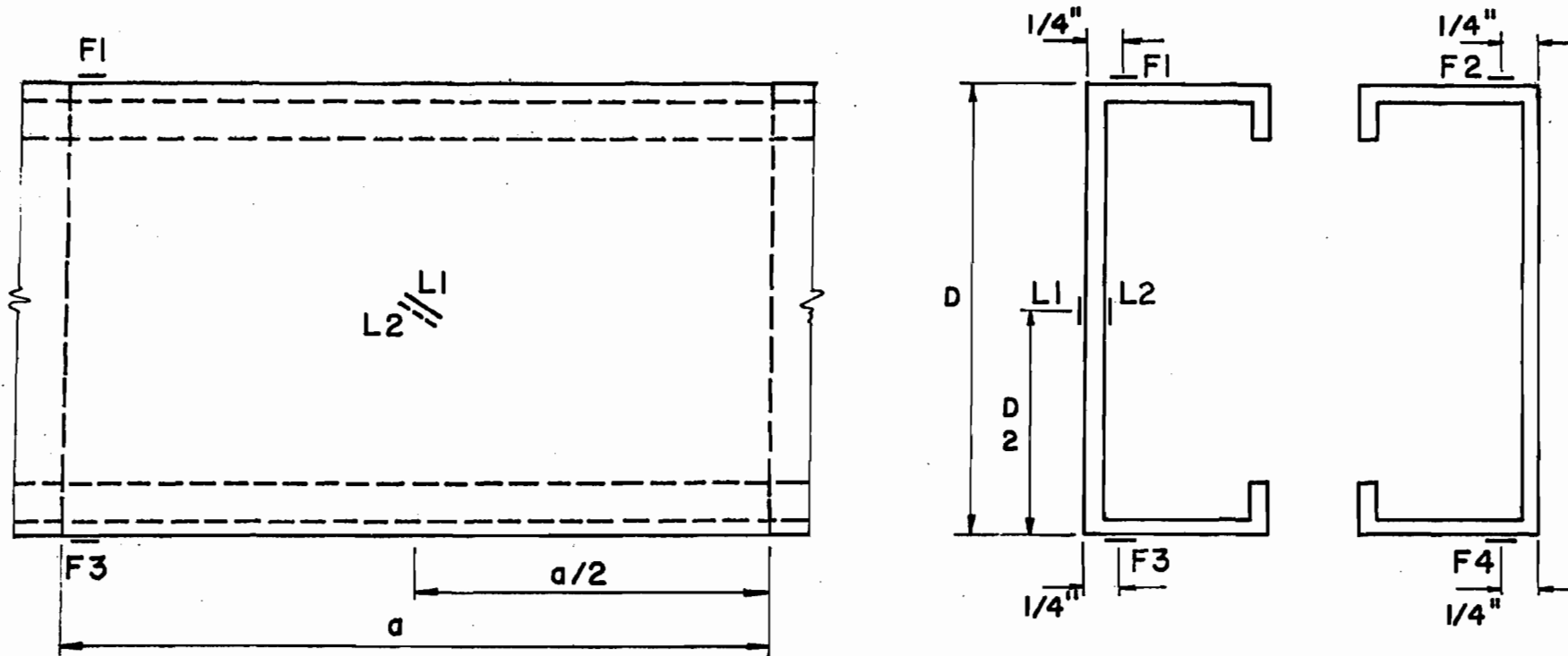
Figure 31. Location of Strain Gages for Beam Specimens (Shear Test Setups -A and C)
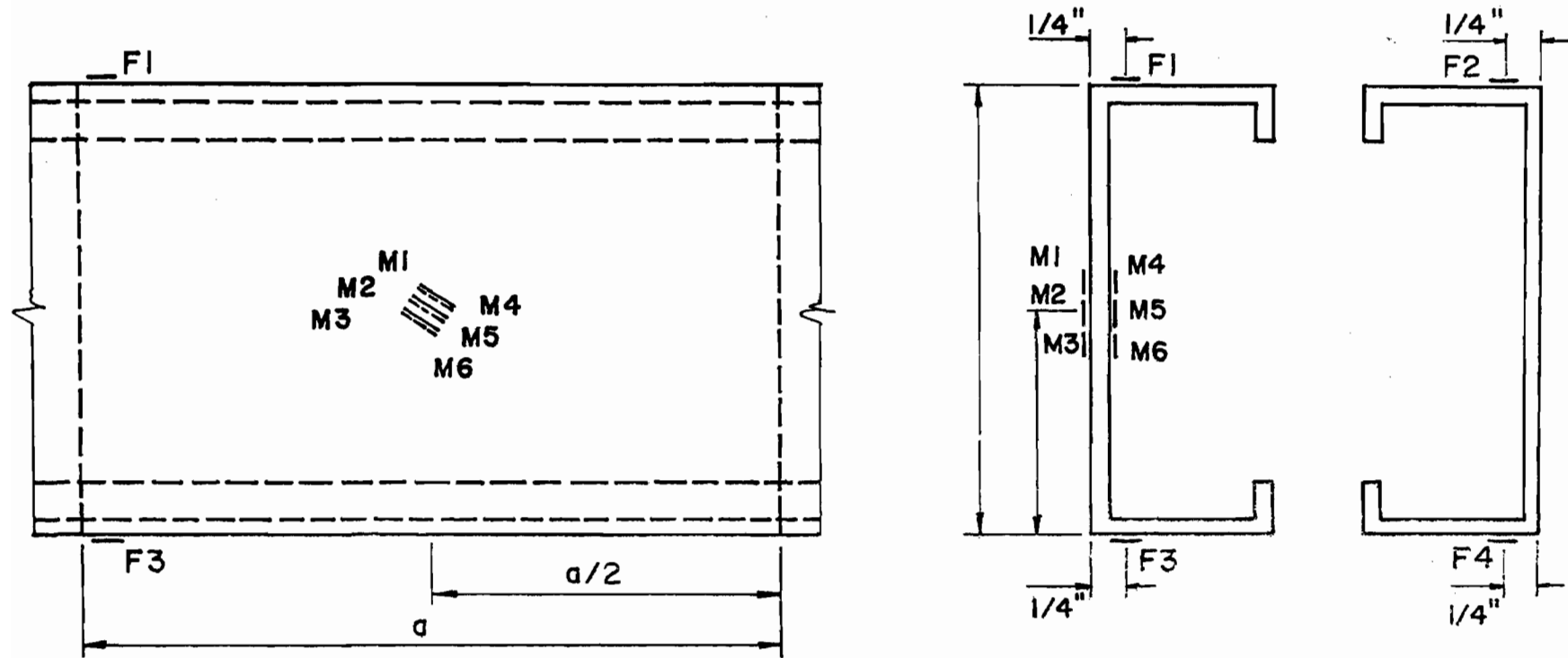
Figure 32.   Location of Strain Gages for Beam Specimens (Shear Test Setups-B and D)
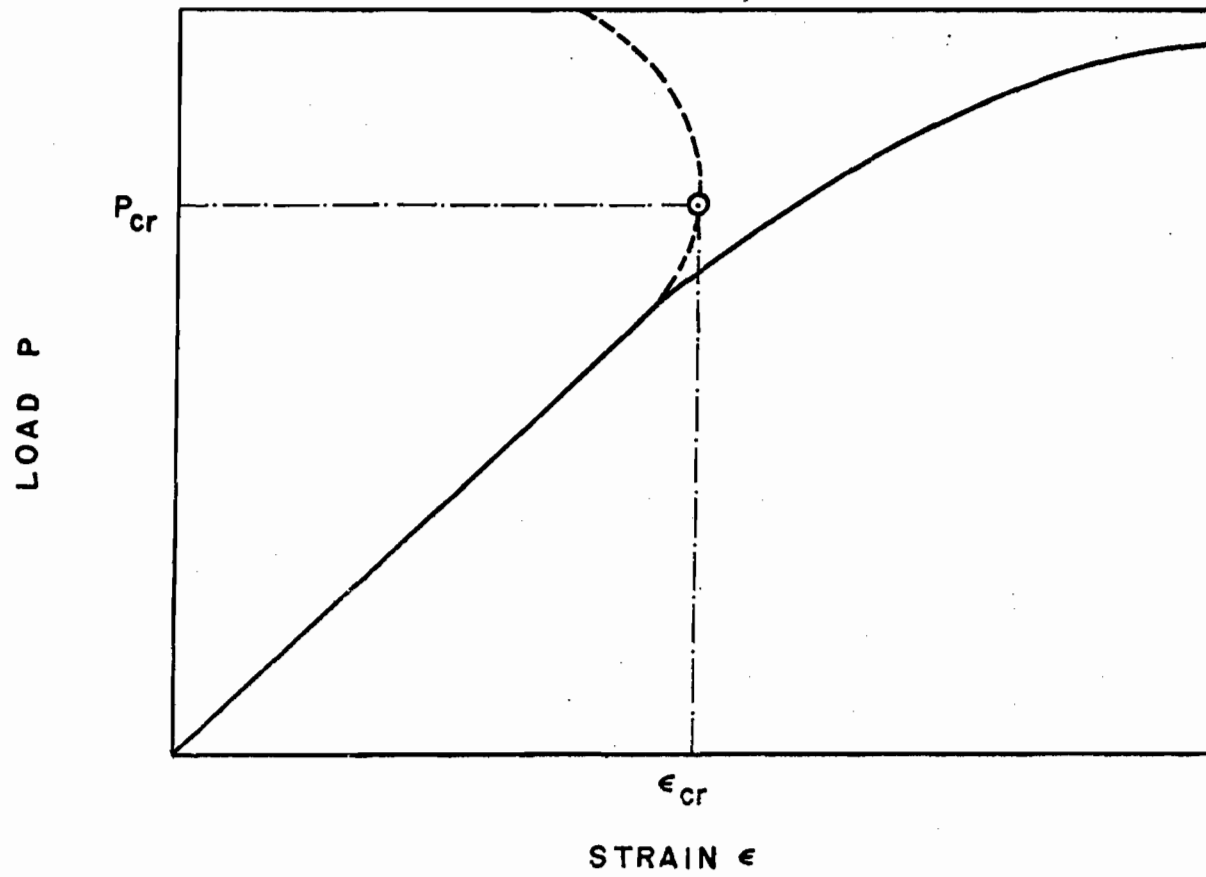
Figure 33. Typical Load-Strain Diagram
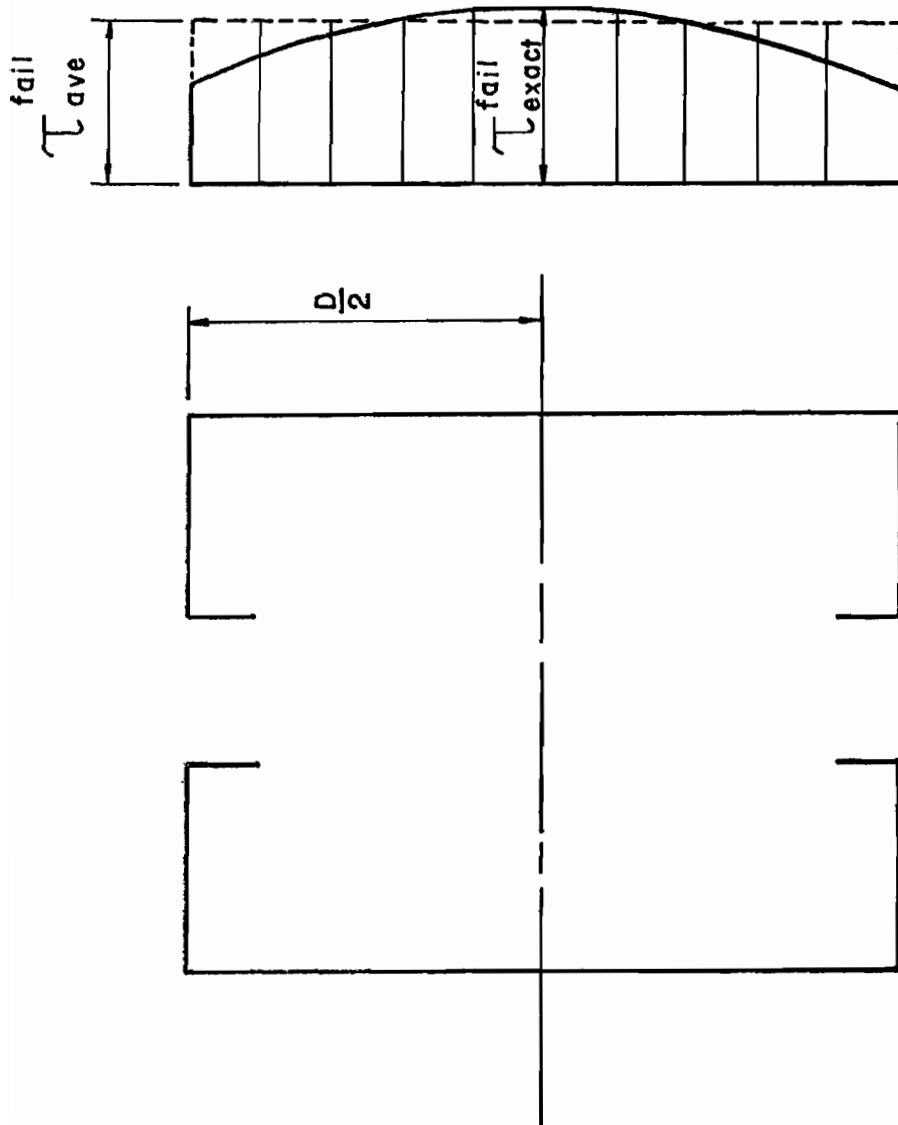
Figure 34. Shear Stress Distribution in Webs
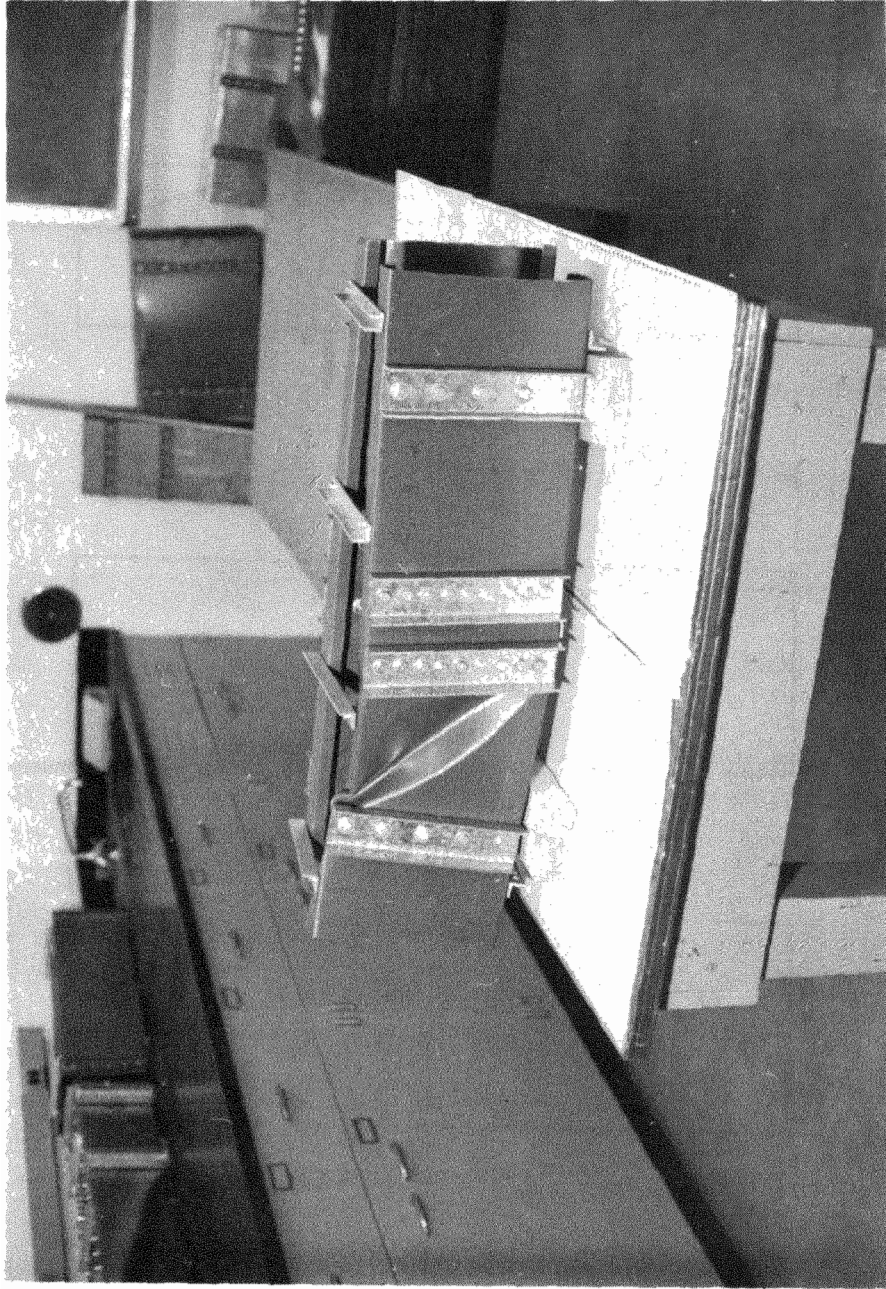
Figure 35. Typical Failure Pattern for Shear Test Specimens (Test Setup-A)

Figure 36. Typical Failure Pattern for Shear Test Specimens (Test Setup-D)

LATERAL DEFLECTION, IN.

Initial

P = 6.5 kips

P = 29.2 kips

P = 8.2 kips

Scale

1.0

.5

0

WEB DEPTH, IN.

P

a

a

3"

6.5 kips = Observed Buckling Load

8.2 kips = Theoretical Buckling Load

29.2 kips = Failure Load
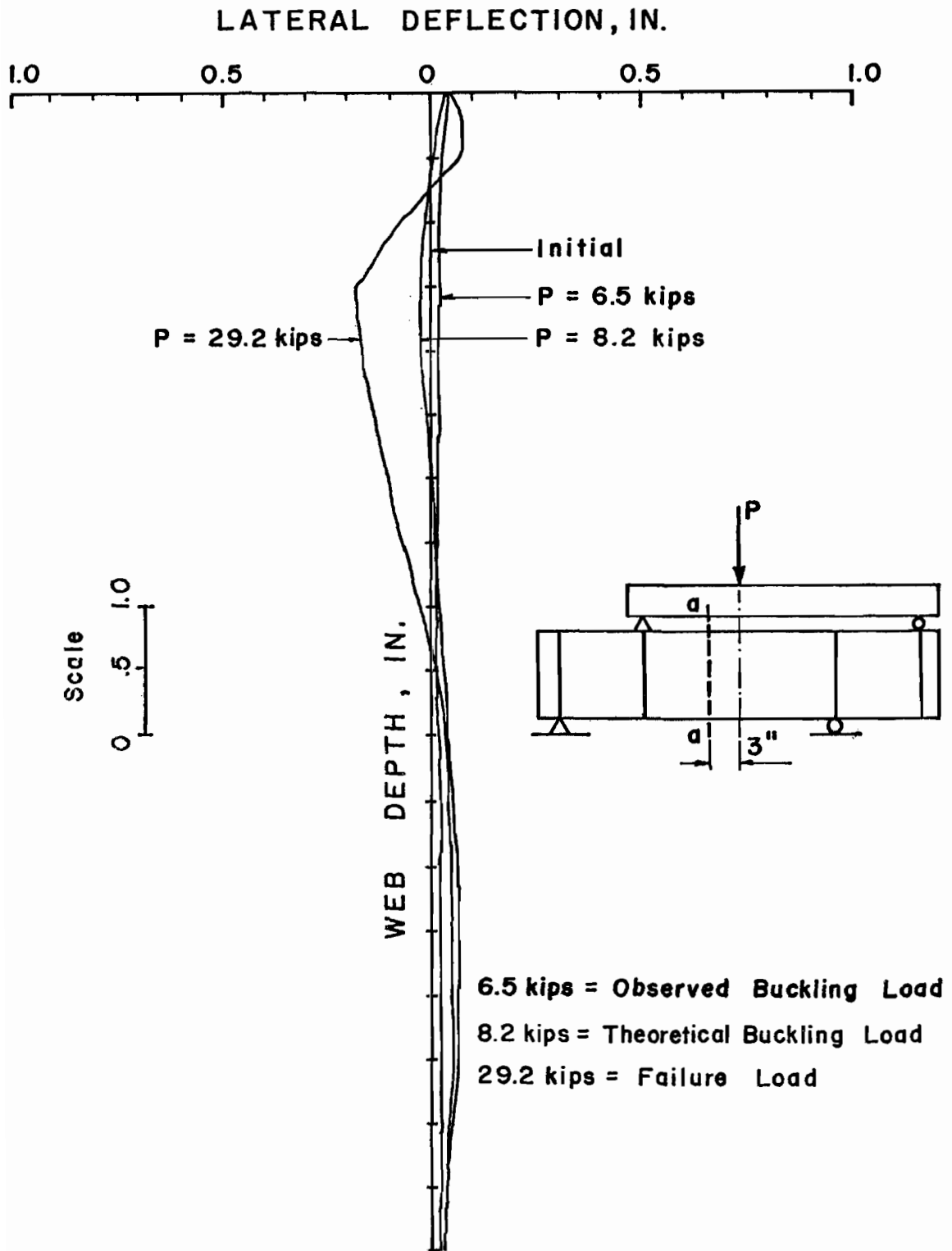
Figure 37. Web Profile of Shear Test Specimen No. S-7-2
at Cross-Section a-a

LATERAL   DEFLECTION, IN.

1.0   0.5   0   0.5   1.0

Initial

P = 6.5 kips

P = 29.2 kips

P = 8.2 kips

Scale

1.0 .5 0

WEB DEPTH, IN.

P

b

b

1.5"

6.5 kips = Observed Buckling Load

8.2 kips = Theoretical Buckling Load

29.2 kips = Failure Load
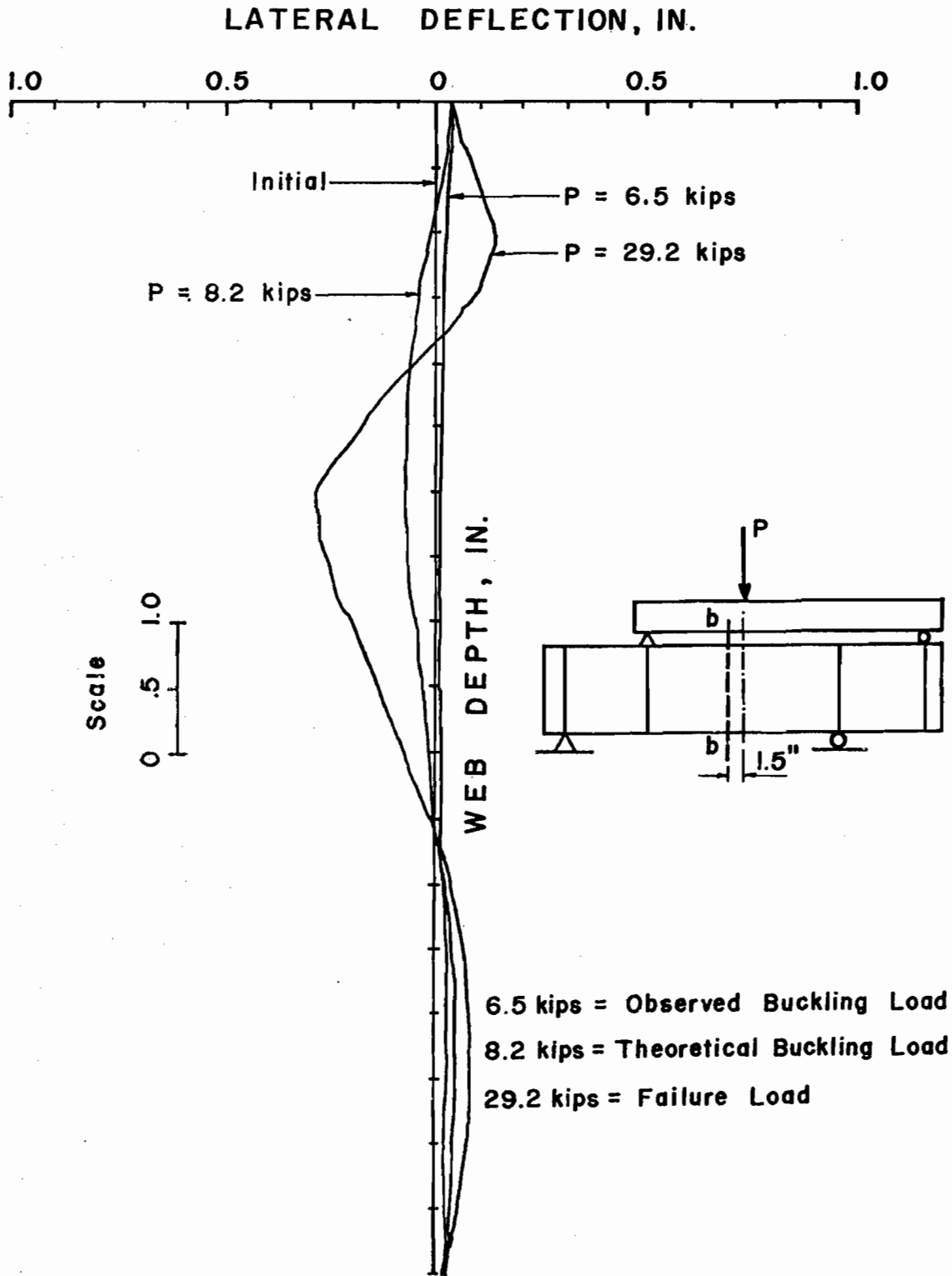
Figure 38.   Web Profile of Shear Test Specimen No. S-7-2
at Cross-Section b-b
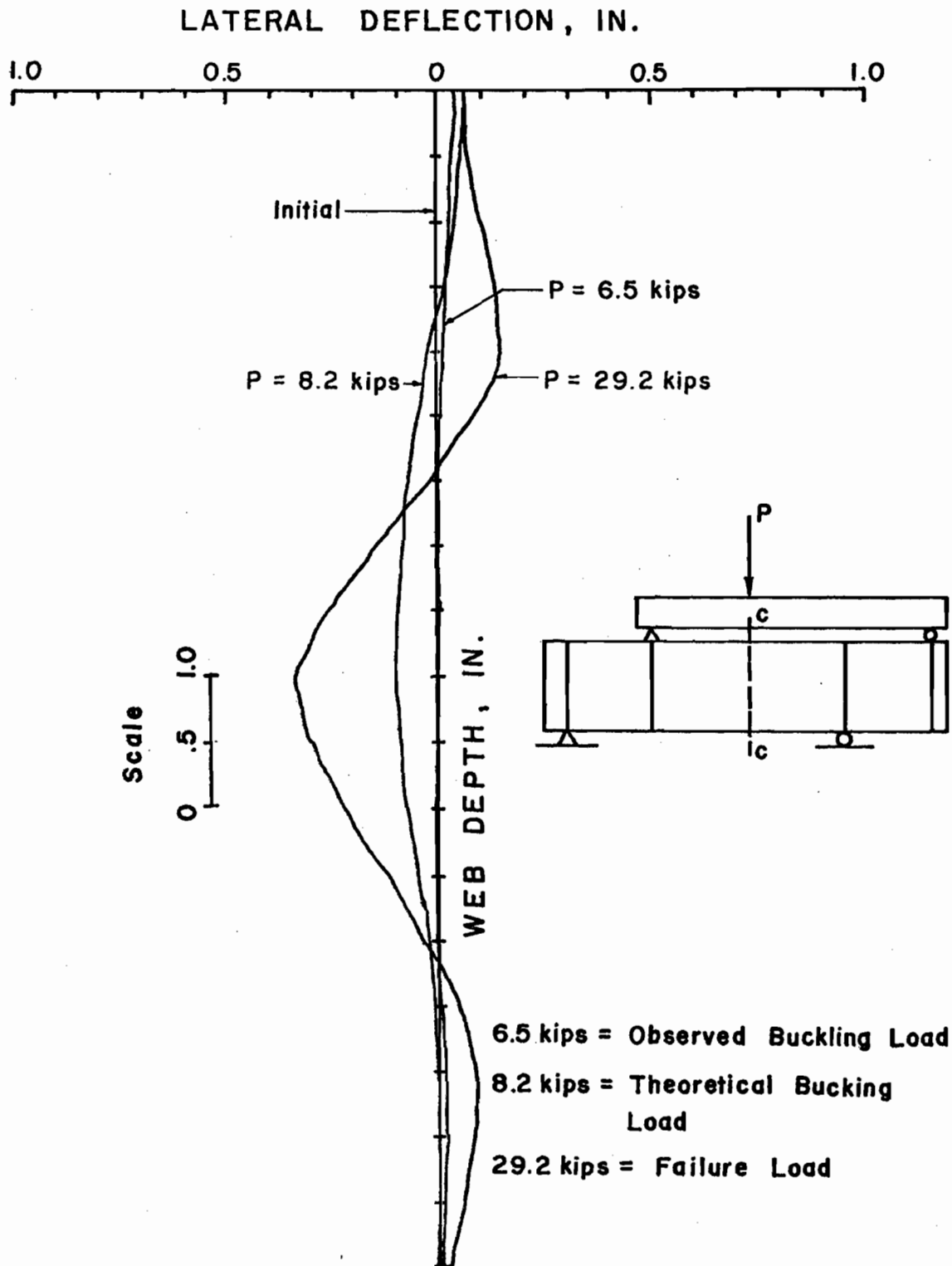
Figure 39. Web Profile of Shear Test Specimen No. S-7-2
at Cross-Section c-c

LATERAL DEFLECTION, IN.
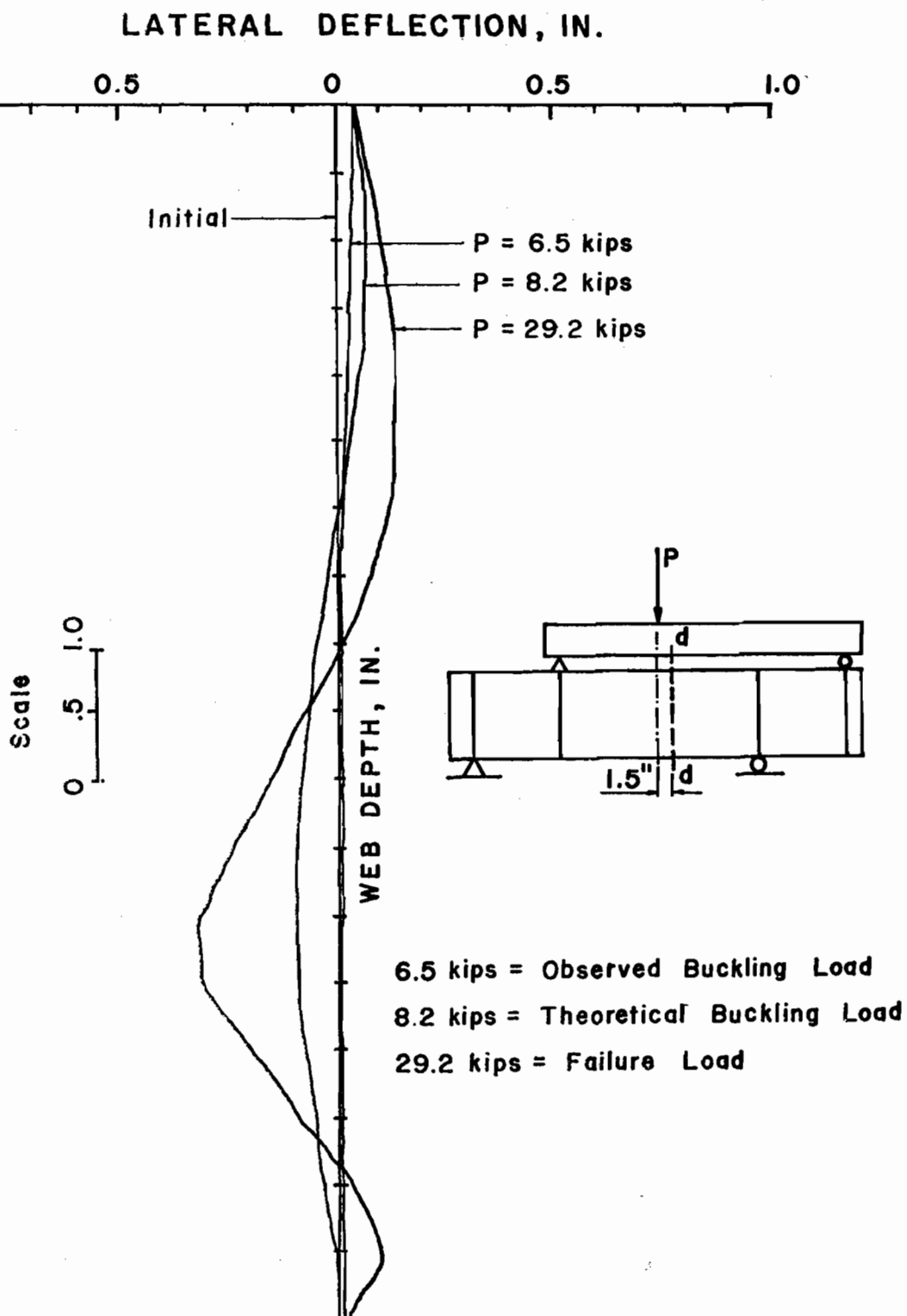
Figure 40. Web Profile of Shear Test Specimen No. S-7-2
at Cross-Section d-d

LATERAL DEFLECTION, IN.

Initial —

P = 6.5 kips

P = 8.2 kips

P = 29.2 kips

WEB DEPTH, IN.

Scale

P

e

e

3"

6.5 kips = Observed Buckling Load

8.2 kips = Theoretical Buckling Load

29.2 kips = Failure Load
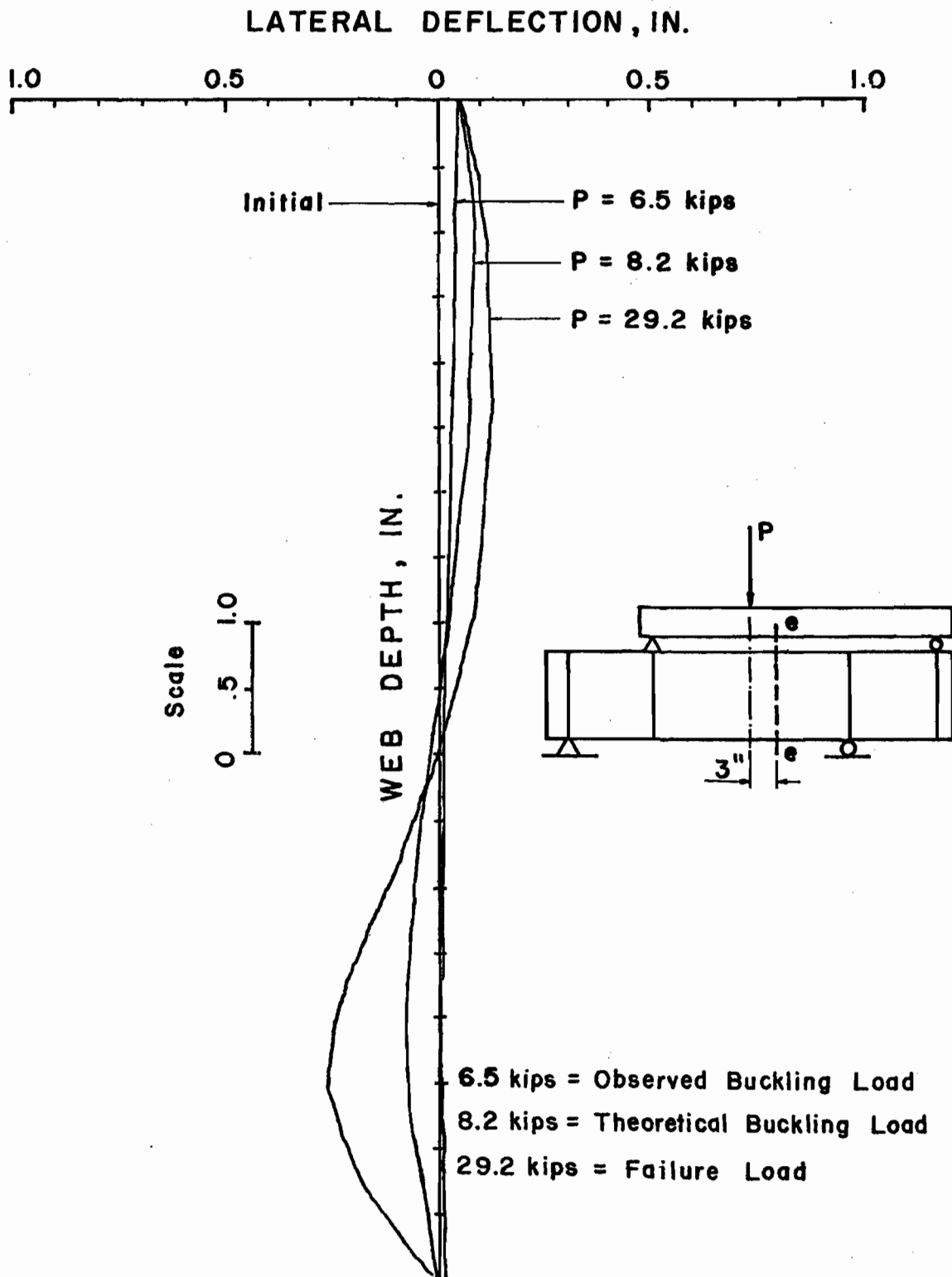
Figure 41. Web Profile of Shear Tests Specimen No. S-7-2
at Cross-Section e-e
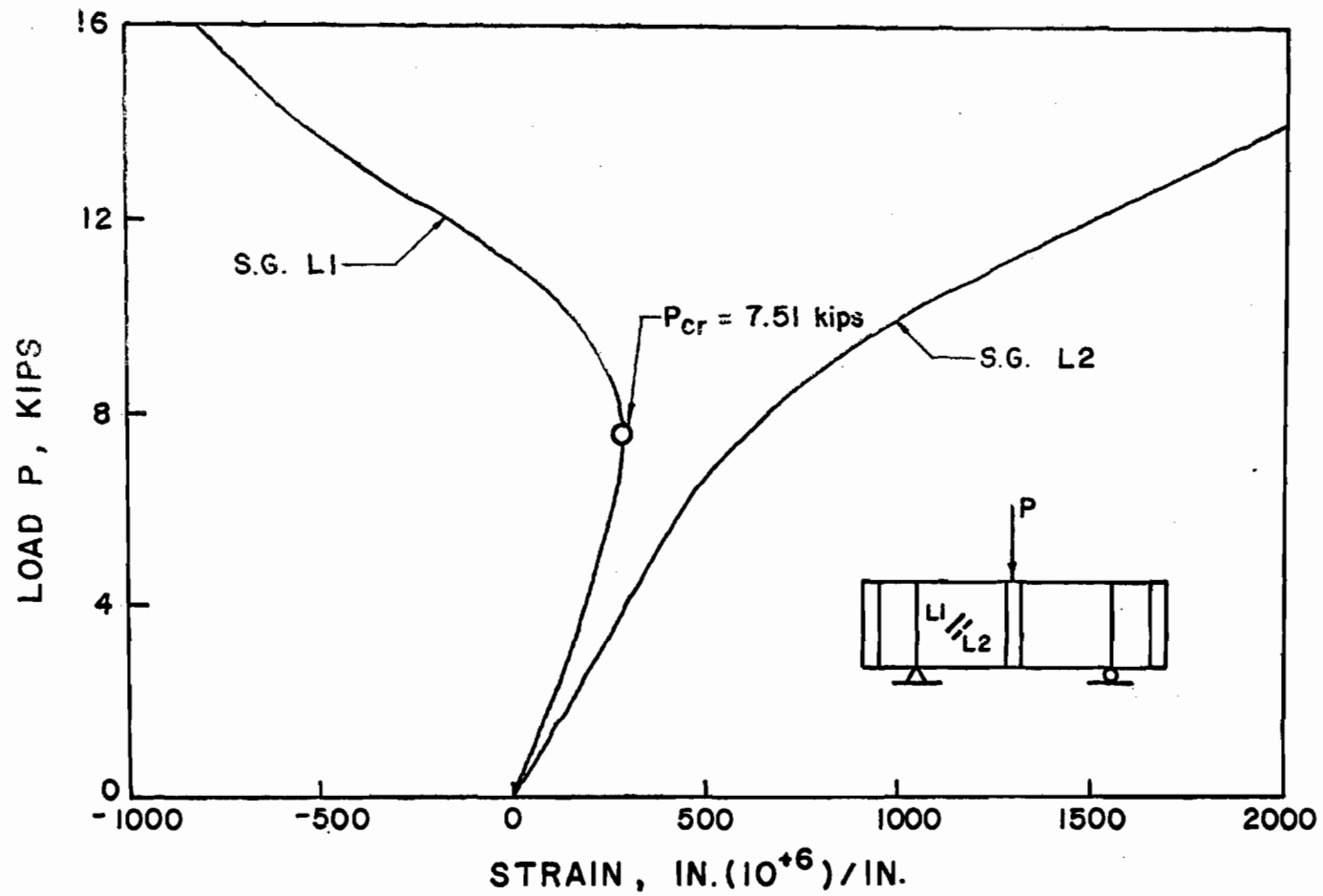
Figure 42. Load-Strain Curve of Specimen No. S-4-1
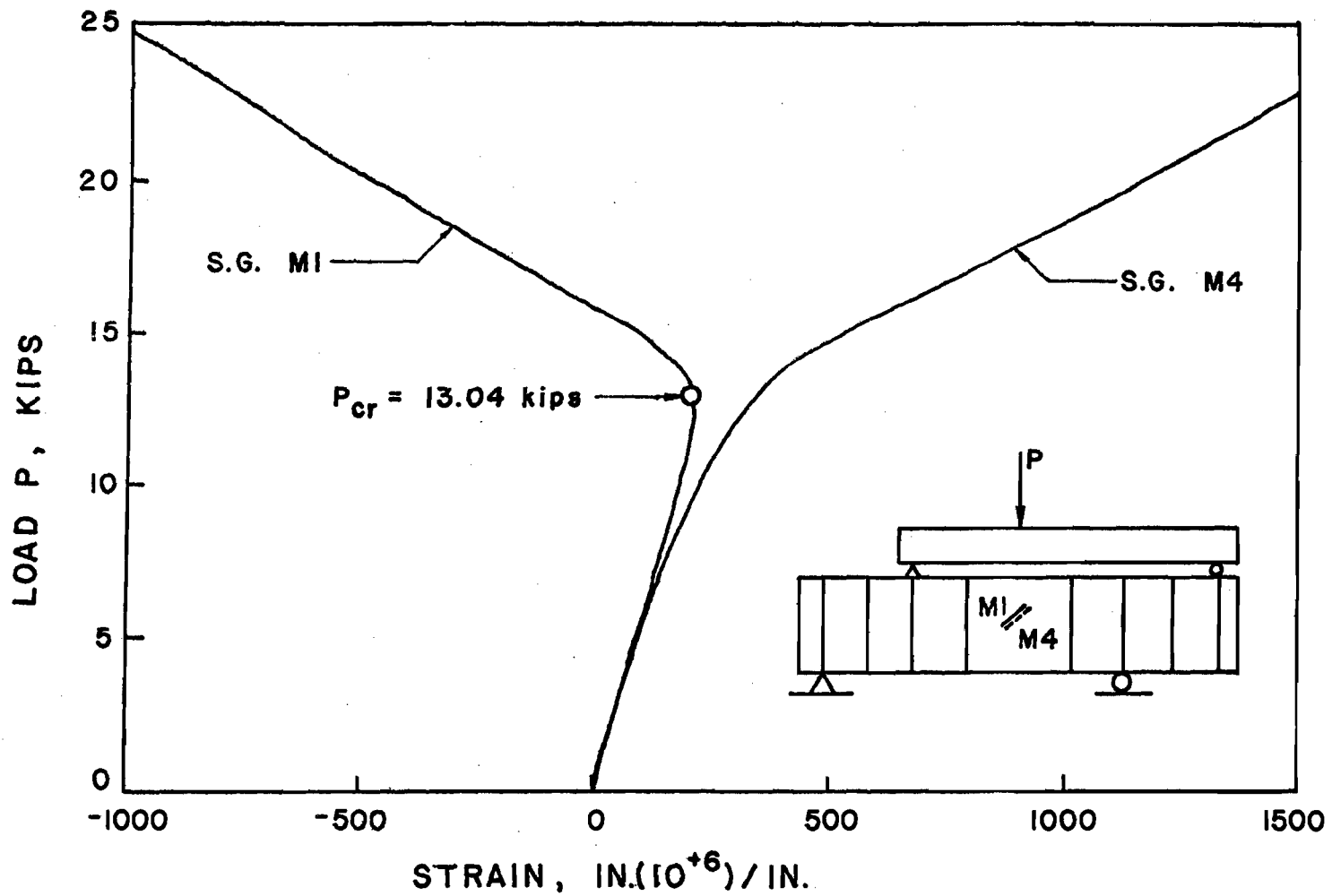
Figure 43. Load-Strain Curve of Specimen No. S-5-1 for strain gages M1 and M4
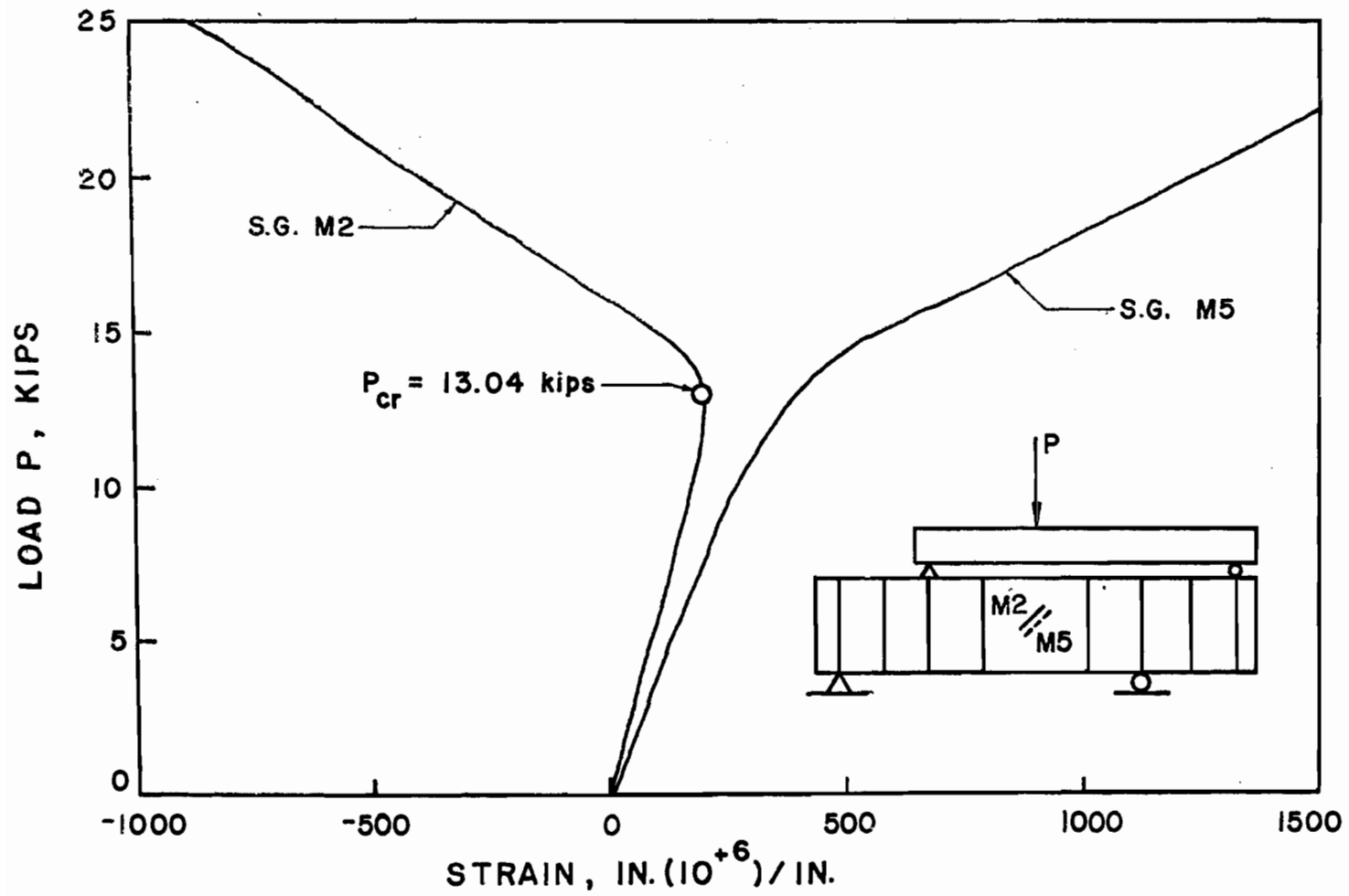
Figure 44. Load-Strain Curve of Specimen No. S-5-1 for Strain Gages M2 and M5
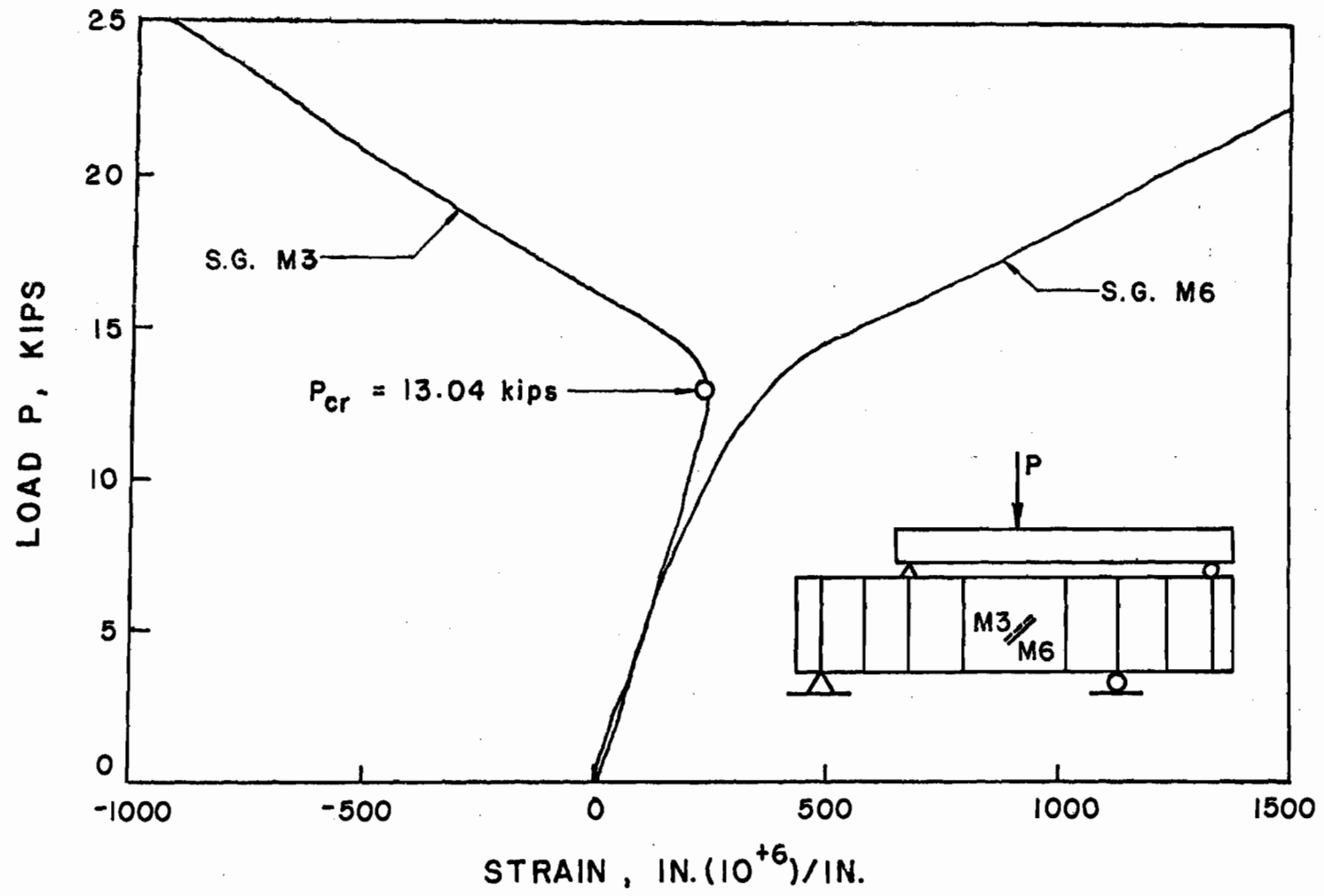
Figure 45. Load-Strain Curve of Specimen No. S-5-1 for Strain Gages M3 and M6
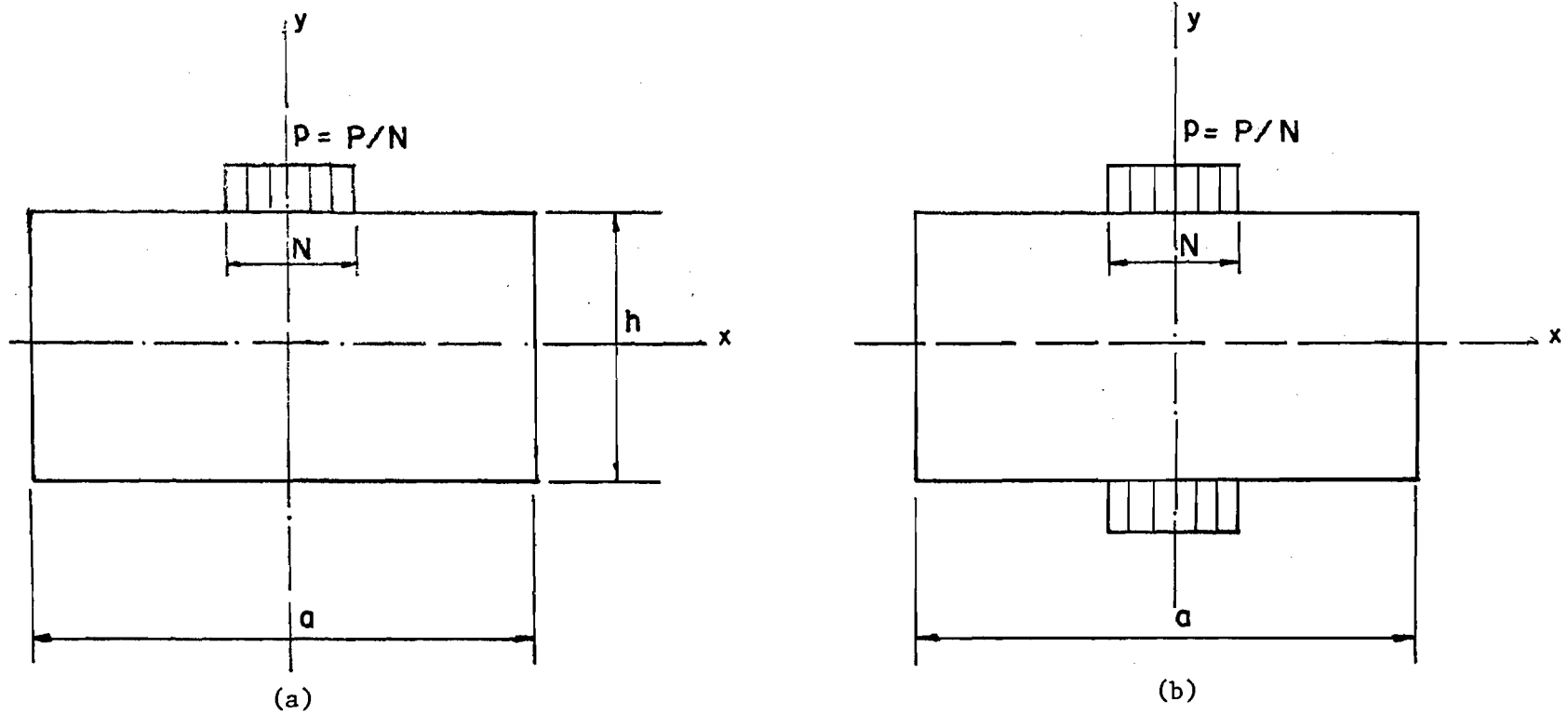
Figure 46. Plates Subjected to Partial Edge Loading
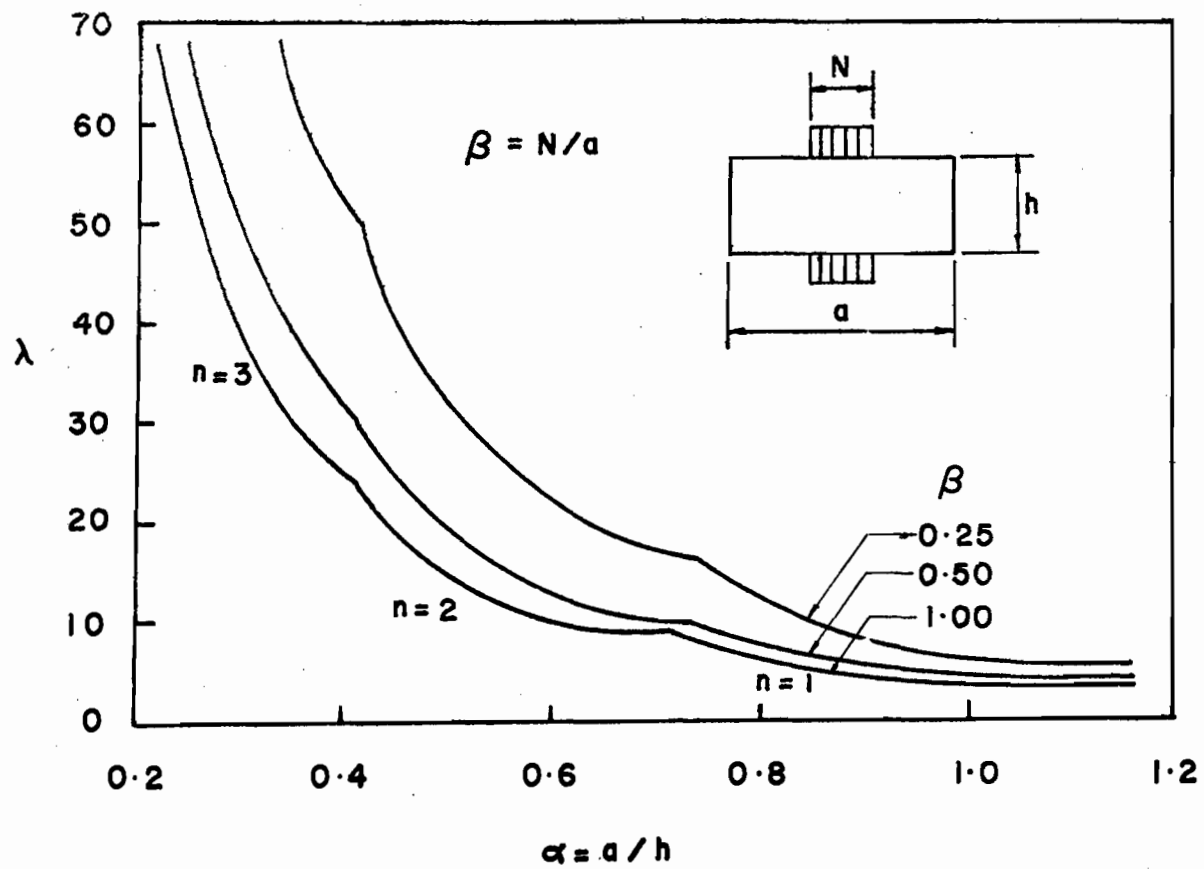
Figure 47. Relationship Between λ and α for Different Buckling Modes
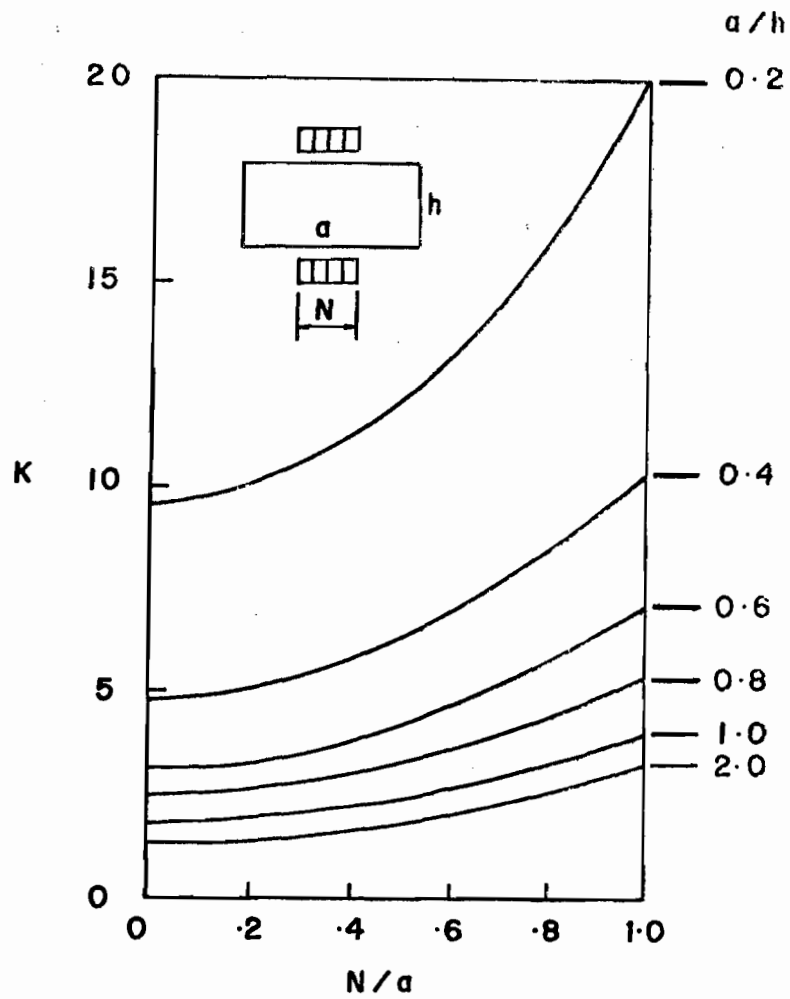
Figure 48. Buckling Coefficient for Simply Supported
Plates Under Partial Loads on Both Edges
Based on UMR Solution
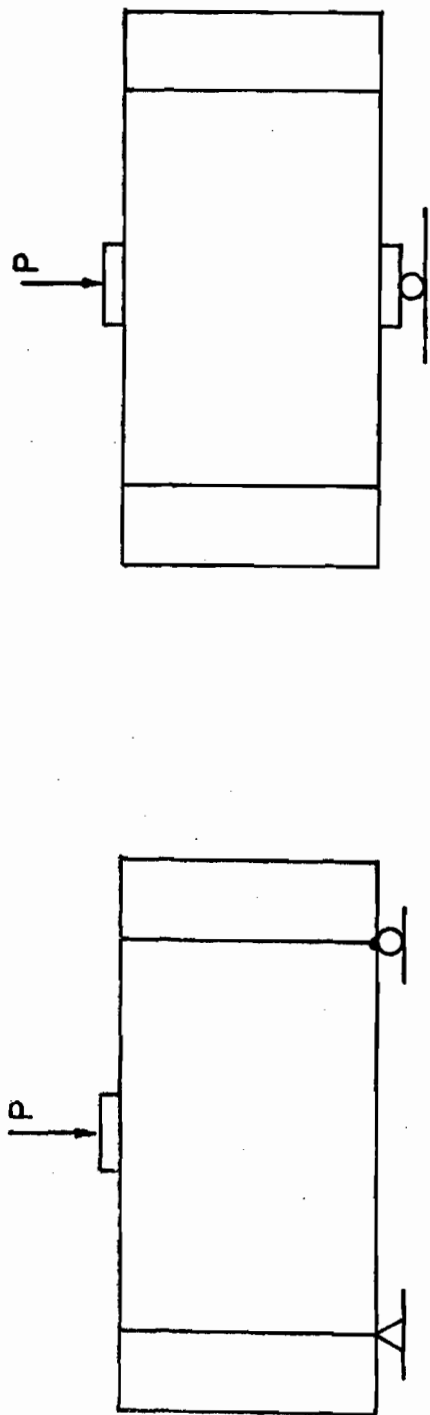
Figure 49. Loading Conditions for Web Crippling Study
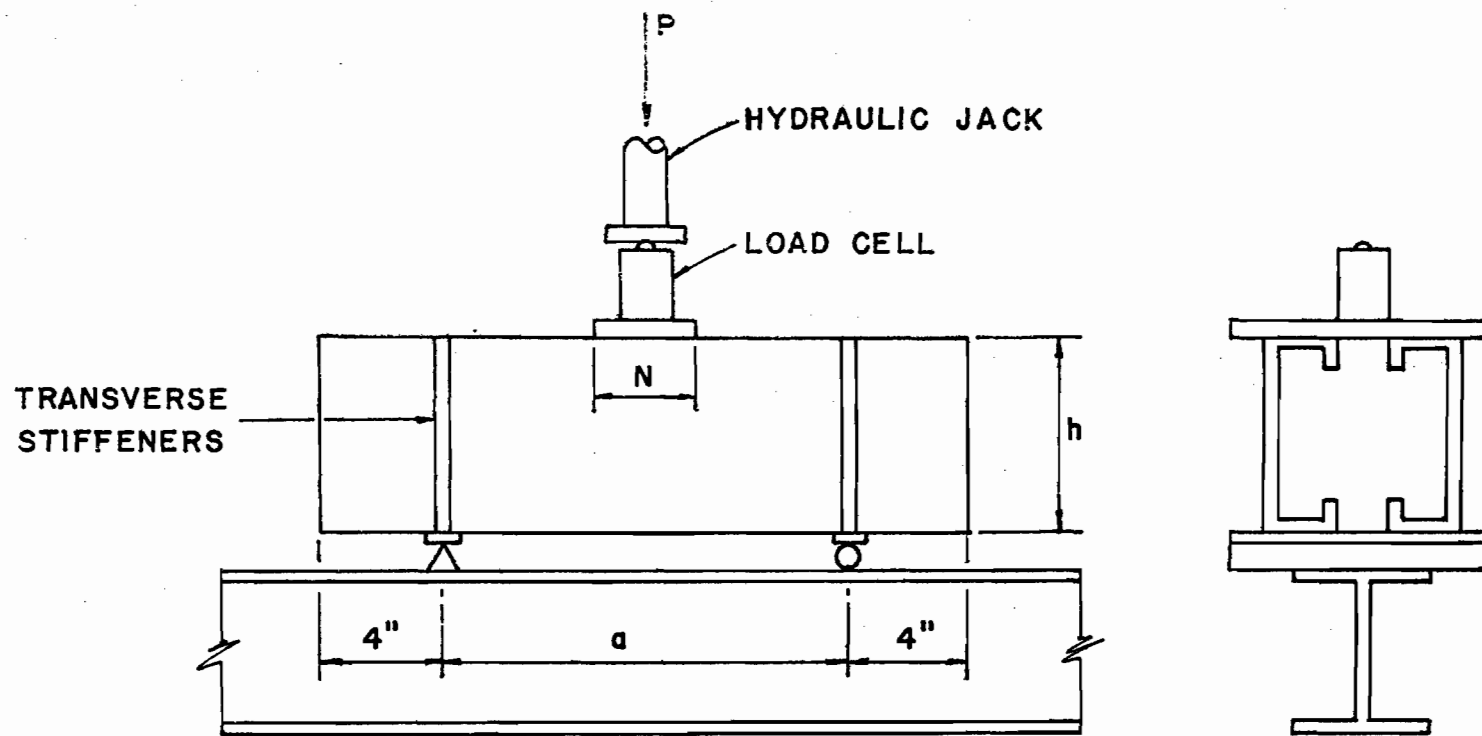
Figure 50.   Test Setup for One-Flange Web Crippling Test (Setup-A)
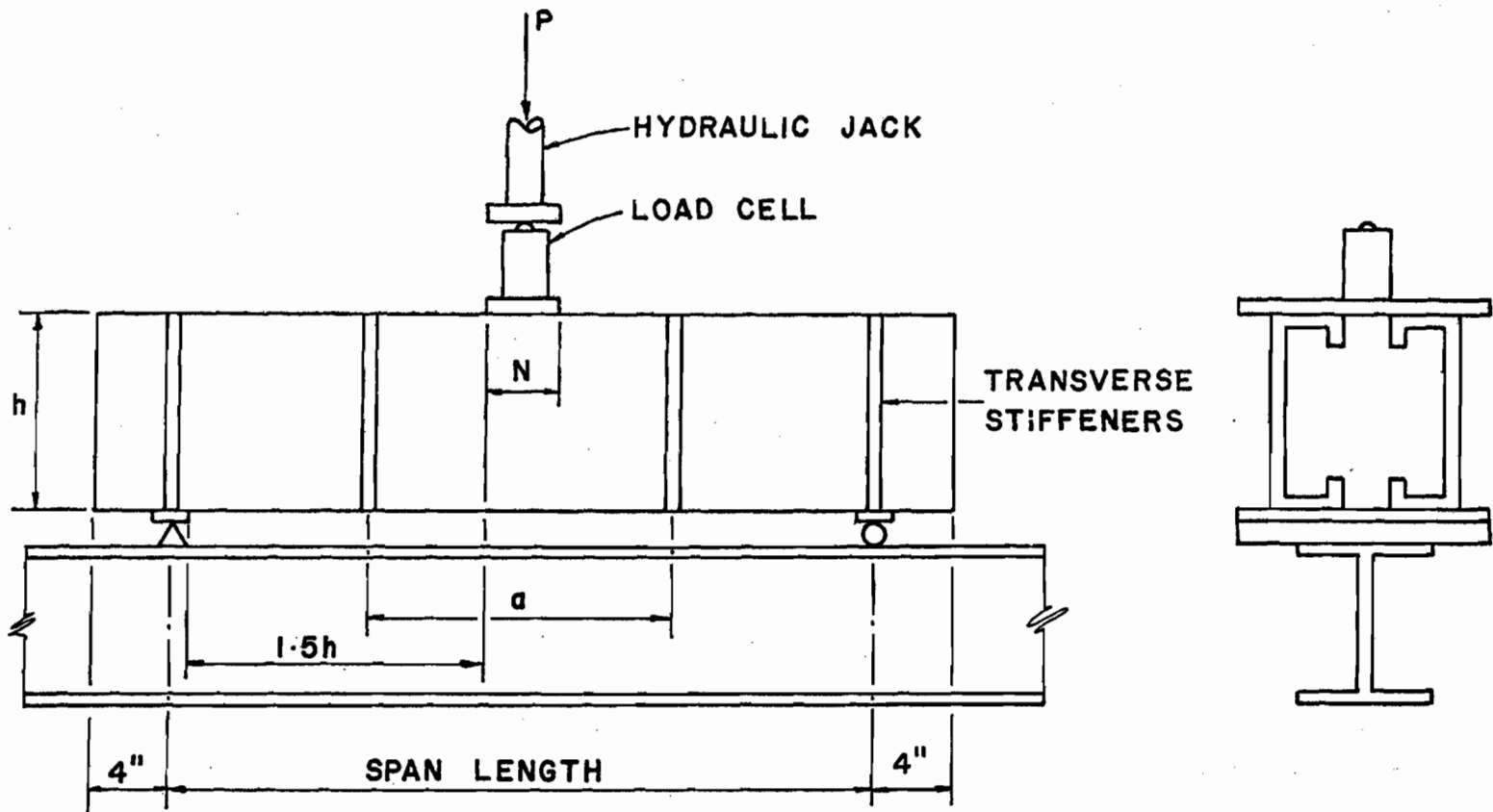
Figure 51. Test Setup for One-Flange Web Crippling Test (Setup-B)
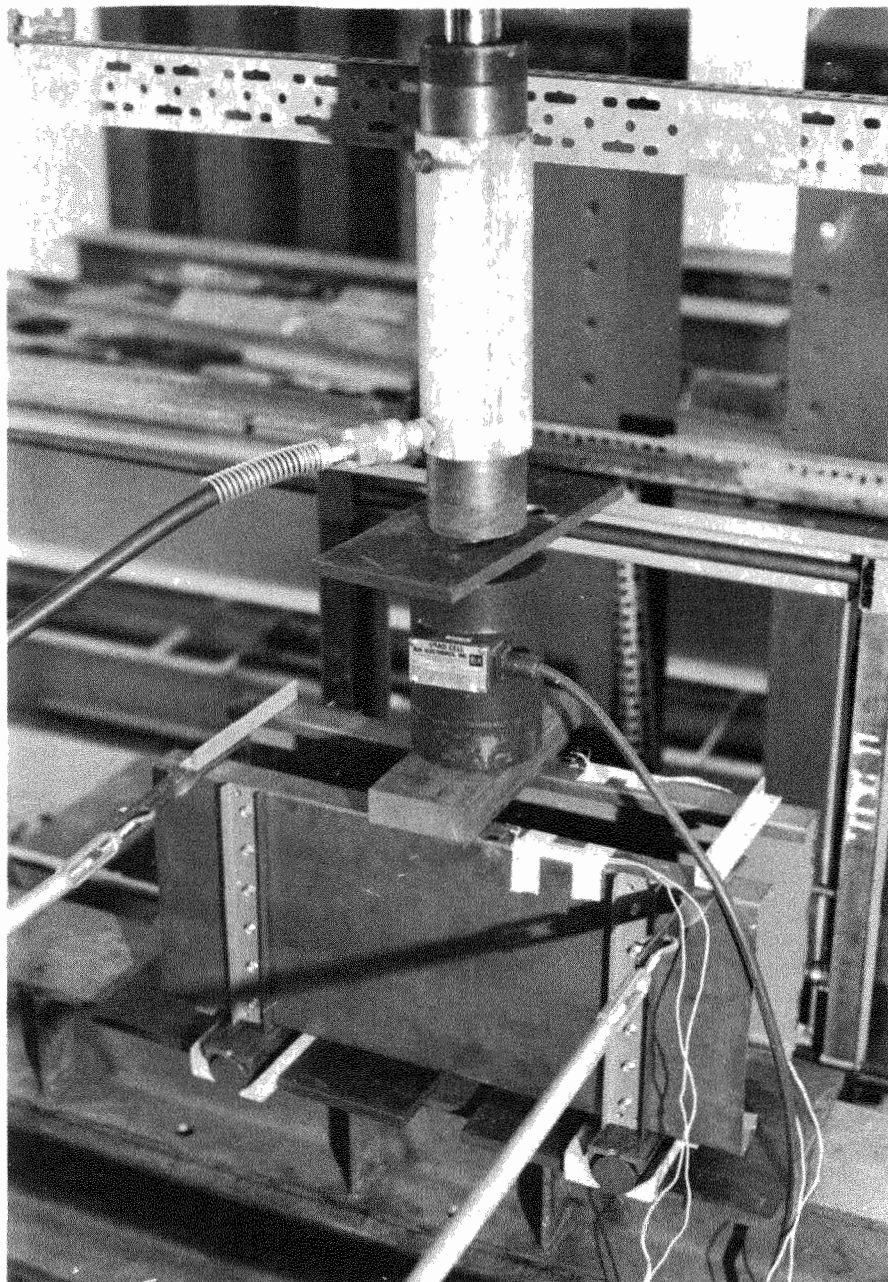
Figure 52. Photograph of Test Setup for One-Flange
Web Crippling Test
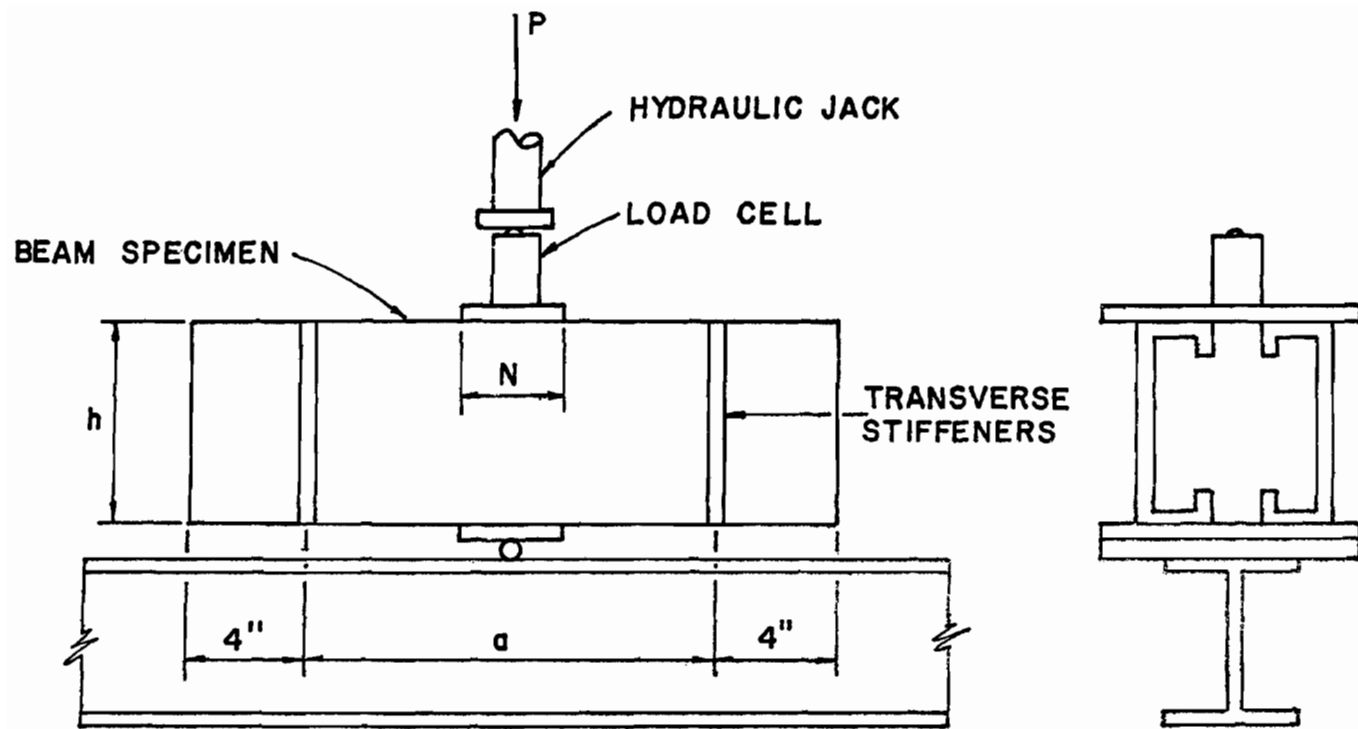
Figure 53. Test Setup for Two-Flange Web Crippling Test
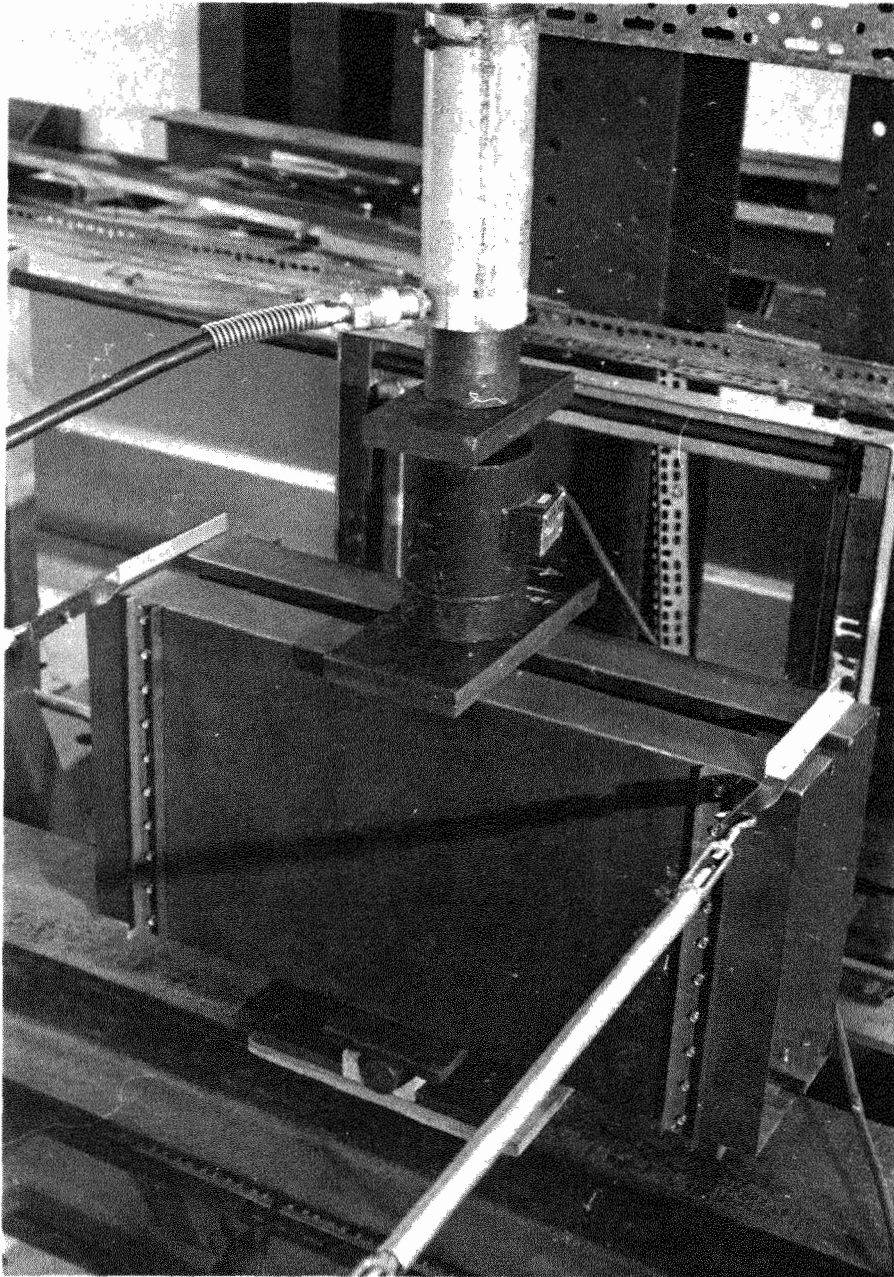
Figure 54.   Photograph of Test Setup for Two-Flange
             Web Crippling Test

Figure 55. Typical Failure Pattern for One-Flange Web Crippling Test Specimen
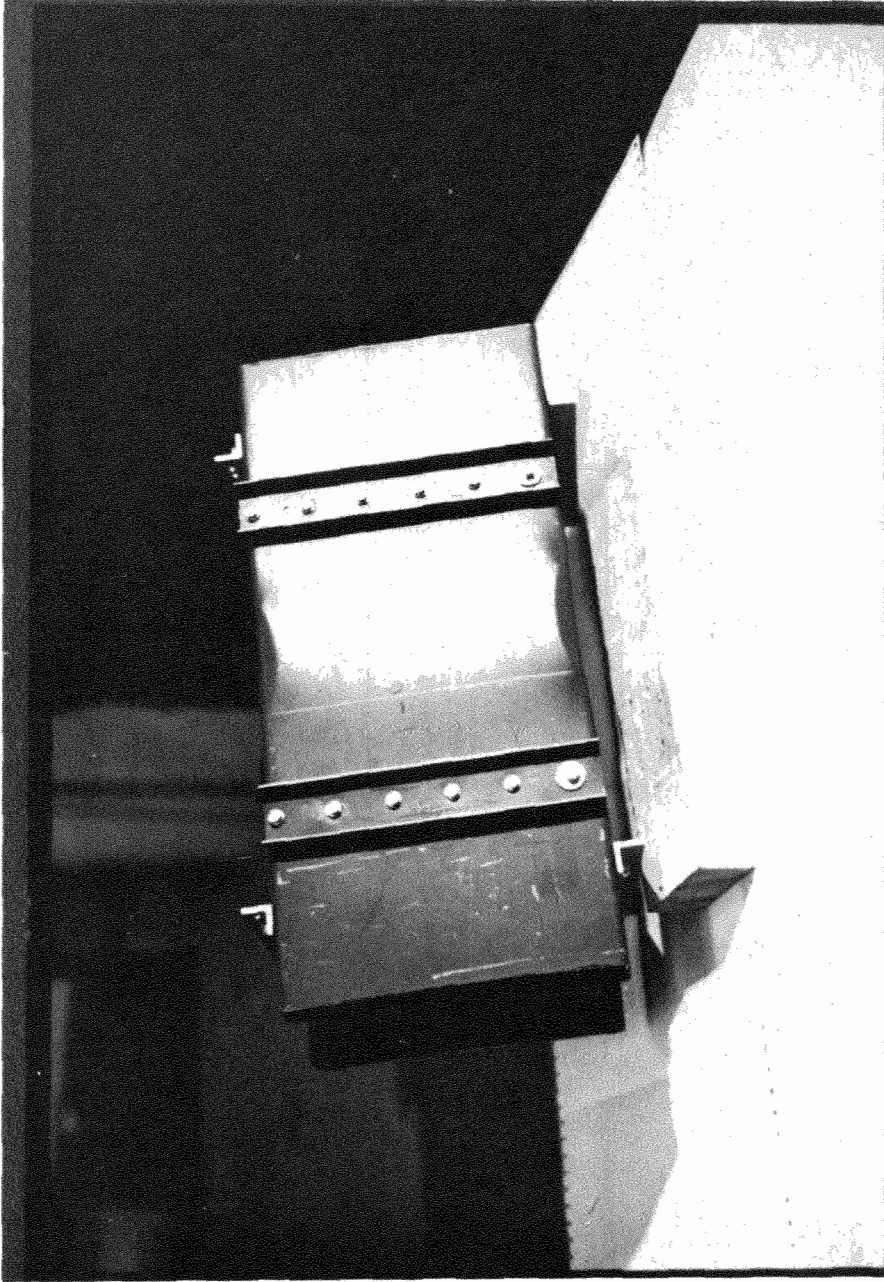
Figure 56. Typical Failure Pattern for Two-Flange Web Crippling Test Specimen
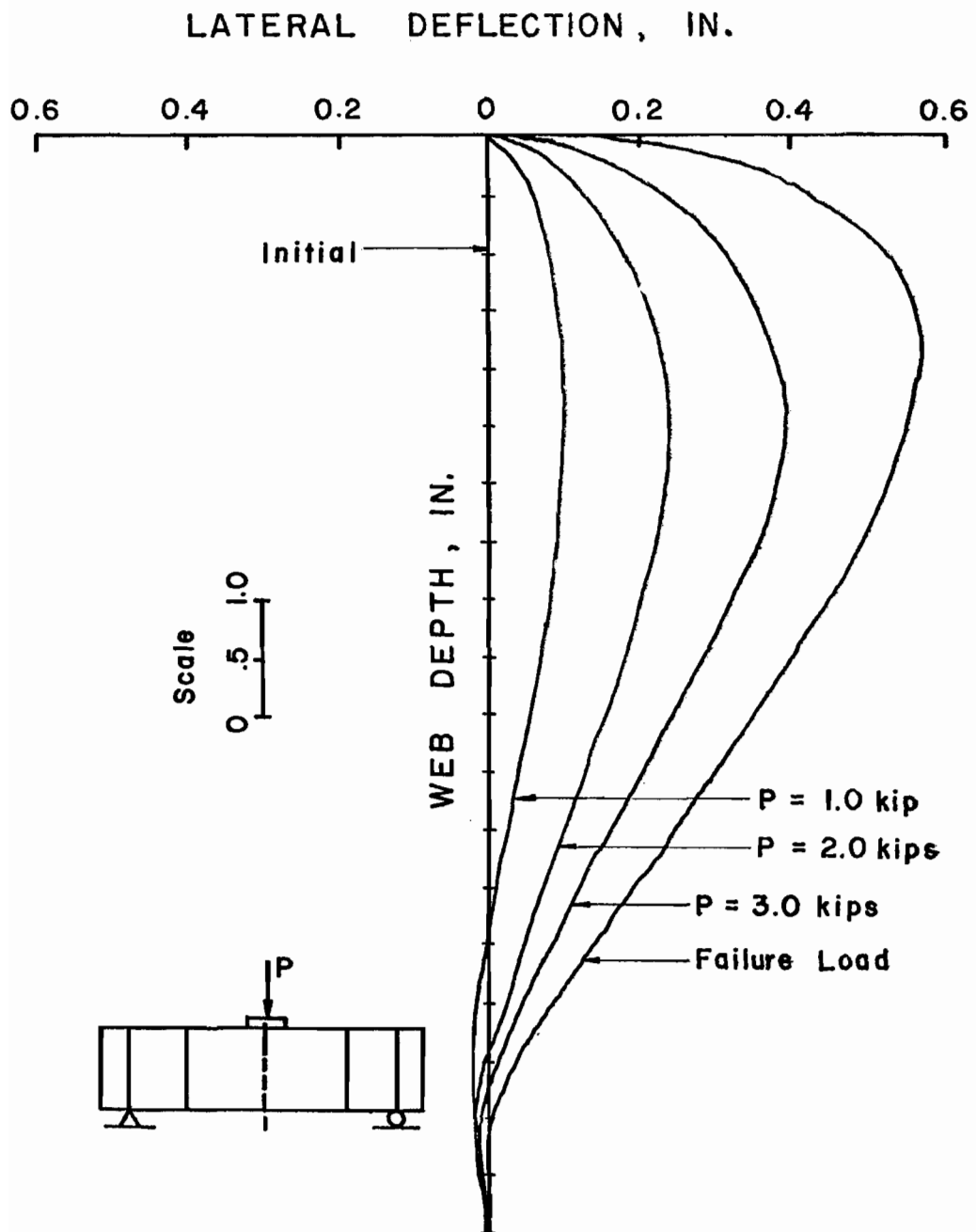
Figure 57. Web Profile of Specimen MWC-OF-4-10

LATERAL DEFLECTION, IN.

0.5　　　　0.25　　　　0　　　　0.25　　　　0.5

Initial

P = 1.0 kip

P = 2.0 kips

Failure Load

Scale

1.0

.5

0

WEB DEPTH, IN.

P
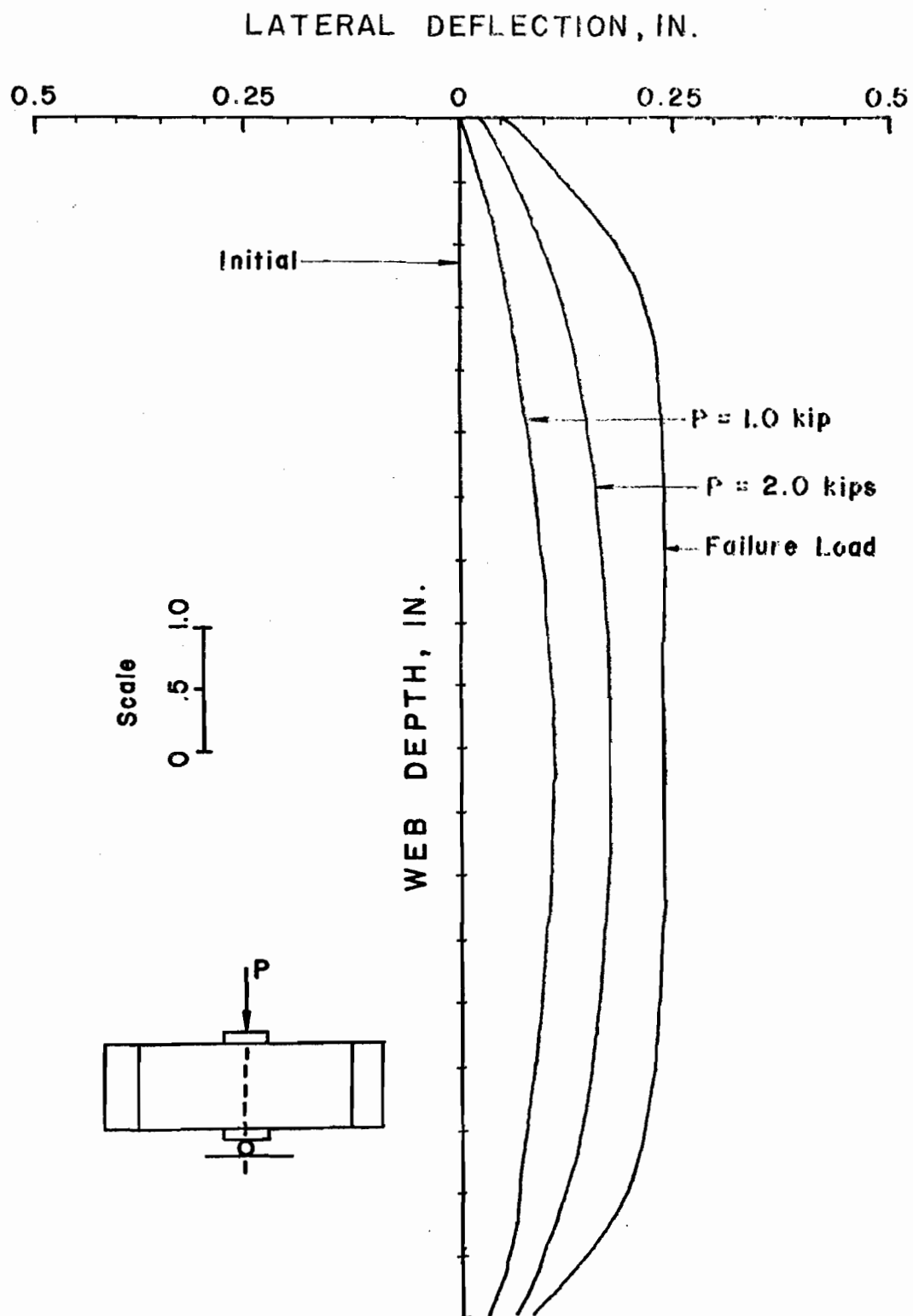
Figure 58.　Web Profile of Specimen WC-TF-6-20
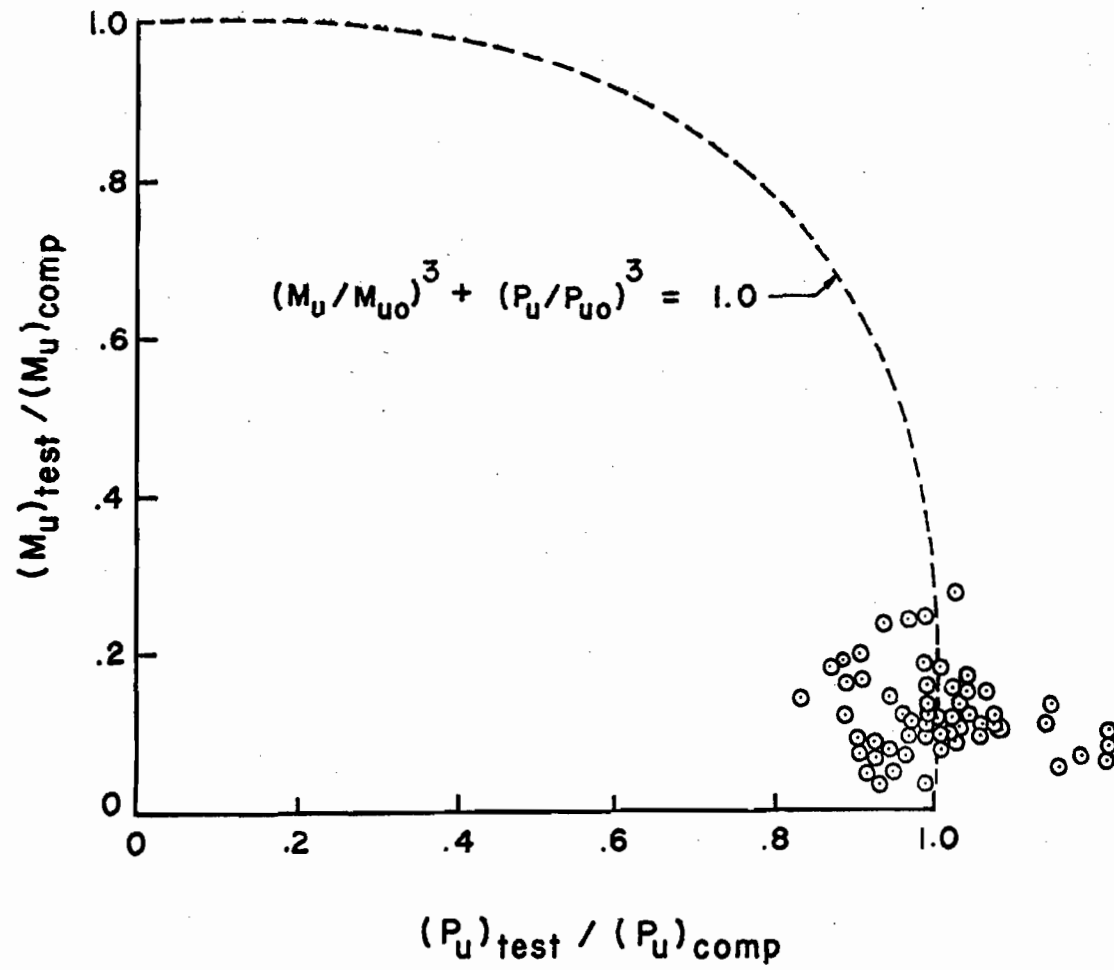
Figure 59. Intereaction of Bending and Web Crippling for One-Flange Test Specimen

The figure shows a plot with vertical axis labeled $(M_u)_{test} / (M_u)_{comp}$ ranging from 0 to 1.0, and horizontal axis labeled $(P_u)_{test} / (P_u)_{comp}$ ranging from 0 to 1.0. The dashed curve represents:

$$(M_u/M_{uo})^3 + (P_u/P_{uo})^3 = 1.0$$
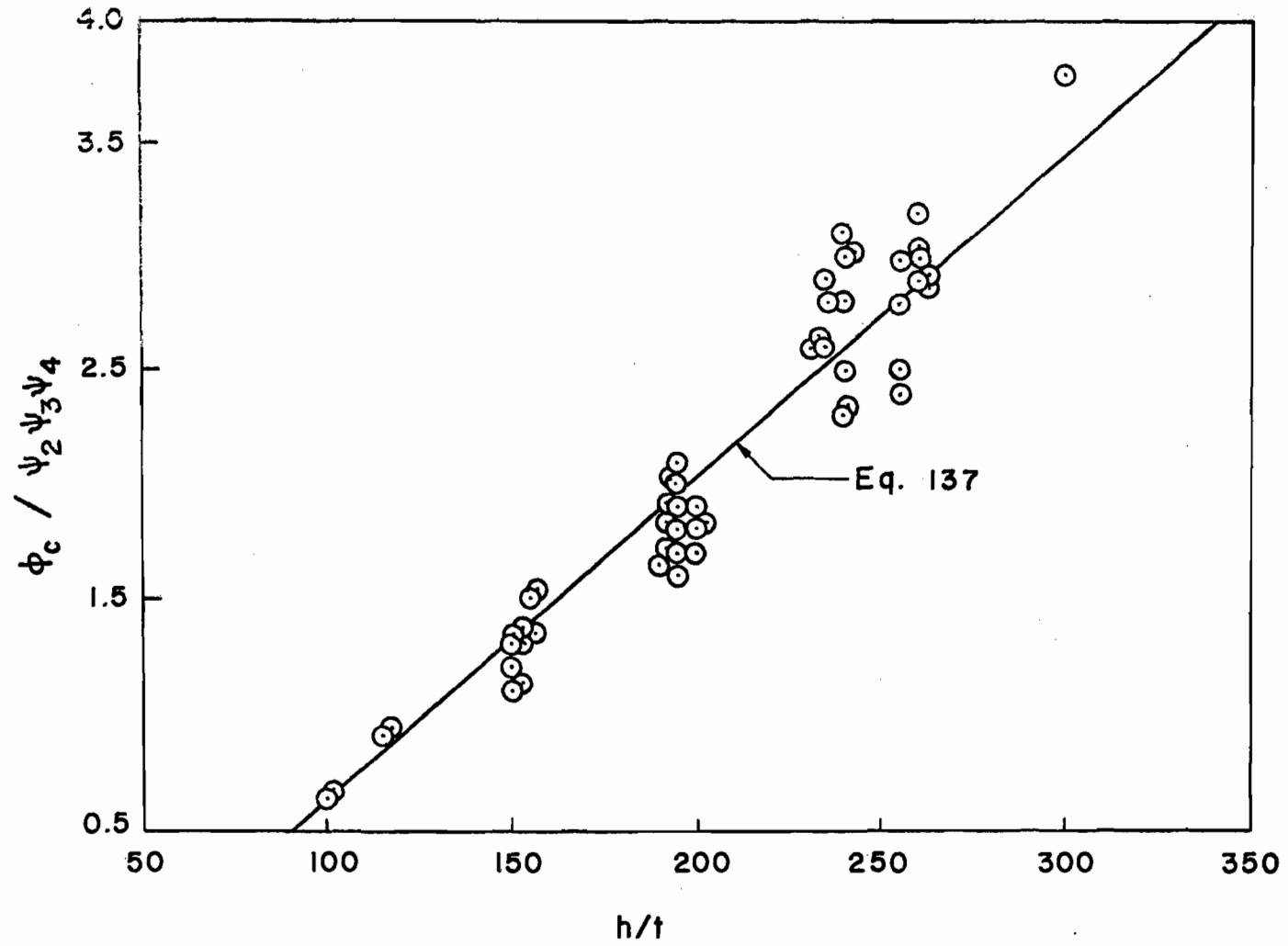
Figure 60.   Variation of Postbuckling Strength Factor with the Ratio h/t for reinforced
Beam Webs Subjected to One-Flange Web Crippling Load
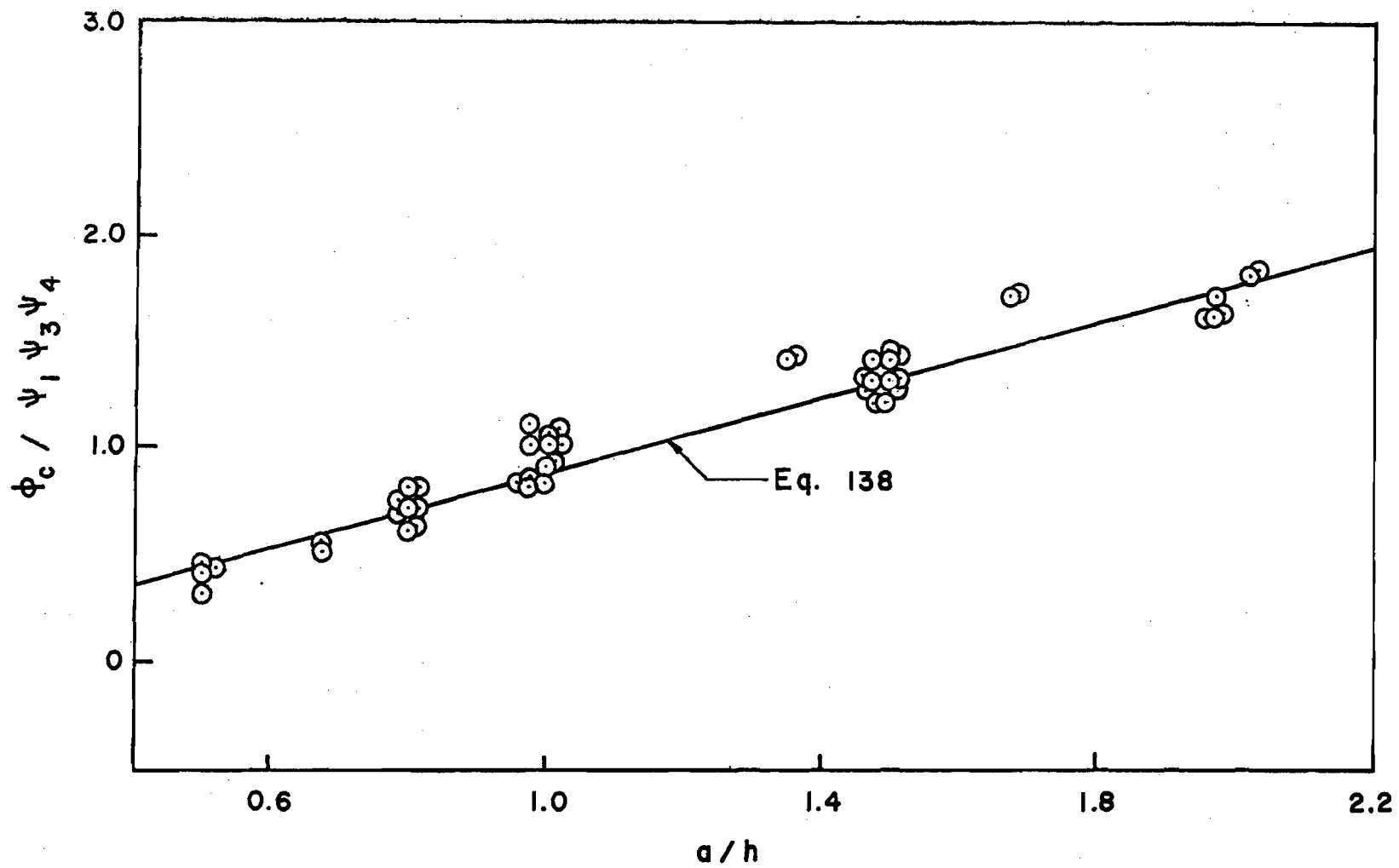
Figure 61. Variation of Postbuckling Strength Factor with the Ratio a/h for reinforced Beam Webs Subjected to One-Flange Web Crippling Load
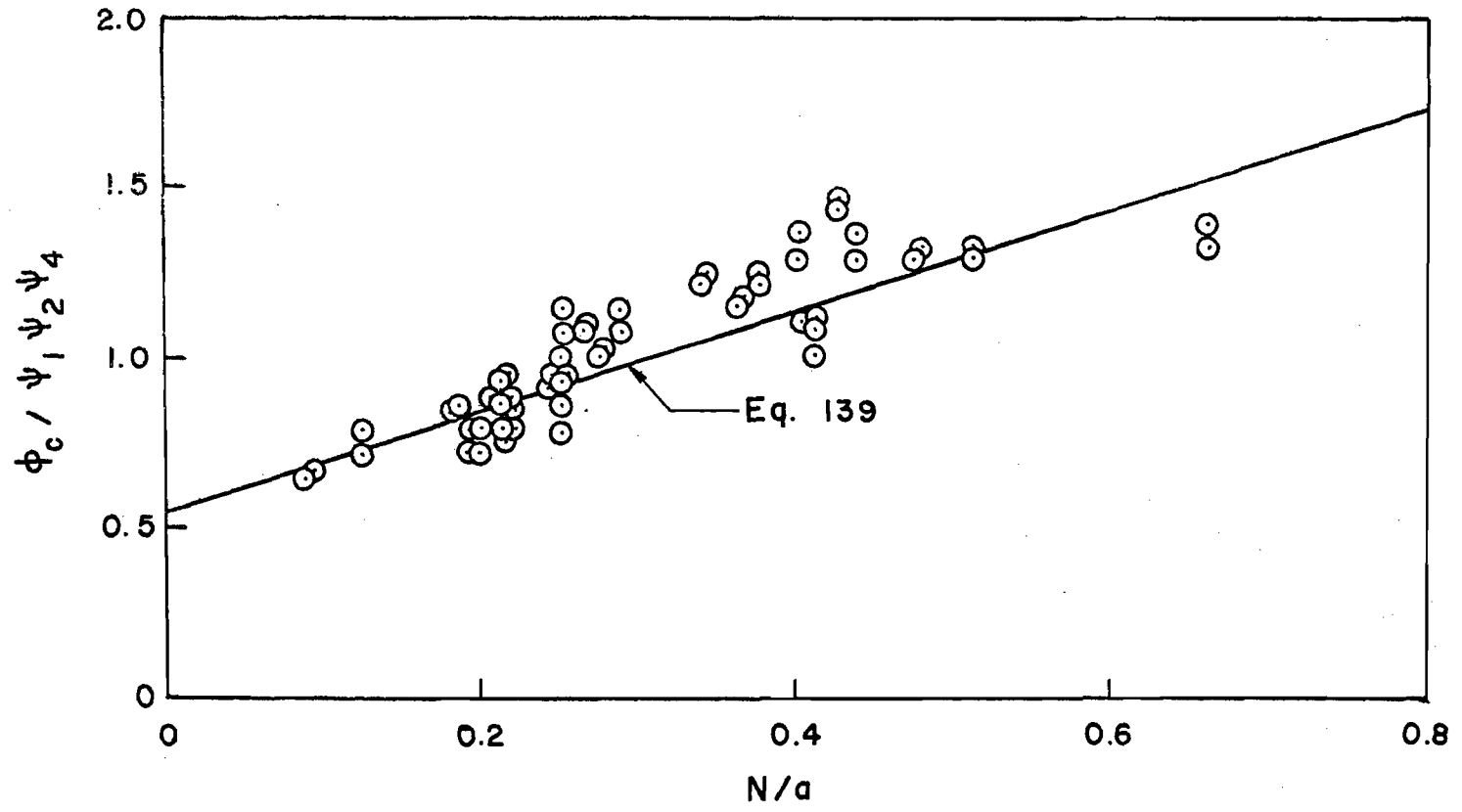
Figure 62. Variation of Postbuckling Strength Factor with the Ratio N/a for Reinforced
Beam Webs Subjected to One-Flange Web Crippling Load
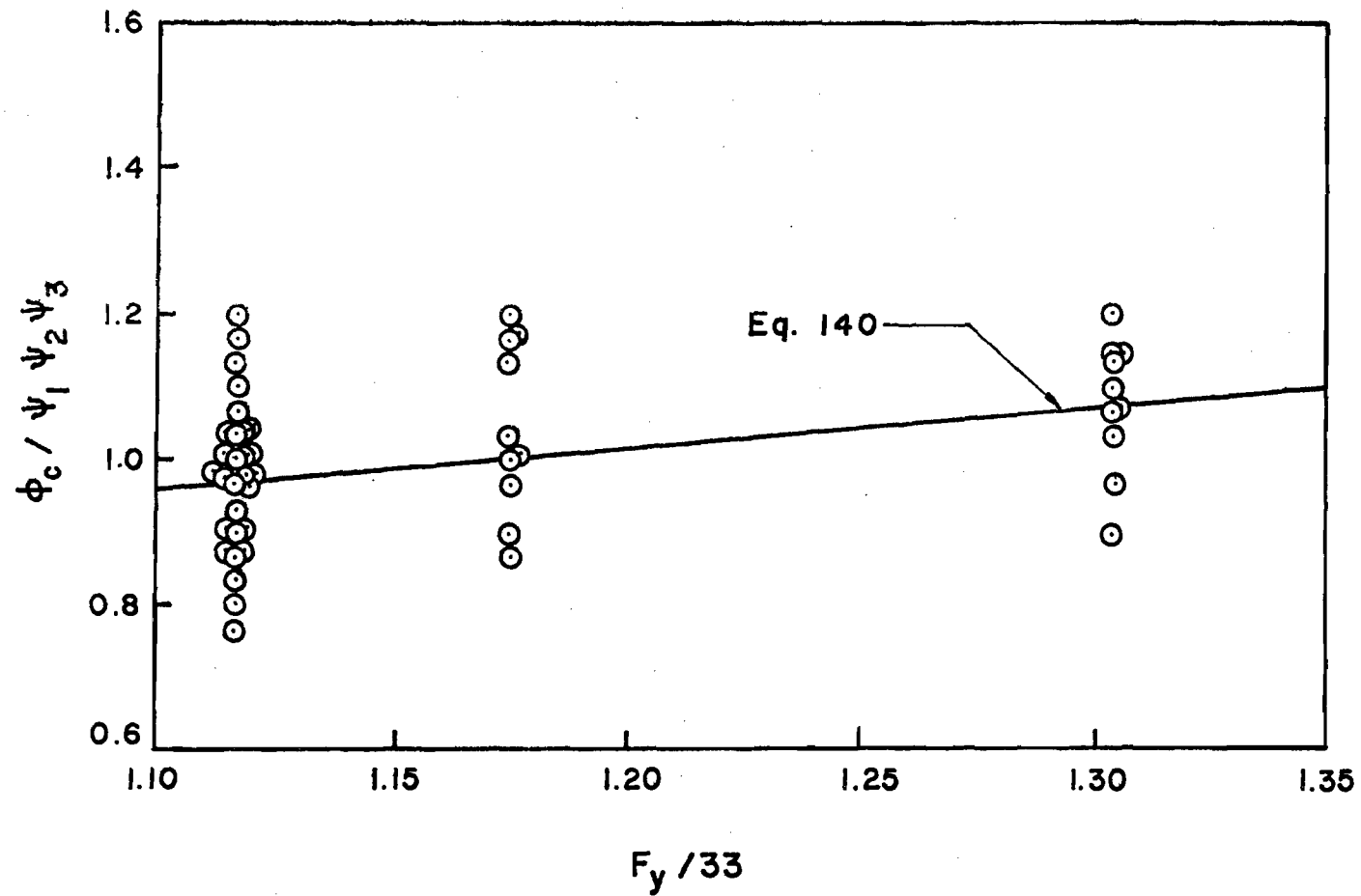
Figure 63. Variation of Postbuckling Strength Factor with the Ratio $F_y/33$ for reinforced
Beam Webs Subjected to One-Flange Web Crippling Load
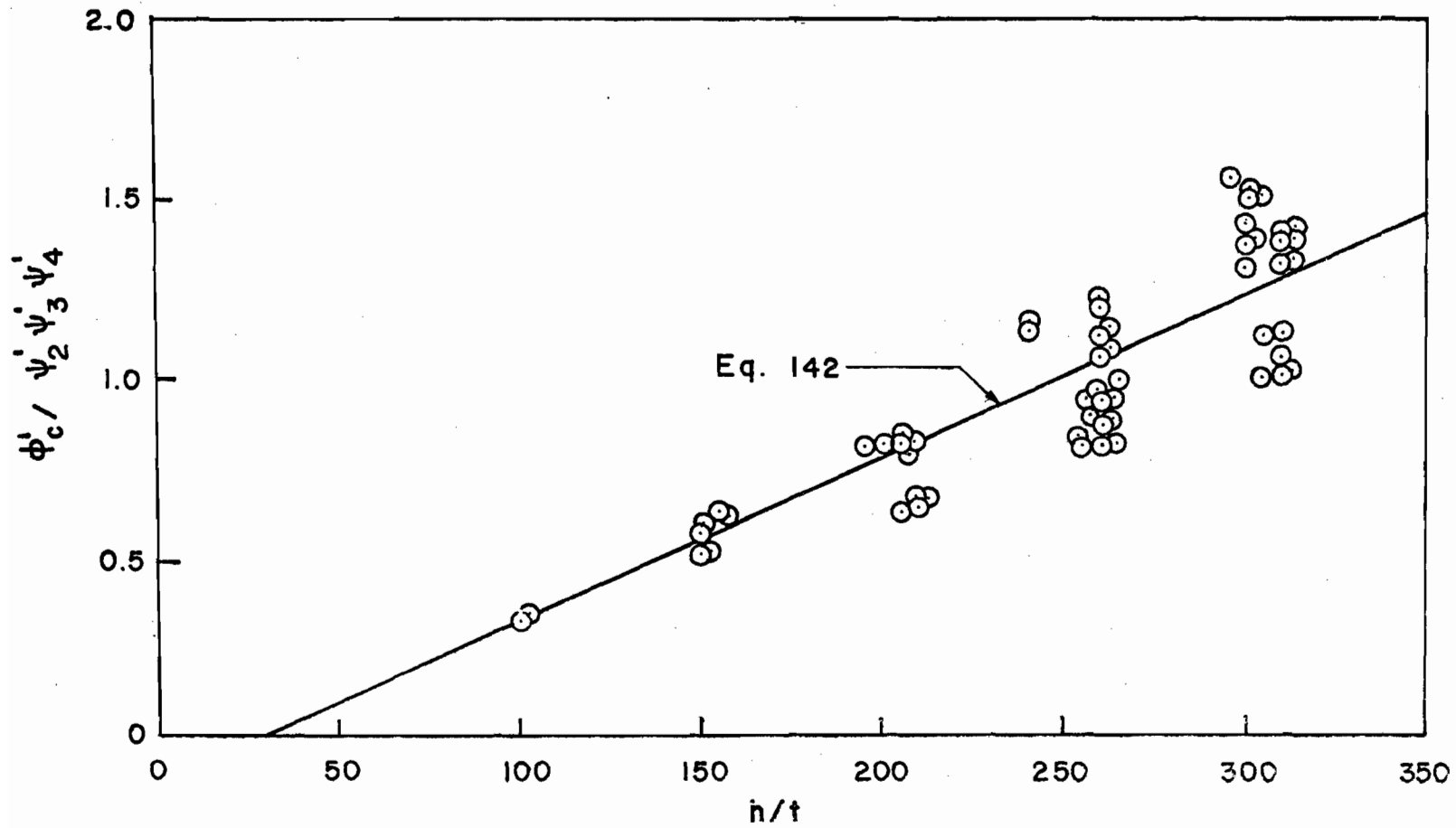
Figure 64.   Variation of Postbuckling Strength Factor with the Slenderness Ratio h/t for Reinforced Beam Webs Subjected to Two-Flange Web Crippling Load
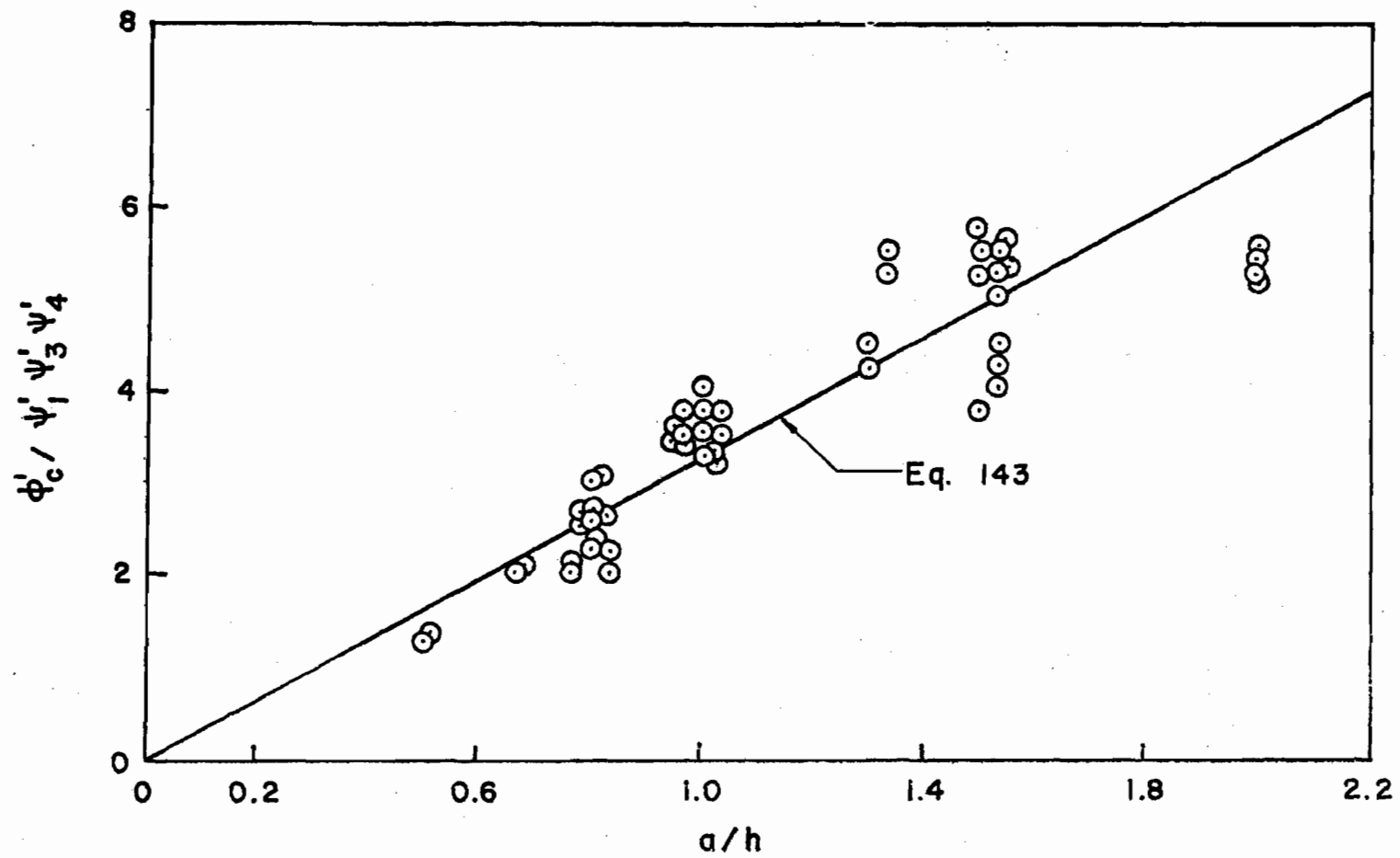
Figure 65. Variation of Postbuckling Strength Factor with the Ratio a/h for Reinforced Beam Webs Subjected to Two-Flange Web Crippling Load
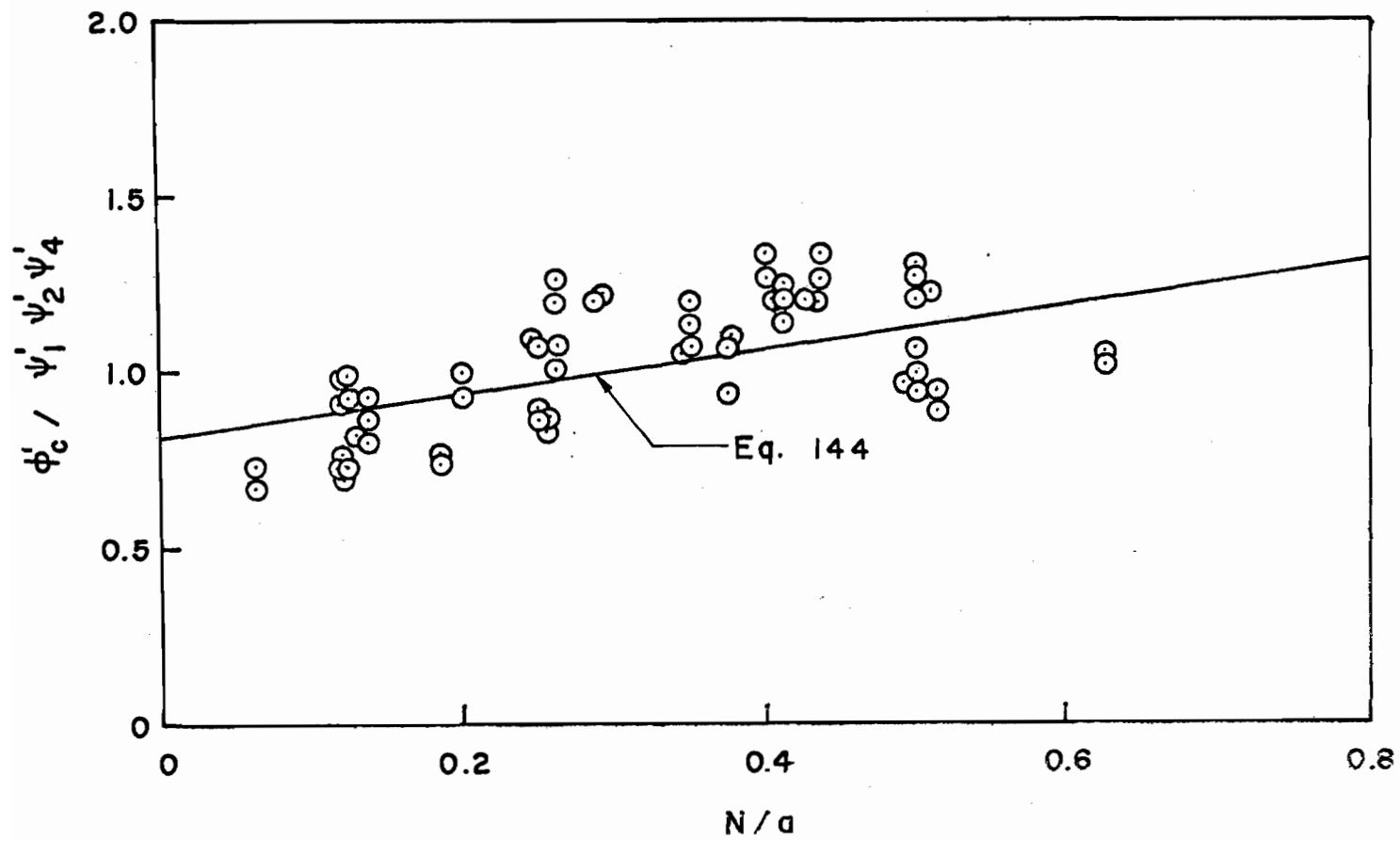
Figure 66. Variation of Postbuckling Strength Factor with the Ratio N/a for Reinforced Beam Webs Subjected to Two-Flange Web Crippling Load
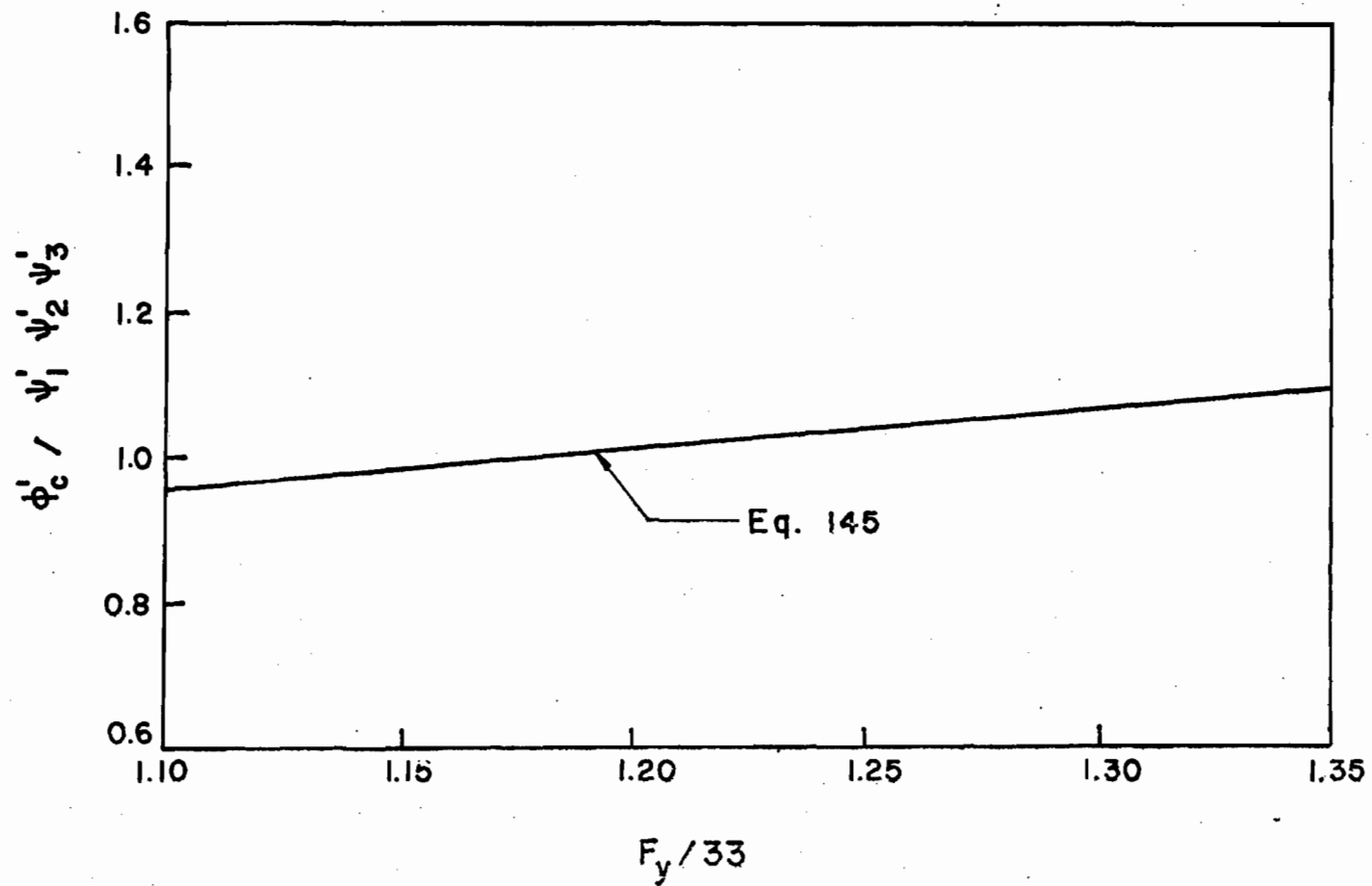
Figure 67. Variation of Postbuckling Strength Factor with the Ratio $F_y/33$ for Reinforced Beam Webs Subjected to Two-Flange Web Crippling Load
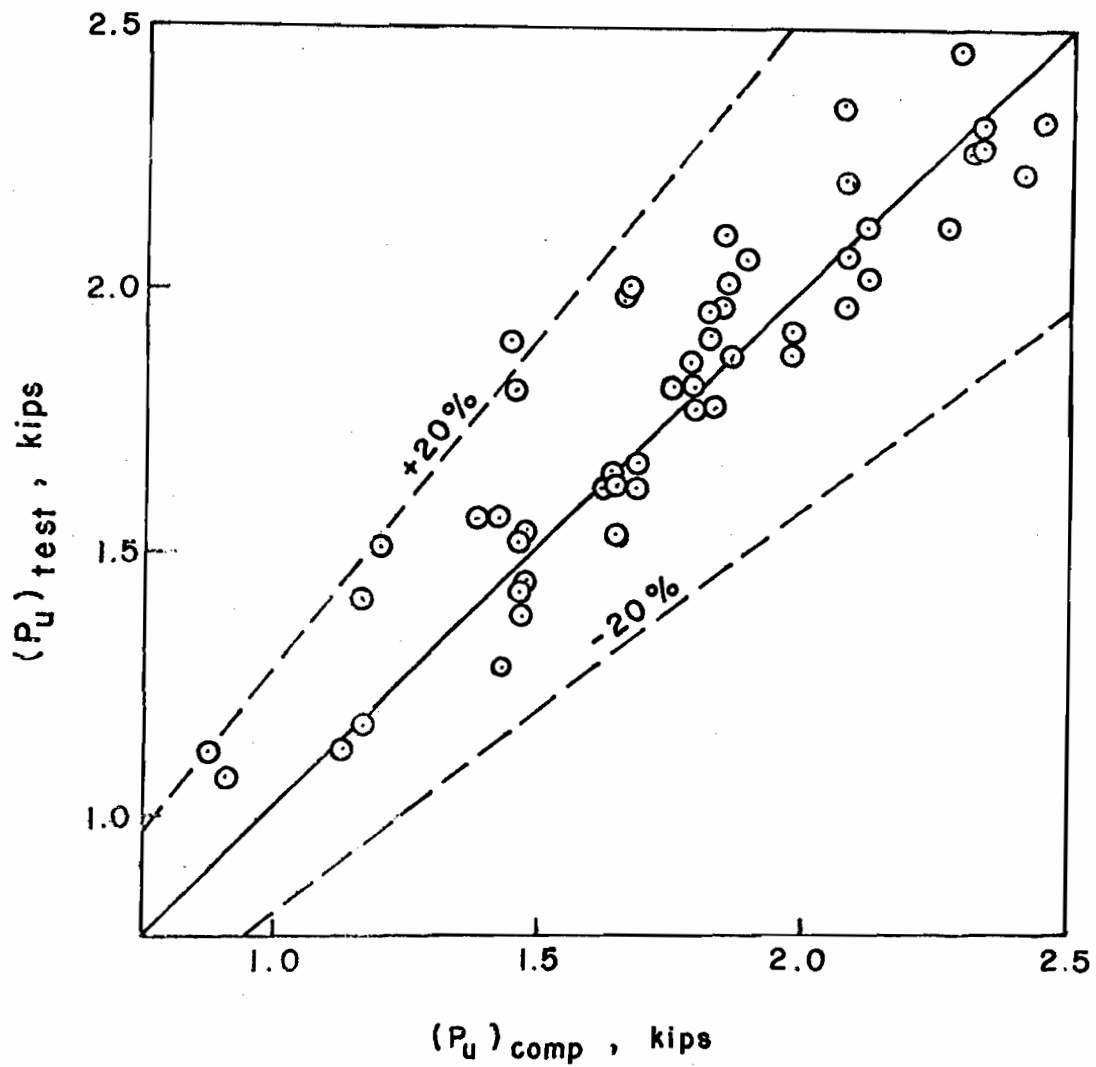
Figure 68. Comparison Between the Tested and Computed Web Crippling
Loads for One-Flange Loading Based on the Ultimate Load
Method
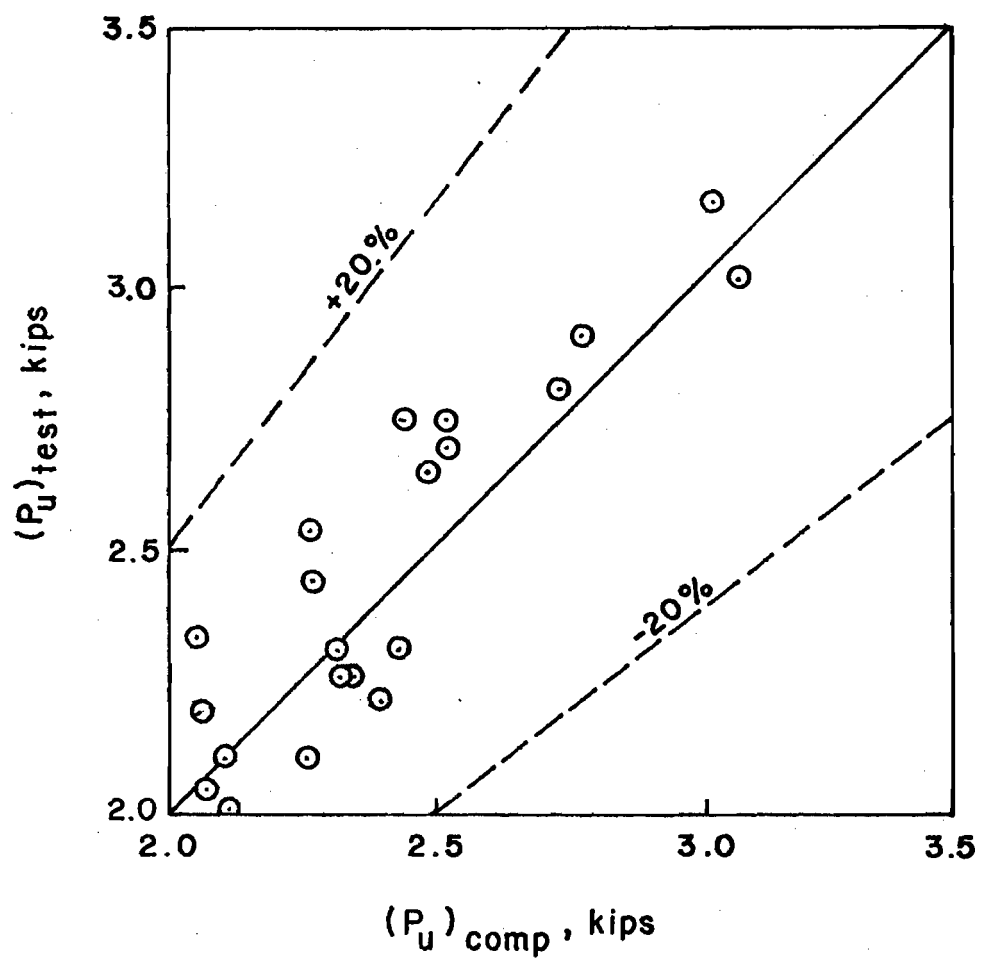
Figure 68. (continued)
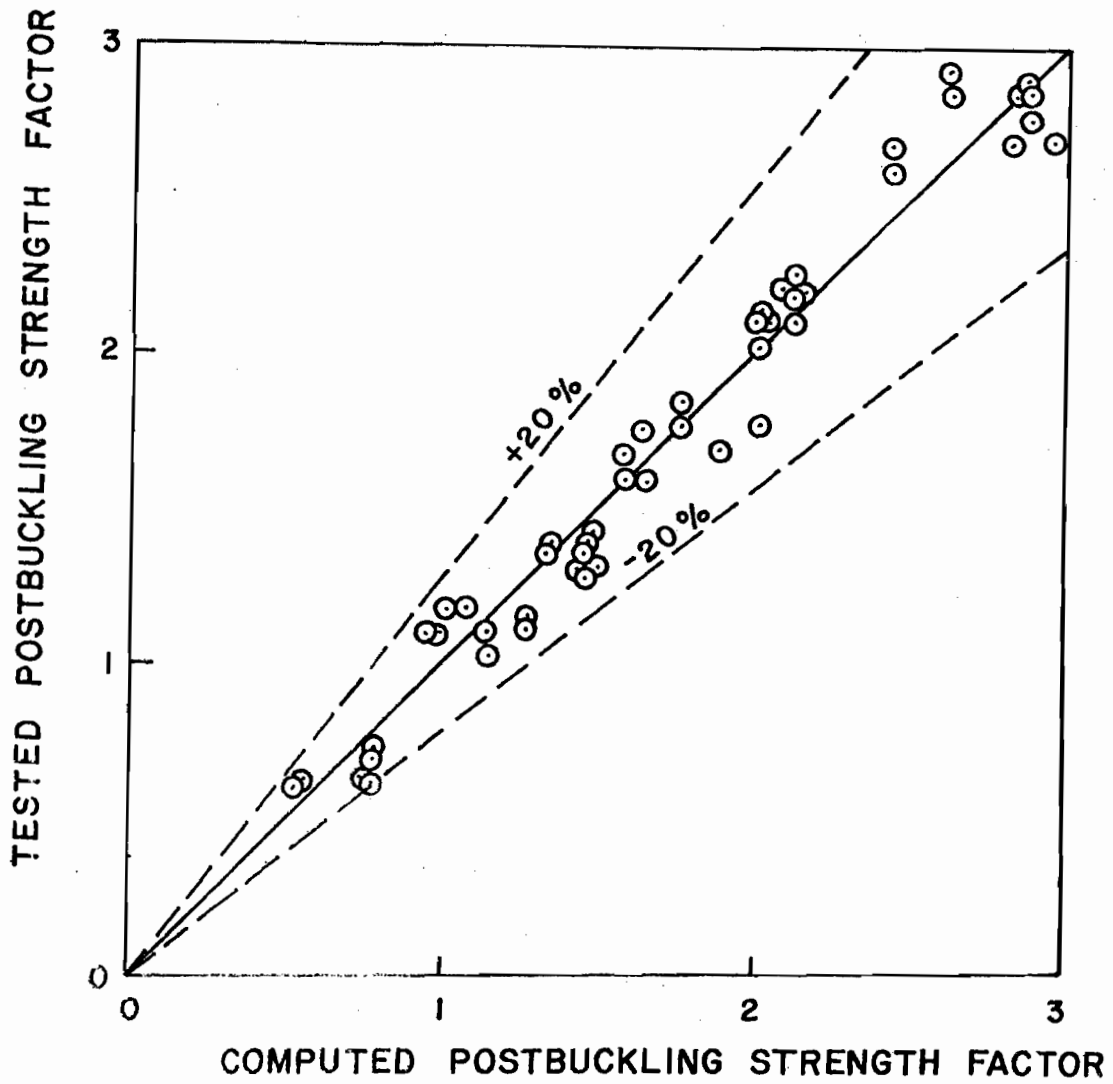
Figure 69. Comparison Between the Tested and Computed Postbuckling Strength Factor for Reinforced Beam Webs Under One-Flange Loading
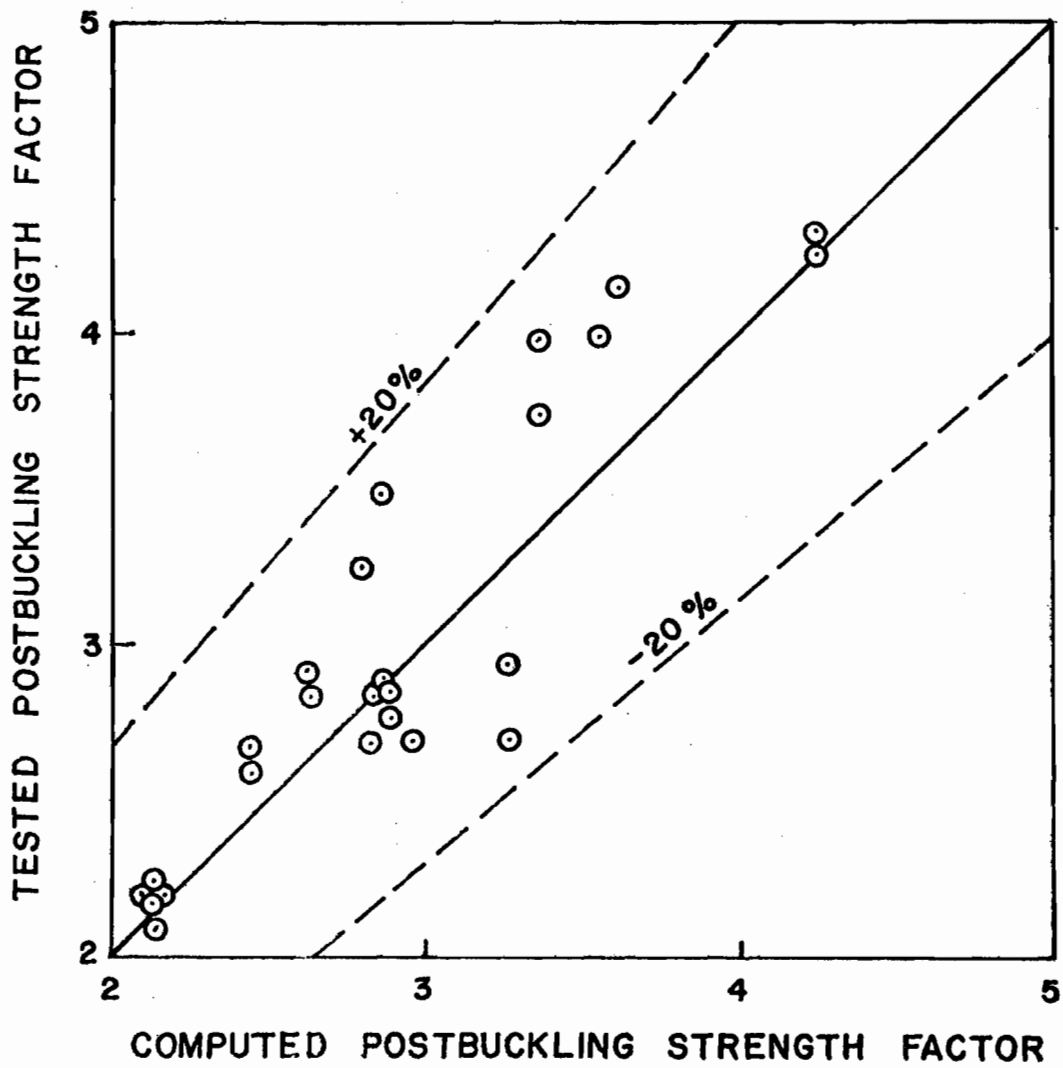
Figure 69. (continued)
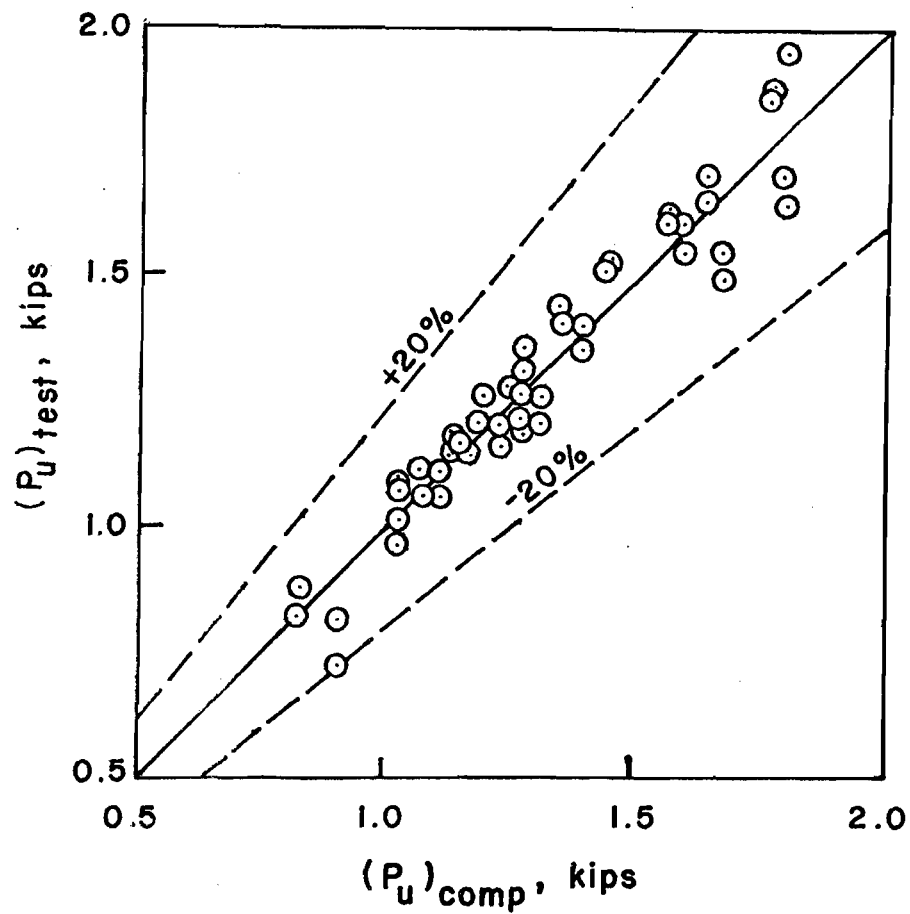
Figure 70. Comparison Between the Tested and Computed Web
Crippling Loads for Two-Flange Loading Based on the
Ultimate Load Method
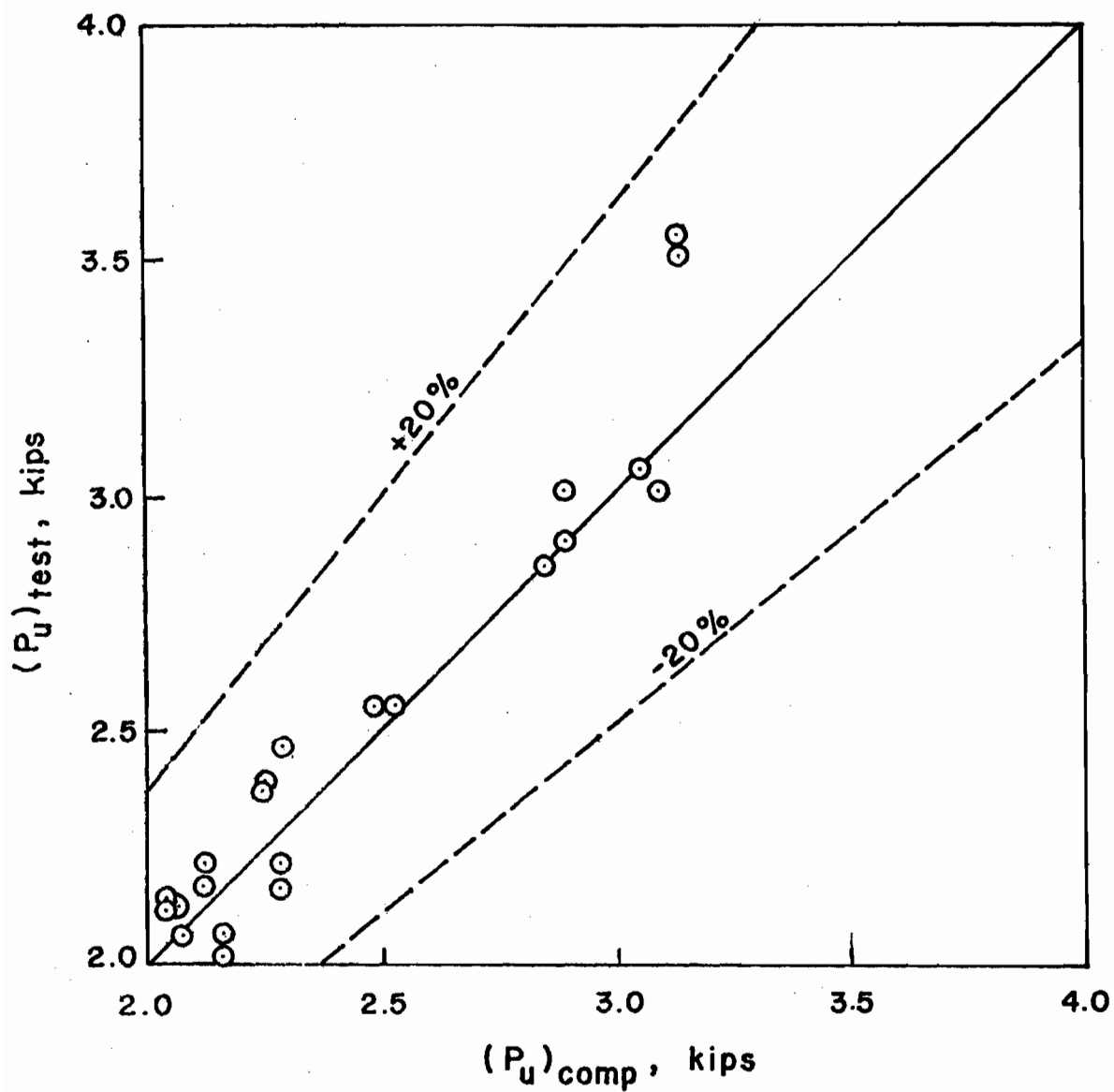
Figure 70. (continued)
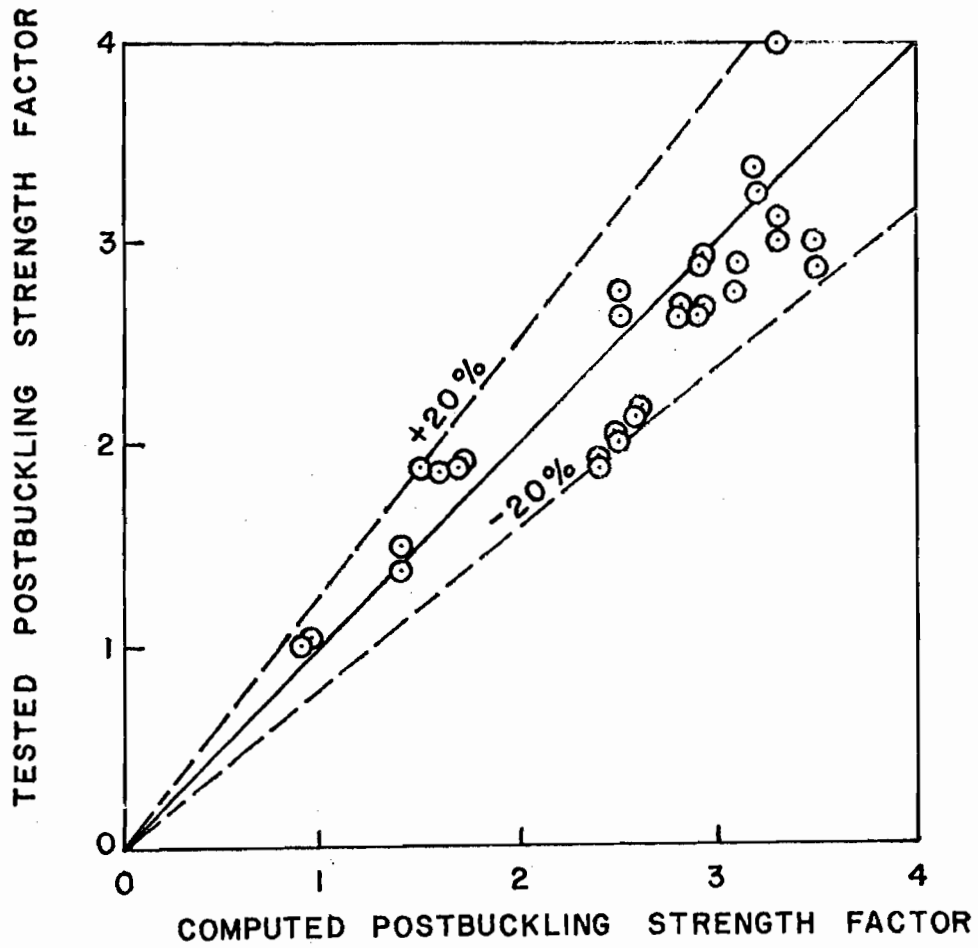
Figure 71. Comparison Between the Tested and Computed Postbuckling Strength Factor for Reinforced Beam Webs Under Two-Flange Loading
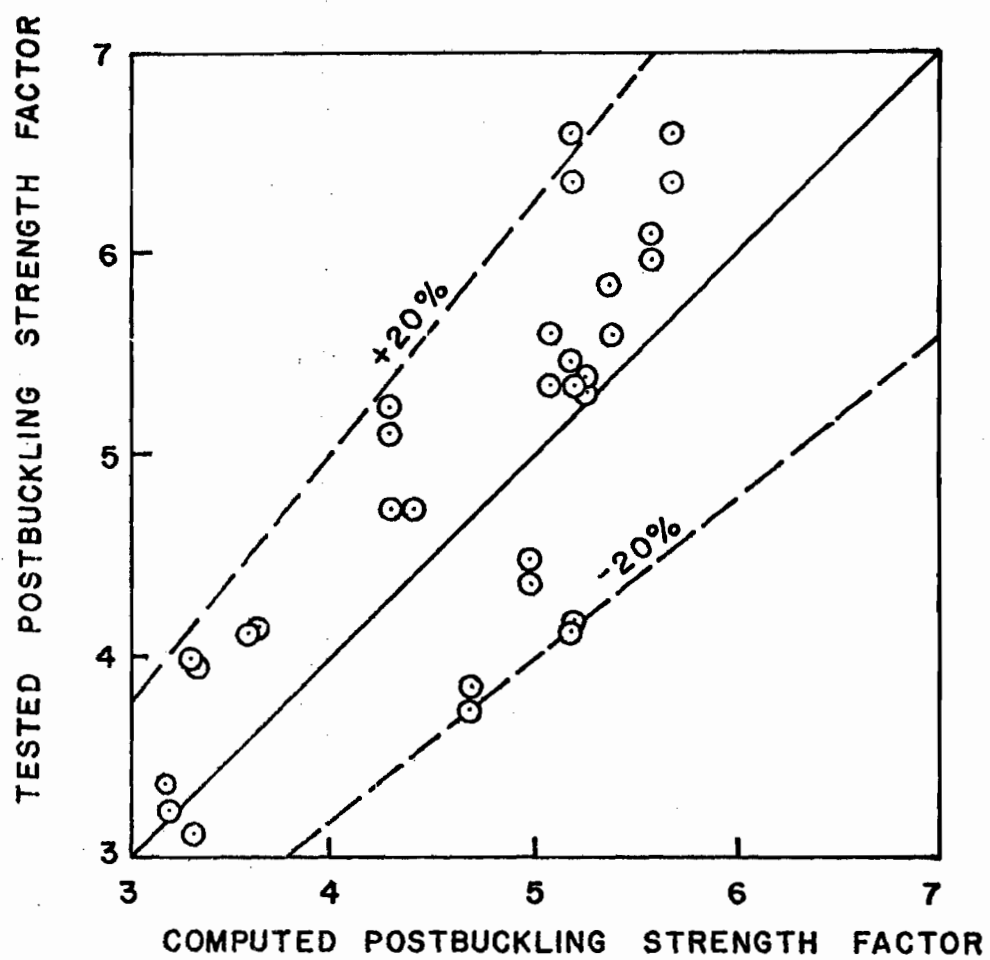
Figure 71. (continued)
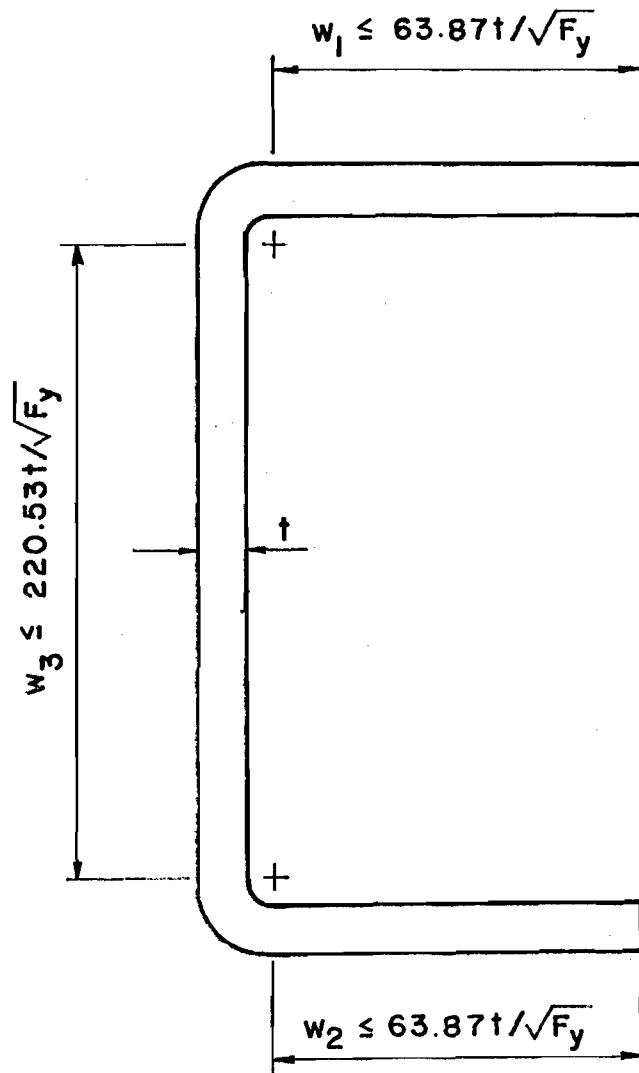
Figure 72. Limiting Dimensions of Cold-Formed Steel
Transverse Stiffeners
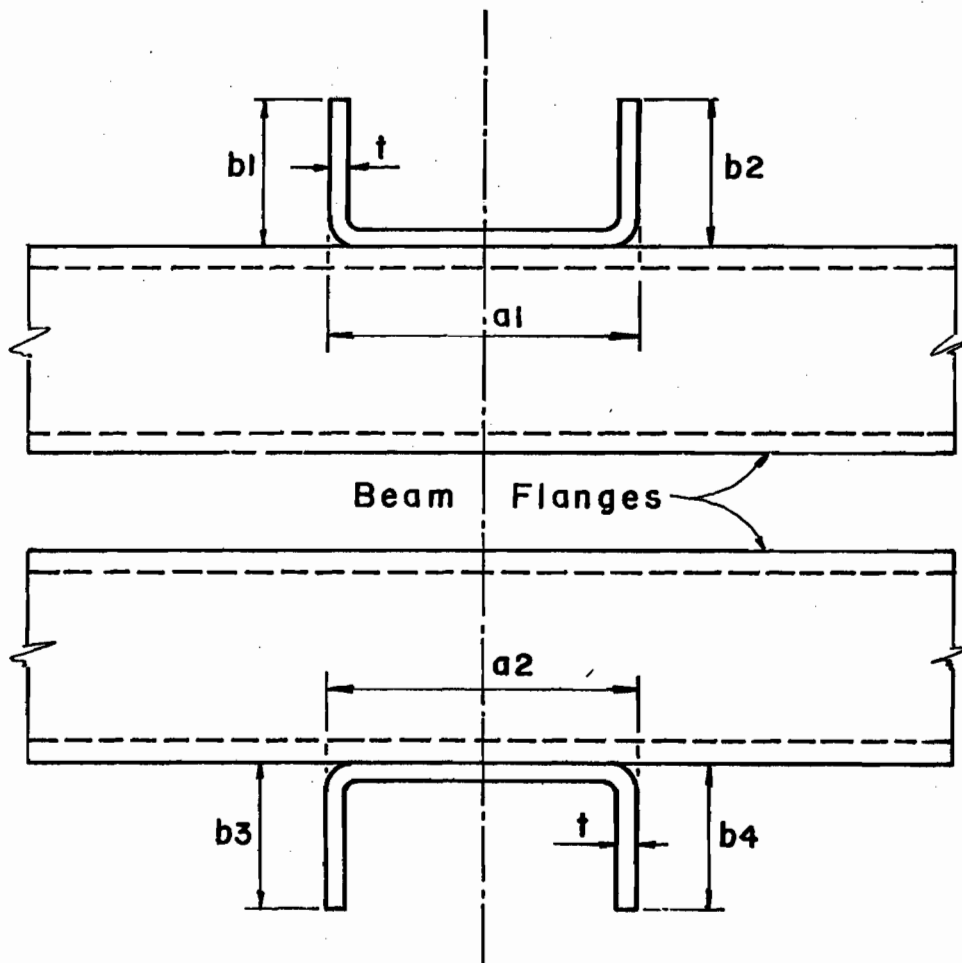
Figure 73. Dimensions of Cold-Formed Steel
Transverse Stiffeners
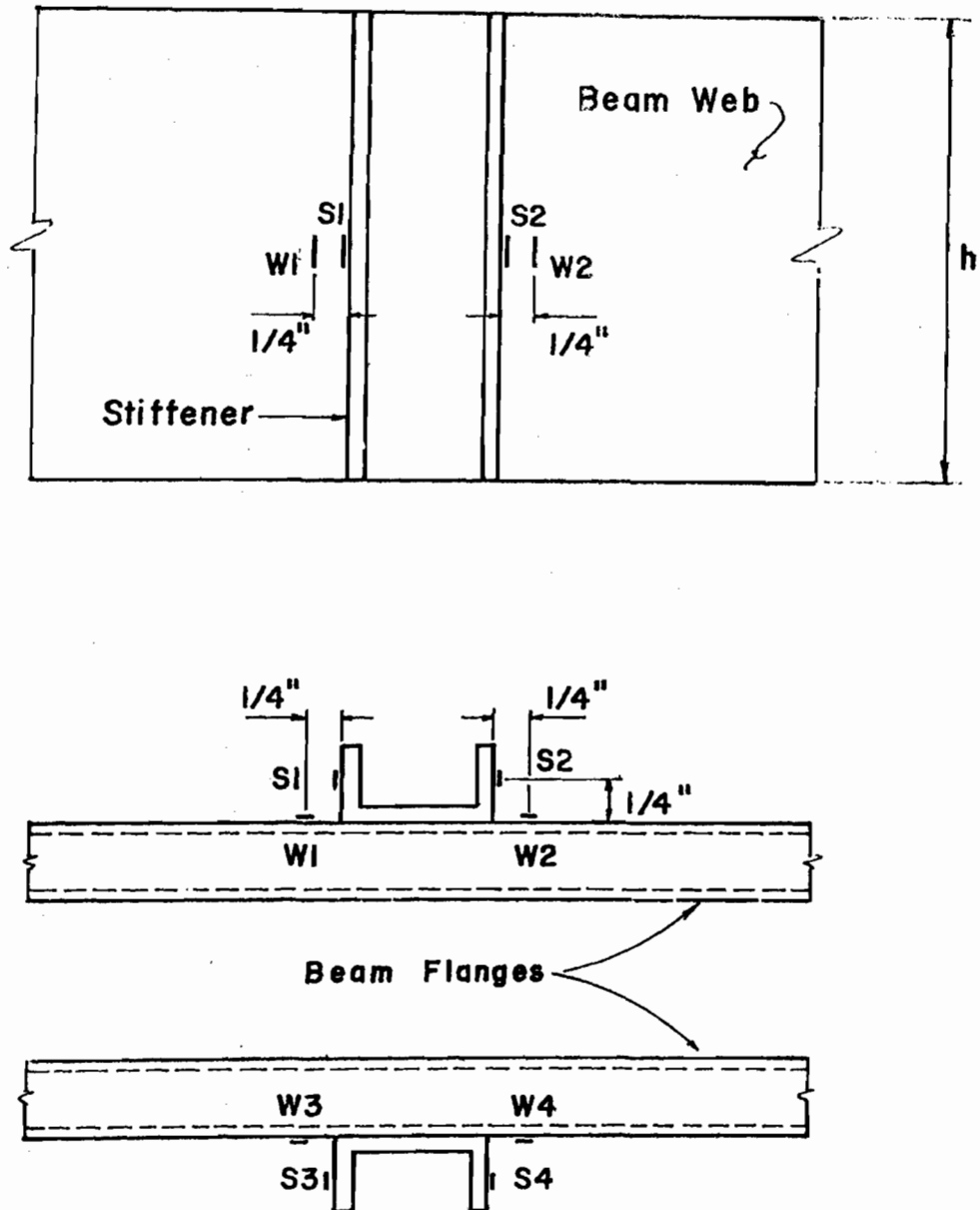
Figure 74. Location of Strain Gages for Transverse Stiffener Tests
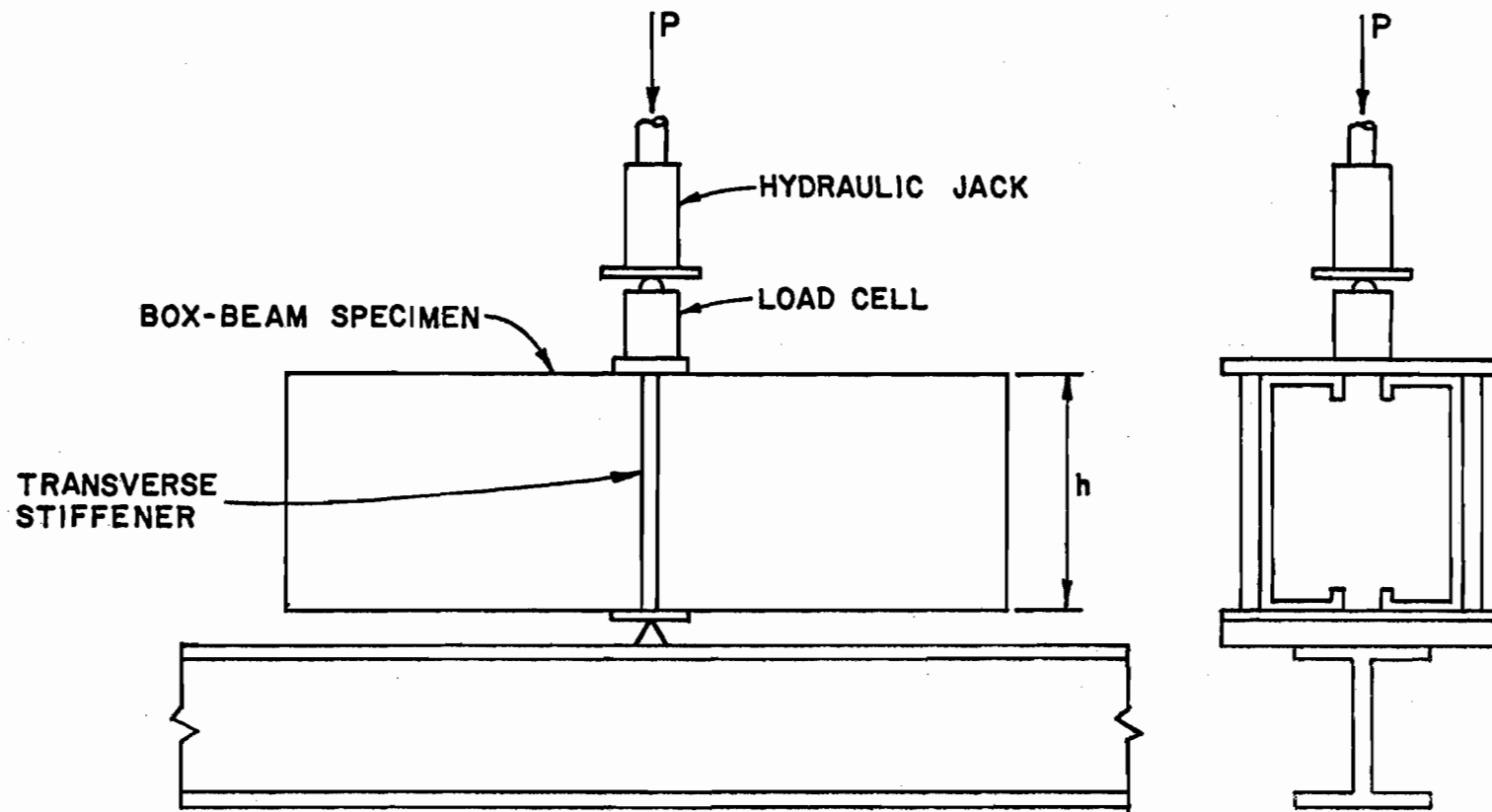
Figure 75. Test Setup for Intermediate Stiffener Tests
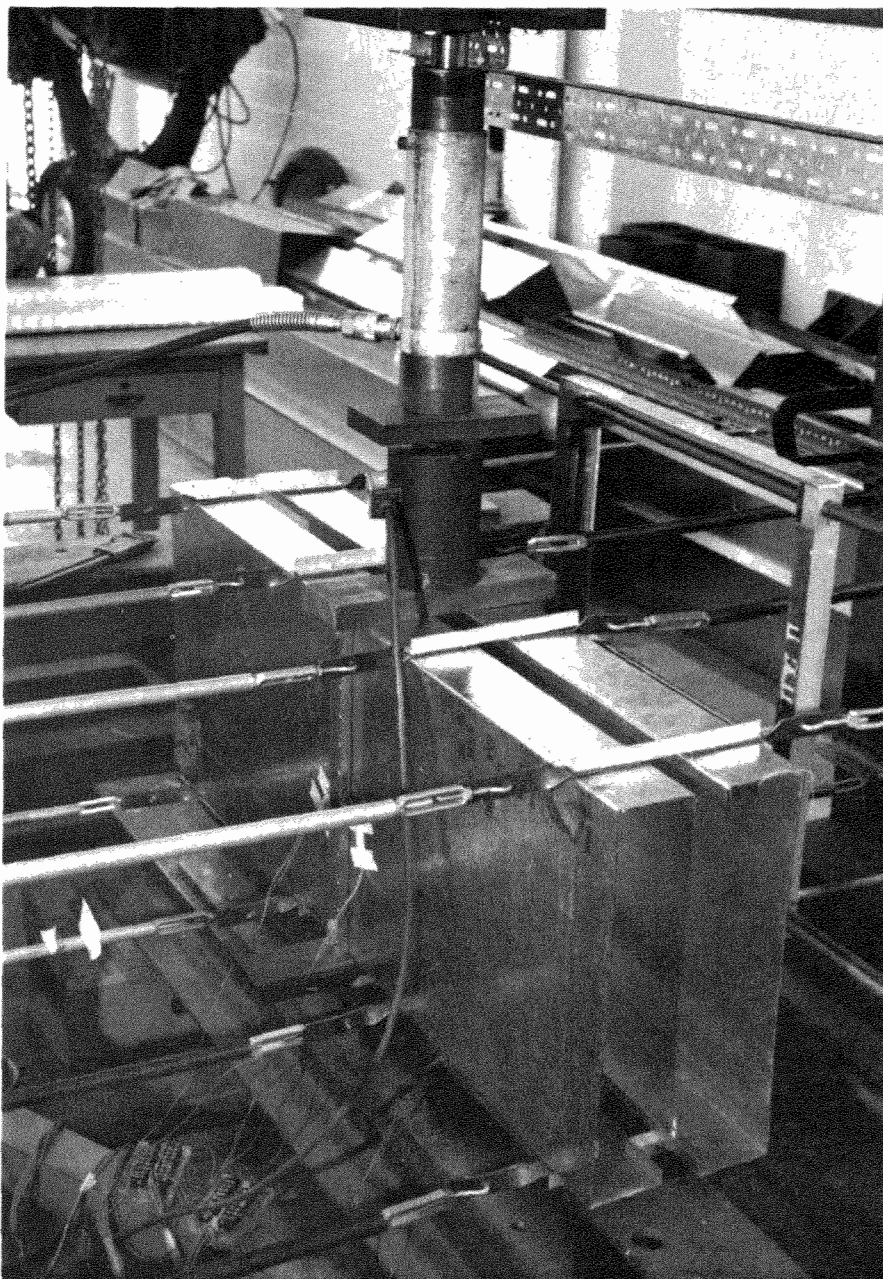
Figure 76. Photograph of Test Setup for Intermediate
Stiffener Tests
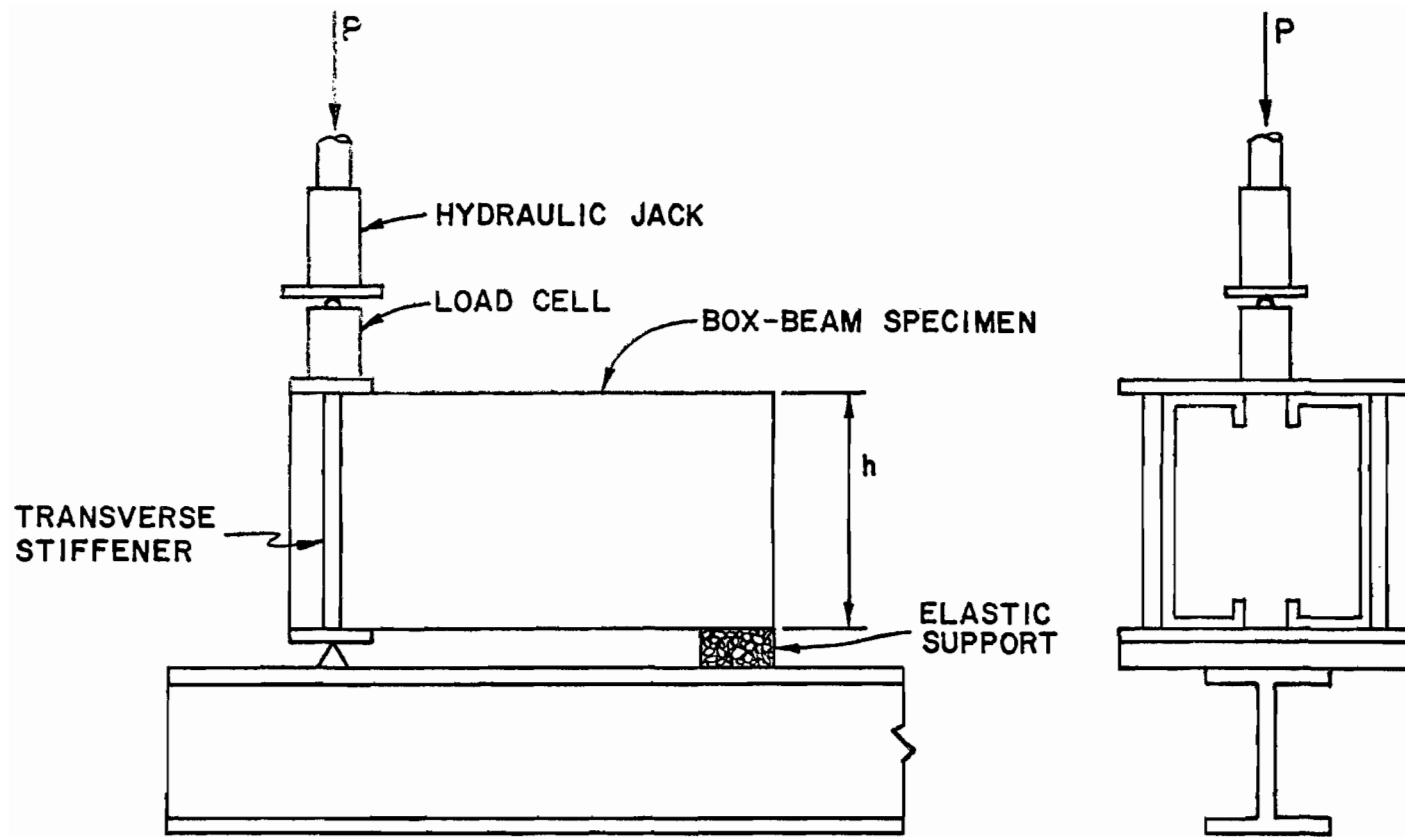
Figure 77. Test Setup for End Transverse Stiffener Tests
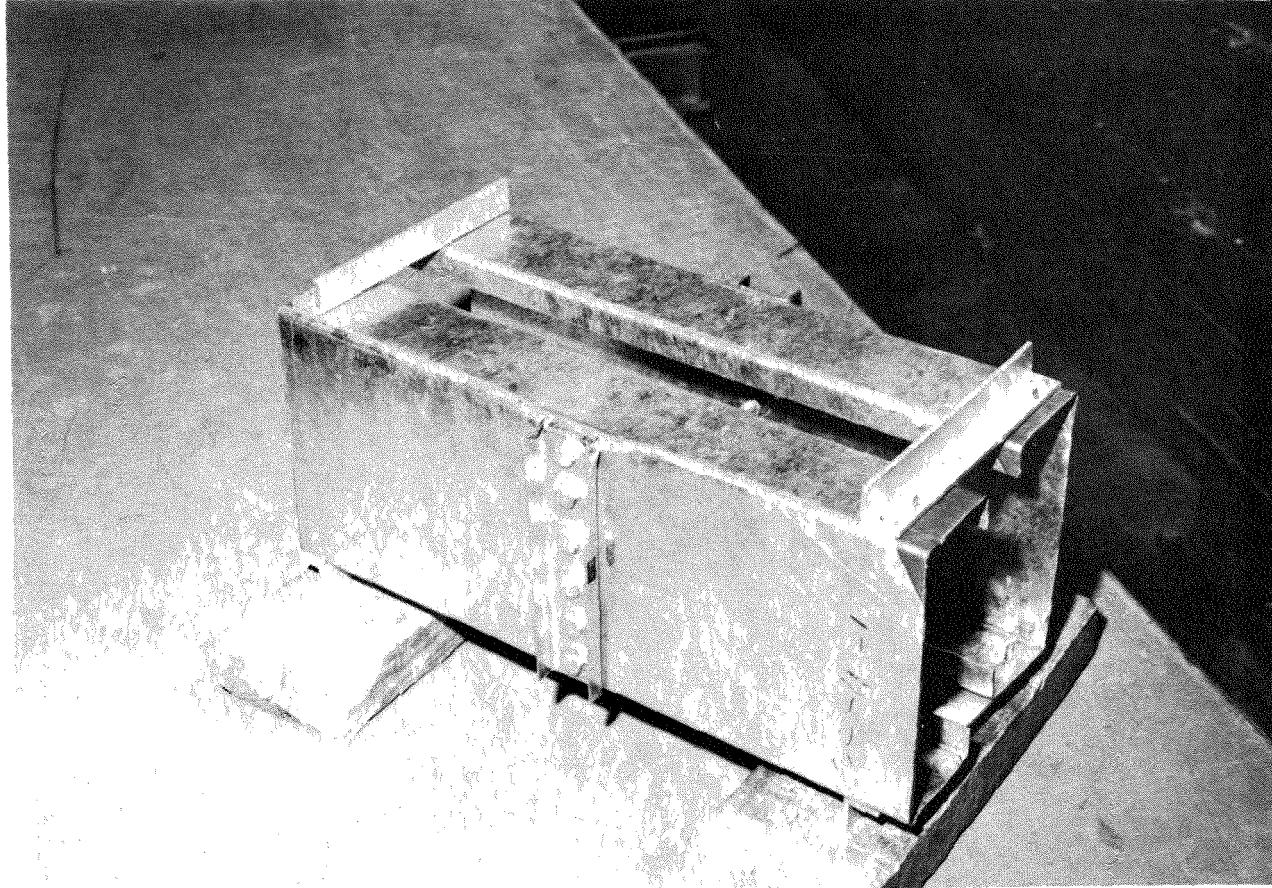
Figure 78. Photograph of End Crushing Failure Mode for Intermediate
Stiffener Tests
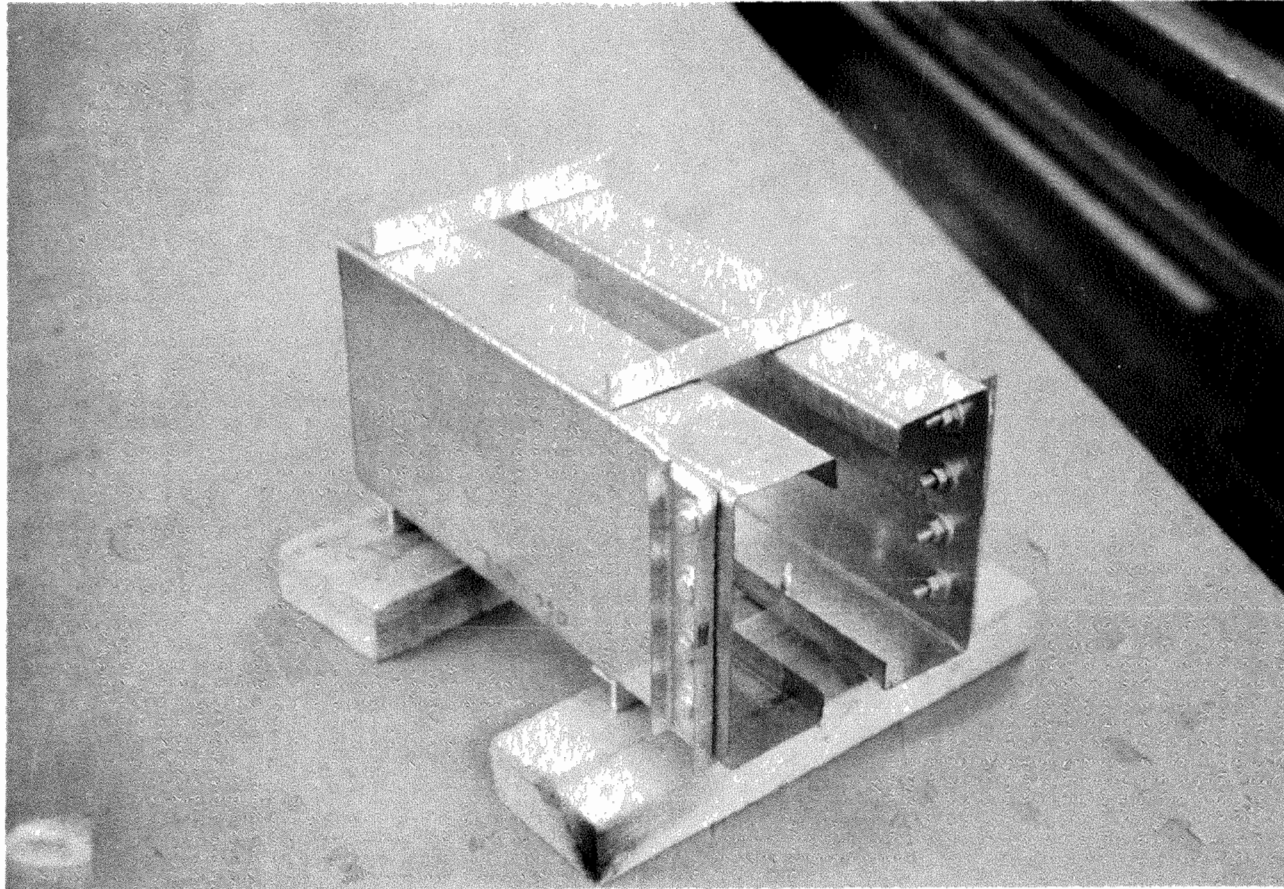
Figure 79. Photograph of End Crushing Failure Mode for End Transverse
Stiffener Tests
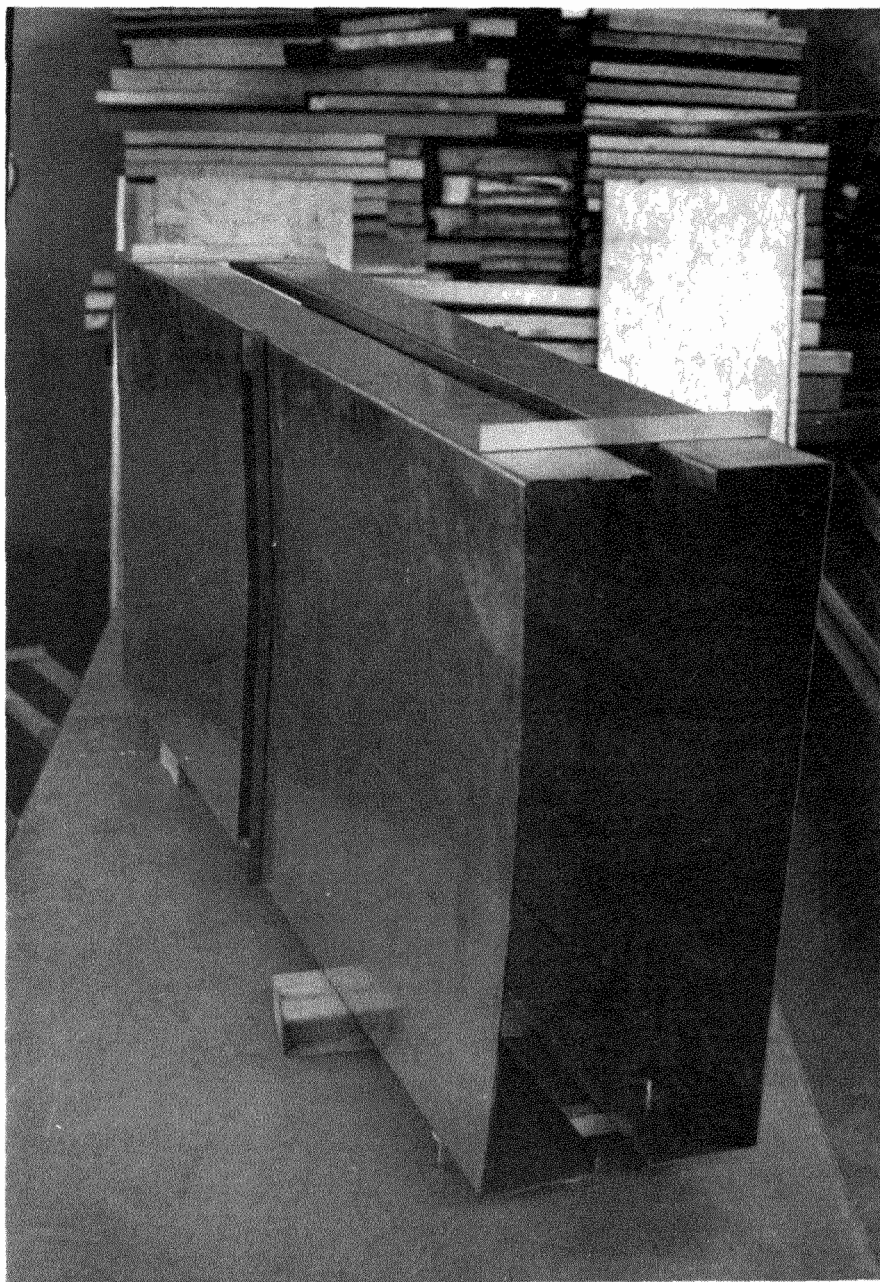
Figure 80.   Photograph of Stability Failure Mode for
Intermediate Stiffener Tests
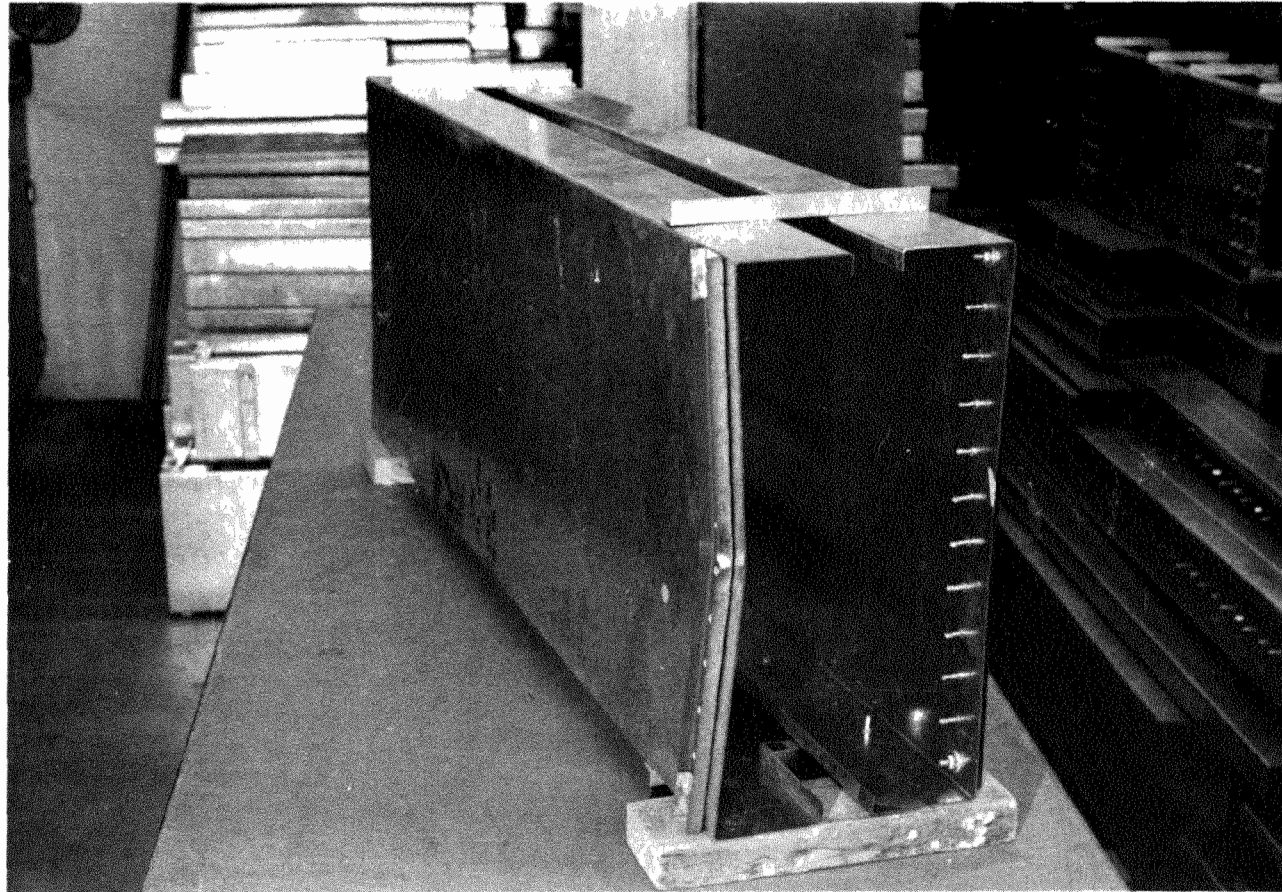
Figure 81. Photograph of Stability Failure Mode for End Transver Stiffener
         Tests
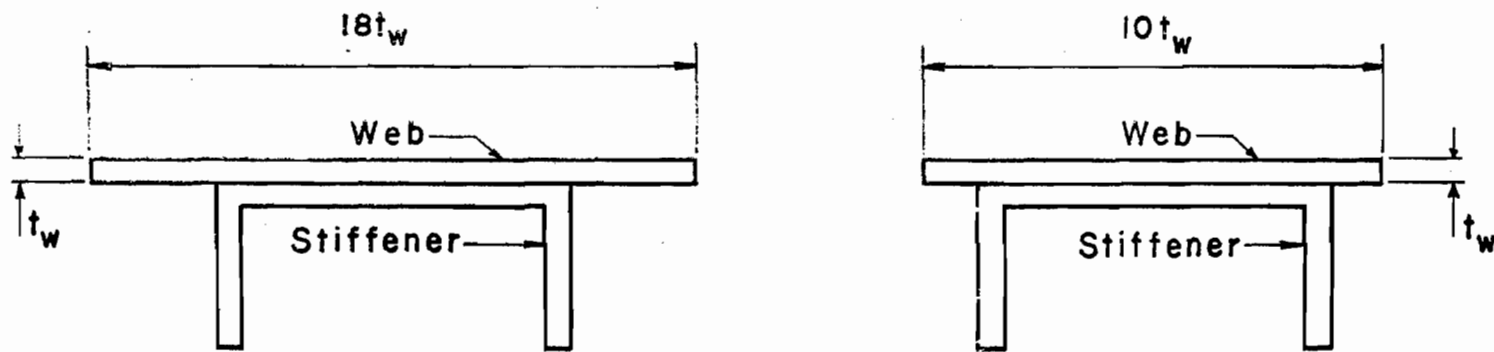
Figure 82. Effective Widths of Beam Webs for Transverse Stiffeners
Under End Crushing Failure
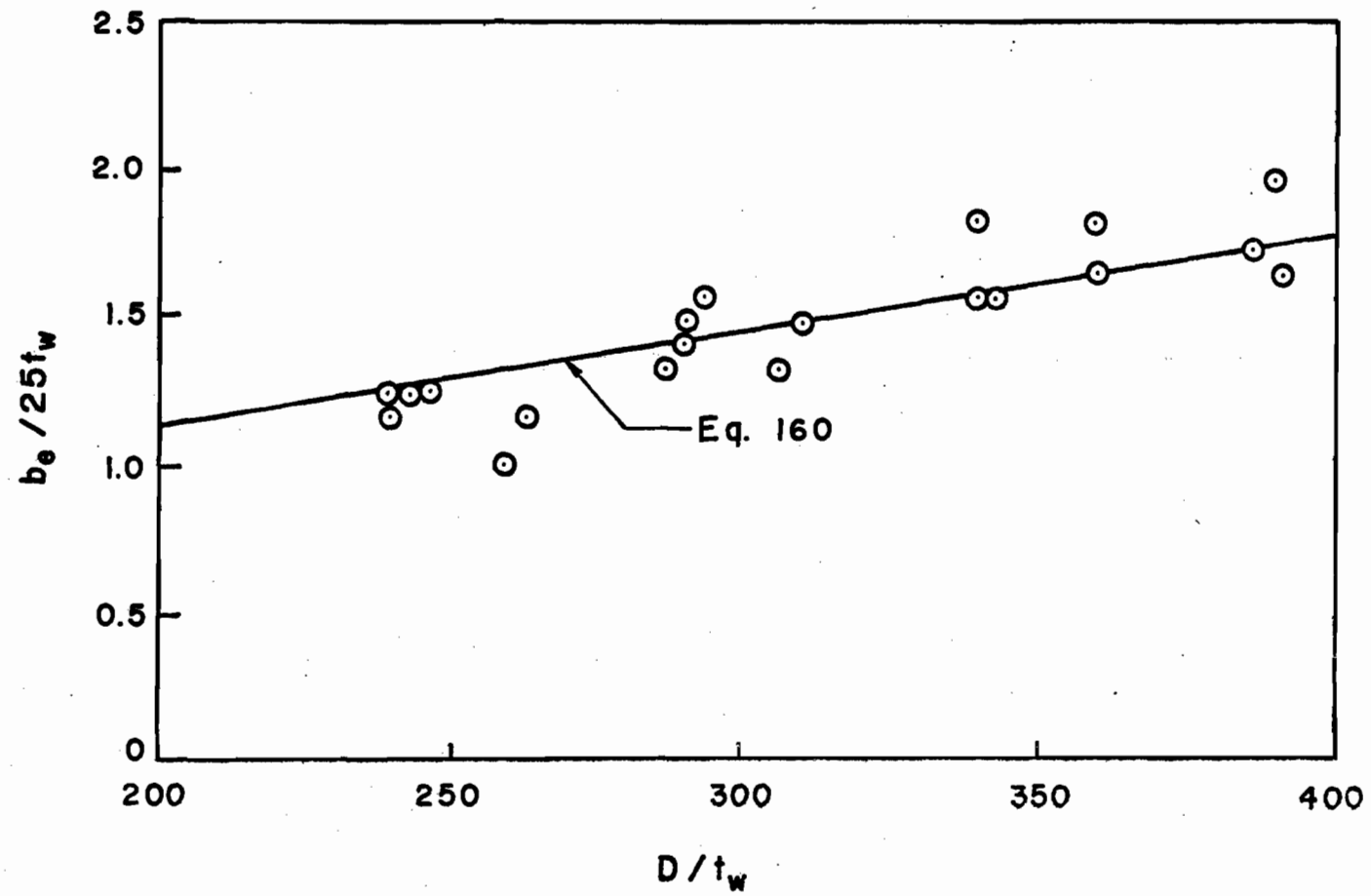
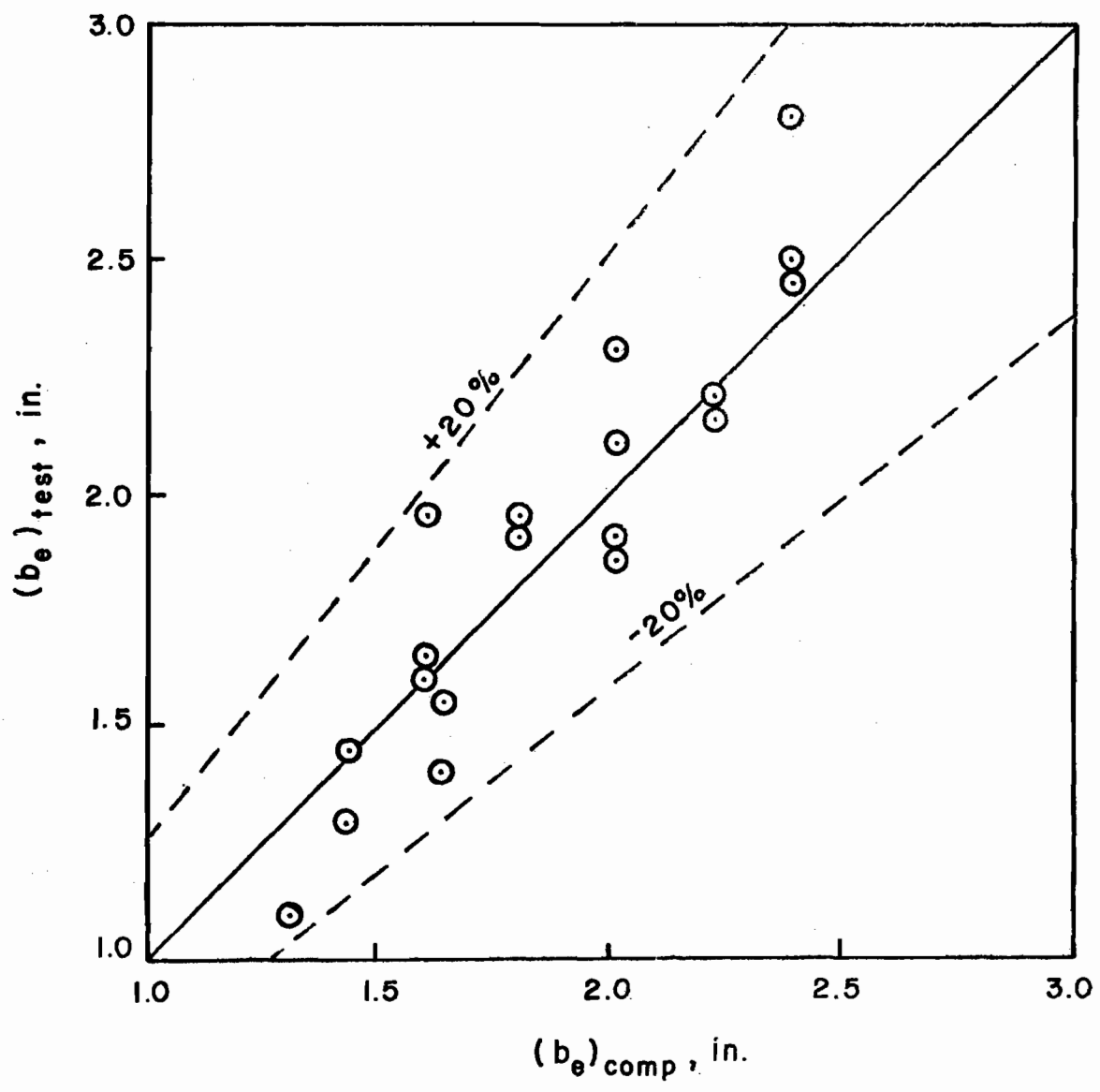Figure 83. Plot of $b_e/25t_w$ versus D/t_w for Intermediate Stiffeners

Figure 84. Comparison of Tested and Computed Effective Widths
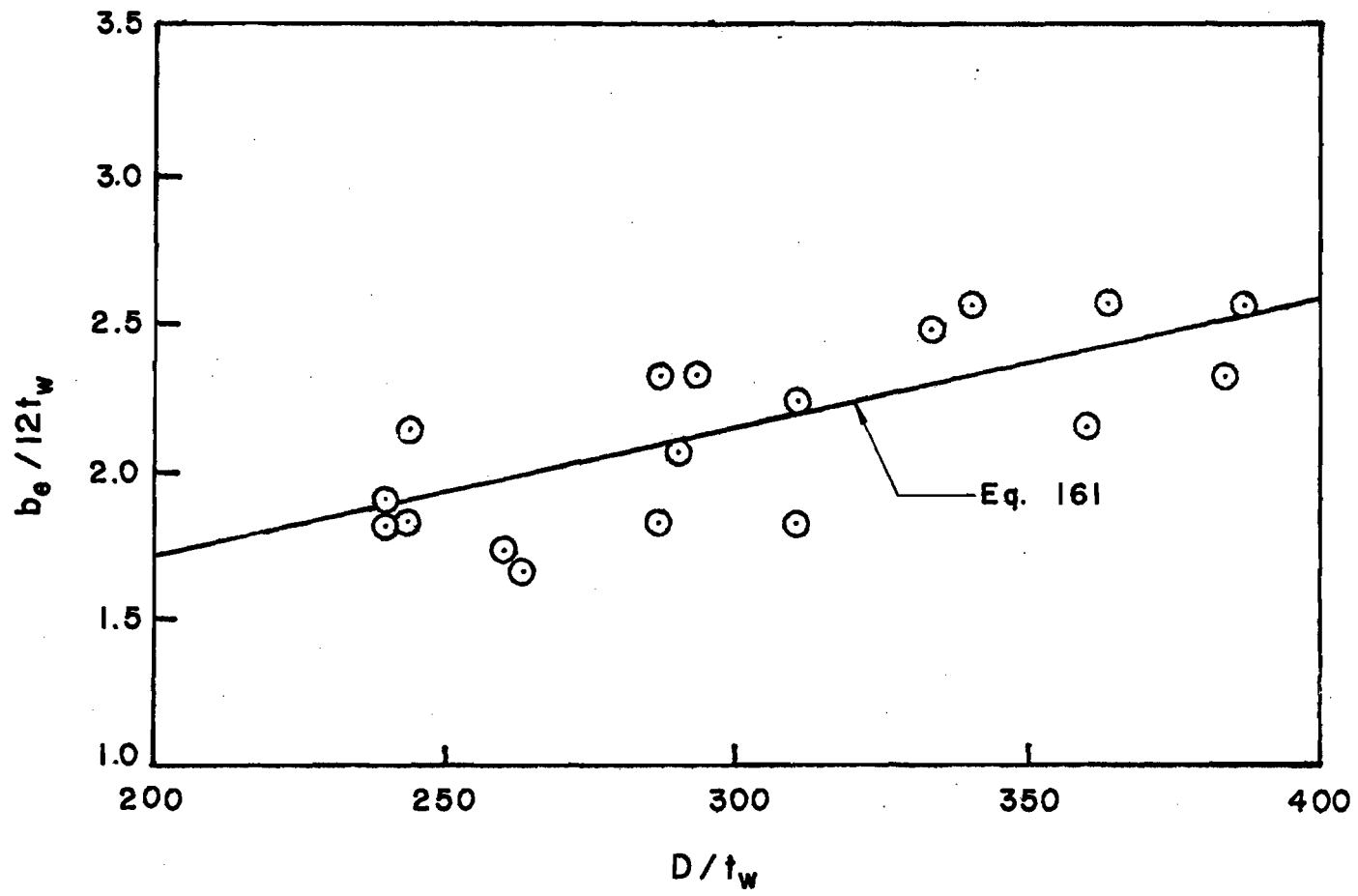for Intermediate Stiffeners Under Stability Failure

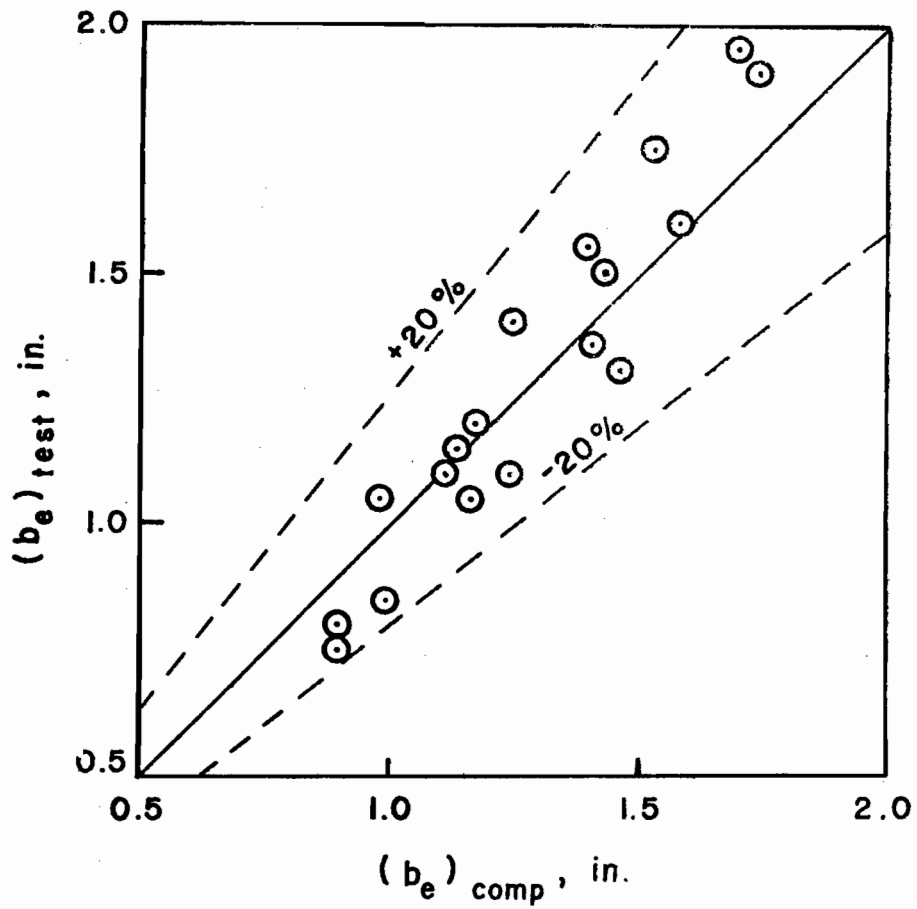Figure 85. Plot of $b_e/12t_w$ versus D/t_w for End Transverse Stiffeners

Figure 86. Comparison of Tested and Computed Effective
Widths for End Transverse Stiffeners